The role of 11β-Hydroxysteroid Dehydrogenase type 2 in protection against inflammation during atherogenesis: Studies in the Apoe$^{-/-}$ /11β-HSD2$^{-/-}$ double knockout mouse.

Danielle Louise Armour

Doctor of Philosophy
University of Edinburgh
2009

Declaration

I hereby declare that this thesis has been composed entirely by myself and that no part of this work has been submitted for any other degree or professional qualification. All work presented was executed by myself except where otherwise acknowledged.

Danielle L Armour.

Abstract

It is well established that atherosclerosis, an inflammatory response to chronic injury in the blood vessel wall, plays a leading role in the development and progression of cardiovascular disease. Mineralocorticoid receptor (MR) over-activation has been implicated in atherosclerosis. In mineralocorticoid-target tissues, 11β-Hydroxysteroid dehydrogenase type 2 (11β-HSD2) inactivates glucocorticoids, conferring aldosterone specificity upon the normally unselective MR. Recent evidence suggests that 11β-HSD2 may also afford protection of MR in the cells of the vasculature, providing possible mechanisms by which MR activation may directly promote atherosclerosis. Consistent with this, *Apoe*$^{-/-}$/11β-HSD2$^{-/-}$ double knockout (DKO) mice show accelerated atheroma development.

The present thesis tested the hypothesis that inactivation of 11β-HSD2, allowing inappropriate activation of MR in cells of the vasculature, accelerates atherogenesis through promotion of a pro-inflammatory environment with increased endothelial cell expression of adhesion molecules and subsequent macrophage infiltration into plaques.

DKO mice received either the MR antagonist eplerenone (200mg/kg/day) or vehicle in normal chow diet from 2 months of age for 12 weeks. Eplerenone significantly decreased atherosclerotic burden in brachiocephalic arteries of DKO mice, an effect that was accompanied by alterations in the cellular composition of plaques such that a more stable collagen- and smooth muscle cell- rich plaque was formed. Eplerenone treatment was also associated with a reduction in vascular inflammation as demonstrated by a significant reduction in macrophage infiltration into DKO plaques. The accelerated atherogenesis in DKO mice was clearly evident by 3 months of age, a time point at which *Apoe*$^{-/-}$ mice were completely lesion free. By 6 months, some *Apoe*$^{-/-}$ mice had developed lesions whilst all DKO mice at this age showed much larger plaques. Compared to *Apoe*$^{-/-}$ mice, the cellular composition of DKO plaques was altered favouring vulnerability and inflammation, with increased macrophage and lipid content and decreased collagen content. To investigate the

possible underlying mechanisms responsible for increased inflammatory cell content, the expression of vascular cell adhesion molecule 1 (VCAM-1) was compared in DKO and *Apoe*$^{-/-}$ brachiocephalic arteries. VCAM-1 immunostaining was significantly greater on the endothelial cells of DKO arteries at 3 months compared to age-matched *Apoe*$^{-/-}$ mice. At 6 months, DKO and *Apoe*$^{-/-}$ mice had similar expression of VCAM-1.

Finally, mouse aortic endothelial cells (MAECs) were used to investigate the mechanism of adhesion molecule up-regulation in the absence of 11β-HSD2. Both aldosterone and TNF-α, included as a positive control, dramatically increased VCAM-1 expression in MAECs. Spironolactone pre-treatment blocked the effect of aldosterone, suggesting an MR-mediated mechanism. Corticosterone alone had no effect on VCAM-1 expression. However, inhibition of 11β-HSD2 by pre-treatment with glycyrrhetinic acid allowed corticosterone to induce a significant increase in the number of VCAM-1-stained MAECs, demonstrating functional expression of 11β-HSD2 in MAECs. Consistent with 11β-HSD2 involvement, VCAM-1 up-regulation by corticosterone in the presence of glycyrrhetinic acid was reversed by blockade of MR with spironolactone.

In conclusion, loss of 11β-HSD2 activity leading to inappropriate activation of MR in atherosclerotic mice promotes plaque vulnerability and increases vascular infiltration of macrophages which accelerates plaque growth, possibly through enhanced MR- mediated endothelial cell expression of VCAM-1.

Acknowledgements

I am fortunate to have received excellent mentoring and supervision throughout my PhD. I am very grateful to both Yuri Kotelevtsev and Karen Chapman for their constant and much appreciated support, advice, and encouragement. I am very lucky to have had two supervisors that complement each other so well, the balance between Karen's methodical and focused approach and Yuri's creative and thought-provoking ideas was ideal.

I am also very grateful to Jon Henderson in the animal unit for his help with all aspects of the mouse colonies. David Brownstein and Graeme Deuchar both provided much appreciated technical advice and help throughout. The Picrosirius red staining was performed by Susan Harvey and Bob Morris in the histology department and I am also thankful to them for general histological advice. I am particularly grateful to Nick Kirkby for his help and patience with all machine and computer related issues, of which there were many.

I am very lucky to have obtained the four-year Wellcome Trust PhD position and am thankful to John Mullins and Rudolph Riemersma for admitting me to this programme. I would also like to thank Gillian Gray for her valued input during thesis committee meetings.

My time in the vascular biology lab has been made so enjoyable by the great friends I have made during the course of my PhD. There are too many names to mention here but all members, past and present, have been great to both work and socialise with.

Last but not least, I am very thankful to Paul for his support throughout and I'm extremely happy to have become his fiancé during this PhD.

Abbreviations

11β-HSD2	11β-Hydroxysteroid dehydrogenase type 2
ACE	Angiotensin converting enzyme
ACTH	Adrenocorticotrophic hormone
Ang II	Angiotensin II
ApoE	Apolipoprotein E
APS	Ammonium Persulphate
AQP2	Aquaporin-2
AT_1	Angiotensin receptor type 1
BSA	Bovine serum albumin
CBG	Corticosteroid-binding globulin
CHD	Coronary heart disease
CNS	Central nervous system
CRH	Corticotrophin-releasing hormone
CVD	Cardiovascular disease
DAB	Diaminobenzidine
DKO	Double knockout mouse (*Apoe*$^{-/-}$/11β-HSD2$^{-/-}$)
DMSO	Dimethyl Sulphoxide
DNA	Deoxyribonucleic acid
DOCA	Deoxycorticosterone acetate
DTT	Dithiothreitol
EBM-2	Endothelial Basal Medium 2

EC	Endothelial cell
ECM	Extracellular matrix
EDTA	Ethylene diamine tetraacetic acid
EEL	External elastic lamina
ELISA	Enzyme-linked immunosorbent assay
EMSA	Electromobility shift assay
ENaC	Epithelial sodium channel
eNOS	Endothelial nitric oxide synthase
EPHESUS	Eplerenone Post-AMI Heart Failure Efficacy and Survival Study
FCS	Foetal calf serum
GR	Glucocorticoid receptor
GRE	Glucocorticoid-responsive elements
HPA	Hypothalamic-pituitary-adrenal axis
HRP	Horseradish Peroxidase
HUVECs	Human umbilical vein endothelial cells
ICAM-1	Intercellular adhesion molecule-1
IEL	Internal elastic lamina
IFN-γ	Interferon-γ
iNOS	Inducible nitric oxide synthase
KRDKO	Kidney rescue DKO mouse
LDL	Low density lipoprotein
MAC-2	Macrophage specific galectin-3
MAECs	Mouse aortic endothelial cells

MCP-1	Monocyte chemoattractant protein-1
M-CSF	Macrophage colony stimulating factor
MMP	Matrix metalloproteinase
MR	Mineralocorticoid receptor
MRE	Mineralocorticoid-responsive elements
mRNA	Messenger Ribonucleic acid
N0	Nitric oxide
NFM	Non-fat milk
NF-κB	Nuclear factor kappa-light-chain-enhancer of activated B cells
nNOS	Neuronal nitric oxide synthase
OCT	Optimum cutting temperature compound
OPD	o -Phenylenediamine dihydrochloride
PBS	Phosphate buffered saline
PBST	PBS-Tween
PCR	Polymerase chain reaction
PECAM-1	Platelet-endothelial cell adhesion molecule 1
PMSF	Phenyl methyl sulphonyl fluoride
RALES	Randomized Aldactone Evaluation Study
RAS	Renin-angiotensin system
ROS	Reactive oxygen species
SAME	Syndrome of apparent mineralocorticoid excess
SARA	Selective aldosterone receptor antagonist

SFM	Serum free culture medium
SMA	Smooth muscle cell α-actin
sVCAM-1	Soluble VCAM-1
TEMED	N,N,N',N'-Tetramethylethylenediamine
TNF-α	Tumour necrosis factor-α
UST	United States trichrome
VCAM-1	Vascular cell adhesion molecule-1
VSMCs	Vascular smooth muscle cells

Table of Contents

Declaration…….. I
Abstract……..II
Acknowledgements……..….IV
Abbreviations……...V
Table of Contents……...IX
List of Figures…….....XIV
List of Tables……...XVI

1 Chapter 1: Introduction 1

1.1 Atherosclerosis 2
1.1.1 The normal arterial wall: Structure and function 2
1.1.2 Pathogenesis of atherosclerosis 5
1.1.3 Plaque stability 8
1.1.4 Animal models of atherosclerosis 9
1.2 Adrenal steroids 12
1.2.1 Physiological actions of steroid hormones 12
1.2.2 Regulation of steroid action 14
1.2.3 Steroid hormone receptors 16
1.2.4 Tissue specific metabolism 17
1.3 Adrenal steroids and cardiovascular pathologies 21
1.3.1 Increased glucocorticoids and cardiovascular risk 21

1.3.2 Vascular steroid action 22
1.3.3 Activation of MR in cardiovascular pathology 25
1.4 The *Apoe*$^{-/-}$/11β-HSD2 double knockout mouse 28
1.5 Hypothesis and aims 32
1.5.1 Hypothesis 32
1.5.2 Aims 32

2 Chapter 2: Materials and methods 33

2.1 Materials 34
2.1.1 Buffers and Solutions 38
2.1.2 Drugs 40
2.2 DKO and *Apoe*$^{-/-}$ Mice 41
2.2.1 Generation of DKO Mice 41
2.2.2 DNA Extraction 42
2.2.3 Genotyping 42
2.2.4 Drug Administration 43
2.3 Characterisation of Atherosclerotic Phenotype 44
2.3.1 Organ harvest and preparation 44
2.3.2 Histology and Immunohistochemistry 45
2.3.3 Image Analysis 54
2.3.4 Serum Cholesterol Measurements 54
2.4 Cell Culture 55
2.4.1 Cells and General Principles 55
2.4.2 Drug Treatments 56
2.4.3 Immunocytochemistry 57

2.4.4 Enzyme-Linked ImmunoSorbent Assay (ELISA) 58
2.4.5 Electrophoretic Mobility Shift Assay (EMSA) 61
2.5 Statistics 63

3 Chapter 3: Effect of Mineralocorticoid Receptor Blockade on the DKO Atherosclerotic Phenotype 65

3.1 Introduction 66
3.2 Methods 68
3.2.1 Drug administration 68
3.2.2 Assessment of atherosclerosis 68
3.2.3 Statistical analysis 68
3.3 Results 71
3.3.1 Influence of MR blockade on vascular remodelling and atherogenesis in DKO brachiocephalic arteries 71
3.3.2 Effect of MR blockade on the cellular composition of brachiocephalic plaques in DKO mice 74
3.3.3 Effect of MR blockade on brachiocephalic plaque inflammation in DKO mice 78
3.3.4 Influence of MR blockade on overall plaque stability in DKO mice .. 81
3.4 Discussion 83

4 Chapter 4: Characterisation of the DKO atherosclerotic phenotype 92

4.1 Introduction 93
4.2 Methods 94

4.2.1 Experimental mice 94
4.2.2 Assessment of atherosclerosis 94
4.2.3 Cholesterol Measurement 94
4.2.4 Statistical analysis 94
4.3 Results 95
4.3.1 Effect of 11β-HSD2 inactivation on atherosclerotic burden and vascular remodelling in *Apoe*$^{-/-}$ mice 95
4.3.2 Total plasma cholesterol levels in *Apoe*$^{-/-}$ vs. DKO mice 98
4.3.3 Influence of 11β-HSD2 inactivation on the cellular composition of brachiocephalic plaques in *Apoe*$^{-/-}$ mice 98
4.3.4 Influence of 11β-HSD2 inactivation on overall plaque stability in *Apoe*$^{-/-}$ mice…… 105
4.4 Discussion 107

5 Chapter 5: Mechanisms of enhanced vascular inflammation in the DKO mouse 116

5.1 Introduction 117
5.2 Methods 119
5.2.1 Adhesion molecule expression 119
5.2.2 Semi-quantitative scoring 119
5.2.3 Cytokine expression 119
5.2.4 Statistical analysis 119
5.3 Results 120
5.3.1 Effect of 11β-HSD2 inactivation on the endothelial expression of ICAM-1 in *Apoe*$^{-/-}$ mice 120

5.3.2 Effect of 11β-HSD2 inactivation on the endothelial expression of VCAM-1 in *Apoe*$^{-/-}$ mice 120
5.3.3 Influence of 11β-HSD2 inactivation on levels of sVCAM-1 123
5.3.4 Influence of 11β-HSD2 inactivation on MCP-1 levels 123
5.4 Discussion 125

6 Chapter 6: The role of the endothelial cell in MR-mediated pro-inflammatory pathways 134

6.1 Introduction 135
6.2 Methods 137
6.2.1 Treatment of MAECs 137
6.2.2 Adhesion molecule expression 137
6.2.3 Cytokine expression 137
6.2.4 Electromobility shift assay (EMSA) 137
6.2.5 Statistical analysis 137
6.3 Results 138
6.3.1 The role of endothelial MR activation on VCAM-1 expression 138
6.3.2 The role of endothelial MR activation on ICAM-1 expression 140
6.3.3 The influence of MR activation on MCP-1 secretion in MAECs 140
6.3.4 Involvement of NF-κB in MR-mediated mechanisms 143
6.4 Discussion 145

7 Chapter 7: Discussion 151

7.1 The DKO mouse as a model of atherosclerosis 152

7.2 The role of MR activation in atherosclerosis 154
7.3 Mechanisms of accelerated atherogenesis in DKO mice 156
7.4 Potential clinical significance of results 159
7.5 Future directions 161
7.5.1 The DKO mouse as a ‘test-bed’ 161
7.5.2 MR vs. GR 162
7.5.3 Mechanisms of unstable plaque formation 163
7.5.4 Renal vs. extra-renal MR activation 164
7.6 Conclusions 165

Reference List 166

Publications and Abstracts 199

Appendix 1 200

List of Figures

Figure 1.1 Structure of the arterial wall 3
Figure 1.2 Metabolism of Glucocorticoids 18
Figure 1.3 Pathological factors in the *Apoe*$^{-/-}$/11β-HSD2$^{-/-}$ DKO mouse..... 29
Figure 2.1 Comparison of direct and indirect immunohistochemistry 48
Figure 2.2 ABC method of immunohistochemistry..... 50
Figure 2.3 Specificity of primary antibodies 53
Figure 2.4 Sandwich ELISA 59
Figure 3.1 Anatomical location of brachiocephalic artery..... 69
Figure 3.2 Morphometric and quantitative analysis of brachiocephalic sections 70
Figure 3.3 Eplerenone reduced plaque size in DKO brachiocephalic arteries..... 72
Figure 3.4 Altered composition of atherosclerotic plaques in DKO mice treated with eplerenone 75
Figure 3.5 Eplerenone increased plaque SMC content in DKO mice..... 76
Figure 3.6 Eplerenone increased plaque collagen content in DKO mice 77
Figure 3.7 Eplerenone had no effect on plaque lipid content in DKO mice..... 79
Figure 3.8 Eplerenone reduced plaque macrophage content in DKO mice..... 80
Figure 3.9 Eplerenone improved plaque stability in DKO mice..... 82
Figure 4.1 Atherosclerotic burden is increased in DKO brachiocephalic arteries..... 96
Figure 4.2 Total plasma cholesterol levels were comparable in Apoe$^{-/-}$ and DKO mice..... 99
Figure 4.3 Smooth muscle cell content is not altered in brachiocephalic plaques from DKO mice 100
Figure 4.4 Collagen content is reduced in DKO plaques..... 102
Figure 4.5 Lipid content is increased in DKO plaques 103
Figure 4.6 Macrophage content is increased in DKO plaques..... 104
Figure 4.7 Effect of 11β-HSD2 inactivation on the stability of plaques..... 106
Figure 5.1 Loss of 11β-HSD2 activity has no effect on endothelial expression of ICAM-1 121
Figure 5.2 Loss of 11β-HSD2 activity increases endothelial expression of VCAM-1 122

Figure 5.3 11β-HSD2 inactivation has no effect on sVCAM-1 levels in plasma ... 124
Figure 6.1 VCAM-1 is induced following MR activation in MAECs 139
Figure 6.2 ICAM-1 is not regulated by MR-mediated mechanisms in MAECs 141
Figure 6.3 MCP-1 secretion is not affected by MR activation in MAECs 142
Figure 6.4 Activation of MR in MAECs activates the NF-κB pathway 144
Figure 7.1 Mechanisms of atherogenesis in DKO mice 158

List of Tables

Chapter 2

Table 2.1 Immunohistochemical Staining Conditions 52
Table 2.2 Odyssey Scan Parameters 64

Chapter 3

Table 3.1 Compensatory remodelling maintains luminal area of brachiocephalic arteries 73

Chapter 4

Table 4.1 Morphometric analysis of brachiocephalic arteries reveals maintenance of lumen in DKO mice 97

Chapter 1
Introduction

Cardiovascular disease (CVD) is highly prevalent in the western world and is the leading cause of death and disability in the UK (responsible for a third of all deaths in 2006), with around 2.5 million people living with coronary heart disease. It is well established that atherosclerosis, an inflammatory response to chronic injury in the blood vessel wall, is central to the pathogenesis of CVD. Yet, the initiating events that lead to leukocyte accumulation and fat deposition within the arterial wall remain poorly defined, partly because atherogenesis in humans occurs silently over many years, making it particularly challenging to study. Blockade of the mineralocorticoid receptor (MR) in patients has revealed an important role for adrenal steroids (mineralocorticoids and glucocorticoids) in the exacerbation of cardiovascular pathologies. The demonstration that glucocorticoid access to the MR is regulated by pre-receptor metabolism in target tissues makes it increasingly important to clarify the roles of the metabolising enzyme, 11β-Hydroxysteroid Dehydrogenase 2 (11β-HSD2), in regulation of MR-mediated pathogenesis. This will improve our understanding of both the role of inappropriate MR activation in regulation of atherosclerosis, and the therapeutic potential of manipulating steroid hormone activity for the treatment of cardiovascular disease.

1.1 Atherosclerosis

Around a half of all cardiovascular deaths in the UK are caused by coronary heart disease (CHD) and, due to the rapid increase in the incidence of cardiovascular risk factors such as obesity and diabetes, this trend may worsen. CHD is caused by the formation of atherosclerotic lesions in the coronary circulation. In order to understand the vascular processes involved in atherogenesis, it is necessary to first consider the structure of the healthy arterial wall and the functions of its component layers.

1.1.1 The normal arterial wall: Structure and function

The healthy arterial wall consists of three distinct layers (Figure 1.1), each of which is described below.

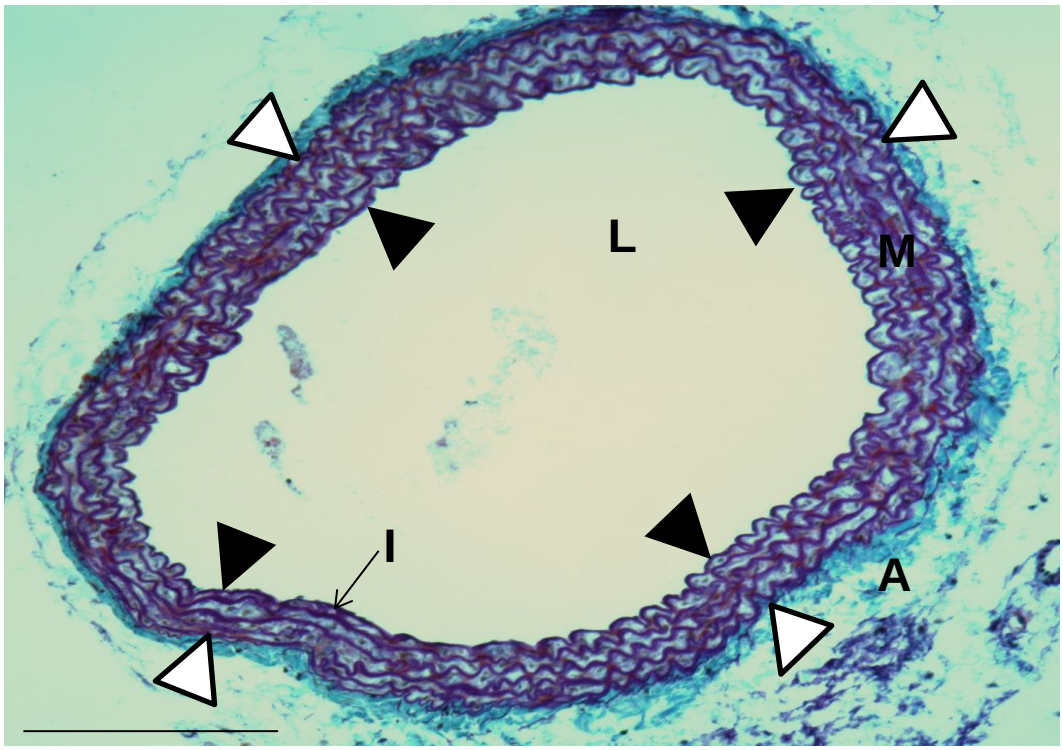

Figure 1.1 Structure of the arterial wall

Transverse section of a wild type mouse brachiocephalic artery stained with United States trichrome (UST) histological stain (elastin, purple; collagen, blue/green; smooth muscle, pink). The tunica adventitia (A) lies outside of the external elastic lamina (EEL, marked by white arrow heads), while the tunica media (M) lies between the EEL and internal elastic lamina (IEL, marked by black arrow heads). The tunica intima (I) consists of only a monolayer of endothelial cells lining the surface of the lumen (L).

1.1.1.1 Tunica intima

This is the innermost layer of the arterial wall, which lines the vascular lumen, and it predominantly consists of a monolayer of endothelial cells sat upon on a basement membrane in mice. In humans, proteoglycans and smooth muscle cells are also found in this layer (Stary, 1989). The internal elastic lamina (IEL) separates the intima from the medial layer. Thickening of the intima occurs during normal development and aging (Velican *et al.*, 1976) and is a common feature of early atherosclerosis (Guyton *et al.*, 1993). The endothelial cells are vital to normal vascular function and it is believed that dysfunction of these cells is an initiating factor in atherogenesis (Moore *et al.*, 1978). Endothelial cells are crucial to the regulation of vascular tone, as they can release a variety of vasodilators (e.g. nitric oxide (N0) (Furchgott *et al.*, 1980; Ignarro *et al.*, 1987) and vasoconstrictors (e.g. endothelin-1) (Masaki, 1989). In addition, the endothelium acts as a barrier between the blood and pro-thrombotic components of the vascular wall, and is an important modulator of inflammation and new blood vessel growth (Levick, 2003).

1.1.1.2 Tunica media

The middle layer of the vessel wall consists of vascular smooth muscle cells (VSMCs) along with extracellular matrix (ECM) proteins. Medial VSMCs are responsible for regulating luminal diameter, and hence blood flow and pressure. They do this by responding to stimulation by blood-borne signals, factors released by the endothelium and neurotransmitters released from nerve endings. Healthy VSMCs display a contractile phenotype whilst differentiation towards a 'synthetic' phenotype is characteristic of vascular pathologies and remodelling (Rensen *et al.*, 2007). The ECM consists of concentric sheets of elastin that enable the vessel to expand and recoil, in order to accommodate blood ejected from the heart (Levick 2003). The ECM also contains collagen, which is important in the maintenance of vessel shape and integrity, and prevents over-expansion of the artery wall (Levick 2003).

1.1.1.3 Tunica adventitia

The outermost layer of the vessel wall is separated from the media by the external elastic lamina (EEL). It consists of connective tissue, VSMCs, fibroblasts and

macrophages. The adventitia can also contain nerve cells and small blood vessels (vasa vasorum), which supply the vessel wall with nutrients (Levick 2003). The adventitia gives the blood vessel stability and strength, and physically connects it to surrounding tissues. In addition to this, the adventitia can also regulate vascular structure and function, e.g. NO can be released from the adventitia via the action of inducible nitric oxide synthase (iNOS) (Muller *et al.*, 2000) and neuronal nitric oxide synthase (nNOS) (Pluta, 2006). The adventitia may also influence vascular remodelling, as it has been proposed that proliferation and migration of adventitial fibroblasts contributes to the development of atherosclerotic lesions (Xu *et al.* 2007).

1.1.2 Pathogenesis of atherosclerosis

Atherosclerosis is the thickening of an artery wall due to the presence of an atheromatous plaque and it is primarily a disease of the large and medium-sized arteries. Atherosclerosis is characterised by the accumulation of lipids and fibrous material within the arterial wall. Development of atherosclerotic plaques usually occurs silently, with their presence only being noticed upon display of clinical symptoms associated with interruption of the blood supply. For example, arterial occlusion in the coronary circulation results in loss of blood supply to the myocardium, which can produce angina or myocardial infarction, the hallmarks of CHD. Whilst luminal narrowing is clearly a detrimental feature of atherosclerosis, the current opinion is that rupture of unstable plaques, leading to acute thrombosis, is the most clinically significant consequence of atherosclerosis (Davies *et al.*, 1984; Falk, 1983; Horie *et al.*, 1978).

Atherosclerotic plaques are classically described on the basis of pathological studies (Badimon *et al.*, 1993; Stary, 1989; Wissler, 1992) and are usually divided into three main types of lesion (Ross *et al.*, 1976a; Ross *et al.*, 1976b): the fatty streak, the fibrous plaque and the complicated lesion, representing initial, progressive and final complicated stages of atherosclerosis.

1.1.2.1 Initiation of atherosclerosis

Due to their complexity, the initiating events of atherosclerosis are not fully understood, although it is widely accepted that lesion development begins as an excessive wound-healing response to injury in the blood vessel wall (Ross, 1999;

Ross, 1986; Ross, 1993). This hypothesis proposes that atherogenesis occurs in response to injury induced by local formation of vasculotoxic factors after exposure to risk factors for atherosclerosis, including cigarette smoking, diabetes mellitus, hyperlipidemia and hypertension. Initially, damage to the endothelium stimulates an inflammatory response, partially a reaction to the incorporation of cholesterol into the vascular wall, leading to fatty streak formation.

The incorporated cholesterol is bound by the low density lipoprotein (LDL) complex and is subject to oxidation in the vessel wall, a process that confers pro-inflammatory and pro-atherogenic properties upon the modified complex (Glass *et al.*, 2001). In response to these inflammatory stimuli the overlying endothelial cells express a variety of adhesion molecules that aid the recruitment and uptake of leukocytes into the vessel wall. P-selectin mediates the rolling of leukocytes (Carlos *et al.*, 1994) whilst the tethering of these inflammatory cells to the vessel wall is mediated by vascular cell adhesion molecule 1 (VCAM-1) (Carlos *et al.*, 1994; Cybulsky *et al.*, 2001). Subsequently, chemoattractant molecules, such as monocyte chemoattractant protein 1 (MCP-1), stimulate the entry of these bound leukocytes into the intimal space via platelet-endothelial cell adhesion molecule 1 (PECAM-1) (Carlos *et al.*, 1994). The incorporated leukocytes, along with oxidised LDL, can induce further endothelial expression of MCP-1, which acts in a self-propagating fashion to stimulate the further uptake of more inflammatory cells (Gu *et al.*, 1998). Within the intima, macrophage colony stimulating factor (M-CSF) instigates the differentiation of migrating monocytes into macrophages (Smith *et al.*, 1995) and these cells express the scavenger receptors via which oxLDL is taken up (Yamada *et al.*, 1998). Macrophage accumulation of cholesterol in this way gives rise to lipid-laden foam cells that are characteristic of fatty streaks (Brown *et al.*, 1983). Activated plaque macrophages and T cells express a variety of cytokines, such as interferon γ (IFNγ), tumour necrosis factor α and β (TNFα/ β), and interleukin-1 (IL-1), that recruit and activate further leukocytes, and stimulate endothelial cells and VSMCs to produce additional inflammatory mediators (Libby, 2008b). These processes lead to the reversible formation of a fatty streak, containing lipid and leukocytes. However, with continued exposure to risk factors for atherosclerosis, this inflammatory response will continue and atherogenesis progresses indefinitely.

1.1.2.2 Progression to fibrous plaque

Immigration of medial smooth muscle cells into the intimal space symbolises the progression from the relatively innocuous fatty streak to the fibrous plaque. Continued injury and inflammation produces a cascade of proliferative and chemotactic factors that promote activation of VSMCs, and their migration to, and proliferation in, the intima. This results in the development of a fibrous plaque with a smooth muscle cell-rich cap. VSMCs within the developing plaque change phenotype from a 'contractile' state into a 'synthetic' state and secrete ECM components, which contribute to cap formation (Chamley-Campbell *et al.*, 1981). It is thought that SMCs are the major cellular source of collagen in plaques (Rekhter, 1999) and that collagen deposition is required for SMC migration (Rocnik *et al.*, 1998), illustrating the inter-dependent and self-propagating nature of atherogenesis. Intimal SMCs also take up modified lipoproteins, thereby contributing to foam cell formation (Glass *et al.*, 2001).

1.1.2.3 The complicated lesion

Further expansion and development of the fibrous plaque results in the formation of a complicated lesion with characteristic necrosis, calcification, thinning of the fibrous cap and protrusion into the lumen (Wissler 1992). Continuation of the inflammatory response increases the numbers of macrophages and T lymphocytes in the lesion, augmenting the release of degradative enzymes, cytokines, and growth factors (Ross 1999). In turn, these inflammatory cytokines, such as IFNγ, can induce macrophage apoptosis, contributing to the development of the necrotic core (Inagaki *et al.*, 2002). The lesion continues to increase in size and becomes structurally modified, with the fibrous cap covering a core of lipid and necrotic tissue.

These advanced lesions may be subject to silent, non-occlusive episodes of plaque rupture and thrombosis (Weissberg 2000), resulting in platelet adhesion and activation, platelet derived growth factor (PDGF) release and thrombin formation. Further VSMC recruitment, proliferation and ECM synthesis ensues (Libby, 2008a) , and thus the formation of a new fibrous cap over the thrombus occurs. In this way, atherosclerotic plaques can grow periodically due to repeated episodes of rupture and repair (Weissberg 2000).

As mentioned above, many clinical consequences of atherosclerosis are the result of plaque rupture and occlusive thrombosis (Libby *et al.*, 1995). Thrombosis occurs when the contents of an atherosclerotic plaque come into direct contact with circulating clotting factors. Tissue factor, the main mediator of thrombosis in atheroma, is produced by macrophages in response to stimulation by T cell-derived CD40 (Mach *et al.* 1997), and also by endothelial cells (Bevilacqua *et al.* 1984) and VSMCs (Schecter *et al.* 1997) exposed to inflammatory cytokines. This reinforces the proposed link between inflammation and thrombosis in atherosclerosis (Libby & Simon 2001). Thrombotic clots can produce sudden occlusion of the vascular lumen, resulting in the clinical sequalae associated with atherosclerotic disease, i.e. myocardial infarction or stroke.

1.1.3 Plaque stability

It is now widely accepted that plaque rupture is the main mechanism that precipitates the thrombotic events prerequisite to clinical symptoms in atherosclerosis (Weissberg 2000) . In this model, plaque stability is not determined by size or degree of luminal obstruction, but by its composition. The homogeneity of plaque development throughout the vasculature, and indeed across species, might mask the fact that plaques are not all uniform in their characteristics. Two major morphological classifications exist; stenotic and non-stenotic. A smaller lipid core and thick fibrous cap, indicating stability, are typical of stenotic plaques (Libby *et al.*, 2005). Due to lack of compensatory vascular enlargement these plaques encroach on the lumen, eventually resulting in ischaemic damage. Non-stenotic lesions are so-called because positive vascular remodelling maintains luminal diameter. These plaques are often characterised by large necrotic cores and thin fibrous caps, rendering them vulnerable to rupture (Libby *et al.*, 2005).

Plaque ruptures associated with acute myocardial infarction generally occur at the shoulder regions of the plaque and are more likely to occur in lesions with thin fibrous caps, a high concentration of lipid-filled macrophages, and large necrotic cores (Davies *et al.*, 1993; Lee *et al.*, 1997). Collagen provides much of the biomechanical strength of the fibrous cap, and plaques with a thick cap are more able to resist local mechanical stresses created by blood flow (Libby 2000). Thus, a low plaque collagen content is associated with reduced strength and therefore a less

stable plaque. It is also thought that a lack of VSMCs, particularly at the shoulder regions of a plaque, can contribute to instability (Lendon *et al.* 1991; van der Wal *et al.* 1994). The susceptibility of plaque shoulder regions to rupture is increased when inflammatory cell content is high in these areas (Davies 1996). Macrophages are generally the most populous inflammatory cell type found in atherosclerotic plaques and the formation of macrophage-derived foam cells, via uptake of plaque lipids, is associated with necrosis and plaque vulnerability. A large lipid core is a key feature of unstable plaques (Glass *et al.*, 2001) as it consists of soft gruel like material that lacks mechanical strength, increasing the stress exerted on the fibrous cap (Lee *et al.*, 1997). It has been suggested that the presence of buried fibrous caps in a plaque indicate instability as they are thought to represent previous plaque ruptures (Williams *et al.*, 2002). Overall, a vulnerable plaque might be described as having a low collagen and smooth muscle cell content and a high content of macrophages and lipids.

Plaque stability can be reduced in several ways. Inflammatory cytokines have wide ranging effects including increasing the expression of matrix metalloproteinase (MMP) enzymes in macrophages and VSMCs, which degrade collagen in the cap (Galis *et al.* 1994a) and inducing apoptosis in VSMCs (Geng *et al.* 1996). Activated macrophages can induce VSMC apoptosis by direct cell-cell contact (Boyle *et al.*, 2001a). In addition to enzymic decomposition there is evidence for inhibition of ECM protein synthesis by intraplaque cytokines liberated from activated T-cells (Amento *et al.*, 1991), such as IFN-γ. This mechanism is thought to have particular impact on lesion stability as T-cells accumulate at the rupture-prone shoulder regions of the plaque (van der Wal *et al.*, 1994). In this way inflammation clearly plays an active role in mediating plaque stability.

1.1.4 Animal models of atherosclerosis

The slow and silent development of atherosclerosis makes investigation of lesion development in humans extremely difficult. Indeed, information on lesion pathology obtained from post-mortem and atherectomy specimens provides only a ‘snapshot’ in the life of a plaque. Vascular imaging techniques (e.g. angiography, intra-vascular ultrasound, and magnetic resonance imaging (MRI)) can provide information on luminal narrowing and lesion size, but give little or no information on the molecular,

biochemical and cellular events involved in lesion formation. These obstacles to clinical investigations into the pathogenesis of atherosclerosis have resulted in much of our knowledge of these processes being gained from animal models.

1.1.4.1 Common models of atherosclerosis

There is no ideal animal model that completely replicates the stages of human atherosclerosis, but cholesterol feeding and mechanical endothelial injury are two common features shared by most animal models of atherosclerosis. Species used in experimental models of lesion formation can be broadly divided into large animals, such as the pig, dog and non-human primate, and small animals, including the rabbit, rat and mouse (Mehta *et al.*, 1996; Narayanaswamy *et al.*, 2000). Small animals are increasingly favoured as they are readily available, cost relatively little, are easy to handle and their small size reduces the amount of drug needed for intervention studies. Also, the rapid growth of lesions in small animals allows a quick assessment of atherogenesis, and it is possible to include large numbers in each group for more powerful statistical analysis.

The cholesterol-fed rabbit, first described by Anichkov in 1913 (Finking *et al.*, 1997) is a widely used model as it develops severe hypercholesterolemia and accumulates lipid and macrophages in the intima of the aortic arch and thoracic aorta (Dhanya *et al.*, 2008). Also, Watanabe heritable hyperlipidemic rabbits, which are massively hyperlipidemic due to a single genetic defect, develop spontaneous atherosclerotic lesions without the need for cholesterol feeding (Watanabe, 1980). However, the lesions that form in rabbits rarely advance beyond the fatty streak stage (Prior *et al.*, 1961), and so only replicate the early stages of atherosclerosis. In addition, rats and mice do not even develop these early lesions of atherosclerosis when fed a high-fat diet (Wissler *et al.*, 1968), as a result of differences in lipid handling compared with humans (Paigen *et al.*, 1994). Despite this, murine models of atherosclerosis have provided valuable information about the processes that lead to lesion formation and progression (Smith *et al.*, 1997). This stems from the generation of mice harbouring disruptions in genes involved in lipoprotein metabolism/cholesterol transport. Transgenic techniques have been used to generate mice that are prone to the development of atherosclerosis, such as the low density lipoprotein (LDL) receptor

and Apolipoprotein E (ApoE) knockout mice (Breslow, 1993). Furthermore, these techniques make it possible to assess lesion development in animals with transgenic deletion of key factors involved in atherogenesis, allowing the molecular mechanisms involved in lesion formation to be investigated at a genetic level.

1.1.4.2 The *Apoe*$^{-/-}$ mouse model of atherosclerosis

Apolipoprotein E (ApoE) is a glycoprotein synthesized mainly in the liver and brain, and it is a constituent of all lipoprotein complexes except low-density lipoproteins (LDL). It serves as a ligand for receptor-mediated removal of chylomicrons and very low density lipoproteins (VLDL) from the blood. Consequently, mice lacking ApoE (*Apoe*$^{-/-}$) develop hypercholesterolemia and atherosclerotic lesions (Plump *et al.*, 1992; Zhang *et al.*, 1992) which are morphologically similar to human lesions and occur at similar sites in the vasculature (Nakashima *et al.*, 1994; Reddick *et al.*, 1994; VanderLaan *et al.*, 2004). Indeed, advanced lesions in the brachiocephalic artery characteristic of vulnerable plaques found in humans have been reported (Rosenfeld *et al.*, 2000), indicating the clinical significance of this model. However, there is controversy as to whether or not plaque rupture, the cause of clinical symptoms in humans, occurs in *Apoe*$^{-/-}$ mice. One study reported that plaque rupture in atherosclerosis prone mice is rare, restricted to older animals, and is not augmented by a high fat diet (Calara *et al.*, 2001) whereas a more recent study demonstrated signs of rupture; including buried fibrous caps, intraplaque haemorrhage, and breaks in the fibrous cap; in brachiocephalic plaques from fat-fed *Apoe*$^{-/-}$ mice (Johnson *et al.*, 2005). Nonetheless, despite the controversy over the clinical relevance of the atherosclerosis in *Apoe*$^{-/-}$ mice, this mouse remains the most widely used model for investigations of atherosclerotic disease.

1.1.4.3 Double knockout models on the *Apoe*$^{-/-}$ background

The generation of double knockout (DKO) mouse models has allowed investigations of the effects of other genes on atherosclerosis. The majority of available models have studied genes that are thought to be pro-atherogenic and so the atherosclerotic burden is reduced in the DKO mice. For example it was reported that knockout of ICAM-1 (Bourdillon *et al.*, 2000), iNOS (Ponnuswamy *et al.*, 2009), PECAM-1 (Stevens *et al.*, 2008), angiotensin II type 1 receptor (AT1) (Eto *et al.*, 2008), the

receptor for advanced glycation end products (RAGE) (Soro-Paavonen *et al.*, 2008), and cyclooxygenase 1 (COX 1) (McClelland *et al.*, 2009) on the *Apoe*$^{-/-}$ background all decreased atherogenesis compared to single *Apoe*$^{-/-}$ mice. These studies are important as they reveal possible targets in the treatment of atherosclerosis and confirm the roles of inflammatory and oxidative pathways in atherogenesis. On the other hand, there are fewer investigations into possible 'athero-protective' genes, which could be important in determining individual susceptibility to atherosclerotic disease. It was found that knockout of apelin (Kojima *et al.*, 2008) and the urotensin II receptor (Bousette *et al.*, 2009) on the *Apoe*$^{-/-}$ background resulted in exacerbation of atherosclerosis. These studies suggest that novel therapeutic strategies to enhance the availability of certain factors may be worth investigating. Overall, DKO mice not only aid the study of the roles of specific gene products in atherosclerosis but they also demonstrate the contributions of distinct phenotypes (e.g. hypercholesterolemia and hypertension or oxidative stress) to atherogenesis.

1.2 Adrenal steroids

Glucocorticoids (cortisol in man and corticosterone in rodents) and mineralocorticoids (aldosterone) are steroid hormones synthesised from cholesterol in the adrenal cortex, and released from the adrenal gland into the systemic circulation. These steroids share the initial part of their biosynthetic pathway with the last step mediated by either aldosterone synthase (for aldosterone) or 11β-hydroxylase (for corticosterone). These enzymes are differentially expressed within the adrenal cortex with aldosterone synthase present in the zona glomerulosa (Williams *et al.*, 2003) and 11β-hydroxylase found in the zona reticularis (Borkowski *et al.*, 1972).

1.2.1 Physiological actions of steroid hormones

1.2.1.1 Glucocorticoids

Glucocorticoids exert a host of wide-ranging effects throughout the central and systemic body systems, and regulate a number of important metabolic and

homeostatic processes. One of the most important physiological roles of glucocorticoids is thought to be during the stress response (Munck *et al.*, 1984), during which increased levels act to alter metabolism to increase blood glucose levels, preparing the body for the 'fight or flight' response. Glucocorticoids play a major role in metabolism, particularly in organs such as the liver, adipose tissue, and muscle, where they enhance the conversion of stored energy (in glycogen, triglycerides and protein) into fuel (glucose, free fatty acids and amino acids) (Dallman *et al.*, 1993). The anti-inflammatory properties of glucocorticoids are well characterised and endogenous glucocorticoids can regulate both the adaptive and innate immune systems (Franchimont *et al.*, 2002). Glucocorticoids are known to modulate the physiology of blood vessels, inflammatory cells and mediators of inflammatory responses (Barnes *et al.*, 1993) such that their anti-inflammatory properties are pleiotropic in nature. They ultimately alter the recruitment of immune cells, such as neutrophils and monocytes, to the site of inflammation and also decrease the activation and proliferation of leukocytes (Barnes *et al.*, 1993). Glucocorticoids also display diverse effects on the cardiovascular system, with cardiac, renal and vascular actions documented. Glucocorticoids can regulate the contractility of the heart such that cardiac output is altered (Ishikawa *et al.*, 1984; Krosch *et al.*, 1977) and they also regulate fluid and electrolyte balance by increasing renal sodium retention and plasma volume expansion by the kidney (Montrella-Waybill *et al.*, 1991). Glucocorticoids also have direct effects on vascular tone through modulation of the sensitivity of the vessel wall to vasoconstrictors and vasodilators (Ullian, 1999).

1.2.1.2 Mineralocorticoids

Much of our knowledge of the physiological actions of aldosterone has come from investigations of pathologies arising from dysfunction of aldosterone synthesis and activity. The finding that hyperaldosteronism resulting from an adrenal tumor in Conn's syndrome presented with hypertension and hypokalaemia (Conn, 1955) defined a clear role for aldosterone in regulation of electrolyte balance and blood pressure homeostasis. The classical actions of aldosterone are on the kidney where it acts on the principal cells of the distal tubule and the collecting duct to increase the permeability of the apical membrane such that potassium is secreted into the urine

whilst sodium is reabsorbed into the blood stream (Williams *et al.*, 2003). Aldosterone increases sodium transport through its stimulatory actions on the synthesis of the epithelial sodium channel (ENaC) (Rossier, 1997). Water is reabsorbed along with sodium due to changes in fluid osmolarity thereby increasing blood volume and hence blood pressure. Aldosterone also plays a role in acid/base balance through stimulation of H^+ secretion by intercalated cells of the renal collecting duct, regulating plasma bicarbonate levels (Wagner *et al.*, 2009). In addition to this, aldosterone acts on the posterior pituitary gland in the central nervous system to stimulate the release of anti-diuretic hormone which, in turn, promotes conservation of water by direct actions on tubular reabsorption. In addition to these classical mineralocorticoid effects, it is now widely recognised that aldosterone has important actions in non-epithelial tissues. It has been shown that aldosterone in combination with excess sodium can regulate inflammation and fibrosis in the cardiovascular system (Brilla *et al.*, 1992; Rocha *et al.*, 1998; Rocha *et al.*, 2002a). These pathological consequences of aldosterone action are introduced later in section 1.3.

1.2.2 Regulation of steroid action

Due to their varied and vital physiological functions throughout the body, the actions of steroid hormones are subject to regulation on several levels.

1.2.2.1 Aldosterone

Aldosterone is stimulated by several factors, which generally alter the activity of one or both of the two major steps involved in its biosynthetic pathway (Aguilera *et al.*, 1982; Albano *et al.*, 1974; Balla *et al.*, 1985; Boyd *et al.*, 1971). The renin-angiotensin system (RAS) is a major regulator of aldosterone secretion. When blood volume is low, the kidney secretes renin which stimulates the conversion of angiotensinogen to angiotensin I, which in turn is converted into the main bioactive effector of the RAS, angiotensin II (Ang II) by angiotensin converting enzyme (ACE) (Paul *et al.*, 2006). Within the adrenal cortex, Ang II acts upon the membrane bound angiotensin 1 (AT_1) receptor (Ouali *et al.*, 1993) to activate protein kinase C (PKC) and raise intracellular calcium levels (Capponi *et al.*, 1984), thereby stimulating the enzymes involved in aldosterone synthesis. Potassium plays a key

role in regulating aldosterone production (Quinn *et al.*, 1988), with increased plasma levels stimulating adrenal glomerulosa cells to secrete aldosterone. Potassium depolarises the plasma membrane leading to activation of voltage-dependent calcium channels (Quinn *et al.*, 1987) and, reminiscent of Ang II action, the resultant increased intracellular calcium levels activates aldosterone synthetic enzymes (Kojima *et al.*, 1985a). This activation of aldosterone secretion by increased potassium is a very important mechanism as aldosterone then acts to return potassium to physiological levels. It is thought that Ang II and potassium act synergistically to stimulate aldosterone secretion as it has been shown that the potassium feedback is inoperative in the absence of Ang II (Pratt, 1982). Whilst not as potent a regulator as potassium, sodium also has a role in aldosterone production (Quinn *et al.*, 1988). Reduced plasma sodium levels, as detected by osmotic pressure sensors (Schneider *et al.*, 1985), stimulate aldosterone secretion with the aim of increasing reabsorption of sodium in the kidney. A further level of regulation is exerted by factors secreted from the pituitary gland in the central nervous system; including adrenocorticotrophic hormone (ACTH), melanocyte stimulating hormone (MSH), and β-endorphins (Quinn *et al.*, 1988). Of these factors, ACTH is the most potent aldosterone secretagogue but it only plays a minor role in the overall regulation of aldosterone secretion (Quinn *et al.*, 1988). Membrane bound G-protein coupled receptors on adrenal cells allow ACTH to activate intracellular pathways that ultimately result in increased calcium levels and stimulation of aldosterone production (Fujita *et al.*, 1979; Kojima *et al.*, 1985b). Finally, sympathetic nervous system drive to the adrenals is known to regulate aldosterone secretion via β-adrenergic receptors (Cugini *et al.*, 1980). Indeed, long term treatment with β receptor blocking drugs associates with decreased plasma Ang II and aldosterone levels, a partial mechanism through which these drugs may reduce blood pressure (Karlberg, 1983).

1.2.2.2 Glucocorticoids

The hypothalamic-pituitary-adrenal (HPA) axis controls the release of glucocorticoids from the adrenal glands. Basal release of glucocorticoids shows a normal diurnal variation, with peak concentrations at the beginning of the active period (Lommer *et al.*, 1976). Glucocorticoid release can also be stimulated by

physiological stimuli such as stress, injury, or infection, which increase the secretion of corticotrophin-releasing hormone (CRH). CRH is released from the hypothalamus (Vale *et al.*, 1981) and acts to stimulate CRH receptors in the anterior pituitary, resulting in the secretion of ACTH into the systemic circulation (Horrocks *et al.*, 1990). As mentioned in the previous section, ACTH stimulates adrenal cells to synthesise steroids, a reaction catalysed by members of the cytochrome P450 oxidative enzyme family, finally resulting in glucocorticoid secretion. Glucocorticoids exert a negative feedback effect on the HPA axis, at the level of both the hypothalamus and the pituitary, thereby regulating their own release in order to maintain physiological plasma levels (De Kloet, 1991). The bioavailability of plasma glucocorticoids for uptake across cell membranes is regulated by glucocorticoid binding proteins. In the circulation, glucocorticoids are predominantly bound to corticosteroid-binding globulin (CBG) and albumin, and in this way only a small fraction of glucocorticoids are free in the plasma to enter cells (Breuner *et al.*, 2002; Westphal, 1971). Inside the cell, glucocorticoids can bind to and activate both the glucocorticoid receptor (GR) and the mineralocorticoid receptor (MR), which are discussed in detail in the next section (1.2.3). Glucocorticoids exert most of their physiological effects through GR, which are ubiquitously expressed. However, it has been demonstrated that expression levels vary between and within tissues (Reul *et al.*, 1985; Reul *et al.*, 1989), providing a means of tissue-specific sensitivity to glucocorticoids.

1.2.3 Steroid hormone receptors

Steroid hormone receptors are members of the nuclear hormone receptor super family of ligand-activated transcription factors which reside in the cell cytoplasm (Parker, 1993). Aldosterone solely activates the MR whilst glucocorticoids can activate both the GR and the MR (Arriza *et al.*, 1987), however, glucocorticoids predominantly activate the GR due to enzyme-mediated protection of MR from glucocorticoid access in aldosterone target tissues (discussed in detail in the next section, 1.2.4). Whilst GR are ubiquitously expressed throughout the body, receptor density varies considerably between tissues with particularly high expression found in metabolic organs such as the liver, adipose tissue and skeletal muscle (Seckl *et al.*, 2004). In contrast, the expressional pattern of MR is largely restricted to aldosterone

target tissues, including the kidney, gut, and sweat glands, and to some areas of the central nervous system (CNS) and cardiovascular system (Funder, 2005a). Within the cytosol, both MR and GR are complexed with heat shock proteins which maintain the receptors in an inactive state with high affinity for ligands (Funder, 1997). Upon ligand binding, the hormone-receptor complexes dissociate from these chaperone proteins, exposing nuclear localisation signals in the receptors. They are then thought to form homodimers and translocate to the nucleus where the receptors bind specific deoxyribonucleic acid (DNA) sequences through interaction with their DNA binding domains (Funder, 1997). MR and GR DNA binding sequences are called mineralocorticoid-responsive elements (MRE) and glucocorticoid-responsive elements (GRE) respectively. Upon binding of receptors to response elements, transcription or repression of target genes is initiated and the overall effect on gene transcription is dependent upon interaction of the receptor-hormone complex with specific sets of co-activator and co-repressor proteins as well as with other transcription factors (Funder, 1997).

1.2.4 Tissue specific metabolism

The peripheral metabolism of glucocorticoids, resulting in conversion of active steroid into inactive metabolites, provides a means of clearing these hormones from the circulation and, hence, adds another level of control to glucocorticoid activity. Metabolism of glucocorticoids (Figure 1.2) occurs mainly in the liver and the resultant metabolites are then excreted by the kidney. Inter-conversion of corticosterone with its inactive 11-keto metabolite 11-dehydrocorticosterone is catalyzed by the two isozymes of 11β-hydroxysteroid dehydrogenase (11β-HSD1 and 2).

1.2.4.1 The 11β-hydroxysteroid dehydrogenase enzymes

The 11β-HSDs are microsomal enzymes of the short-chain alcohol dehydrogenase super family (Stewart *et al.*, 1999). The inter-conversion of active glucocorticoids with their inert 11-keto forms by 11β-HSD was first described over fifty years ago (Amelung *et al.*, 1953), but its significance has only become apparent more recently. Subsequent studies have identified two isozymes of 11β-HSD with different tissue distributions and physiological roles. The first isozyme (11β-HSD1) to be cloned

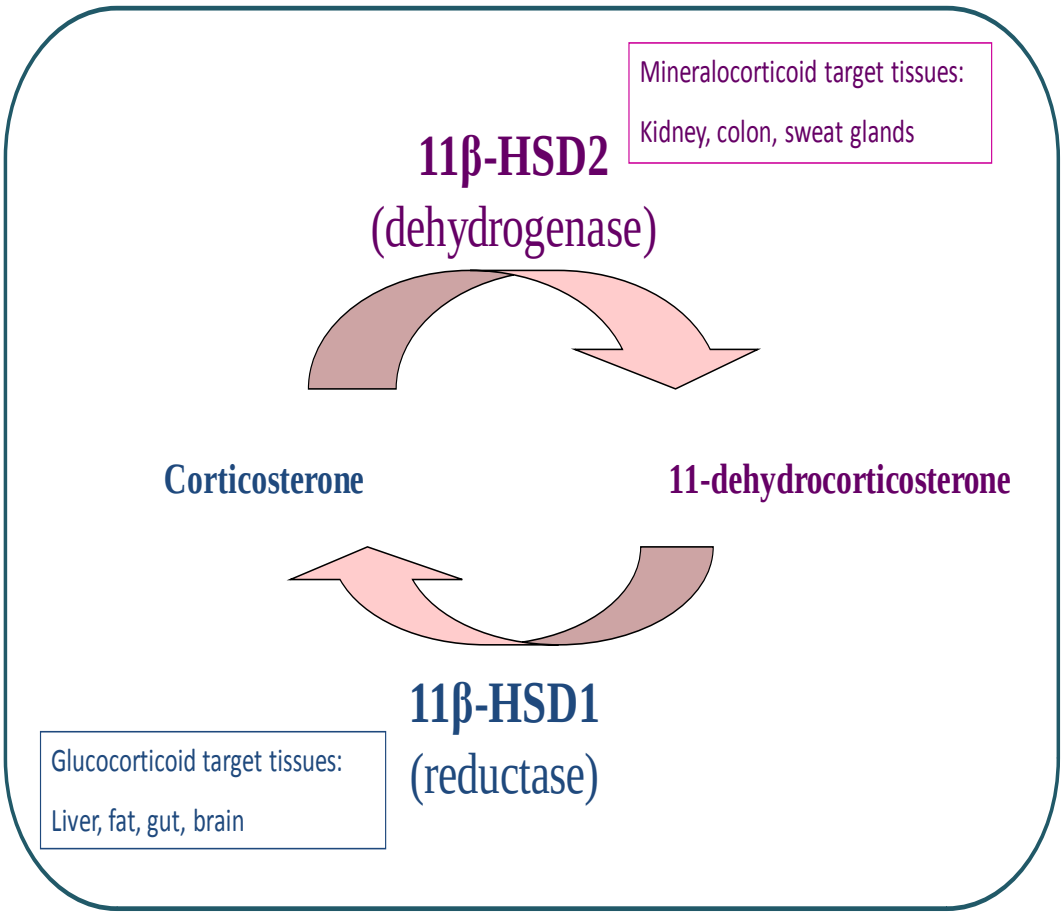

Figure 1.2 Metabolism of Glucocorticoids

This pathway involves the inter-conversion of active (corticosterone) and inactive (11-dehydrocorticosterone) hormone by the isozymes of 11β-hydroxysteroid dehydrogenase (11β-HSD). Local glucocorticoid action is amplified in target tissues by re-generation of active glucocorticoid by 11β-HSD1. In mineralocorticoid target tissues, conversion of cortisone into inactive glucocorticoid by 11β-HSD2 confers aldosterone specificity upon the normally unselective MR.

(Agarwal *et al.*, 1989) and purified from liver homogenates had a Km in the μM range for corticosterone (Lakshmi *et al.*, 1988) and was shown to exhibit NADP(H)-dependent reductase activity *in vivo*. The second isozyme (11β-HSD2) of 11β-HSD, with NAD-dependent dehydrogenase activity and a Km for corticosterone in the nM range, was later identified in the aldosterone target cells of the kidney (Mercer *et al.*, 1992; Naray-Fejes-Toth *et al.*, 1991; Stewart *et al.*, 1994a). The functional role of 11β-HSD1 is to provide the GR with corticosterone, in a tissue-specific manner, by locally re-generating active glucocorticoids from inert metabolites (Stewart *et al.*, 1994b). 11β-HSD1 has a wide expression pattern, being found in a variety of glucocorticoid target tissues including the liver, lung, adipose tissue, brain, vascular smooth muscle, skeletal muscle, anterior pituitary, and adrenal cortex (Stewart *et al.*, 1999; Tomlinson *et al.*, 2004). Glucocorticoids are also potent activators of the MR (Arriza *et al.*, 1987), however, despite a several fold molar excess of circulating glucocorticoids compared to mineralocorticoids, MR remains selective for its physiological ligand aldosterone in target cells (Sheppard *et al.*, 1987). This tight control is a consequence of the pre-receptor metabolism of corticosterone, to inactive 11-ketoglucocorticoids, by 11β-HSD2 in mineralocorticoid target tissues such as the kidney. Due to the fact that its 11-OH cyclises with the aldehyde group on C18, aldosterone is not a substrate for this enzyme. This mechanism serves to protect the MR from illicit activation by glucocorticoids, thus conferring aldosterone specificity upon MR. The functional significance of this pre-receptor metabolism of glucocorticoids has subsequently been explored in greater detail, particularly since the generation of mice with selective transgenic disruption of each isozyme (Kotelevtsev *et al.*, 1999; Kotelevtsev *et al.*, 1997).

1.2.4.2 11β-HSD1

In tissues with few MR but abundant GR, 11β-HSD1 reactivates glucocorticoids suggesting that the physiological role of 11β-HSD1 is to amplify local glucocorticoid concentrations in glucocorticoid target tissues (Seckl *et al.*, 2001). It was initially suggested that 11β-HSD1 might be bi-directional, with both dehydrogenase and reductase activities observed *in vitro* (Monder *et al.*, 1989). However, it is now accepted that any dehydrogenase activity of 11β–HSD1 is attributable to release of enzyme from damaged cells in culture, and dissociation from hexose-6-phosphate

dehydrogenase, which maintains the NADP concentrations necessary for reductase activity (Bujalska *et al.*, 2005; Hewitt *et al.*, 2005). In intact cells in liver (Jamieson *et al.*, 1995), adipose tissue (Bujalska *et al.*, 1997), neurones (Rajan *et al.*, 1996) and vascular smooth muscle (Brem *et al.*, 1995), 11β-HSD1 predominantly acts in the reductase direction. These results are supported by studies in 11β-HSD1 deficient mice, which cannot convert 11-dehydrocorticosterone to corticosterone *in vivo* (Kotelevtsev *et al.*, 1997).

1.2.4.3 11β-HSD2

The importance of 11β-HSD2 activity is most convincingly displayed in the 11β-HSD2 knockout mouse, which models the human 'syndrome of apparent mineralocorticoid excess' (SAME) with characteristic hypertension associated with sodium retention, low plasma renin and hypokalemia (Kotelevtsev *et al.*, 1999). Deficiency of 11β-HSD2 in humans and mice results in impaired inactivation of cortisol/corticosterone to cortisone/11-dehydrocorticosterone (Monder *et al.*, 1986; Shackleton CH, 1985; Ulick *et al.*, 1979) and consequent inappropriate binding of glucocorticoids to MR in the kidney. This phenotype can also be recapitulated by ingestion of licorice derivatives, such as glycyrrhetinic acid, which inhibit 11β-HSD2 at the messenger RNA level and therefore allow illicit activation of MR (Whorwood *et al.*, 1993). As well as protecting the MR by reducing the local glucocorticoid concentrations, 11β-HSD2 may also provide an additional level of protection through the generation of inactive 11-dehydrocorticosterone. It has been shown that 11-dehydrocorticosterone can inhibit the binding of aldosterone to the MR (Morris *et al.*, 2009) and the subsequent aldosterone-induced anti-natriuresis (Brem *et al.*, 1993). Perhaps, this inert metabolite can also limit binding of active glucocorticoid to MR.

It is clear that rather than merely representing a clearance mechanism, pre-receptor metabolism by 11β-HSD enzymes in target tissues is an essential component in regulating tissue-specific responses to glucocorticoids (Seckl *et al.*, 2001). Consequently, in addition to its role in rare conditions such as SAME, tissue-specific pre-receptor metabolism of glucocorticoids is now thought to contribute to the

pathogenesis of common conditions such as obesity, insulin resistance, essential hypertension and cardiovascular disease.

1.3 Adrenal steroids and cardiovascular pathologies

It has been known for some time that aldosterone, acting via the MR, in combination with salt is pro-inflammatory and pro-fibrotic in the cardiovascular system with detrimental effects on the heart, blood vessels and the kidney. Despite their potent anti-inflammatory properties, there is emerging evidence to suggest that glucocorticoids may exacerbate inflammatory diseases such as atherosclerosis. This is likely through activation of MR and may help to explain why MR antagonists are beneficial in patients with low aldosterone levels.

1.3.1 Increased glucocorticoids and cardiovascular risk

Given their anti-inflammatory actions, glucocorticoids have been extensively used in the clinic to treat a variety of allergic, inflammatory and autoimmune disorders, including arthritis and asthma. However, it was recently demonstrated in a large case-control study that patients receiving oral glucocorticoids had a 25% higher risk of cardiovascular disease than those receiving non-oral glucocorticoid treatment (Souverein *et al.*, 2004). This study also found that associations between oral glucocorticoids and cardiovascular disease were independent of confounding factors such as smoking and BMI. This suggests that excess circulating glucocorticoids are directly associated with adverse cardiovascular outcomes. Indeed, patients with rheumatoid arthritis have an increased risk of developing cardiovascular disease (White *et al.*, 2006), a connection thought to be associated with the exogenous glucocorticoid treatment employed in this condition (Davis *et al.*, 2005; Morand *et al.*, 2006). In addition to exogenous glucocorticoid pharmacotherapy, there is a well established link between increased levels of endogenous glucocorticoids and cardiovascular disease. The most significant causes of morbidity and mortality in patients with Cushing's syndrome, who have increased systemic glucocorticoid concentrations, are cardiovascular diseases (Ross *et al.*, 1982). Cushing's patients often demonstrate intimal thickening, increased arterial stiffness and a higher incidence of atherosclerotic plaques in the carotid artery (Faggiano *et al.*, 2003). Enhanced activation of the HPA axis, with consequent increases in glucocorticoid

secretion, can also be observed in non-Cushing's patients. This could be caused by programming events during early life (Seckl 2004), leading to cardiovascular and metabolic disorders in adulthood. This form of hypercortisolemia has also been associated with hypertension, hyperglycemia and dyslipidemia in several studies (Walker, 2006b).

There is evidence to suggest that increased tissue sensitivity to glucocorticoids is associated with cardiovascular risk factors (Walker, 2006a; Walker *et al.*, 1998). Individuals vary in their sensitivity to glucocorticoids and sensitivity between tissues within an individual can also vary. Since tissue-specific metabolism is a major regulator of local glucocorticoid activity, it might be proposed that variations in 11β-HSD enzyme activity are involved in altered sensitivity to glucocorticoids. In line with this, central obesity in humans is associated with dysregulation of 11β-HSD1 activity in adipose tissue (Rask *et al.*, 2001) and transgenic mice over-expressing 11β-HSD1 selectively in adipose tissue (Masuzaki *et al.*, 2001) or liver (Paterson *et al.*, 2004) display features of the metabolic syndrome.

Animal and cell culture experiments also support a role for glucocorticoids in atherosclerosis. A study utilising pharmacological inhibition of 11β-HSD1, reported that atherosclerotic plaque formation in *Apoe*$^{-/-}$ mice was significantly decreased by inhibition of intracellular corticosterone activation (Hermanowski-Vosatka *et al.*, 2005). In addition to this, it was found that treatment of human umbilical vein endothelial cells (HUVECs) with the synthetic glucocorticoid dexamethasone resulted in an increase in free radical production and a decrease in nitric oxide (NO) production (Iuchi *et al.*, 2003), implicating a direct pro-atherogenic action of glucocorticoids on cells on the vascular wall.

1.3.2 Vascular steroid action

Systemic effects of glucocorticoids such as obesity, hypertension and dyslipidemia are clearly very important in cardiovascular pathologies, however, there is also evidence that adrenal steroids can act directly upon the vascular wall to alter structure and function (Hadoke *et al.*, 2006).

1.3.2.1 Vascular steroid receptors and metabolism

The ability of steroid hormones to interact with the vascular wall indicates the presence of receptors in cells of the vasculature. Indeed, both GR and MR have been found in freshly isolated vessels (Christy *et al.*, 2003; Kornel *et al.*, 1982) and in cultured VSMCs (Scott *et al.*, 1987) and endothelial cells (Caprio *et al.*, 2008; Golestaneh *et al.*, 2001; Inoue *et al.*, 1999). The finding that blockade of GR with RU38486 inhibited induction of ACE activity in rat aortic endothelial cells (Sugiyama *et al.*, 2005) shows functional activity of vascular GR. Similarly, the functional ability of vascular MR was demonstrated by the finding that antagonism of MR inhibits Ang-II-induced hypertrophy of VSMCs (Hatakeyama *et al.*, 1994) and aldosterone-induced swelling of endothelial cells (Oberleithner *et al.*, 2003).

In addition to receptors, the expression of both 11β-HSD1 and 11β-HSD2 in the vasculature suggests that pre-receptor metabolism of glucocorticoids may influence steroid action within the vessel wall. There is some controversy over the precise cellular localisation of these enzymes. In the mouse aorta 11β-HSD1 is localised to VSMC whilst 11β-HSD2 resides in endothelial cells (Christy *et al.* 2003), however in cultured human and rat cells both isoforms exist in VSMCs (Cai *et al.*, 2001; Hatakeyama *et al.*, 1999) and endothelial cells (Brem *et al.*, 1998; Caprio *et al.*, 2008). Therefore, the cellular distribution of these enzymes may vary between species, and with the anatomical location of the vessel (Hadoke *et al.* 2006).

1.3.2.2 Actions of adrenal steroids on the vascular wall

Whilst many of the cardiovascular actions of aldosterone are attributed to activation of renal MR with consequent changes in electrolyte and blood volume balance, increasing evidence suggests that aldosterone may directly alter the function of the vascular wall through activation of extra-renal MR. A very early study in dogs and rats showed that administration of the mineralocorticoid Deoxycorticosterone acetate (DOCA) induced hypertension, despite the fact that these animals had been bilaterally nephrectomised (Langford *et al.*, 1959). Later studies suggest that this may be due to direct effects of mineralocorticoids on the VSMC MR (Kornel, 1993; Kornel *et al.*, 1993). As well as this, enhancement of vascular contractility by glucocorticoids has been implicated in the development of hypertension (Brem,

2001). Evidence for a direct effect of glucocorticoids on the vascular wall in this comes from the finding that selective GR agonists, such as dexamethasone, increase blood pressure in the absence of an increase in sodium retention or plasma volume (Whitworth, 1992). Possible mechanisms may be associated with the observations that glucocorticoids can reduce the release of vasodilators (e.g. prostaglandins, NO) (Rosenbaum *et al.*, 1986; Whitworth *et al.*, 2002), whilst increasing the release of vasoconstrictors (e.g. angiotensin II, endothelin-1) (Mendelsohn *et al.*, 1982; Morin *et al.*, 1998), from endothelial cells.

Various effects of aldosterone on the endothelium have also been documented (Schiffrin, 2006a). Studies using HUVECs have defined a role for aldosterone in processes associated with endothelial dysfunction such as endothelial cell swelling (Oberleithner *et al.*, 2004), stiffening and vulnerability to shear stress (Oberleithner *et al.*, 2006), and decreased NO production (Oberleithner *et al.*, 2007). A role for aldosterone in vascular oxidative stress has been repeatedly shown (Brown, 2008) and involves activation of NADPH oxidase in endothelial and VSMCs (Callera *et al.*, 2005). Aldosterone has also been shown to enhance VSMC hypertrophy (Duprez *et al.*, 2000) and aortic fibrosis (Benetos *et al.*, 1997), consistent with the known pro-fibrotic actions of aldosterone. In contrast to this, glucocorticoids are known to inhibit smooth muscle cell migration and proliferation as well as inflammation in the vasculature (Hadoke *et al.*, 2009). Glucocorticoids also inhibit angiogenesis via a GR-dependent mechanism (Small *et al.*, 2005). Overall, these studies suggest a negative effect of glucocorticoids and a positive effect of mineralocorticoids on vascular remodelling.

However, caution must be employed when determining the overall effects of glucocorticoids on vascular function. Activation of GR might be expected to protect against the pathogenesis of vascular dysfunction whilst activation of MR by glucocorticoids might mimic the effects of aldosterone, resulting in disease. Whilst the presence of 11β-HSD2 in cells of the vasculature will normally protect MR from illicit activation by glucocorticoids, perhaps under conditions of disease this protective mechanism is overcome.

1.3.3 Activation of MR in cardiovascular pathology

Recently there has been a surge in research aiming to investigate the pathological consequences of MR activation in non-epithelial tissues, such as the heart and vasculature. This has been stimulated by the fact that MR antagonists, administered at doses that do not significantly lower blood pressure, improve survival in patients with heart failure and acute myocardial infarction (Pitt *et al.*, 2001; Pitt *et al.*, 1999), suggesting cardiovascular effects independent of renal control of blood pressure. Much of the knowledge of the detrimental effects of MR activation in CVD stems from studies employing the MR antagonists spironolactone and eplerenone. The beneficial effects of these drugs are undeniable yet the mechanisms by which they produce these effects are largely unknown.

Spironolactone, a competitive aldosterone antagonist, has long been the MR blocking drug of choice for treating patients with heart failure. It is a member of the class of drugs called the potassium sparing diuretics and it competes with aldosterone for occupation of MR in renal distal tubules. However, spironolactone also has affinity for androgen and progesterone receptors and so produces off-target effects with prolonged treatment. Selective aldosterone receptor antagonists (SARA) have been developed which are similar in structure to spironolactone, but are much more selective for the MR (Delyani, 2000). Eplerenone is one of these selective MR blockers and is being preferentially used over spironolactone in an increasing number of studies.

Several studies in humans and rodents have reported detrimental effects of MR activation in cardiovascular pathologies. Mineralocorticoid over-production causes pathophysiological changes in the arterial wall (Wexler *et al.*, 1978) possibly by stimulating production of vasoactive peptides such as angiotensin II (Ang II) or endothelin 1 (ET-1) (Letizia *et al.*, 1996; Rossi *et al.*, 2001), or reducing NO activity (Ikeda *et al.*, 1995; Rajagopalan *et al.*, 2001). Also, another study reported that eplerenone improved endothelial cell function and reduced superoxide production in cholesterol fed rabbits (Rajagopalan *et al.*, 2002). Pro-inflammatory changes in endothelial cells underlie the pathogenesis of atherosclerosis and it has been consistently shown that activation of MR produces an endothelial inflammatory

phenotype. Indeed, a study in human vascular endothelial cells found that aldosterone mediated activation of MR lead to up-regulation of ICAM-1 mRNA and protein (Caprio *et al.*, 2008). Also, MR antagonism in mice with heart failure resulted in reduced expression of ICAM-1 (Kuster *et al.*, 2005). Furthermore, it was recently reported that aldosterone significantly increased VCAM-1 mRNA in HUVECs (Hashikabe *et al.*, 2006) and that MR blockade in aldosterone-treated rats reduced aortic expression of VCAM-1 mRNA (Hirono *et al.*, 2007). These mechanisms could be important in the promotion of CVD since endothelial dysfunction is known to be a crucial initiating event. A recent study demonstrated that administration of aldosterone to *Apoe*$^{-/-}$ mice for 1 month led to accelerated atherogenesis; a mechanism mediated, at least in part, by MR and AT_1 receptors (Keidar *et al.*, 2004). Furthermore, eplerenone significantly reduced atherosclerosis in mice (Suzuki *et al.*, 2006a) and in non-human primates (Takai *et al.*, 2005) fed a high cholesterol diet without affecting blood pressure. The authors suggest that the plaque reduction may have been due to effects of eplerenone on decreasing levels of oxidized LDL and improving endothelial cell function (Takai *et al.*, 2005). Pro-inflammatory effects of MR activation have been reported in several studies. Rats treated with aldosterone/salt for 5 weeks developed a pro-inflammatory and fibrogenic heart phenotype which was attenuated by MR blockade with spironolactone (Sun *et al.*, 2002). Also, a role for MR in stimulating MCP-1 expression has been shown in the rat heart, where treatment with aldosterone and salt resulted in increased MCP-1 mRNA, an effect that was reversed by MR blockade with spironolactone (Sun *et al.*, 2002). Perhaps, this effect of MR activation on MCP-1 might partially explain the finding that blockade of MR in mice reduced monocyte infiltration into the failing heart (Kuster *et al.*, 2005). In addition to this, a role for MR in macrophage biology has been demonstrated in other studies where MR activation was found to be involved in macrophage oxidative stress in mice (Keidar *et al.*, 2003) and in macrophage adherence to endothelial cells *in vitro* (Caprio *et al.*, 2008). Given the important role of the macrophage in atherogenesis, it is likely that MR-mediated effects on these cells are involved in the pro-atherogenic properties of MR agonists.

The implication of these studies is that aldosterone-mediated activation of MR has wide ranging effects on the cardiovascular system. However, as mentioned previously, MR is not only activated by mineralocorticoid, but is also a high affinity glucocorticoid receptor (Arriza *et al.*, 1987). Given the fact that glucocorticoids acting via the GR are generally anti-inflammatory, it is tempting to postulate that the increased cardiovascular risk asociated with excess glucocorticoids is due to inappropriate activation of the MR. Support for a role for glucocorticoid-mediated activation of MR in cardiovascular pathologies is found in studies using MR antagonists. The patients in the RALES and EPHESUS trials who benefited from MR blockade had pre-treatment plasma aldosterone levels that were in the low normal range (Funder, 2006). Also, a sub-hypotensive dose of eplerenone attenuated coronary vascular inflammation and heart failure in hypertensive Dahl salt-sensitive rats, despite the fact that these animals had low aldosterone levels (Nagata *et al.*, 2006). The finding that MR blockade was beneficial in the setting of low to normal mineralocorticoid levels in these studies implicates activation of MR by glucocorticoids as an important mechanism in cardiovascular disease promotion. In agreement with this, it was reported that 11β-HSD blockade with carbenoxolone in uninephrectomised rats produces a coronary perivascular inflammatory response similar to that observed with mineralocorticoid treatment in rats (Young *et al.*, 2003b). This effect was completely blocked by coadministration of eplerenone, providing evidence for a detrimental effect of endogenous glucocorticoids via MR activation. Also, evidence for a direct effect of glucocorticoids on vascular cell MR comes from a study in cultured human VSMCs which demonstrated cortisol-mediated activation of mineralocorticoid response elements only when 11β-HSD2 was inhibited (Jaffe *et al.*, 2005). Taken together, these studies suggest an important pathophysiological role for glucocorticoid-mediated activation of MR under conditions of compromised 11β-HSD2 activity.

1.4 The *Apoe*$^{-/-}$/11β-HSD2$^{-/-}$ double knockout mouse

Despite this wealth of evidence linking activation of MR with the pathogenesis of cardiovascular diseases, the mechanisms by which MR activity exacerbate atherosclerosis have yet to be fully established. In order to dissect out the importance and contribution of inappropriate activation of MR, along with the protective role of 11β-HSD2, to atherosclerotic disease, the *Apoe*$^{-/-}$; 11βHSD2$^{-/-}$ double knockout mouse (DKO) was generated. A null mutation of the *Hsd11b2* gene was originally generated by replacing the genomic fragment encompassing exons 2–5 with a neomycin resistance cassette through homologous recombination in mouse 129 ES cells (Kotelevtsev *et al.*, 1999). In order to generate the *Apoe*$^{-/-}$/11β-HSD2$^{-/-}$ DKO mouse, the *Hsd11b2* null allele was transferred onto a C57B1/6J genetic background and crossed with *Apoe*$^{-/-}$ mice (Zhang *et al.*, 1992) on a C57B1/6 background and double homozygotes (DKO) were identified by PCR. This model promises several potential advantages over existing models of atherogenesis: (i) both mutations are on a pure C57Bl/6 background, minimizing variations associated with modifier loci, (ii) rapid atherogenesis develops on a normal chow diet, (iii) this occurs in young adults (6 months) rather than in senescence and (iv) the mice are fully viable beyond puberty, enabling successful breeding and the generation of sustainable colonies.

The schematic in Figure 1.3 illustrates the suitability of the DKO mouse for investigations concerning MR activation in atherosclerosis. It shows that the DKO mouse combines the atherosclerosis prone nature of the *Apoe*$^{-/-}$ mouse with the moderate hypertension and increased MR activity of the 11β-HSD2$^{-/-}$ mouse. Whilst a human presenting with defects in both *Apoe* and 11β-HSD2 genes would be an extremely rare find, the clinical relevance of this model stems from the fact that a large proportion of western populations do suffer from hypercholesterolemia and hypertension. Also, the cardioprotective effects of MR blockade in patients indicates that people with underlying cardiovascular pathologies may indeed have increased activation of MR.

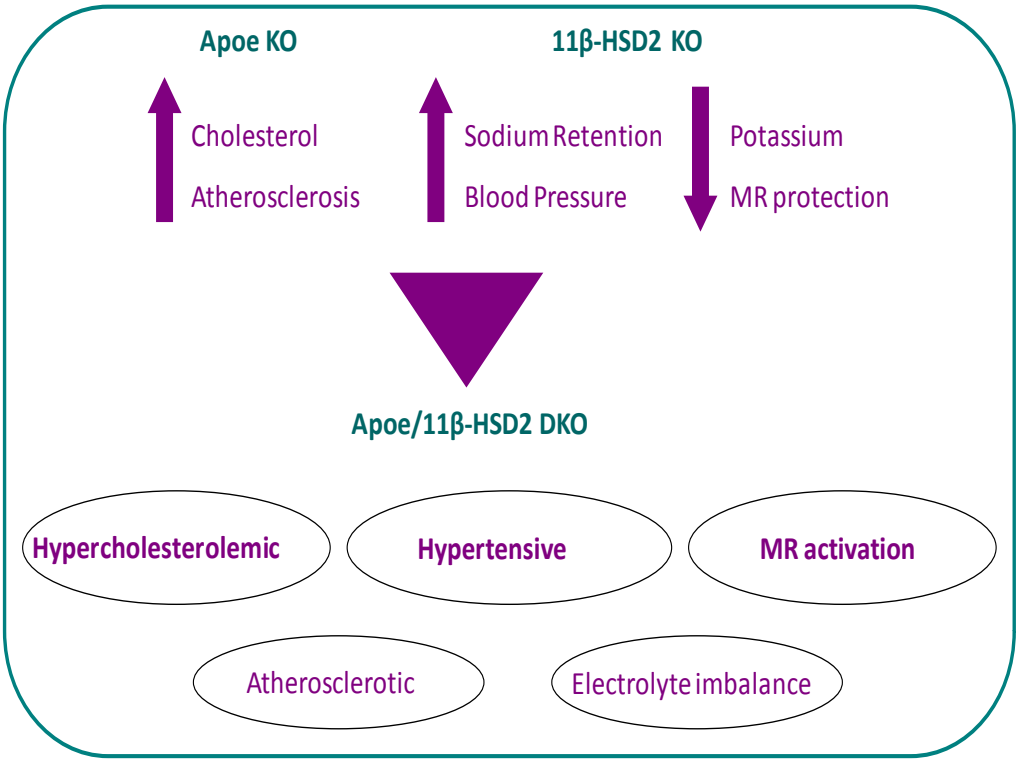

Figure 1.3 Pathological factors in the *Apoe*$^{-/-}$/11β-HSD2$^{-/-}$ DKO mouse

The *Apoe*$^{-/-}$/11β-HSD2$^{-/-}$ DKO mouse combines the hypercholesterolemia and atherosclerotic nature of the *Apoe*$^{-/-}$ mouse with the hypertension and MR activation of the 11β-HSD2$^{-/-}$ mouse. The DKO also has an electrolyte imbalance due to activation of renal MR. The combined phenotype of the DKO mouse is reminiscent of humans suffering from cardiovascular pathologies.

Initial investigations revealed that in contrast to *Apoe*$^{-/-}$ mice, DKO mice fed on a normal chow diet showed a high incidence of sudden death, with around 50% of animals dying by 6-7 months of age. The original studies in 11β-HSD2 single KO mice found an increased incidence of sudden death (Kotelevtsev *et al.*, 1999), particularly at the neonatal stage, suggesting that this phenotype in DKO mice is due to loss of 11β-HSD2-mediated protection of MR. The cause of sudden death in DKO mice is unknown but may be associated with the massive cardiac enlargement observed upon post-mortem examination (Deuchar *et al.*, 2009). Whilst some of the older DKO mice had near occlusive atheroma in the origins of the coronary arteries, histopathological analysis showed no evidence of myocardial infarction, plaque ruptures, or thrombosis (Deuchar *et al.*, 2009). Thus, it appears as though the DKO mice do not die of their atherosclerotic disease. However, coronary atherosclerosis may have exacerbated the heart disease by inducing cardiac ischaemia. DKO mice also show fibrosis of the heart and kidney, which could be a result of local MR activation leading to collagen deposition (Pellman *et al.*, 2009) or of haemodynamic changes associated with activation of renal MR.

Compared to *Apoe*$^{-/-}$ mice, DKO mice also demonstrate much larger more occlusive atherosclerotic lesions in the aortic arch, thoracic aorta and the major branches, with the brachiocephalic artery being particularly affected. Quantification revealed accelerated atherogenesis in DKO mice compared to age-matched *Apoe*$^{-/-}$ mice. In addition to this, the plaques from DKO mice had a greater number of submerged fibrous caps than those from *Apoe*$^{-/-}$ mice. Since these caps are thought to be an indication of plaque rupture (Johnson *et al.*, 2005), it could be suggested that DKO mice have vulnerable plaques.

This initial characterisation of the DKO mouse did not dissect out the mechanisms responsible for the severe phenotype observed. The important role of 11β-HSD2 in protection of renal MR against inappropriate activation by glucocorticoids is highlighted in the 11β-HSD2 knockout mouse and in patients with SAME. The question now arises as to whether or not the 11β-HSD2 present in cells of the vasculature has this same protective role over vascular MR. That this is likely is suggested by the fact that 11β-HSD2 knockout mice have endothelial cell dysfunction (Hadoke *et al.*, 2001) and that blockade of MR, without blood pressure

reduction, is beneficial in vascular disease. Therefore, with the aim of determining the contributions of renal and extra-renal MR activation to the DKO atherosclerotic phenotype, a drug study was performed. The effects of a sub-hypotensive dose of the MR antagonist eplerenone were compared with those of the blood pressure reducing drug amiloride. In this way, the role of renal hypertension in atherosclerosis in the DKO mouse could be investigated. The results demonstrated a significant reduction in both global and brachiocephalic atherosclerotic burden in eplerenone treated animals without a reduction in blood pressure (Deuchar *et al*, 2009). Conversely, treatment of DKO mice with the epithelial sodium channel (ENaC) blocker amiloride did significantly reduce blood pressure but had no impact upon atherogenesis (Deuchar *et al.,* 2009). Amiloride may also inhibit uPA (Vassalli *et al.*, 1987) and, given the role of uPA in thrombolysis, this in itself could affect atherosclerotic processes. Together these results suggest that activation of extra-renal MR, and not hypertension brought about by activation of renal MR, is important in the DKO atherosclerotic phenotype.

1.5 Hypothesis and aims

1.5.1 Hypothesis

Activation of MR has been implicated in the pathogenesis of atherosclerosis and *Apoe*$^{-/-}$ mice deficient in 11β-HSD2 activity have accelerated atherogenesis. Pharmacological inhibition of MR in animals and humans has been shown to reduce atherosclerosis yet the mechanisms remain unclear. Therefore, it was hypothesised that loss of 11β-HSD2-mediated protection in the vasculature allows glucocorticoids to illicitly activate the MR resulting in a pro-inflammatory vascular phenotype and accelerated atherogenesis. It was proposed that activation of vascular cell MR would directly alter plaque composition rendering DKO plaques more vulnerable to rupture. Lastly, it was anticipated that activation of endothelial cell MR would be key in mediating the enhanced pro-inflammatory environment associated with atherosclerosis in DKO mice.

1.5.2 Aims

In order to address this hypothesis, the aims of this thesis were:

(i) To determine the role of MR activation in the DKO atherosclerotic phenotype.

(ii) To determine the cellular and molecular mechanisms by which 11β-HSD2 protects against atherogenesis and the formation of unstable plaques.

(iii) To investigate the effects of 11β-HSD2 deficiency on vascular, and in particular endothelial cell, inflammation.

Chapter 2

Materials and Methods

2.1 Materials

COMPANY	PRODUCT(S)	PRODUCT APPLICATION
Sigma-Aldrich Company Ltd. The Old Brickyard New Road Gillingham Dorset SP8 4XT	All chemicals except where specified	
	Bovine serum albumin	Immunohistochemistry and Protein Assay
	Mouse anti-mouse α-smooth muscle actin antibody	Immunohistochemistry
	Aldosterone Corticosterone Spironolactone Glycyrrhetinic acid	Cell Culture Cell Culture Cell Culture Cell Culture
	Weigert's iron haematoxylin A and B solutions	United States Trichrome
	NP40	Nuclear Protein Extraction
	Bradford reagent	Protein Assay
	Ethidium Bromide	Gel electrophoresis
	Hydrogen peroxide 30% solution	Immunohistochemistry
	Tween20	Immunohistochemistry
	Acrylamide/ bisacrylamide 19:1	EMSA
Fisher Scientific UK Ltd Bishop Meadow Road Loughborough Leicestershire LE11 5RG	All solvents except where specified	
	Harris Haematoxylin	Histology
	Ammonium persulfate	EMSA
Vector Laboratories Ltd. 3 Accent Park Bakewell Road Orton Southgate Peterborough	Biotinylated secondary antibodies	Immunohistochemistry
	Control IgG	Immunohistochemistry

PE2 6XS	Normal serum	Immunohistochemistry
	Vectastain ABC reagent	Immunohistochemistry
	Diaminobenzidine substrate kit (DAB)	Immunohistochemistry
Lonza Wokingham Ltd 1 Ashville Way Wokingham Berkshire RG41 2PL	Endothelial basal medium 2 (EBM-2)	Cell culture
	PBS solution	Cell culture
	Trypsin/EDTA	Cell culture
	Penicillin/streptomycin	Cell culture
	L-Glutamine	Cell culture
Promega UK Delta House Southampton Science Park Southampton SO16 7NS	Dioxyribonucleotide triphosphate (dNTPs)	PCR
	100bp DNA ladder	PCR
	Blue/orange loading dye	PCR
	Agarose	Gel electrophoresis
Bioline Ltd 16 The Edge Business Centre Humber Road London NW2 6EW	Taq polymerase	PCR
	10x PCR buffer	PCR
	$MgCl_2$ solution	PCR
Invitrogen Ltd. 3 Fountain Drive Inchinnan Business Park Paisley PA4 9RF	Foetal Calf Serum	Cell Culture
	Dithiothreitol (DTT)	Nuclear protein extraction
	HEPES buffer	Nuclear protein extraction
	MCP-1 ELISA kit	ELISA
R & D Systems Ltd. 19 Barton Lane Abingdon Science Park Abingdon Oxfordshire OX3 7BZ	sVCAM-1 quantikine ELISA kit	ELISA
	Goat anti-mouse ICAM-1 polyclonal antibody	Immunohistochemistry

Thermo Scientific 93-96 Chadwick Road Astmoor Runcorn Cheshire WA7 1PR	Microtome cutting blades Sequenza microplate coverslides	Histology Immunohistochemistry
VWR International Ltd. Hunter Boulevard Magna Park Lutterworth Leicestershire LE17 4XN	Superfrost plus microscope slides DPX mounting media	Histology Histology
Fine Science Tools GmbH Heidelberg Germany	Forceps Spring Scissors	Dissection Dissection
Bright Instrument Co. Ltd St Margarets Way Huntingdon Cambridgeshire PE29 6EU	Optimum Cutting Temperature (OCT) Compound	Cryosectioning
Starstedt Ltd 68 Boston Road Beaumont Leys Leicester LE4 1AW	Lithium/Heparin microvette blood collection tubes	Plasma Collection
Eurofins MWG Operon 318 Worple Rd Rayned Park London SW20 8QU	11β-HSD2 and neo resistance cassette genotyping primers	PCR
Perbio Science Unit 9 Atley Way North Nelson Industrial Estate Cramlington Northumberland NE23 1WA	O-phenylenediamine dihydrochloride (OPD)	Immunocytochemistry
Roche Diagnostics East Sussex BN7 1LG	Phenylmethylsulphonyl fluoride (PMSF) Proteinase K	Nuclear protein extraction DNA extraction and Immunohistochemistry
LI-COR Biosciences UK Ltd St John's Innovation Centre Cowley Road Cambridge	NF-κB IRDye 700-labelled DNA oligonucleotides	EMSA

CB4 0WS	EMSA buffer kit	EMSA
VH Bio Ltd. Unit 11b Station Approach Team Valley Trading Estate Tyne & Wear NE11 0ZF	Rat anti-mouse MAC2 antibody	Immunohistochemistry
Bio-Rad Laboratories UK Ltd. Bio-Rad House Maylands Avenue Hemel Hempstead Herts HP2 7DX	TEMED	EMSA
Merck Chemicals Ltd. Boulevard Industrial Park Padge Road Beeston Nottingham NG9 2JR	Cholesterol/cholesteryl ester quantification kit	Total plasma cholesterol assay
Viagen Biotech Inc 3530 Wilshire Blvd Los Angeles California USA	DirectPCR (tail) buffer	DNA extraction
Cambridge Bioscience 25 Signet Court Newmarket Road Cambridge CB5 8LA	Rat anti-mouse VCAM-1 antibody	Immunohistochemistry
AbD Serotec Kidlington Oxford OX5 1JE	TNF-α	Cell Culture
Abcam plc 330 Cambridge Science Park Cambridge CB4 0FL	Rabbit anti-mouse NF-κB p65 antibody (CHIP grade)	EMSA
Other NRIE Pharmacy Sainsbury supermarket	 Eplerenone Gelatin Non-fat Milk	 Drug study Drug study Immunocytochemistry

2.1.1 Buffers and Solutions

2.1.1.1 Electrophoresis

50x Tris acetate EDTA (TAE) buffer: 242g of Tris base and 57.1mL of glacial acetic acid were mixed with 100mL of 0.5M EDTA (pH 8). The volume was made up to 1L with water.

5x Tris Borate EDTA (TBE) buffer: 54g of tris base and 27.5g of boric acid were mixed in 980mL of water and 20mL of 0.5M EDTA (pH 8) was added to make the final volume up to 1L.

10% Ammonium Persulfate (APS): 100mg of APS was dissolved in 1mL 0.5x TBE buffer.

2.1.1.2 Histology and Immunohistochemistry

PBS-Tween (PBST): 250µL of Tween20 was added to 100mL of commercially available PBS solution.

Tris EDTA (TE) buffer: 5mL of 1M Tris-Cl (pH 7.5) was mixed with 1mL 0.5M EDTA (pH 7.8) and made up to 500mL with water.

Proteinase K antigen retrieval solution (20µg/mL): 200µL of 10mg/mL proteinase K stock solution was dissolved in 100mL TE buffer. Fresh solution was made up immediately prior to each experiment.

3% Hydrogen peroxide (H_2O_2): 10 mL of commercially available 30% H_2O_2 solution was diluted in 100mL PBS. This solution was kept for up to 2 weeks at 4^0C.

1% Bovine serum albumin (BSA): 1g of BSA was dissolved in 100mL PBS. Fresh solution was made up immediately prior to each experiment.

2.5% Non-fat milk (NFM): 2.5g of NFM was dissolved in 100mL PBS. Fresh solution was made up immediately prior to each experiment.

Gomori's aldehyde fuchsin: 5 g of pararosaniline base was dissolved in 500 mL of 60% ethanol. To this 1 mL of hydrochloric acid (HCl) and 2 mL of fresh paraldehyde

were added, and the mixture was allowed to blue at room temperature for at least two days. Before use the solution was filtered.

Gomori's trichrome: 3 g of phosphotungstic acid was dissolved in 500 mL of distilled water. To this 3 g of chromotrope 2R and 1.5 g of fast green FCF were added and mixed until dissolved, then 5 mL of acetic acid were added. The solution was filtered before use.

Weigert's iron haematoxylin: Equal volumes of Weigert's iron haematoxylin solution A and solution B were mixed and filtered before use.

0.3% Potassium permanganate in 0.3% aqueous sulphuric acid: Prepared from stock solutions of 1% potassium permanganate (5 g dissolved in 500 mL distilled water) and 3% sulphuric acid (15 mL concentrated sulphuric acid made up to 500 mL with distilled water), made up to the appropriate volume with distilled water.

2% Oxalic acid: 10 mL of a commercially available solution was diluted in 490 mL of distilled water.

5% Phosphotungstic acid: 250 mL of a commercially available solution was diluted in 250 mL of distilled water.

0.2% Aqueous acetic acid: 1mL of glacial acetic acid was dissolved in 499mL distilled water.

2.1.1.3 Nuclear Protein Extractions

Buffer A: 100µL Hepes-KOH (made by adding concentrated KOH solution to 1M Hepes buffer until pH 7.9 was reached); 100µL 1M KCl (made by dissolving 7.45g KCL in 100mL water); 15µL 1M $MgCl_2$ (made by dissolving 9.52g $MgCl_2$ in 100mL water); 100µL 50mM DTT (made by dissolving 77.1mg DTT in 10mL water); 100µL 50mM PMSF (made by dissolving 87.1mg in 10mL isopropanol) made up to final volume of 10mL with water. This gives final solution: 10mM Hepes-KOH (pH 7.9), 10mM KCl, 1.5mM $MgCl_2$, 0.5mM DTT, and 0.5mM PMSF.

Buffer C: 4.2mL 1M NaCl (made by dissolving 5.84g NaCl in 100mL water); 100µL Hepes-KOH (pH 7.9); 15µL 1M $MgCl_2$; 20µL 0.5M EDTA (made by

dissolving 14.61g EDTA in 100mL water); 2.5mL 100% glycerol; 100µL 50mM DTT; 100µL 50mM PMSF made up to final volume of 10mL with water. This gives final solution: 420mM NaCl, 10mM Hepes-KOH (pH 7.9), 1.5mM $MgCl_2$, 0.2mM EDTA, 25% glycerol, 0.5mM DTT, and 0.5mM PMSF.

Buffer D: 2mL Hepes-KOH (pH 7.9); 7.5mL 1M NaCl; 20µL 0.5M EDTA; 20mL 100% glycerol; 1mL 50mM PMSF made up to final volume of 100mL with water. This gives final solution of 20mM Hepes-KOH (pH 7.9), 75mM NaCl, 0.1mM EDTA, 20% glycerol, and 0.5mM PMSF.

2.1.2 Drugs

2.1.2.1 Cell Culture Drugs

Tumour necrosis factor α (TNF-α): Recombinant mouse TNF-α protein (0.1mg/mL) was diluted 1:100 in serum free cell culture medium (SFM) to obtain a 1µg/mL solution.

Aldosterone: 3.6mg of aldosterone was dissolved in 1mL ethanol to obtain a 10^{-2}M solution. Serial dilutions of this were made in 1mL SFM to produce a range of aldosterone concentrations (10^{-4}M to 10^{-7}M).

Corticosterone: 3.5mg of corticosterone was dissolved in 1mL ethanol to obtain a 10^{-2}M solution. Serial dilutions of this were made in 1mL SFM to produce a range of corticosterone concentrations (10^{-4}M to 10^{-7}M).

Spironolactone: 4.2mg of spironolactone was dissolved in 1mL ethanol to obtain a 10^{-2}M solution. Serial dilutions of this were made in 1mL SFM to produce a range of spironolactone concentrations (10^{-4}M to 10^{-6}M).

Glycyrrhetinic acid: 4.7mg of glycyrrhetinic acid was dissolved in 1mL ethanol to obtain a 10^{-2}M solution. Serial dilutions of this were made in 1mL SFM to produce a range of glycyrrhetinic acid concentrations (10^{-4}M to 10^{-6}M).

2.1.2.2 Drug Study

Eplerenone: Based on the average mouse weighing 30g and eating 10g of food per day; in order to achieve a dosage of 200mg/kg of body weight/day for each mouse, every 1kg of diet contained 600mg of eplerenone. The diet was made up as follows: 40g of gelatine was dissolved in 300ml boiling water and 600mg eplerenone was dissolved in 300ml cold water (eplerenone was omitted from the water in vehicle diet). Following cooling of the gelatine, the two solutions were added together and 360g of powdered chow diet was mixed in to form a paste. The paste was packed tightly into 50ml tubes and frozen until needed.

2.2 DKO and *Apoe*$^{-/-}$ Mice

2.2.1 Generation of DKO Mice

A null mutation of the *Hsd11b2* gene was originally generated by replacing the genomic fragment encompassing exons 2–5 with a neomycin resistance cassette through homologous recombination in mouse 129 ES cells (Kotelevtsev *et al.*, 1999). In order to generate the 11β-HSD2$^{-/-}$/*Apoe*$^{-/-}$ double knockout mouse, the *Hsd11b2* null allele was transferred onto a C57B1/6J genetic background and crossed with *Apoe*$^{-/-}$ mice (Zhang *et al.*, 1992) on a C57B1/6 background and double homozygotes (DKO) were identified by PCR. DKO and *Apoe*$^{-/-}$ mice were maintained under controlled conditions of light (lights on 0800h-2000h) and temperature (21-22^{o}C), and allowed free access to standard chow (Special Diet Services, U.K.) with water *ad libitum*. Animal experiments were carried out under the auspices of the UK Home Office Animals (Scientific Procedures) Act, 1986. Mice were killed by Schedule 1 procedures according to Home Office guidelines.

2.2.2 DNA Extraction

DNA was extracted from mouse ear notches for use in genotyping PCR. Ear notches were immersed in 100µL of DirectPCR buffer containing 0.3mg/mL proteinase K and were placed in a rotating hybridising oven (Techne, hybridiser HB-1D) at 55^0C for 16 hours overnight. The crude lysates were then incubated at 85^0C for 45 minutes and allowed to cool before storing at -20^0C until use.

2.2.3 Genotyping

DNA extracted from ear notches at weaning was used in PCR reactions to genotype the mice. This DNA (2µL) was subjected to 32 cycles of PCR amplification with primers specific to the wild type 11β-HSD2 allele (forward: 5'-AGGCTGATGATAGATTCACGAGAC-3'; reverse: 5'-CGAATGTGTCCATAAGCAGTGC-3') and the neomycin resistance cassette present only in the mutant allele (forward: 5'-AGGCTGATGATAGATTCACGAGAC-3'; reverse: 5'-GCGAATGGGCTGACCGCTTCCTCG-3').

The final PCR mix (DNA, 1 X Taq buffer, 2.5mM $MgCl_2$, 200µM dNTPs, 10µM primers, 1 unit Taq polymerase, and dH_2O to a final volume of 20µL) was amplified in a PTC-200 lightcycler (MJ Research) under the following conditions: initial denaturation at 94^0C for 3 minutes, 72^0C for 2 minutes, followed by amplification for 32 cycles of denaturation at 94^0C for 30 seconds, annealing at 55^0C for 1 minute, and extension at 72^0C for 2 minutes. To finish, a final extension period of 5 minutes at 72^0C was used.

To prepare a 2% gel, 2 g of agarose were melted in 100 mL 1x TAE buffer. Following the addition of 10µL of ethidium bromide (10µg/mL), the gel was allowed to set at room temperature before being placed in a tank containing 1x TAE running buffer. 8µL of each reaction was analysed by electrophoresis with a 100bp DNA ladder used to verify product size. Products were visualised under UV light (Uvitec, BXT-20-M), the wild-type allele gave a band of 981bp whilst the knockout allele

gave a 562bp product. Heterozygous animals had both the wild-type and the knockout band.

2.2.4 Drug Administration

2.2.4.1 Eplerenone

Spironolactone, a competitive aldosterone antagonist, has long been the drug of choice for treating patients with heart failure. It is a member of the class of drugs called the potassium sparing diuretics and it competes with aldosterone for occupation of MR in renal distal tubules. However, spironolactone also has affinity for androgen and progesterone receptors and so produces off-target effects with prolonged treatment. Selective aldosterone receptor antagonists (SARA) have been developed which are similar in structure to spironolactone, but are much more selective for the mineralocorticoid receptor (Delyani, 2000). Eplerenone is one of these selective MR blockers and has been shown to provide benefits independent of blood pressure lowering effects in patients and mouse models of cardiovascular disease (Pitt *et al.*, 2001; Wang *et al.*, 2004).

2.2.4.2 Eplerenone Administration in Mouse Diet

Eplerenone is commonly administered in mouse chow diet and so food containing either eplerenone or vehicle was made. It was previously established that the mice eat around 10g of food per day (observation by Graeme Deuchar) and so the food was made up to ensure that each mouse received the correct daily dose of eplerenone (200mg/kg of body weight/day). To make up 1kg of food the mixture contained 360g of powdered diet, 600mL H_2O, 40g gelatin, and 600mg eplerenone. Briefly, the gelatin was dissolved in boiling water and the eplerenone was dissolved, and formed a suspension, in cold water. The powdered diet was added slowly to the mixture of gelatin (once sufficiently cooled) and eplerenone (or water in the vehicles) and mixed to form a paste with the drug as evenly distributed as possible throughout. The diet was tightly packed into tubes and frozen until given to the animals.

2.2.4.3 Drug Study Mice

To study the effect of MR blockade on the inflammatory component of atherosclerosis in DKO mice, at 2 months of age male DKO mice received diet containing 200mg/kg of body weight/day eplerenone (n=5) or vehicle (n=4). The mice were fed their respective diets for 12 weeks until they reached 5 months of age. This time course of treatment was chosen as a previous drug study in DKO mice (Deuchar *et al.*, 2009) demonstrated that eplerenone caused a significant reduction in atherogenesis that was independent of blood pressure lowering.

2.3 Characterisation of Atherosclerotic Phenotype

2.3.1 Organ harvest and preparation

2.3.1.1 Culling and Blood Sampling

DKO and *Apoe*$^{-/-}$ mice at 3 or 6 months of age, or at 5 months of age in the drug study, were killed by asphyxiation with CO_2. Terminal blood samples were taken from the left ventricle of the heart by cardiac puncture with a 19.5G needle (0.5 inch) fitted to a 1ml syringe, collected into heparin/lithium coated tubes to prevent blood clotting, and centrifuged (Sorvall, Biofuge fresca) at 894 x g for 10 minutes at 4^0C to separate the plasma fraction (upper layer) from the whole blood. Plasma samples were stored at -80^0C until use.

2.3.1.2 Collection and Fixation of Organs

The heart was exposed and the vasculature perfused via the left ventricle with 10mL phosphate buffered saline (PBS) followed by 10mL 10% neutral buffered formalin (for paraffin embedded samples) in order to flush out blood cells and maintain the structure of the blood vessels. However, perfusion under constant physiological pressure would have been more appropriate for measurements of vessel dimensions. The chest cavity was then cleaned of fat and connective tissue so that the aortic arch and its' major branches could be located. Due to its' predisposition to developing atherosclerotic plaques, the brachiocephalic artery was of interest and therefore preferentially used in these studies. The arch with attached brachiocephalic artery

(excised from the arch to the bifurcation of the right subclavian and carotid arteries) and the thoracic aorta were taken out, remaining fat was removed under the dissecting microscope (Nikon, SMZ-2B), and either fixed in 10% neutral buffered formalin for 24 hours or rapidly frozen in Optimum Cutting Temperature (OCT) compound. Formalin fixation, by cross-linking proteins, preserves tissues from degradation and helps to maintain the structure of cells and sub-cellular components. However, this process can mask some antigens, so some vessels were frozen in OCT compound which removes the need for formalin fixation and thus preserves antigenic sites.

2.3.1.3 Processing and Sectioning of Vessels

Tissues contain a high water content and since paraffin embedding medium is immiscible with water, the vessels were processed through increasing concentrations of alcohols and xylene to dehydration then infused with paraffin wax using an automatic tissue processing machine (Shandon, U.K.). They were then placed vertically in embedding moulds with molten paraffin wax which was allowed to cool and set into a solid block. A microtome (Leitz Wetzlar, 1512) was used to cut 4µm thick transverse sections which were floated on a water bath at 37^0C to remove folds and wrinkles. In the case of the frozen organs, 8µm thick sections were cut on a cryostat (Leica, CM1900) and stored at -20^0C until use. A cutting strategy was employed to maximise the number of useful sections gained from a vessel, which involved cutting in from the proximal end of the vessel, taking the first sections at the beginning of a lesion. Four serial sections were taken every 50µm until the plaque disappeared. Sections were collected onto positively charged superfrost plus microscope slides and dried in an oven for 16 hours at 37^0C (fixed tissues) or stored at -20^0C (frozen tissues).

2.3.2 Histology and Immunohistochemistry

2.3.2.1 Slide Preparation

Prior to staining, paraffin embedded sections require to be dewaxed and rehydrated, this was carried out by immersion in sequential baths of: xylene (x2) for 5 minutes

each, 100% ethanol for 1 minute, 74 O.P. (x2) (A solution of 99.5% ethanol and 0.5% methanol) for 1 minute each, and finally tap water for 5 minutes.

2.3.2.2 United States Trichrome

The United States Trichrome (UST) stain is a histological procedure which combines Gomori's aldehyde fuchsin stain for elastin with Gomori's one-step trichome stain (Hadoke *et al.*, 1995). It colours cell cytoplasms pink-red, nuclei blue-black, elastic fibres deep purple, and collagen blue-green. The staining procedure was carried out in an automated staining machine (Varistain Gemini; Thermo Shandon, U.K.). Sections were dewaxed and rehydrated, 0.3% potassium permanganate in 0.3% aqueous sulphuric acid was applied and, after rinsing in water, sections were decolourised in 2% aqueous oxalic acid. Sections were rinsed in water and 70% ethanol and then immersed in Gomori aldehyde fuchsin. After differentiating in 70% ethanol and washing in water, Weigert's iron haematoxylin was applied. The slides were then left to blue in running tap water, before 5% aqueous phosphotungstic acid was applied, which prepares the tissue for the trichrome stain. After washing in water, sections were immersed in Gomori trichrome stain for 20 minutes before rinsing in 0.2% aqueous acetic acid, dehydrating and clearing in xylene. Given its ability to differentially stain numerous plaque components, the UST stain is particularly useful in the evaluation of plaque composition and stability. UST was employed for the purposes of assessing general plaque composition and for making measurements of lipid content (Johnson *et al.*, 2005).

2.3.2.3 Picrosirius Red Stain

In order to assess plaque collagen content, the Picrosirius red histological stain was employed (Puchtler *et al.*, 1973). This stain was carried out by Susan Harvey and Bob Morris (histology technicians) in an automated staining machine (Varistain Gemini; Thermo Shandon, U.K.) and involved dewaxing and rehydrating sections before immersion in a solution of Sirius red and saturated aqueous picric acid for 1 hour in order to stain collagen fibres red.

2.3.2.4 Principles of Immunohistochemistry

Immunohistochemistry is the process of localizing specific proteins in the cells of a tissue section and it exploits the principle of antibodies binding specifically to antigens. This technique is widely used in the diagnosis of abnormal cells, e.g. in tumours, but it is also very useful in basic research to understand the distribution and localization of specific biomarkers. The two types of antibody employed in immunohistochemistry are called primary and secondary antibodies. Primary antibodies are raised against an antigen of interest and can be either monoclonal or polyclonal. Polyclonal antibodies are made by injecting an animal, e.g. a rat, with the antigen of interest from another species, e.g. mouse. This induces the rats B-cells to produce IgG immunoglobulins specific for the mouse antigen and these antibodies can be collected and purified from the serum. Most antigens induce multiple B-cell clones and so polyclonal antibodies are therefore a heterogeneous mix of antibodies that recognise several epitopes on an antigen. On the other hand, monoclonal antibodies are produced by one type of B-cell which are all clones of a single parent cell, selected for its ability to produce the most specific and stable antibodies, and are thus considered to be more specific. Secondary antibodies are raised against primary antibodies and recognise immunoglobulins, or immunoglobulin fragments, of a particular species.

There are two methods of immunohistochemistry, direct or indirect, and they are summarised in Figure 2.1. The direct method involves a one-step staining protocol with a labelled primary antibody and whilst it is simple and rapid, it suffers from problems with sensitivity. The most commonly used method is the indirect one which uses a two-step protocol with an unlabelled primary and labelled secondary antibody. This method has greater sensitivity due to the signal amplification conferred by the ability of one primary antibody to bind numerous secondary antibodies.

Formalin fixation causes protein cross-linking in tissues and although this helps to maintain cell morphology it can also mask some antigens. The demonstration of many antigens can be significantly improved in formalin-fixed tissues by pre-

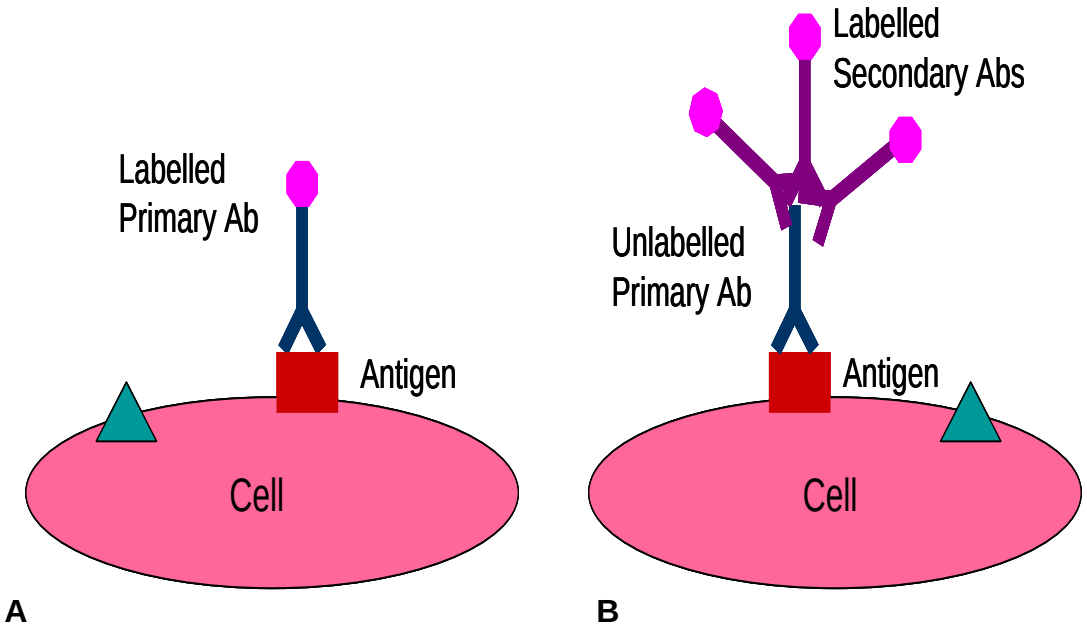

Figure 2.1 Comparison of direct and indirect immunohistochemistry

Direct immunohistochemistry (A) employs a labelled primary antibody and suffers from insensitivity due to lack of signal amplification. Indirect immunohistochemistry (B) is a two-step method which exploits the ability of one unlabelled primary antibody to bind numerous labelled secondary antibodies, thereby gaining signal amplification.

treatment with an antigen retrieval reagent. The two major methods of antigen retrieval are Heat Induced Epitope Retrieval (HIER) and Proteolytic Induced Epitope Retrieval (PIER). HIER utilises a source of heat, e.g. microwave or pressure cooker, in combination with a citrate or TRIS-EDTA buffer to unmask antigenic sites. PIER uses proteolytic enzymes such as proteinase K or trypsin to digest the protein cross-links and reveal the antigen.

Prior to incubating sections with antibodies, various blocking steps need to be performed to prevent non-specific binding of the primary antibody to proteins. The main cause of non-specific background staining is non-immunological binding of the specific immune sera by hydrophobic and electrostatic forces to certain sites within tissue sections. When using the Horse Radish Peroxidase (HRP) method of detection (discussed below) it is important to quench endogenous peroxidase activity in a tissue, this is most commonly done by pre-treating the section with 3% hydrogen peroxide (H_2O_2). In order to reduce non-specific staining by antibodies, sections are incubated with non-immune serum from the species that the secondary antibody is raised in. Bovine Serum Albumin (BSA) and Non-Fat Milk (NFM) are also commonly used to block non-specific protein and lipid sites and can be used as a diluent for the primary antibody. The general immunohistochemistry procedure employs the avidin-biotin complex (ABC) method outlined in Figure 2.2. Briefly, the specific primary antibody binds to the antigen of interest and the biotinylated secondary antibody binds the primary antibody. A complex of streptavidin linked to HRP is added and the biotin molecules on the secondary antibody can each bind three streptavidin-HRP molecules. The HRP substrate Diaminobenzidine (DAB) is then applied which forms an insoluble brown precipitate at the antigenic site.

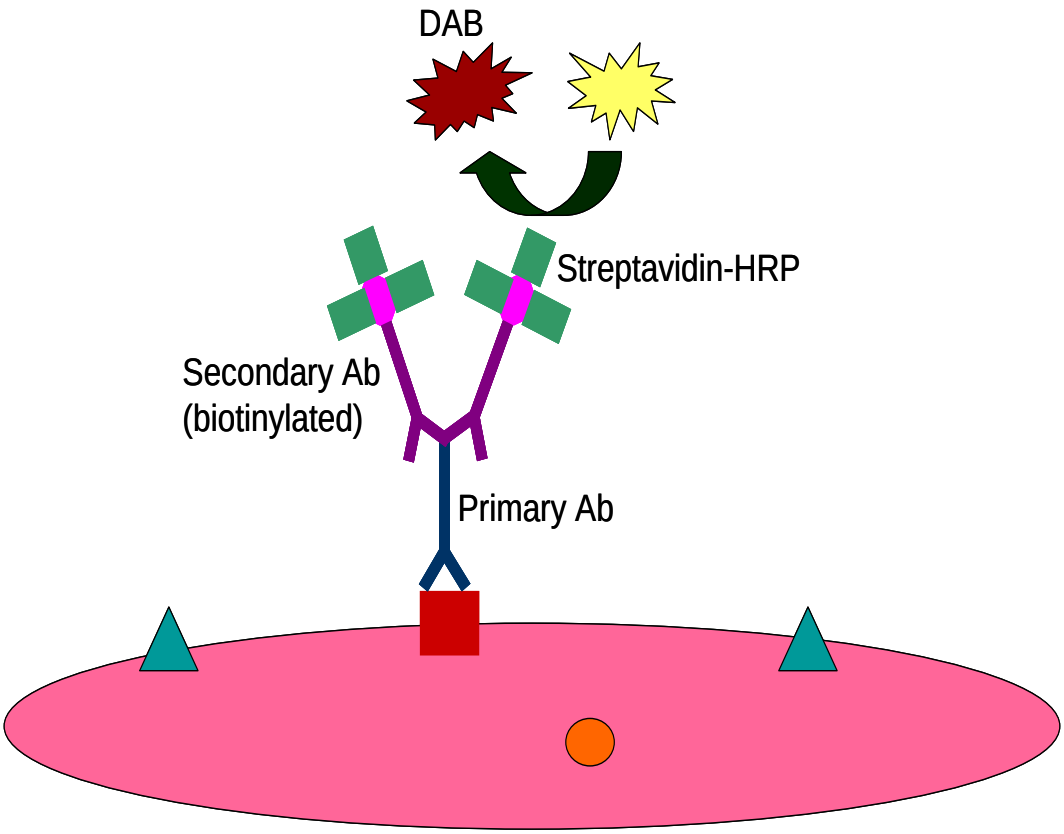

Figure 2.2 ABC method of immunohistochemistry

Immunohistochemical method employed in this thesis based on the indirect procedure described in figure 2.1. Antigen of interest is recognised by primary antibody which, in turn, is bound by species-specific biotinylated secondary antibodies. Following addition of the ABC complex, the biotin binds three molecules of streptavidin-linked HRP, further amplifying the primary signal. Reaction of HRP with its substrate DAB produces an insoluble brown precipitate at the antigenic site.

2.3.2.5 Immunohistochemistry in Brachiocephalic Artery Sections

Immunohistochemistry using primary antibodies against smooth muscle cell α-actin (SMA), macrophage specific galectin-3 (MAC2) (Ho *et al.*, 1982), and intracellular adhesion molecule 1 (ICAM-1) was performed on paraffin-embedded brachiocephalic artery sections, and vascular cell adhesion molecule 1 (VCAM-1) on frozen sections, from DKO and *Apoe*$^{-/-}$ mice. Immunohistochemistry was performed in sequenza racks using microplate holders (Shandon, UK) which minimises the volume of reagents required (150µL/slide). The specific conditions associated with each primary antibody are detailed in Table 2.1. Generally, following quenching of endogenous peroxidase activity for 15 minutes with 3% Hydrogen Peroxide (H_2O_2), sections were washed 3 x 150µL with PBS then blocked with 20% non-immune serum from the species that the secondary antibody was raised in for 20 minutes to 1 hour. Sections were then exposed to primary antibodies at pre-determined dilutions in 150µL PBS or 1% BSA at 4 ^{0}C overnight or room temperature (RT) for 30 minutes. Controls included substitution of the primary antibody with an equal concentration of IgG from the species that the primary antibody was raised in. Following washing with 3 x 150µL PBS, biotinylated secondary antibodies were incubated at pre-determined dilutions in 150µL PBS with the sections at RT for 30 minutes or 1 hour. Subsequently, bound secondary antibodies were detected with ABC reagent (streptavidin-biotin peroxidase ABC kit) at RT for 30 minutes. The sections were then stained with the HRP substrate DAB, for a time determined specifically for each batch of staining, then washed in tap water for 5 minutes. Counterstaining with haematoxylin was carried out for 1 minute prior to dehydration through graded alcohols and clearing in xylene in preparation for coverslipping with DPX mountant. Examples of specific staining are shown by comparison with a negative control for each antibody (figure 2.3).

Primary Antibody	Dilution and Incubation Time	Blocking	Secondary Antibody	Dilution and Incubation Time
Rat anti-Mouse MAC2	1:6000 (1% BSA) O/N at 4^0C	20% GS	Goat anti-Rat IgG	1:200 1h at RT
Mouse anti-Mouse SMA	1:400 (1% BSA) 1h at RT	2.5% BSA/2.5% NFM 20% GS	Goat anti-Mouse IgG	1:400 30 min at RT
Goat anti-mouse ICAM-1	1:1000 (PBS) O/N at 4^0C	3% NFM/20% RS	Rabbit anti-Goat IgG	1:400 1h at RT
Rat anti-mouse VCAM-1	1:1000 (PBS) O/N at 4^0C	3% NFM/20% RS	Rabbit anti-Rat IgG	1:200 1h at RT

Table 2.1 Immunohistochemical Staining Conditions

The conditions detailed in this table were used during immunohistochemistry on paraffin-embedded sections, with the exception of VCAM-1 staining which was performed on frozen sections. MAC2 = macrophage-specific galectin-3; SMA = smooth muscle actin; ICAM-1 = intracellular adhesion molecule 1; VCAM-1 = vascular cell adhesion molecule 1; BSA = bovine serum albumin; GS = goat serum; RS = rabbit serum; NFM = non-fat milk; RT = room temperature; O/N = overnight.

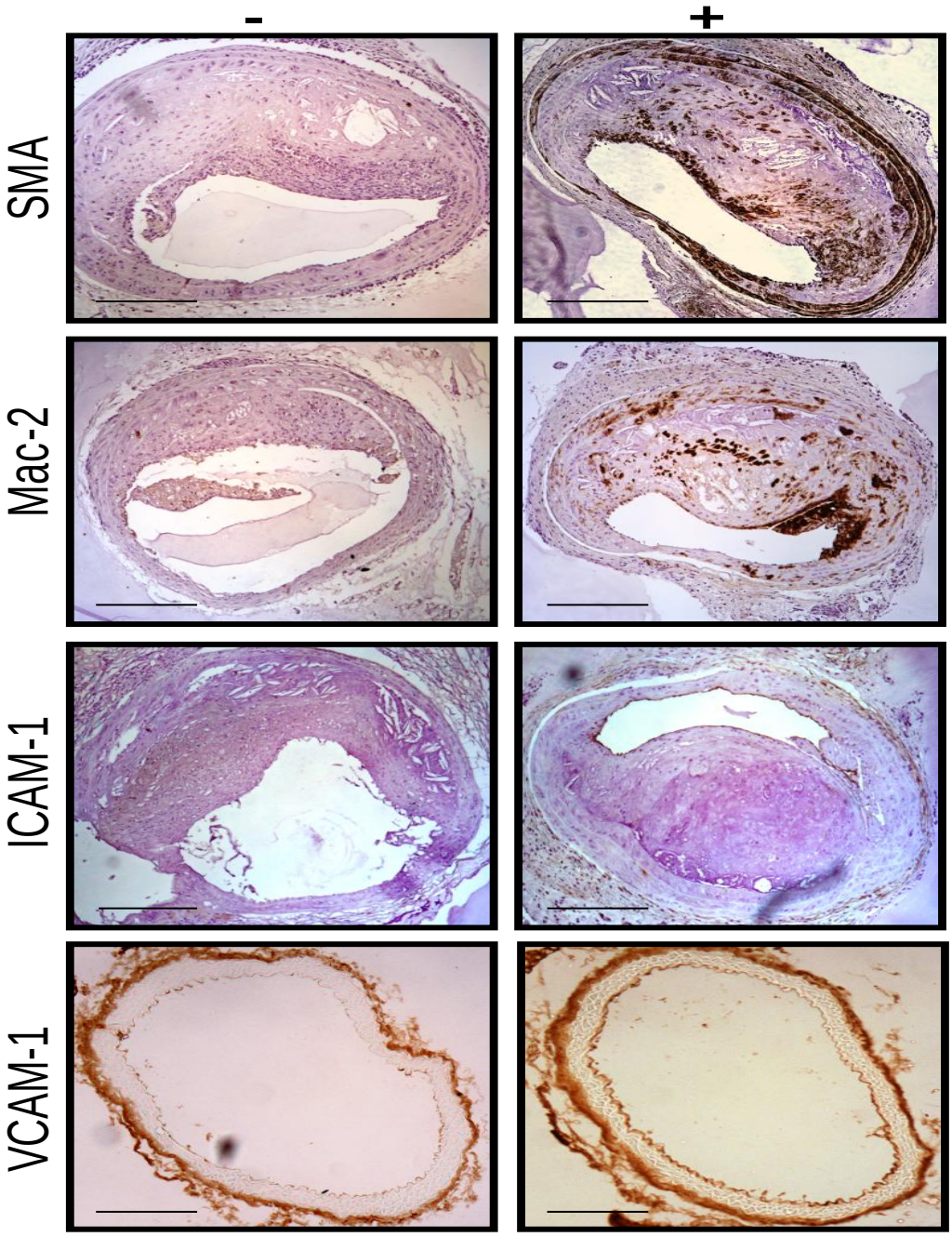

Figure 2.3 Specificity of primary antibodies

Sections of brachiocephalic arteries from DKO mice were stained with antibodies against SMA, Mac-2, ICAM-1 and VCAM-1 (right-hand panel). The specificity of each antibody was demonstrated by absence of specific staining in negative control images (left-hand panel), in which the primary antibody was substituted with IgG. Captured at x10 magnification, scale bar = 250 µm.

2.3.3 Image Analysis

2.3.3.1 Light Microscopy

Images of stained sections were digitised using a light microscope (Zeiss Axioskop) coupled to a Photometrics CoolSnap camera (Tucson, U.S.A.) via a microcolour liquid crystal turnable RGB filter (Cambridge Research and Instrumentation Inc., Woburn, U.S.A.). Microcomputer Imaging Device software (MCID; Imaging Research Inc., St. Catharines, Canada) was used to integrate the microscope and camera and images were taken at x10 and x40 magnifications.

2.3.3.2 Morphometric Analysis

Photoshop CS3 Extended software was used to perform measurements on images of stained brachiocephalic artery sections. The measurement scale was calibrated such that pixels were converted into microns for quantifying images taken on the Zeiss Axioskop microscope at x10 magnification. Total plaque area was measured and by instructing the software to measure the area of positive staining within plaques, it was possible to express the area of stained cells as a percentage of plaque size. For each separate staining experiment a colour template, which tells the software which colour to measure, is created for one image and applied to all other images in the same set. Measurements were performed blinded to genotype and age.

2.3.4 Serum Cholesterol Measurements

Total serum cholesterol levels were measured in *Apoe*$^{-/-}$ and DKO mice using a cholesterol/cholesteryl ester quantification kit (Calbiochem), following the manufacturer's instructions. Briefly, samples and cholesterol standards (0-10µg) were prepared in cholesterol reaction buffer and 50µL of each was added to appropriate wells in triplicate in a 96-well plate. To each of these, 50µL of reaction mix (cholesterol reaction buffer, cholesterol probe, enzyme mix, supplied with the kit) was added and the plate was incubated at 37^0C in the dark for 1 hour. The absorbance at 590nm was read in a plate reader (Dynatech labs, MRX) and the cholesterol concentration in each sample was calculated from the cholesterol standard curve.

2.4 Cell Culture

2.4.1 Cells and General Principles

2.4.1.1 Mouse Aortic Endothelial Cells (MAECs)

Mouse Aortic Endothelial Cells (MAECs) were obtained from the lab of Dr Saito at Tsurumi University in Japan (Nishiyama *et al.*, 2007). These immortalised cells were isolated from the aortas of p53-deficient mice and the group initially cultured the MAECs for over 100 passages to ensure they retained endothelial cell (EC) properties, such as cobblestone morphology, active uptake of acetylated low-density lipoprotein, and expression of EC markers (Nishiyama *et al.*, 2007). As well as this, tumour necrosis factor α (TNF-α) treatment promoted lymphocyte adhesion to MAECs (Nishiyama *et al.*, 2007), lending these cells to the study of inflammatory responses and atherosclerosis.

2.4.1.2 Culture Conditions

MAECs were preserved by freezing aliquots (10^6 cells) in FCS with 10% Dimethyl Sulphoxide (DMSO) and storing in liquid nitrogen freezers. MAECs were cultured in Endothelial Basal Medium 2 (EBM-2) supplemented with 10% fetal calf serum (FCS) and penicillin/streptomycin (250U/250U) mix under standard culture conditions (5% CO_2 at 37^0C). Cells were grown to confluence in T75 culture flasks and passaged every 3-4 days, with around 10^6 cells used for continuing culture and the remaining cells (around 5 x 10^6) plated out for experimental use as required. Sterile cell culture techniques were employed at all times in order to minimise risk of infection.

2.4.1.3 Passaging

Once confluent, MAECs were washed twice with 10mL PBS to remove any traces of FCS (this inhibits trypsin) and then incubated at 37^0C with 3ml trypsin-versene EDTA mixture (1X) for 3 to 5 minutes to dissociate the cells, checked microscopically. Following this, trypsin was inactivated by the addition of 9mL complete growth medium and the cell suspension was centrifuged (Heraeus, labofuge 400R) at 112 x g for 5 minutes. The cell pellet was resuspended in 10mL EBM-2 and 2ml (1:5 split) was added to a T75 flask to continue culture whilst the remaining

cells were plated out at densities specific to individual experiments, see below for details.

2.4.2 Drug Treatments

2.4.2.1 Justification of treatments

TNF-α was chosen as a positive control treatment in all studies as it is a potent pro-inflammatory stimulus well known to up-regulate a wide variety of inflammatory responses in endothelial cells (Wajant *et al.*, 2003). Aldosterone and corticosterone were the main focus of the treatments as they both act on MR and are expected to be dysregulated in DKO mice. Spironolactone is a competitive antagonist of the MR and thus prevents the actions of aldosterone and corticosterone at this receptor. The glycyrrhetinic acid metabolite, 3-Beta-D-(monoglucuronyl)18-beta-glycyrrhetinic acid, inhibits 11β-HSD2 activity (Bujalska *et al.*, 1997) and was used in these studies to determine whether or not 11β-HSD2 actively protects MR from illicit activation by glucocorticoids in endothelial cells.

2.4.2.2 Drug specifics and treatment conditions

MAECs were treated with various hormones at near physiological concentrations such that *in vitro* conditions mirrored *in vivo* conditions as closely as possible. The following hormones and drugs were employed at the indicated concentrations: TNF-α (10ng/mL, 0.5μM), Aldosterone (1nM), Corticosterone (1nM), Spironolactone (1μM), and glycyrrhetinic acid (1μM). MAECs were seeded into either 6-well (500 000 cells), 12-well (250 000 cells), 96-well (10 000 cells), or 10cm (10^6 cells) plates and grown to 80-100% confluency before complete growth medium was substituted with serum free medium (SFM). In all studies, MAECs were first pre-treated with the inhibitor drugs (spironolactone or glycyrrhetinic acid) for 2 hours prior to the addition of the hormone treatments to ensure maximal inhibition at the time of treatment.

2.4.3 Immunocytochemistry

2.4.3.1 Preparation and Treatment of Cells

MAECs were seeded onto circular glass coverslips (sterilised in ethanol and thoroughly washed in PBS) in 12-well plates (250 000 cells) for Vascular Cell Adhesion Molecule 1 (VCAM-1) staining or directly onto the plastic in 96-well plates (10 000 cells) for Intercellular Cell Adhesion Molecule 1 (ICAM-1) staining. Cells were grown in complete medium to around 80% confluency before substitution with SFM and treatment with the aforementioned drugs for 24 hours.

2.4.3.2 MAEC staining conditions

Treated MAECs were fixed in methanol containing 5% Dimethyl Sulphoxide (DMSO) and, following 3 x 5 minute washes with 250 µL PBS containing 0.05% Tween (PBST), endogenous peroxidase was quenched with a 0.3% solution of H_2O_2 in methanol (250µL). Following further PBST washing and blocking with 3% non-fat milk/10% normal serum (250µL), cells were exposed to either a 1:50 dilution of rat anti-mouse VCAM-1 primary antibody (12-well plates with coverslips) or a 1:1000 dilution of goat anti-mouse ICAM-1 primary antibody (96-well plates) at 4^0C overnight. Substitution of the primary antibody with rat IgG or goat IgG was employed as a negative control. Dilutions of primary and control antibodies were made in 250 µL blocking solution. Primary antibody was removed by 3 x 5 minute washes with PBST and then goat anti-rat (VCAM-1) or rabbit anti-goat (ICAM-1) biotinylated secondary antibodies were applied at 1:200 or 1:600 dilutions in 250µL PBS respectively at room temperature for 1 hour. Cells were washed with PBST and bound secondary antibodies were detected with a streptavidin-biotin peroxidase ABC kit (see section 2.3.2.4 for details). For VCAM-1 detection the cells were then stained with 250µL of the HRP substrate DAB for 1 to 2 minutes. For ICAM-1 detection, the DAB was replaced with the soluble HRP substrate o-Phenylenediamine dihydrochloride (OPD) which forms a yellow product upon reaction with peroxidase. After 1 minute, the reaction was stopped by the addition of 2M sulphuric acid which turns the product orange. The intensity of staining, which

correlates with the amount of ICAM-1 protein present, was measured colorimetrically at a wavelength of 490nm in a plate reader (Dynatech labs, MRX).

2.4.3.3 Image Analysis

Following DAB staining of MAECs to detect VCAM-1 expression, the glass coverslips, with adherent cells, were removed from the wells and dehydrated through alcohols and xylene. The coverslips were then mounted cell-surface down onto microscope slides with DPX non-aqueous mounting media. Slides were subsequently viewed under a light microscope (Zeiss Axioskop) coupled to a Photometrics CoolSnap camera (Tucson, U.S.A.) via a microcolour liquid crystal turnable RGB filter (Cambridge Research and Instrumentation Inc., Woburn, U.S.A.). Microcomputer Imaging Device software (MCID; Imaging Research Inc., St. Catharines, Canada) was used to integrate the microscope and camera and images were taken at x10 and x40 magnifications. The number of positively stained cells per field (x40) were counted in four randomly selected fields per slide for each treatment and this procedure was repeated in five individual cell culture experiments.

2.4.4 Enzyme-Linked ImmunoSorbent Assay (ELISA)

2.4.4.1 Principles of ELISA

The ELISA was developed as a safer alternative to the radioimmunoassay for assessing the expression level of specific antigens in biological samples (Van Weemen et al, 1971). It utilises enzyme-linked (e.g. HRP) antibodies in place of radioactively-labelled antibodies and exploits the colorimetric reactions catalysed by these enzymes as a means of measuring antigenic expression. A variant of this technique called the solid phase sandwich ELISA is a commonly used method of measuring the amount of specific antigen between two layers of antibodies (capture and detection antibodies). Figure 2.4 depicts the general principles of the sandwich ELISA in which a capture antibody, immobilised on the surface of a 96-well plate, binds the specific antigen in a sample and this in turn is bound by a biotinylated detection antibody specific to that same antigen. Streptavidin-labelled HRP enzyme is added and this binds to the biotin on the detection antibody where it catalyses the

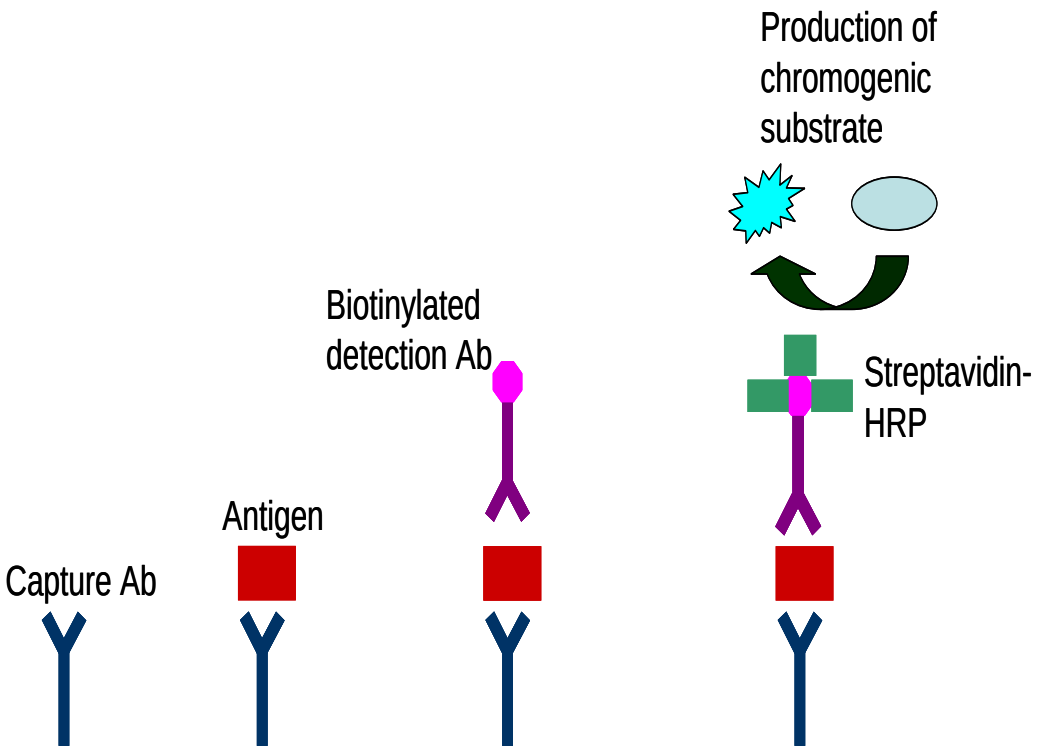

Figure 2.4 Sandwich ELISA

Sandwich ELISA method of measuring antigen levels in serum or cell culture media. The antigen of interest is captured by a specific primary antibody, coated onto the surface of a well in a 96-well plate, and detected by the addition of a biotinylated antigen-specific antibody, which binds to the captured antigen. The addition of streptavidin-linked HRP followed by reaction with an HRP substrate allows chromogenic detection of the antigen where the colour intensity is directly related to the levels of antigen present in the original sample.

production of a chromogenic substrate, allowing antigenic expression levels to be determined by measurement of colour intensity.

2.4.4.2 MCP-1 and sVCAM-1 sandwich ELISA

Around 500 000 MAECs were seeded onto 6-wells plates in complete growth medium and incubated until 100% confluency was reached. Cells were then treated with the aforementioned hormones/drugs in SFM for 16h and the culture media were collected for analysis of MCP-1 or sVCAM-1 secretion by ELISA. A mouse MCP-1 (Invitrogen) or sVCAM-1 (R&D Systems) sandwich ELISA kit was used according to the manufacturer's instructions. Briefly, standards (0-2500pg/mL and 0-20ng/mL, supplied with kits) and samples (100µL) were added to appropriate wells in a 96-well plate containing the immobilised capture monoclonal antibody specific to mouse MCP-1 or sVCAM-1, and incubated at room temperature for 2 or 3 hours, respectively. Following removal of unbound components by washing with a mild detergent (supplied with the kit), a biotinylated anti-mouse MCP-1 or sVCAM-1 detection antibody (supplied with the kit) was applied to the wells for 45 minutes or 1 hour respectively at room temperature. Wells were washed to remove unbound antibody and a solution of streptavidin-HRP (supplied with the kit) was added for a further 45 minutes and, subsequently, excess was removed by washing. Stabilised chromogen (supplied with the kit) was then applied and a yellow product was formed, the intensity of which was dependent upon the amount of antigen present in the cell culture media. The chromogen was incubated for 15 (MCP-1) or 30 (sVCAM-1) minutes before a stop solution (supplied with the kit) was added, turning the colour from yellow to blue. The colour intensity was measured at a wavelength of 450nm in a plate reader (Dynatech labs, MRX) and the concentration of MCP-1 or sVCAM-1 in the samples was inferred from the standard curve produced by plotting the absorbance readings of the standards against the standard concentration.

2.4.5 Electrophoretic Mobility Shift Assay (EMSA)

2.4.5.1 Principles of EMSA

The electrophoretic mobility shift assay (EMSA) is widely used to study the interaction of proteins with DNA and it relies on the principle that a DNA-protein complex will have a retarded mobility during electrophoresis compared to non-bound DNA (Garner *et al.*, 1981). The shifts can be visualised on a native acrylamide gel using labelled DNA to form the DNA-protein binding complex. The majority of protocols to date use DNA labelled with radioisotopes, digoxygenin, or biotin. However, it is now possible to perform an EMSA using specific oligonucleotides labelled with an infrared dye, removing the need for hazardous radioisotopes, gel transfer, and lengthy film exposure. The Odyssey® infrared imaging system is used in combination with IRDye® 700 EMSA oligonucleotides in standard EMSA protocols to detect DNA-protein interactions.

2.4.5.2 Bradford Protein Assay

Protein concentration measurements were performed using Bradford's reagent (Bradford, 1976). To prepare the standard curve, a 2mg/mL solution of BSA was made up and serial dilutions gave standards with the range 0 – 2mg/mL. In a 96-well plate, 2µL of standard or sample was mixed with 98µL of Bradford's reagent and incubated at RT for 5 minutes. Absorbance at 595nm was measured in a plate reader (Dynatech labs, MRX) and the standard curve was used to determine the protein concentration of nuclear protein extracts.

2.4.5.3 MAEC Nuclear Protein Extractions

MAECs (10^6 cells) were grown in complete medium to confluency in 10cm dishes prior to treatment with the aforementioned hormones/drugs in SFM for 2 hours, ten 10cm dishes were used for each treatment. Following treatment, nuclear proteins were extracted using a modified version of the protocol described by Dignam et al (Dignam JD, 1983). MAECs were washed in ice cold PBS w/o calcium and magnesium, scraped in 2mL ice cold PBS, and collected into 15mL falcon tubes for counting. The ten dishes per treatment typically yielded around 50 million cells. The MAECs were then collected by centrifugation at 112 x g (Heraeus, labofuge 400R) for 10 minutes, resuspended in 5 packed cell volume (PCV) of buffer A

(10mM Hepes-KOH pH 7.9, 10mM KCl, 1.5mM $MgCl_2$, 0.5mM DTT, and 0.5M PMSF), and allowed to swell on ice for 10 minutes. Following this, cells were again collected by centrifugation at 112 x g (Heraeus, labofuge 400R) for 10 minutes and resuspended in 2.5 PCV buffer A with 0.1% NP40. Cells were then lysed with 12 strokes in a pre-chilled glass homogeniser with tight-fitting pestle then centrifuged at 447 x g (Heraeus, labofuge 400R) for 10 minutes to collect the nuclei, which were subsequently washed in 2mL buffer A without NP40. This solution was centrifuged at 18000 x g (Beckman, Optima MAX-E ultracentrifuge) for 15 minutes to pellet the nuclei which were then resuspended in 2.5 nuclei pellet volume buffer C (420mM NaCl, 10mM Hepes-KOH pH 7.9, 1.5mM $MgCl_2$, 0.2mM EDTA, 25% glycerol, 0.5mM DTT, and 0.5mM PMSF) and homogenised with 10 strokes with a tight fitting pestle as before. The lysed nuclei were then stirred slowly for 30 minutes at 4^0C followed by centrifugation for 30 minutes at 25000 x g (Beckman, Optima MAX-E ultracentrifuge). The supernatant, containing the nuclear proteins, was dialysed against 50 volumes of buffer D (20mM Hepes-KOH pH 7.9, 75mM NaCl, 0.1mM EDTA, 20% glycerol, and 0.5mM PMSF) at 4^0C for 3 hours in order to remove the salt from the protein extracts. Bradford's protein assay (see section 2.4.5.2) was employed to determine the concentration of nuclear proteins in the extracts, which were aliquoted and stored at -80^0C until use.

2.4.5.4 5% Polyacrylamide Gels

Native polyacrylamide gels (6%) were made with TBE buffer for electrophoresis of EMSA reactions. Glass plates and spacers are assembled such that the resulting gel is 1mm thick, and a 2% agarose solution is used to seal the edges of the glass plates to prevent leaking. The gel is made by mixing 3g of acrylamide/bisacrylamide (19:1) with 50mL of 0.5x TBE buffer (diluted 1:10 from 5x TBE stock) and adding 300µL of 10% ammonium persulfate (APS). Immediately prior to pouring, 40µL of TEMED is added to the gel mixture to aid polymerisation, which normally occurred within 10 to 20 minutes of carefully pouring the gel between the glass plates and inserting the comb. Before loading, the gel was pre-run at 20mA for 30 minutes in 0.5x TBE buffer.

2.4.5.5 NF-κB EMSA

The activity of NF-κB in nuclear protein extracts was determined by EMSA. NF-κB IRDye 700-labelled DNA oligonucleotides were obtained from LI-COR. Crude nuclear extract (10µg/reaction) was incubated for 20 min on ice in binding buffer (EMSA buffer kit, LI-COR UK) containing 25mM DTT/2.5% Tween20, 1µg/mL Poly (dI-dC), and with or without 1µg NF-κB antibody (Abcam). Following this, 1µL of the IR-labelled oligonucleotides encoding the consensus NF-κB site 5'-AGTTGAGGGGACTTTCCCAGGC-3' was added to each reaction (total volume 20µL) and incubated for 30 minutes on ice. Orange loading dye (1µL) was added and samples were separated by electrophoresis at 20mA in pre-run 6% polyacrylamide gels for around 2 hours. The glass plates were then removed from the electrophoresis apparatus and placed directly onto the Odyssey infrared imaging system flatbed (LI-COR). The gel was scanned using the parameters detailed in Table 2.2 and odyssey 3.0 software was used to generate a .tiff image.

2.5 Statistics

All data are expressed as mean ± standard error of the mean (sem). Values quoted for n refer to the number of different mice used in each experiment. GraphPad Prism 5 software was used to create graphs and perform statistical analyses. Data were analysed by unpaired t test, One or Two Way Analysis of Variance (ANOVA) followed by post hoc tests, or the non-parametric Kruskal wallis test, as appropriate. $p<0.05$ was considered significant.

Scanning Channel	Scan Intensity	Focus Offset	Resolution
700	8.0	3mm	169µm

Table 2.2 Odyssey Scan Parameters

The parameters detailed in this table were used to scan EMSA gels using the LI-COR odyssey infrared imaging system. The scanning channel refers to the dye that is linked to the oligo of interest and the intensity is that recommended in the manufacturer's instructions. The focus offset is the glass plate thickness (2.5mm) + ½ the gel thickness (0.5mm) and the resolution is preset for a DNA gel.

Chapter 3

Effect of Mineralocorticoid Receptor Blockade on the DKO Atherosclerotic Phenotype

3.1 Introduction

The major aim of the work described in this thesis was to determine the cellular and molecular mechanisms underlying the accelerated development of atherosclerosis in the *Apoe*/11β-HSD2 DKO mouse. In order to do this, it was first necessary to assess the role of MR activation in atherogenesis in the DKO mouse. Given the loss of 11β-HSD2-mediated protection of MR in DKO mice it is likely that illicit MR activation is implicitly involved in this phenotype.

Several studies in humans and rodents have reported detrimental effects of MR activation in cardiovascular pathologies (see section 1.3). Loss of 11β-HSD2-mediated protection of MR in DKO vessels may produce the vascular dysfunction necessary to drive the progression of atherosclerosis. In support of this proposal, a recent study demonstrated that administration of aldosterone to *Apoe*$^{-/-}$ mice for 1 month led to accelerated atherogenesis; a mechanism mediated, at least in part, by MR and AT_1 receptors (Keidar *et al.*, 2004). Recently there has been a surge in research aiming to investigate the pathological consequences of MR activation in non-epithelial tissues, such as the heart and vasculature. This has been stimulated by the fact that MR antagonists, administered at doses that do not significantly lower blood pressure, improve survival in patients with heart failure (Pitt *et al.*, 2001; Pitt *et al.*, 1999), suggesting cardiovascular effects *independent* of renal control of blood pressure.

The mechanisms by which the selective MR antagonist eplerenone exerts its cardioprotective effects are largely unknown, highlighting the necessity for continued research in this area. Given that the DKO mouse combines the atherosclerosis-prone nature of the *Apoe*$^{-/-}$ with the inappropriate MR activation of the 11β-HSD2$^{-/-}$, it is an ideal model for investigating the effects of MR activation on atherogenesis and may, thereby, aid in dissecting out the mechanisms of eplerenone action. A previous drug study in the DKO mice demonstrated a significant reduction in both global and brachiocephalic atherosclerotic burden in eplerenone treated animals without a reduction in blood pressure (Deuchar *et al*, 2009). Conversely, treatment of DKO mice with the epithelial sodium channel (ENaC) blocker amiloride did significantly reduce blood pressure but had no impact upon atherogenesis.

Together these results suggest that activation of *extra-renal* MR, and not hypertension brought about by activation of renal MR, is important in the atherosclerotic phenotype and so based on this, it was hypothesised that blockade of MR would alter the cellular components of the DKO atherosclerotic plaque, favouring stability by reducing vascular inflammation. The specific aims of this chapter were:

(i) To assess the effects of a sub-hypotensive dose of eplerenone on the cellular composition and stability of plaques from DKO mice.

(ii) To determine whether or not the reduction in plaque size with MR blockade is associated with decreased vascular inflammation.

3.2 Methods

3.2.1 Drug administration

Male *Apoe*$^{-/-}$/11β-HSD2$^{-/-}$ DKO mice received either vehicle (n=4) or 200mg/kg of body weight/day eplerenone (n=4) in standard chow diet from 2 months of age (for diet preparation, see section 2.2.4). Treatment was for 12 weeks and at 5 months of age mice were culled by asphyxiation with CO_2. This particular treatment regime was based on the previous drug study in DKO mice which demonstrated an effect of eplerenone on lesion size without significantly altering blood pressure (Deuchar *et al.*, 2009).

3.2.2 Assessment of atherosclerosis

For detailed methods on the characterisation of atherosclerosis see section 2.3. The brachiocephalic artery (anatomical location depicted in Figure 3.1) was preferentially used in these studies due to its propensity to develop advanced lesions. Histological and immunohistochemical techniques were performed according to the methods detailed in section 2.3.2. Total plaque area was measured in transverse sections by drawing around the lesion and by instructing the software to measure the area of positive staining within plaques, it was possible to express the area of stained cells as a percentage of plaque size (see Figure 3.2a). For each separate staining experiment a colour template, which tells the software which colour to measure, is created for one image and applied to all other images in the same set. Measurements were performed blind to genotype and age. Additional parameters measured were: buried fibrous caps (% of animals with buried caps), mean area (μm^2) inside the external elastic lamina (EEL), internal elaαstic lamina (IEL) and lumen (see Figure 3.2b). These measurements could then be uαsed to calculate the area of the media (area inside EEL – area inside IEL). Three evenly spaced sections were chosen to represent each artery when calculating the mean parameters in a group.

3.2.3 Statistical analysis

Data are mean ± sem and were analysed by students' unpaired t-test.

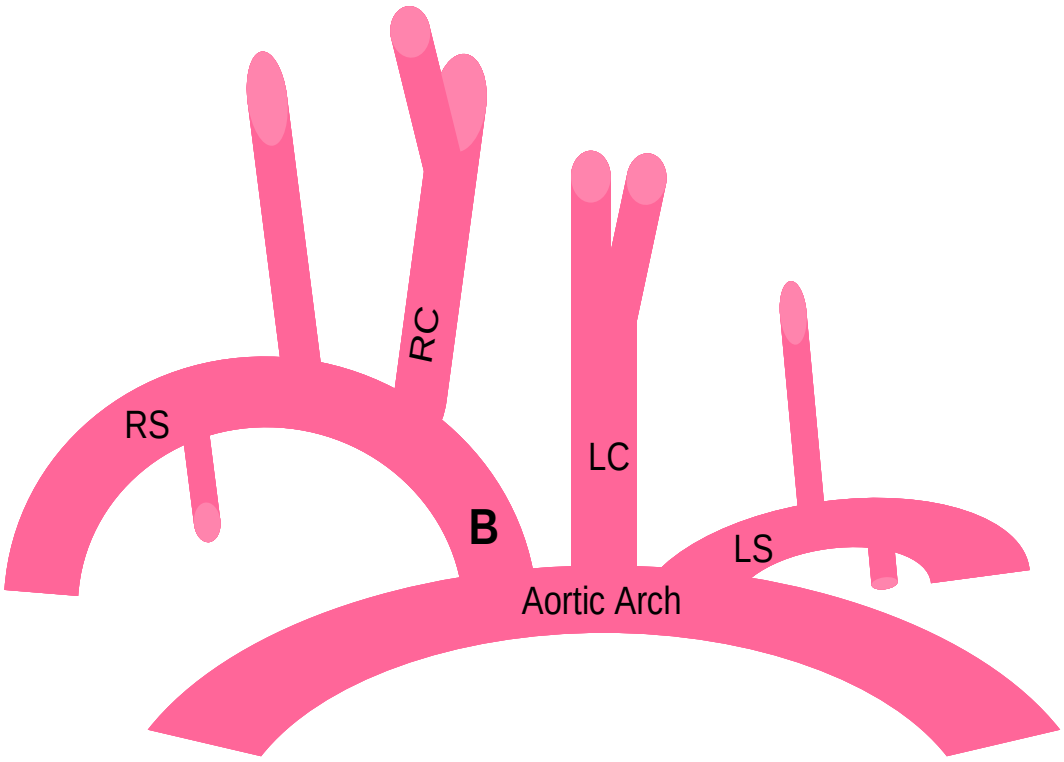

Figure 3.1 Anatomical location of brachiocephalic artery

Schematic diagram of the aortic arch with its' major branches, of which the brachiocephalic artery (B) is studied in this thesis. The brachiocephalic artery (also called the innominate artery) is the first branch off the aortic arch and it supplies blood to the right arm, the head, and the neck. Soon after it emerges, the brachiocephalic artery divides into the right αcommon carotid artery (RC) and the right subclavian artery (RS). The second and third major branches off the aortic arch are the left common carotid artery (LC) and the left subclavian artery (LS).

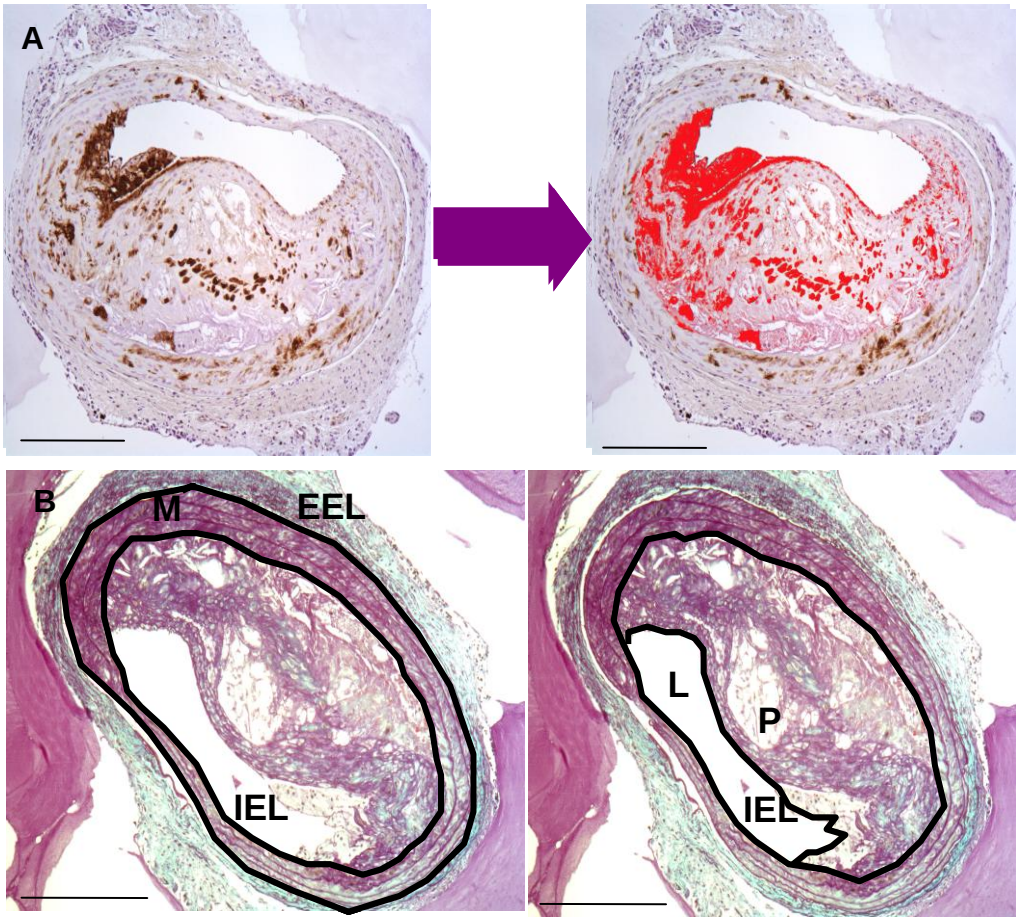

Figure 3.2 Morphometric and quantitative analysis of brachiocephalic sections

Photoshop CS3 Extended software was used to quantify: (A) immunohistochemical staining in brachiocephalic artery sections. A line was drawn around the plaque and the brown staining, macrophages in this example, within the area of interest was then selected and highlighted (red in the right-hand image) and, by dividing the area of the highlighted regions by the total plaque area the percentage contribution of the stained cell type to the plaque can be calculated. (B) Vascular remodelling was quantified by measuring the mean area (μm^2) inside the external elastic lamina (EEL), and by subtracting the mean area inside the internal elastic lamina (IEL), the medial area (M) could be calculated (left panel). Luminal patency was determined by subtracting the plaque area (P) from the area inside the IEL in order to measure lumen are (L) (right panel). Images at x10 magnification. Scale bar = 250µm.

3.3 Results

3.3.1 Influence of MR blockade on vascular remodelling and atherogenesis in DKO brachiocephalic arteries

To determine whether or not inappropriate MR activation played a causative role in the DKO atherosclerotic phenotype, DKO mice received either the selective MR antagonist eplerenone (n=5) (at a dose that does not alter blood pressure) or vehicle (n=4) administered for 12 weeks in their diet from 2 months of age. In order to confirm the findings of the previous drug study in DKO mice (Deuchar *et al.*, 2009), plaque size was compared in brachiocephalic arteries from vehicle and eplerenone treated DKO mice. Haematoxylin stained sections revealed smaller plaques in eplerenone (EPL) treated animals compared to vehicle (VEH) treated animals (
Figure 3.3a). Quantitative analysis of three evenly spaced sections per vessel, using Photoshop CS3 Extended software, confirmed that antagonism of MR significantly reduced plaque size in DKO brachiocephalic arteries compared to vehicle treatment (Figure 3.3b).

The formation of atherosclerotic lesions is often associated with remodelling of the blood vessel such that a compensatory enlargement of the vessel occurs to accommodate the plaque and maintain the lumen (Glagov *et al.*, 1987). Vascular remodelling was investigated in vehicle and eplerenone treated DKO brachiocephalic arterial sections to determine whether or not the reduction in plaque size with MR blockade was associated with alterations in other vascular parameters. The results are shown in Table 3.1 and indicate that eplerenone treatment significantly reduced both the area inside the EEL and the area inside the IEL, thereby maintaining the medial area. Despite a reduction in plaque area, the luminal area was not altered by eplerenone, an effect that may be explained by the reduction in the area inside the IEL in eplerenone treated animals. The percentage of animals containing buried fibrous caps was significantly decreased by eplerenone, and since this feature is indicative of plaque vulnerability, MR blockade may improve plaque stability.

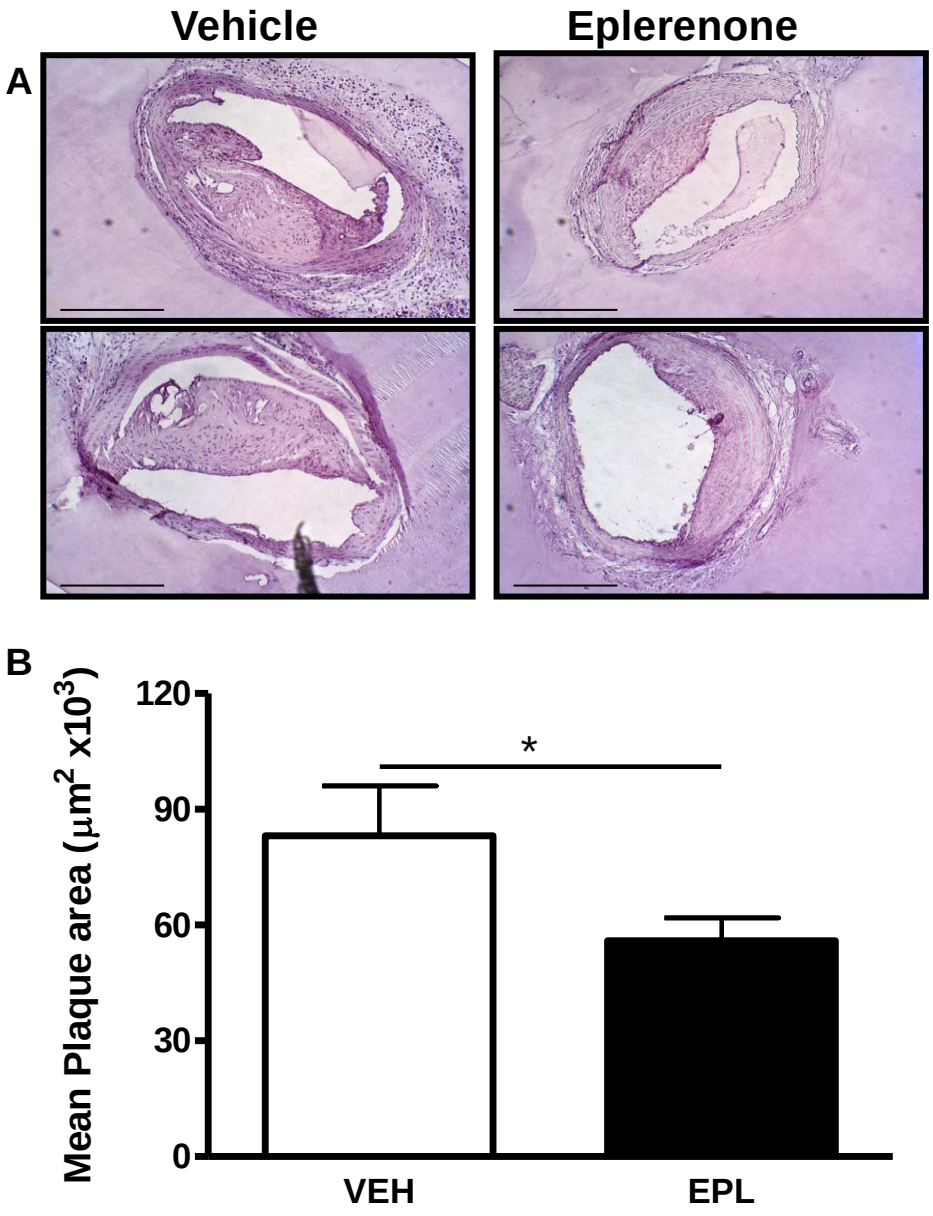

Figure 3.3 Eplerenone reduced plaque size in DKO brachiocephalic arteries

Sections of brachiocephalic arteries from DKO mice treated with 200mg/kg/day eplerenone or vehicle for 12 weeks were stained with haematoxylin (A). Atherosclerotic plaques developed in both groups but appeared smaller in size with eplerenone compared to vehicle treatment. Representative images from two vehicle and two eplerenone treated animals, captured at x10 magnification. Scale bar = 250 µm. The area of atherosclerotic plaque was quantified using Photoshop CS3 Extended software (B). Compared to vehicle, eplerenone administration caused a decrease in plaque area after 12 weeks of treatment. Data are mean ± sem, n= 4-5. Analysed by Student's unpaired t test: * $p<0.05$.

	Vehicle	Eplerenone
Area inside EEL (μm^2)	283600 ± 17630	245400 ± 3995 *
Area inside IEL (μm^2)	182500 ± 12240	144700 ± 5592 **
Medial area (μm^2)	101100 ± 6198	100700 ± 4142
Plaque area (μm^2)	85610 ± 11470	57060 ± 7369 *
Lumen area (μm^2)	108800 ± 6904	94620 ± 6235
Buried fibrous caps (% mice with caps)	75%	20%

Table 3.1 Compensatory remodelling maintains luminal area of brachiocephalic arteries

Sections of brachiocephalic arteries from vehicle and eplerenone treated DKO mice were subjected to morphometric analysis using Photoshop CS3 Extended software. The measurements show that MR blockade reduced the area inside the external elastic lamina (EEL) and internal elastic lamina (IEL) with no change in the medial area. Whilst plaque size was reduced with eplerenone treatment, the luminal area remained comparable with that in vehicle treated mice. Eplerenone also showed a trend to reduce the % of plaques that contained buried fibrous caps. Data are mean ± sem, n = 4-5. Data were analysed by Students unpaired t-test and * < 0.05; ** < 0.005.

3.3.2 Effect of MR blockade on the cellular composition of brachiocephalic plaques in DKO mice

Given the beneficial effect of eplerenone on atherogenesis in DKO brachiocephalic arteries, it was decided to investigate whether or not the cellular composition of plaques was also altered by MR blockade. Thus, brachiocephalic sections from vehicle and eplerenone treated animals were subjected to histological staining and immunohistochemistry using cell-specific antibodies.

3.3.2.1 Smooth Muscle Cells

Immigration of medial smooth muscle cells into the growing plaque signifies the progression from the fatty streak to the more complex lesion. Smooth muscle cells synthesise the extracellular matrix (ECM) proteins that contribute to the development of the fibrous cap, and are generally considered to be a stabilising factor in plaques. Immunohistochemical staining with anti-smooth muscle α-actin antibody revealed a higher density of SMCs in the plaques of eplerenone treated mice compared to vehicle treated mice (Figure 3.4). Quantitative analysis of 2-3 sections per vessel established that plaques from mice in the eplerenone group contained a significantly greater proportion of SMCs than did those from mice in the vehicle group (Figure 3.5).

3.3.2.2 Collagen

Collagen fibres are major components of the ECM that exists to provide stability to both healthy cells and tissues and to atherosclerotic plaques. Collagen content was assessed by staining DKO brachiocephalic sections with Picrosirius red and it was found that plaques from eplerenone treated animals appeared to show more abundant collagen staining when compared to plaques from animals in the vehicle group (Figure 3.4). Quantification of collagen staining in 2-3 sections per vessel confirmed that collagen content was significantly increased in plaques from DKO mice treated with eplerenone, compared to those that received vehicle (Figure 3.6)

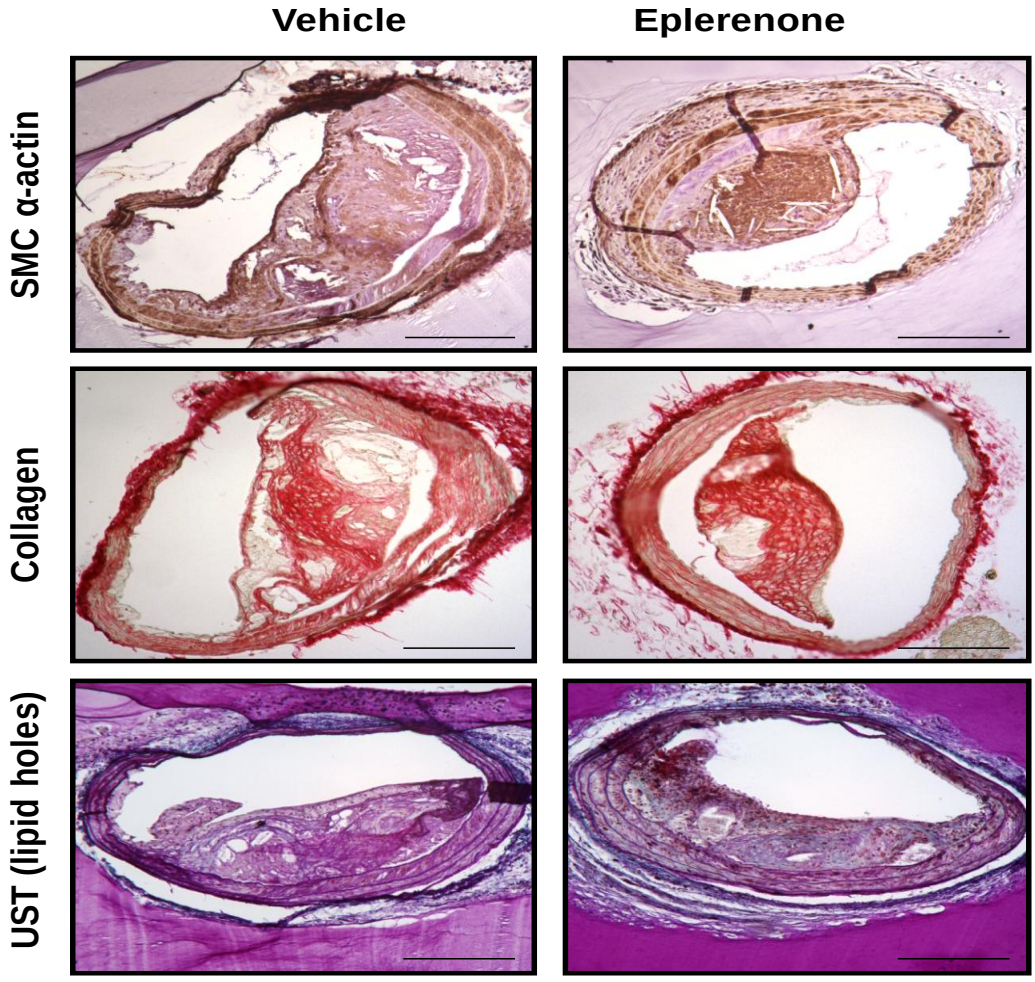

Figure 3.4 Altered composition of atherosclerotic plaques in DKO mice treated with eplerenone

Atherosclerotic plaques from mice treated with 200mg/kg/day eplerenone differed in composition from vehicle-treated controls. Plaques in eplerenone treated animals demonstrated increased staining for SMCs and collagen with no apparent difference in lipid content, compared to those in vehicle treated DKO mice. Representative images from vehicle (n=4) and eplerenone (n=5) treated animals, captured at x10 magnification. Scale bar = 250 µm.

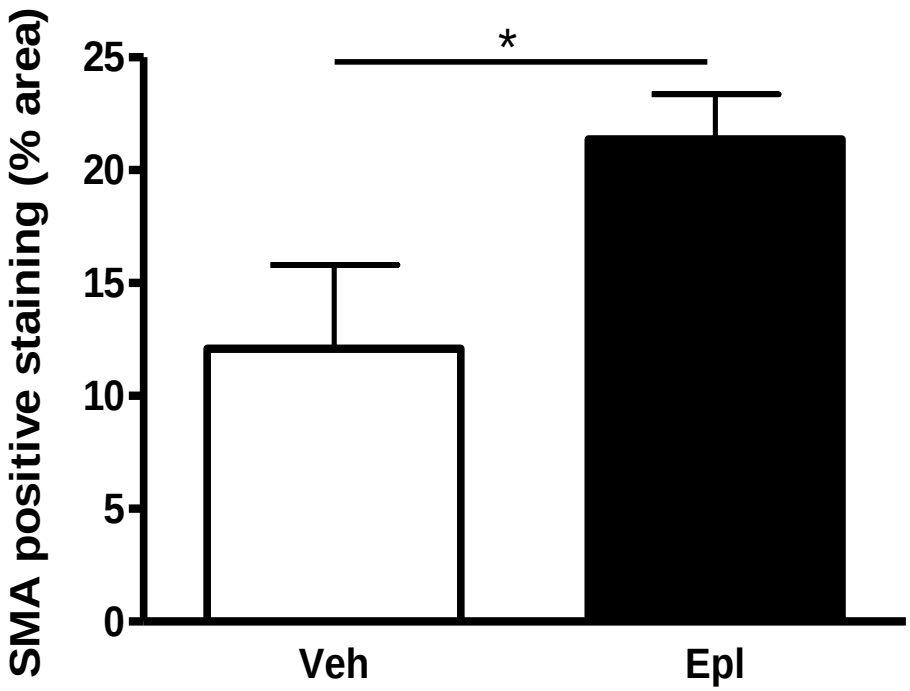

Figure 3.5 Eplerenone increased plaque SMC content in DKO mice

The area of smooth muscle actin staining in animals treated with 200mg/kg/day eplerenone or vehicle was quantified using Photoshop CS3 Extended software and expressed as a % of total plaque area. Eplerenone administration increased plaque SMC content compared to vehicle treatment. Data are mean ± sem, n= 4-5. Analysed by Student's unpaired t test: * $p<0.05$.

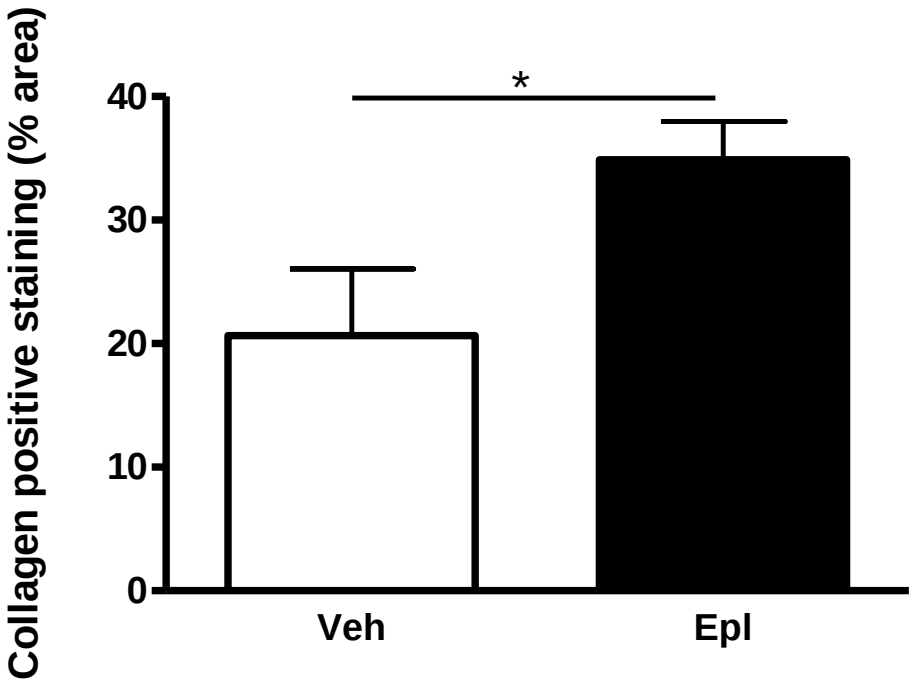

Figure 3.6 Eplerenone increased plaque collagen content in DKO mice

The area of collagen staining in animals treated with 200mg/kg/day eplerenone or vehicle was quantified and expressed as a % of total plaque area. Eplerenone administration increased plaque collagen content compared to vehicle treatment. Data are mean ± sem, n= 4-5. Analysed by Student's unpaired t test: * $p<0.05$.

3.3.2.3 Lipid

With atherosclerotic progression, lipids accumulate within the plaque at the expense of ECM and smooth muscle cells, aiding the formation of a destabilising necrotic lipid core. Thus, as a measure of plaque instability, lipid content was investigated by measuring the lipid holes left behind during histological processing in UST stained brachiocephalic sections. It appeared from observation of plaques from eplerenone and vehicle treated mice that lipid content was comparable between the two groups (Figure 3.4). Indeed, a lack of effect of eplerenone on the area of lipid holes was verified by quantitative analysis (Figure 3.7).

3.3.3 Effect of MR blockade on brachiocephalic plaque inflammation in DKO mice

Infiltration of monocytes into plaques and their subsequent differentiation into macrophage-derived foam cells is an important step in the development and progression of atherosclerosis. To investigate possible mechanisms behind the eplerenone-mediated retardation of atherogenesis in DKO mice, inflammatory cell infiltration was assessed in brachiocephalic plaques from vehicle and eplerenone treated animals. Macrophage content was determined using immunohistochemistry with specific antibodies and, upon microscopic examination, eplerenone treatment appeared to reduce the area of Mac-2 positive staining compared to vehicle treatment (Figure 3.8a). Quantitative image analysis revealed that eplerenone did indeed significantly reduce the macrophage content of plaques in DKO mice compared to vehicle treated mice (Figure 3.8b).

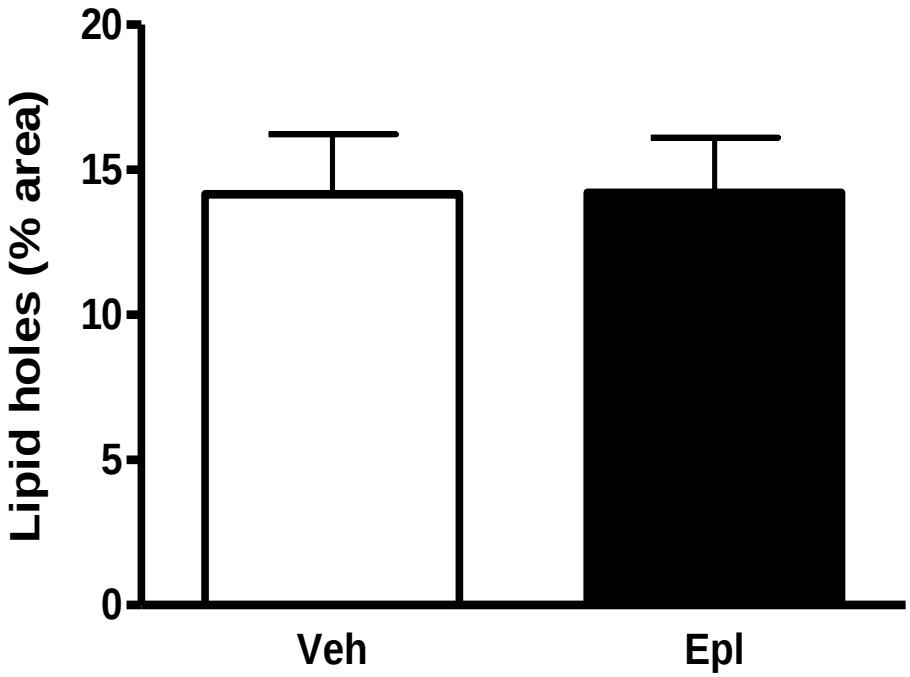

Figure 3.7 Eplerenone had no effect on plaque lipid content in DKO mice

The area of lipid holes in animals treated with 200mg/kg/day eplerenone or vehicle was quantified and expressed as a % of total plaque area. Eplerenone administration had no effect on the lipid content of DKO plaques with levels being comparable to those in vehicle control plaques. Data are mean ± sem, n= 4-5. Analysed by Student's unpaired t test: p = ns.

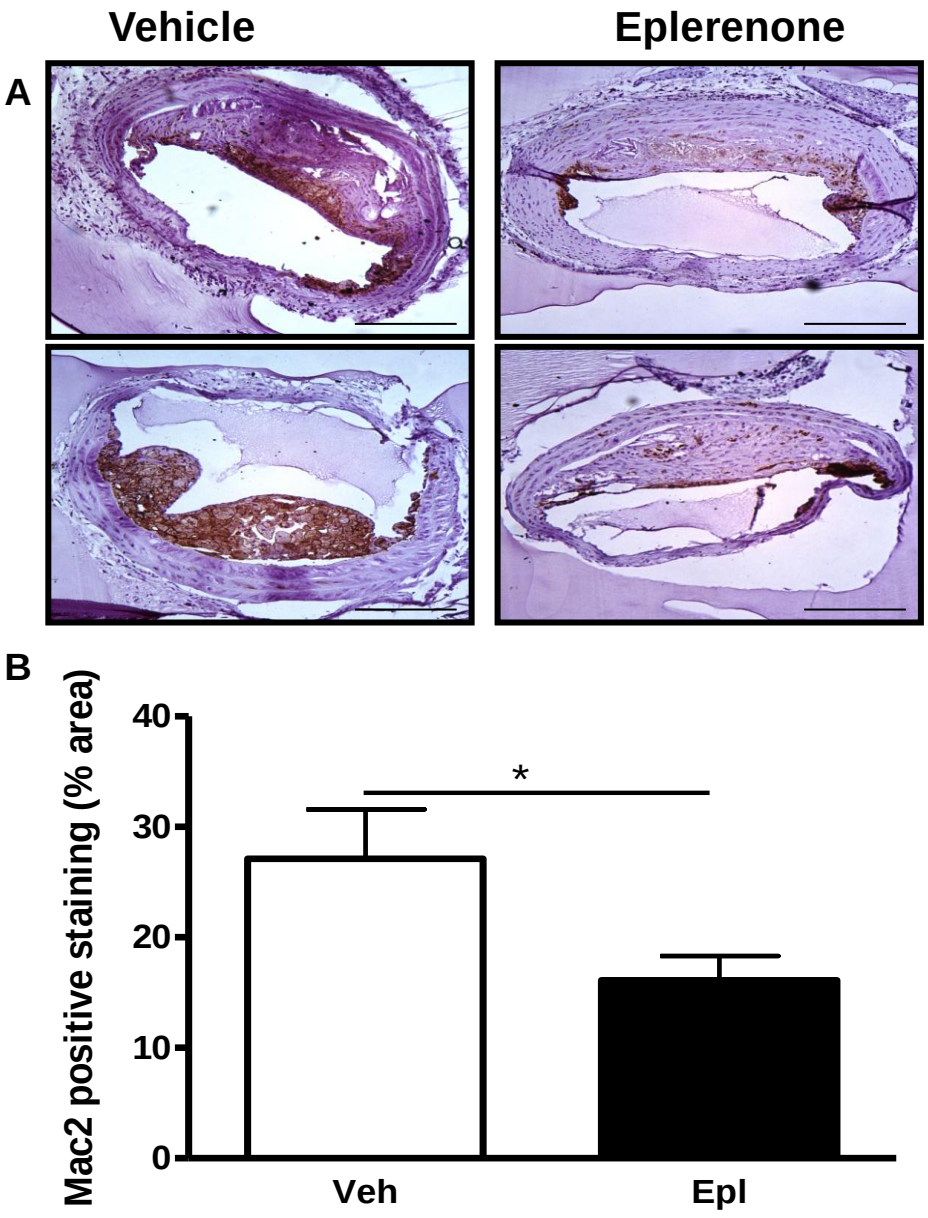

Figure 3.8 Eplerenone reduced plaque macrophage content in DKO mice

Sections of brachiocephalic arteries from animals treated with 200mg/kg/day eplerenone or vehicle for 12 weeks were stained with antibodies against Mac-2 (A). Plaque macrophage abundance appeared reduced with eplerenone compared to vehicle treatment. Representative images from two vehicle and two eplerenone treated animals, captured at x10 magnification. Scale bar = 250 µm. The area of Mac-2 staining was quantified and expressed as a % of total plaque area (B). Eplerenone administration led to a reduction in macrophage content of plaques from DKO mice compared to vehicle control mice. Data are mean ± sem, n= 4-5. Analysed by Student's unpaired t test: * $p<0.05$.

3.3.4 Influence of MR blockade on overall plaque stability in DKO mice

The fate of an advanced dynamic plaque depends on the balance of stabilising (SMCs and collagen) and degrading (lipids and macrophages) forces, the ratio of which is often used as an indication of overall plaque stability (Davies, 1996; Shiomi *et al.*, 2008). Creating a stacked-bar graph, where each stack represents either stabilising or destabilising components, allows a simple comparison of overall plaque composition between vehicle and eplerenone treated mice (Figure 3.9). The graph suggests that eplerenone treatment alters the composition of plaques, favouring a more stable phenotype. Plaques from eplerenone treated mice were made up of 56% stabilising components, largely collagen, and only 30% destabilising components, almost equal lipids and macrophages. In contrast, plaques from vehicle mice consisted of only 33% stabilising components, largely collagen, and 41% destabilising components, mostly macrophages. These four components, however, do not add up to 100% of lesion area and so there must also be other cell types within the plaque that aren't detected by any of the stains employed in this study. Other candidates could include ECM proteins other than collagen (e.g. elastin and fibronectin), minerals such as calcium, or other leukocytes (e.g. T-cells and mast cells).

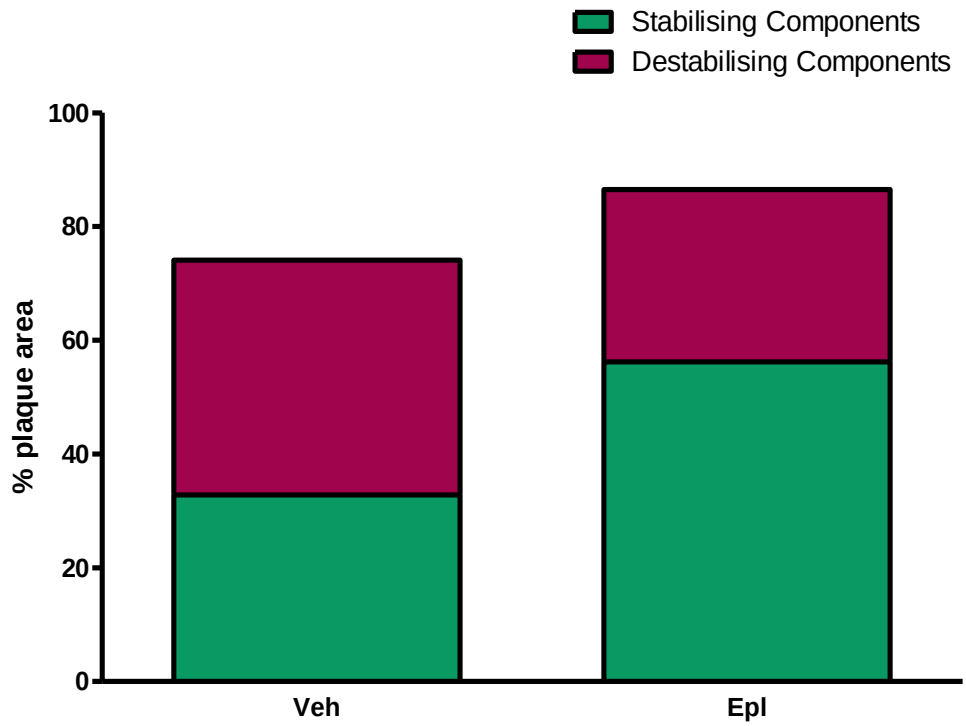

Figure 3.9 Eplerenone improved plaque stability in DKO mice

The contribution that stabilising and destabilising components make to the overall plaque gives an indication of plaque stability. Eplerenone treatment promotes plaque stability by altering plaque composition such that the ratio of stabilising (SMC and collagen) to degrading (lipid and macrophages) forces is increased compared to vehicle treatment.

3.4 Discussion

These studies demonstrated that treatment with eplerenone for 12 weeks slowed the progression of atherosclerosis and vascular remodelling in DKO mice. Plaque composition was altered such that mice receiving eplerenone developed more stable smooth muscle cell- and collagen-rich plaques whilst vulnerable lipid- and macrophage-rich plaques developed in vehicle treated mice. Vascular inflammation in DKO mice was reduced by eplerenone treatment as shown by a decrease in macrophage infiltration.

Effects of eplerenone on atherogenesis and vascular remodelling

Eplerenone was administered in standard chow diet at a dose of 200mg/kg of body weight/day, which was chosen as it reduced brachiocephalic lesion size without altering blood pressure in a previous study in DKO mice (Deuchar *et al.*, 2009). In the current study, eplerenone significantly decreased both plaque size and expansive vascular remodelling, without affecting medial or luminal area in DKO brachiocephalic arteries. This suggests that whilst inappropriate activation of MR accelerates atherogenesis in DKO mice, the lumen is maintained by compensatory expansion of the vascular wall. It is well established that atherosclerosis promotes this type of remodelling (Glagov *et al.*, 1987) and, since a reduction in plaque size with eplerenone was associated with a reduction in vascular remodelling, it is clear that the outward remodelling in DKO mice is a direct consequence of plaque growth, and not due to other effects of MR activation such as hypertension, which was not normalised in eplerenone treated mice (Deuchar *et al.*, 2009). Moreover, remodelling in hypertensive disorders is generally 'inward' and is characterised by medial thickening, decreased luminal patency, and an increased extracellular matrix (Roman *et al.*, 1992; Safar *et al.*, 1998), features that were not observed in brachiocephalic arteries of vehicle or eplerenone treated DKO mice. In addition to this, although MR activation by aldosterone is associated with vascular injury and remodelling in stroke-prone hypertensive rats (Rocha *et al.*, 1998) and in hypertensive humans (Schiffrin *et al.*, 2004), it is the inward type of remodelling and not the expansive type that is found with atherosclerosis. This lends further support

to the notion that the vascular remodelling associated with MR activation in DKO mice is a result of increased plaque size.

The fact that eplerenone significantly reduced plaque size in DKO mice demonstrates that inappropriate MR activation is causal in the accelerated atherogenesis in this model. DKO mice are hypertensive, due to loss of 11β-HSD2-mediated protection of renal MR, and the link between hypertension and atherosclerosis is well established. Indeed, atherosclerosis has been shown to be 3 times more common in patients with hypertension (Doyle, 1990) and *Apoe*$^{-/-}$ mice that are hypertensive due to inactivation of the eNOS gene developed larger lesions than single *Apoe*$^{-/-}$ controls (Knowles *et al.*, 2000). However, the plaque reducing effects of eplerenone in DKO mice occurred at a dose that did not reduce blood pressure, suggesting an important role for MR activation in extra-renal cells in this phenotype. In line with this, reduction of the renal consequences of MR activation by inhibition of ENaC with amiloride did significantly reduce blood pressure but had no effect on the atherosclerotic burden in DKO mice (Deuchar *et al.*, 2009). This is in agreement with the RALES (Pitt *et al.*, 1999) and EPHESUS (Pitt *et al.*, 2001) trials where treatment with sub-hypotensive doses of spironolactone and eplerenone had significant cardio-protective benefits in patients with heart failure.

Cells of the vasculature are prime candidates for a role in MR-mediated atherogenesis; not only are they implicitly involved in all stages of atherosclerosis (Libby *et al.*, 2002) but they also express the necessary components (Takeda, 1993) to be mineralocorticoid/glucocorticoid responsive. The major initiating event in atherosclerosis is endothelial cell dysfunction and, given that 11β-HSD2$^{-/-}$ mice display features of this (Hadoke *et al.*, 2001), it is likely that endothelial dysfunction is an important contributor to the accelerated atherogenesis in DKO mice. An elegant set of studies using HUVECs has defined a role for aldosterone-mediated MR activation in processes associated with dysfunction such as endothelial cell swelling (Oberleithner *et al.*, 2004), stiffening and vulnerability to shear stress (Oberleithner *et al.*, 2006), and decreased nitric oxide (NO) production (Oberleithner *et al.*, 2007). Whilst aldosterone has been shown to have a wide range of detrimental effects on the vasculature (Schiffrin, 2006b), which may be important

in the DKO phenotype, the loss of glucocorticoid inactivation by 11β-HSD2 in DKO mice points towards inappropriate activation of MR by glucocorticoids as a significant mechanism in the accelerated atherogenesis. A recent study in rat vascular smooth muscle cells reported stimulation of MR-dependent signalling pathways by physiological concentrations of corticosterone in the absence of 11β-HSD2 activity (Molnar *et al.*, 2008). This same study also reported that corticosterone acts on intact endothelial cells to enhance the phenylephrine-induced contraction of aortic rings; reduction of this effect by spironolactone showed that this action of corticosterone was at least partially MR-mediated. Thus, glucocorticoids are able to regulate vascular function through MR but the specific role of 11β-HSD2 in mediating these actions remains to be defined.

Mechanisms of eplerenone action

The reduction in plaque size with MR blockade in DKO mice may represent one of the potential mechanisms by which eplerenone exerts its beneficial effects on cardiovascular morbidity and mortality. The question now arises as to how MR blockade results in reduced plaque size. In DKO mice, MR is likely to be continually occupied by glucocorticoids, causing a level of illicit activation that would not commonly be reached in most animals. Thus, it could be that blockade of MR in the DKO would produce effects in this model that wouldn't necessarily be beneficial, or relevant, in other animals. However, evidence from studies using eplerenone in other models, where 11β-HSD2 was not manipulated, suggests that MR blockade does reduce atherosclerotic burden in the absence of 11β-HSD2 inactivation. In support of this, eplerenone significantly reduced atherosclerosis in non-human primates fed a high cholesterol diet without affecting blood pressure (Takai *et al.*, 2005). The authors suggest that the plaque reduction may have been due to effects of eplerenone on decreasing levels of oxidized LDL and improving EC function (Takai *et al.*, 2005). Another study reported that eplerenone improved EC function and reduced superoxide production in cholesterol fed rabbits (Rajagopalan *et al.*, 2002). Taken together, these studies in combination with the present DKO data suggest a detrimental role for endothelial cell MR activation and subsequent dysfunction in promoting atherosclerosis. It is also evident that eplerenone is

efficacious in cardiovascular pathologies even when 11β-HSD2 is present to protect MR, suggesting that either increased mineralocorticoid/glucocorticoid levels or decreased vascular 11β-HSD2 activity may be features of certain diseases. In agreement with this, it was recently reported that tumour necrosis factor α (TNF-α) dose-dependently inhibited 11β-HSD2 activity and mRNA expression in a human bronchial epithelial cell line (Suzuki *et al.*, 2005). Further, an *in vivo* study demonstrated that transgenic over-expression of TNF-α in mice led to reduced 11β-HSD2 activity and mRNA in the kidney (Kostadinova *et al.*, 2005). Thus, it is plausible that in pro-inflammatory states, where TNF-α, and perhaps other cytokines are up-regulated, 11β-HSD2 activity may be compromised. Indeed, TNF-α is known to be expressed in macrophages, smooth muscle cells, and endothelial cells in human blood vessels affected by atheroma, but not in unaffected vessels (Barath *et al.*, 1990). Taken together, these studies support the idea that the normal protection of MR afforded by 11β-HSD2 may be reduced or even lost during atherosclerosis. When the findings from the DKO model are also considered, it could be suggested that pro-inflammatory processes lead to down-regulation of 11β-HSD2 activity thereby promoting illicit activation of MR and accelerating atherogenesis. This may also explain why MR blockade with eplerenone is cardioprotective. However, decreased 11β-HSD2 activity may not be the only mechanism involved in pro-inflammatory regulation of MR activation. It has also been shown that transgenic mice over-expressing TNF-α have increased 11β-HSD1 activity in the liver (Ignatova *et al.*, 2009), providing a mechanism by which inflammatory conditions may enhance local glucocorticoid levels. The combination of decreased 11β-HSD2 activity with increased levels of glucocorticoids in pro-inflammatory states such as atherosclerosis has profound implications for inappropriate MR activation and its subsequent pathological consequences.

Effects of eplerenone on plaque composition and inflammation

Whilst the smaller plaque size in eplerenone treated mice was not associated with a larger lumen in the present study, by retarding the progression of atherogenesis eplerenone may prolong the stability of the lesion. However, a smaller plaque does not necessarily translate into increased stability. The only way to determine whether

or not eplerenone promotes plaque stability is to investigate its effects on the composition of lesions. The reduction in plaque size with eplerenone treatment was accompanied by an alteration in the cellular composition of plaques in DKO mice.

Both smooth muscle cell (SMC) actin and collagen content were significantly increased by eplerenone in brachiocephalic plaques. This implies that MR activation concomitantly increases lesion area whilst decreasing the content of particular cells. Perhaps activation of MR in the SMCs themselves promotes apoptosis or inhibits proliferation and migration. However, evidence suggests the contrary, and activation of MR in human vascular SMCs may promote proliferation by increasing expression of the anti-apoptotic cell cycle gene MDM2 (Nakamura *et al.*, 2006). Smooth muscle cell and collagen biology are intimately linked (Rekhter, 1999) and so it could be that the increased plaque content of both of these components upon MR blockade is a direct result of this relationship. It is known that SMCs are the major cellular source of collagen in plaques (Rekhter, 1999) and that collagen deposition is required for SMC migration (Rocnik *et al.*, 1998). Therefore, does MR activation lead to decreased SMC content, resulting in less collagen secretion or does it lead to decreased collagen content which, in turn, reduces SMC migration into the plaque? It has previously been reported that activation of MR in the heart leads to fibrosis characterised by increased collagen deposition (Chai *et al.*, 2006; Young *et al.*, 1994) and that this can be reversed with MR blockade (Stas *et al.*, 2007; Suzuki *et al.*, 2002). Based on this it might be expected that MR activation in the DKO would increase plaque collagen content; perhaps the discrepancy between prediction and observation is indicative of differential effects of MR activation in different cell types. The amount of collagen present in a plaque is not only determined by its rate of secretion, but also by its degradation. The matrix metalloproteinases (MMPs) are a group of enzymes responsible for degrading extracellular matrix proteins, including collagen (Lee *et al.*, 1997), and are up-regulated in human atherosclerotic plaques, most notably in the vulnerable shoulder regions (Galis *et al.*, 1995). The decreased collagen content due to MR activation in DKO plaques could, therefore, be a result of increased MMP activity. Indeed, it was reported that blockade of MR with eplerenone inhibited MMP activity in the hearts of dogs suffering from

experimentally induced heart failure (Suzuki *et al.*, 2002). Given that macrophages are a key source of MMPs (Welgus *et al.*, 1990) and that plaque macrophage content was decreased by eplerenone in DKO mice, it could be postulated that MR activation promotes macrophage infiltration into DKO plaques, where these cells then secrete MMPs causing increased collagen degradation.

Plaque macrophages not only secrete matrix degrading enzymes, but they are also involved in a host of pro-inflammatory processes that propagate atheroma development and progression (Lucas *et al.*, 2001). The finding that eplerenone treatment was associated with reduced macrophage infiltration into DKO plaques is suggestive of a role for MR activation in the generation of a pro-inflammatory environment. In support of this, administration of aldosterone to rats induced the formation of coronary inflammatory lesions characterized by macrophage infiltration, an effect that was reversed by MR antagonism (Rocha *et al.*, 2002b). Also, other studies have demonstrated effects of MR activation on macrophage oxidative stress in mice (Keidar *et al.*, 2003) and on macrophage recruitment during peritoneal fibrosis in rats (Nishimura *et al.*, 2008). However, the present study is the first to describe a role for vascular 11β-HSD2 in protection against MR-mediated enhancement of macrophage infiltration into murine atherosclerotic plaques. Increased macrophage content in DKO plaques could be due to MR activation in a number of cells. Macrophages express MR (Barish *et al.*, 2005) and it was recently reported that deletion of MR specifically from murine macrophages decreased mineralocorticoid-induced cardiac fibrosis and demonstrated an important role for macrophage MR signalling in cardiovascular pathologies associated with mineralocorticoid excess (Rickard *et al.*, 2009b). However, this study also reported that macrophage recruitment was not affected by loss of MR suggesting that activation of MR in DKO macrophages may not be the mechanism of increased infiltration into plaques. Having said this, whilst macrophage recruitment to the heart was not affected by loss of MR (Rickard *et al.*, 2009a), perhaps macrophage MR activation plays a role in macrophage recruitment to the vascular wall under certain conditions. It could be that activation of MR in macrophages increases their circulating levels or activation status and if this were combined with increased

adhesion molecule and cytokine expression, as is found in atherosclerosis, then the situation could be envisaged where increased capture and infiltration of macrophages occurs at sites of lesion development. However, 11β-HSD2 is not present in macrophages to protect the MR (Gilmour *et al.*, 2006) and so the receptor will normally be occupied by glucocorticoids in these cells. Thus, it seems unlikely that the loss of 11β-HSD2 activity in DKO mice would have a substantial effect on macrophage MR activation, which points towards MR-mediated mechanisms in other cell types as being important in macrophage recruitment to DKO plaques. The endothelium is known to play a vital role in the infiltration of monocytes into the intimal space during the early stages of atherogenesis, partially through the expression of cellular adhesion molecules. This particular issue is investigated and discussed in the following chapters.

The proportion of plaque lipids was not altered by MR blockade with eplerenone and this could be attributable to several reasons. Firstly, DKO mice are on the hypercholesterolemic *Apoe*$^{-/-}$ background and eplerenone treatment is not expected to affect cholesterol levels, as shown in other studies (Keidar *et al.*, 2003; Suzuki *et al.*, 2006b; Takai *et al.*, 2005). Therefore, if circulating cholesterol levels are the main predictor of plaque lipid content, comparable levels between vehicle and eplerenone treated mice would be expected. Secondly, there is little or no evidence in the literature to implicate MR signalling pathways in lipid synthesis/metabolism. Having said this, the one MR-mediated factor that was not altered by eplerenone in DKO mice was blood pressure (Deuchar *et al.*, 2009). It is possible that the lack of effect on plaque lipids is a consequence of the lack of eplerenone efficacy in reduction of blood pressure via renal MR.

Effects of eplerenone on plaque stability

The overall effect of eplerenone on DKO atherogenesis was a stabilisation of the plaque. Mice in the vehicle group exhibited a vulnerable plaque phenotype with a larger lipid + macrophage content compared to SMC + collagen content. MR blockade in the eplerenone group shifted the balance towards a more stable plaque with a higher SMC + collagen content and a reduced lipid + macrophage content.

Collagen, whilst promoting the growth of the atherosclerotic plaque, is thought to be a stabilising material by contributing to the integrity of the fibrous cap (Rekhter, 1999). A loss of collagen content in DKO mice is therefore considered to be a destabilising action of MR activation. Given that MR activation would normally be expected to increase SMC proliferation and collagen deposition in cardiovascular pathologies, and that lipid content was not altered with eplerenone, it seems likely that the beneficial effect of MR blockade in DKO mice is due to the reduction in macrophage infiltration. Further, it could be that increased MR-mediated macrophage infiltration in DKO mice is the underlying mechanism driving the accelerated atherogenesis. Previous studies have demonstrated that macrophages in culture may promote collagen breakdown of human fibrous caps (Shah *et al.*, 1995) and that the mechanical strength of human aortic plaques was reduced when macrophage density was increased (Lendon *et al.*, 1991). This, along with the fact that SMC and collagen content were decreased, either at the expense of or as a direct result of increased macrophage content in vehicle treated DKO plaques, reveals a very important role for the macrophage in the vulnerable plaque. Whilst many studies have shown an inhibitory effect of eplerenone on atherogenesis in various models, there is little information on plaque stabilisation by eplerenone. An investigation in *Apoe*$^{-/-}$ mice found that eplerenone treatment reduced the susceptibility of LDL to oxidation (Keidar *et al.*, 2003). LDL oxidation and its subsequent uptake by macrophages leads to the formation of foam cells which are thought to be detrimental to plaque stability (Ball *et al.*, 1995; Rajagopalan *et al.*, 1996). Taken together, this provides indirect evidence for a plaque stabilising effect of eplerenone. However, the present study provides direct evidence that MR activation leads to a vulnerable plaque phenotype characterised by vascular inflammation and that this can be reversed by treatment with eplerenone. Eplerenone also showed a trend to decrease the incidence of buried fibrous caps in DKO plaques with only one in five of the mice in the eplerenone group showing the presence of buried caps, compared to three out of four mice in the vehicle group. It has been suggested that buried fibrous caps are indicative of previous plaque ruptures, indeed one study found a significant positive correlation between acute plaque rupture and the development of buried fibrous caps (Johnson *et al.*, 2005). It is thought that

plaques grow through continuous cycles of plaque rupture and healing (Heistad, 2003) and so it could be that stabilisation of plaques by MR blockade along with the associated decrease in buried fibrous caps contributes towards the reduced plaque size in eplerenone treated animals.

One final point to consider is that eplerenone treatment was started in DKO mice at 2 months of age and by this stage inappropriate MR activation will be well established, along with some of its phenotypic manifestations. Detrimental alterations in cardiovascular physiology and perhaps anatomy will begin *in utero* and so some of the effects of MR activation may be too advanced by two months of age for eplerenone to have a beneficial impact. Thus, in order to determine more fully the range of effects of MR activation on atherogenesis, a direct comparison needs to be made between DKO and *Apoe*$^{-/-}$ control mice, this is dealt with in the next chapter

Conclusions

Inappropriate activation of MR is causal in the DKO atherosclerotic phenotype. Blockade of MR with eplerenone not only reduces the brachiocephalic atherosclerotic burden, but it also promotes plaque stability by altering the cellular composition of lesions. Eplerenone also reduces macrophage infiltration into plaques indicating an inhibitory effect on vascular inflammation in the DKO mouse. The mechanisms behind the cardio-protective effects of eplerenone are largely unknown and so the knowledge in this area is enhanced by the results of this study. The present study also signifies a vital function of 11β-HSD2 in preventing, or at least slowing, the development of vulnerable atherosclerotic plaques. The fact that eplerenone reduced atherogenesis without altering blood pressure is suggestive of a role for extra-renal MR activation in the DKO atherosclerotic phenotype.

Chapter 4
Mechanisms of accelerated atherogenesis in the DKO mouse

4.1 Introduction

It was determined in the previous chapter that activation of MR in DKO mice is responsible for the accelerated atherosclerosis and a vulnerable plaque phenotype characterised by inflammation. However, to more fully characterise the mechanisms involved in this phenotype, a direct comparison of the atheroma in DKO and *Apoe*$^{-/-}$ brachiocephalic arteries is required. This will not only aid in determining the effects of 11β-HSD2 inactivation on atherogenesis but, by comparing the results with those in eplerenone treated DKO mice, it will also help to distinguish between the consequences of renal and non-renal MR activation.

Preliminary findings showed that compared to *Apoe*$^{-/-}$ mice, DKO mice have accelerated atherogenesis due to over-activation of MR (Deuchar *et al.*, 2009). The studies in the previous chapter advanced the understanding of how MR activation accelerates atherosclerosis by showing effects on the cellular composition and inflammatory environment of the plaque. However, what remains unclear from these studies are the mechanisms by which 11β-HSD2 activity influences atherogenesis, and whether it is via systemic actions on factors such as plasma lipid levels or blood pressure, or caused by a local effect on the cells of the vascular wall. To begin to explore the influence of 11β-HSD2 inactivation on the cellular composition and stability of atherosclerotic plaques, it was hypothesised that loss of 11β-HSD2-mediated protection of MR would alter the cellular composition of lesions and promote a pro-inflammatory environment in DKO brachiocephalic plaques. This was based on the previous observations (chapter 3) that blockade of MR in DKO mice promotes plaque stability by reducing vascular inflammation. With this in mind, the specific aims of this chapter were:

(i) To identify the differences in cellular composition between *Apoe*$^{-/-}$ and DKO plaques that may account for the accelerated atherogenesis.

(ii) To determine the effects of loss of 11β-HSD2 activity on plaque stability and inflammation.

4.2 Methods

4.2.1 Experimental mice

An established colony of *Apoe*$^{-/-}$ and *Apoe*$^{-/-}$/11β-HSD2$^{-/-}$ DKO mice were maintained on standard chow diet with water *ad libitum*. At 3 or 6 months of age, 5-8 male and female (due to lack of sufficient males) mice per group were culled by asphyxiation with CO_2.

4.2.2 Assessment of atherosclerosis

Atherosclerosis was investigated in *Apoe*$^{-/-}$ and DKO mice at two different time points, chosen based on preliminary studies in 3 and 6 month old DKO mice, to represent early and established lesions respectively. For detailed methods on the characterisation of atherosclerosis see section 2.3. Histological and immunohistochemical techniques were performed according to the methods detailed in section 2.3.2. The section with the largest plaque was chosen to represent each artery when calculating the mean parameters in a group.

4.2.3 Cholesterol Measurement

A commercial kit was used to measure cholesterol levels in plasma samples from *Apoe*$^{-/-}$ and DKO mice at 6 months of age (see section 2.3.4).

4.2.4 Statistical analysis

Data are mean ± sem and were analysed by two-way ANOVA or unpaired Students t-test for cholesterol data.

4.3 Results

4.3.1 Effect of 11β-HSD2 inactivation on atherosclerotic burden and vascular remodelling in *Apoe*$^{-/-}$ mice

In order to confirm the findings of previous studies in DKO mice (Deuchar *et al.*, 2009), plaque size was compared in brachiocephalic arteries from *Apoe*$^{-/-}$ and DKO mice at 3 and 6 months of age. These time points were chosen to represent early (3 months) and established (6 months) atherosclerosis in DKO mice. Haematoxylin stained sections (previously subjected to 'test-run' immunohistochemistry for CD31 staining, not employed itself in this thesis) revealed plaques in DKO mice at 3 months whilst *Apoe*$^{-/-}$ mice were completely lesion free at this age (Figure 4.1a). By 6 months, some *Apoe*$^{-/-}$ mice had developed plaques while DKO mice at this age showed much larger plaques (Figure 4.1a). Quantitative analysis of the sections with the largest plaques from each vessel confirmed that plaque size was significantly increased in DKO mice at both 3 and 6 months compared to age-matched *Apoe*$^{-/-}$ controls (Figure 4.1b). This analysis also showed that 3 month DKO plaques are comparable in size to those in 6 month *Apoe*$^{-/-}$ mice (Figure 4.1b).

Vascular remodelling was investigated in *Apoe*$^{-/-}$ and DKO brachiocephalic arterial sections to determine whether or not the accelerated atherogenesis in DKO mice was associated with alterations in other vascular parameters. The results are shown in Table 4.1 and indicate that DKO brachiocephalic arteries are expansively remodelled with an increased area inside the EEL at 3 and 6 months and an increased area inside the IEL at 6 months, compared to age-matched *Apoe*$^{-/-}$ mice. There is also significant medial proliferation in DKO mice at 3 and 6 months compared to *Apoe*$^{-/-}$ controls. Despite an increase in plaque area in DKO mice, the luminal area was maintained due to the outward remodelling in DKO mice compared to *Apoe*$^{-/-}$ mice. Interestingly, 3 month DKO mice and 6 month *Apoe*$^{-/-}$ mice are comparable in all parameters except medial area, which is significantly increased in the DKOs. These results suggest that whilst loss of 11β-HSD2 activity in DKO mice leads to accelerated atherogenesis, it does not affect the luminal patency of brachiocephalic arteries due to compensatory outwards remodelling of the vessel.

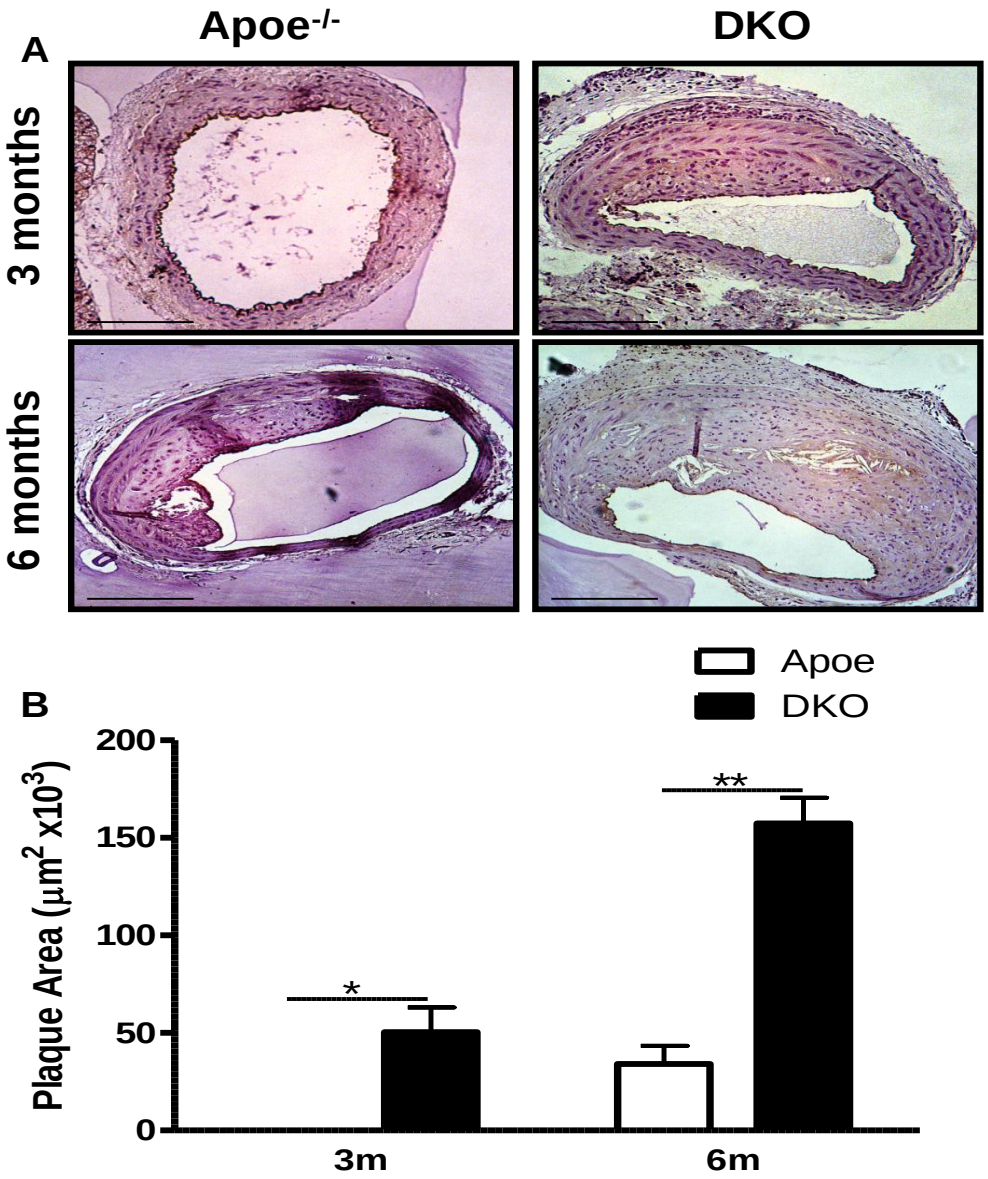

Figure 4.1 Atherosclerotic burden is increased in DKO brachiocephalic arteries

Sections of brachiocephalic arteries from *Apoe*$^{-/-}$ and DKO animals were stained with haematoxylin (A). Atherosclerotic plaques developed in DKO but not *Apoe*$^{-/-}$ mice at 3 months of age and by 6 months *Apoe*$^{-/-}$ mice showed plaques that appeared smaller in size, compared to age-matched DKO mice. Representative images from *Apoe*$^{-/-}$ (n= 6-7) and DKO (n= 7-8) animals, captured at x10 magnification. Scale bar = 250 µm. The area of atherosclerotic plaque was quantified using Photoshop CS3 Extended software (B). DKO plaques were larger than *Apoe*$^{-/-}$ plaques at both 3 and 6 months of age and plaque sizes were comparable between 3 month DKO and 6 month *Apoe*$^{-/-}$ mice. Data are mean ± sem, n= 6-8 per group. Analysed by two-way ANOVA: * $p<0.01$, ** $p<0.001$.

	3 months		6 months	
	Apoe$^{-/-}$	DKO	Apoe$^{-/-}$	DKO
Area inside EEL (μm^2)	100924 ± 17266	253445 ± 34615 *	229724 ± 25376	370073 ± 25604 **
Area inside IEL (μm^2)	58107 ± 11602	147122 ± 24678	157806 ± 19722	256115 ± 22660 *
Medial area (μm^2)	42817 ± 8537	106323 ± 10684 ***	71918 ± 7856	113958 ± 6506 **
Plaque area (μm^2)	0	56767 ± 14399 **	34504 ± 15642	149493 ± 13233 ***
Lumen area (μm^2)	58107 ± 11602	90355 ± 16000	123302 ± 12258	106623 ± 18668
Buried fibrous caps (% mice with caps)	0	57%	33%	75%

Table 4.1 Morphometric analysis of brachiocephalic arteries reveals maintenance of lumen in DKO mice

Sections of brachiocephalic arteries from *Apoe*$^{-/-}$ and DKO mice at 3 and 6 months of age were subjected to morphometric analysis using Photoshop CS3 Extended software. DKO mice showed an increase in the area inside the external elastic lamina (EEL) at 3 and 6 months and an increase in the internal elastic lamina (IEL) at 6 months only compared to *Apoe*$^{-/-}$ mice. DKO mice showed increased medial area at 3 and 6 months compared to *Apoe*$^{-/-}$ mice. Whilst plaque size was increased in DKO mice at 3 and 6 months, the luminal area remained comparable with that in *Apoe*$^{-/-}$ mice at both ages. There was also a trend towards an increase in buried fibrous cap incidence in DKO mice compared to *Apoe*$^{-/-}$ controls. Data are mean ± sem, n = 5-8 per group. Data were analysed by two-way ANOVA and * $p< 0.01$; ** $p< 0.001$; *** $p<0.0001$.

4.3.2 Total plasma cholesterol levels in *Apoe*$^{-/-}$ vs. DKO mice

To determine whether or not the accelerated atherogenesis in DKO mice could be accounted for by increased cholesterol levels, over and above the levels conferred by Apoe knockout, total plasma cholesterol levels were measured in *Apoe*$^{-/-}$ and DKO mice at 6 months of age. As expected, it was found that there was no significant difference in total plasma cholesterol levels between *Apoe*$^{-/-}$ and DKO mice (Figure 4.2) and so this is not a factor in the DKO atherosclerotic phenotype.

4.3.3 Influence of 11β-HSD2 inactivation on the cellular composition of brachiocephalic plaques in *Apoe*$^{-/-}$ mice

Given the detrimental effect of loss of 11β-HSD2 activity on atherogenesis in DKO brachiocephalic arteries, and the benefits observed with MR blockade in the eplerenone study, it was of interest to investigate whether or not this phenotype was associated with alterations in the cellular composition of plaques. Thus, brachiocephalic sections from *Apoe*$^{-/-}$ and DKO animals at 3 and 6 months of age were subjected to histological staining and immunohistochemistry using cell-specific antibodies.

4.3.3.1 Smooth Muscle Cells

Smooth muscle cells (SMC) are generally considered to be a stabilising factor in plaques and the previous chapter showed an increase in the content of these cells following MR blockade, suggesting that 11β-HSD2 inactivation diminishes the SMC content of plaques in *Apoe*$^{-/-}$ mice. In order to determine if this was in fact the case, immunohistochemical staining with anti-smooth muscle α-actin antibody was performed. Quantitative analysis of 5-7 vessels per group established that there was no significant difference in plaque SMC content between *Apoe*$^{-/-}$ and DKO mice at 3 or 6 months of age (Figure 4.3).

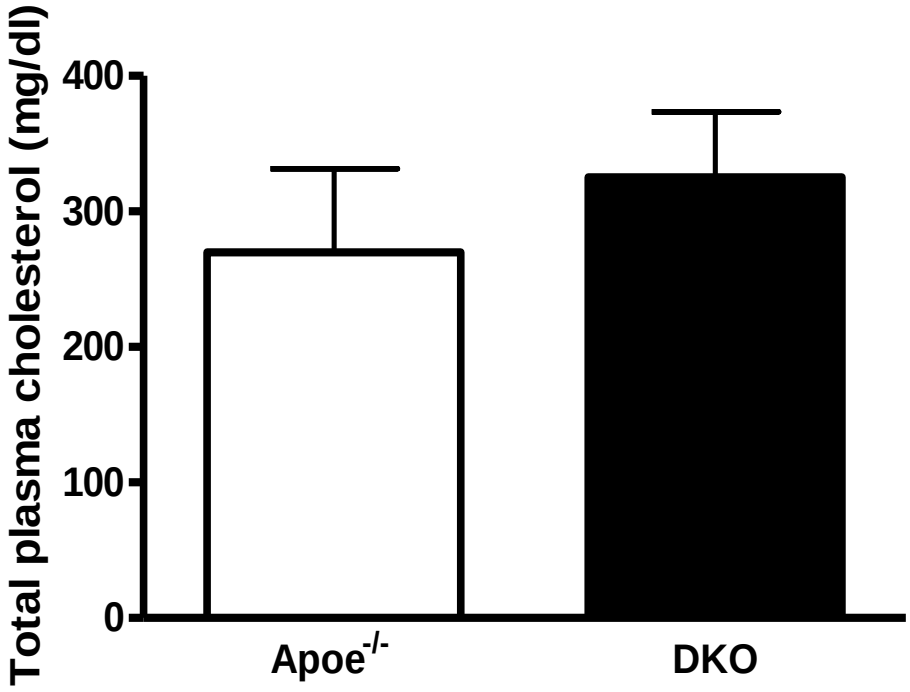

Figure 4.2 Total plasma cholesterol levels were comparable in Apoe$^{-/-}$ and DKO mice

Total plasma cholesterol levels were measured in *Apoe*$^{-/-}$ and DKO mice at 6 months of age using a commercial kit. Cholesterol levels were found to be comparable between DKO and *Apoe*$^{-/-}$ mice. Data are mean ± sem, n= 8 per group. Analysed by Student's t-test: p=ns.

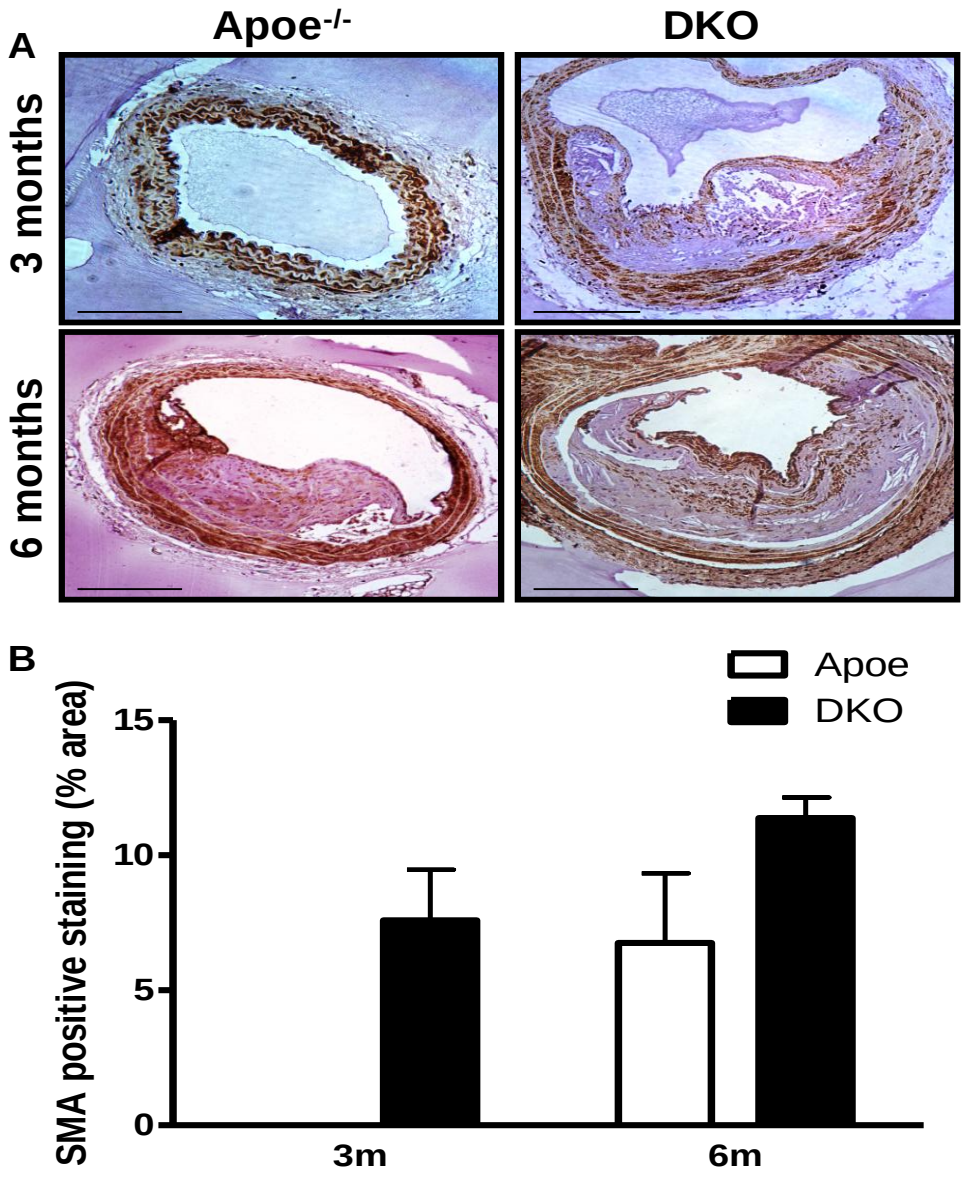

Figure 4.3 Smooth muscle cell content is not altered in brachiocephalic plaques from DKO mice

Representative images of atherosclerotic plaques from *Apoe*$^{-/-}$ and DKO animals stained with specific antibody against smooth muscle α-actin show similar abundance of staining for SMCs (A). Captured at x10 magnification, scale bar = 250 µm. The area of smooth muscle actin staining was quantified using Photoshop CS3 Extended software and expressed as a % of total plaque area (B). There was no difference in the SMC content of plaques between *Apoe*$^{-/-}$ and DKO mice at either 3 or 6 months of age, *Apoe*$^{-/-}$ mice at 3 months lack plaques. Data are mean ± sem, n= 5-7. Analysed by two-way ANOVA: p=ns

4.3.3.2 Collagen

The finding that collagen content was increased by eplerenone treatment in DKO plaques indicates that lack of 11β-HSD2 activity results in a vulnerable collagen-poor plaque. Collagen content was assessed by staining *Apoe*$^{-/-}$ and DKO brachiocephalic sections with Picrosirius red. Plaques from DKO animals at 3 and 6 months show less abundant collagen staining compared to plaques in 6 month old *Apoe*$^{-/-}$ mice (Figure 4.4a). Quantification of Picrosirius red staining in 5-6 vessels per group confirmed that collagen content was significantly decreased at both 3 and 6 months in plaques from DKO mice compared to those from 6 month *Apoe*$^{-/-}$ mice (Figure 4.4b)

4.3.3.3 Lipid

As a measure of plaque instability (Davies, 1996; Shiomi *et al.*, 2008), lipid content was investigated by measuring the lipid holes left behind during histological processing in UST stained brachiocephalic sections. Measurement of hole size suggested that lipid content was greater in plaques of 3 and 6 month DKO than in 6 month *Apoe*$^{-/-}$ mice (Figure 4.5a). Indeed, an enhancing effect of 11β-HSD2 inactivation on plaque lipid content was verified by quantitative analysis (Figure 4.5b).

4.3.3.4 Macrophages

Inflammatory cell infiltration was assessed in brachiocephalic plaques from DKO and Apoe$^{-/-}$ animals by staining for the macrophage specific marker, mac-2. Microscopic examination and quantitative image analysis revealed that loss of 11β-HSD2 activity in *Apoe*$^{-/-}$ mice increased the area of mac-2 positive staining at both 3 and 6 months (Figure 4.6).

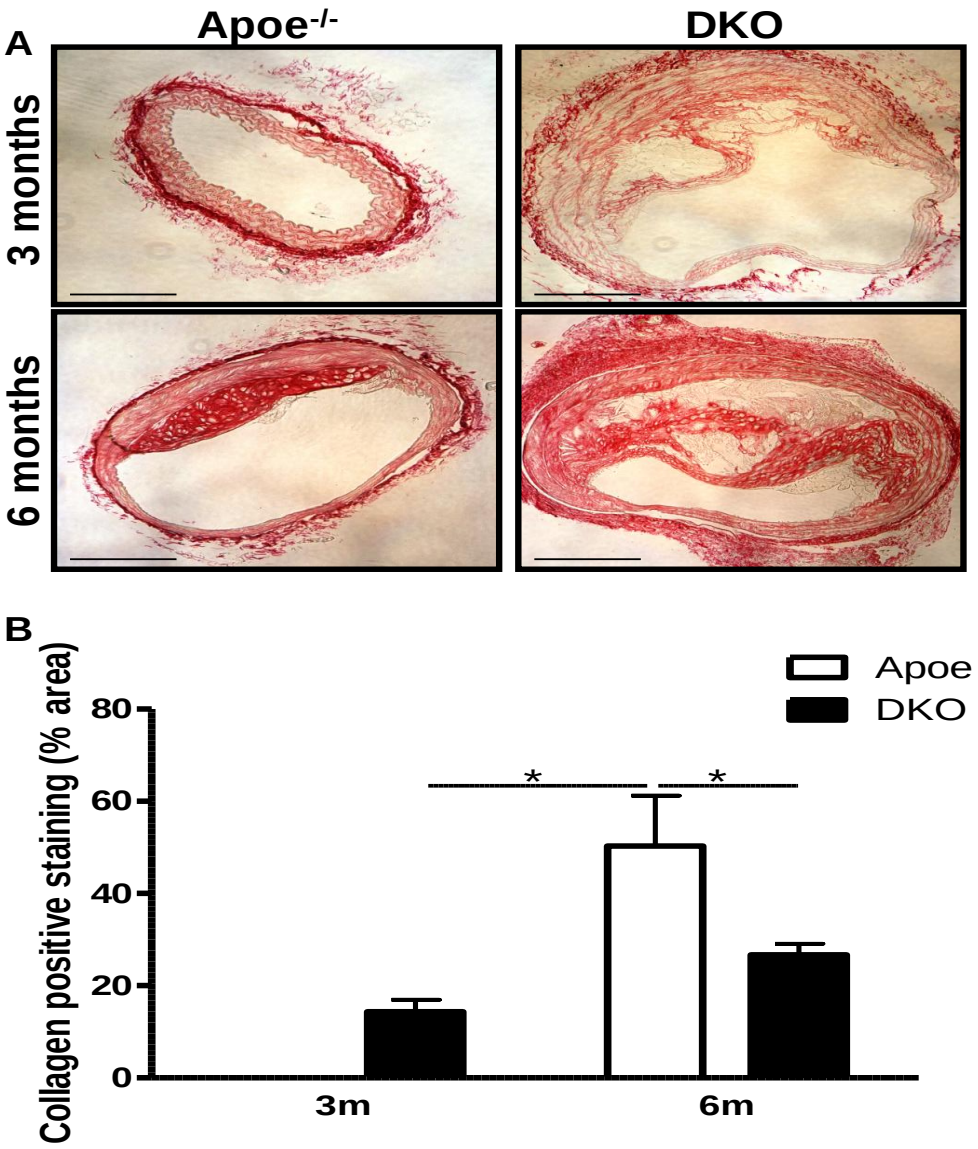

Figure 4.4 Collagen content is reduced in DKO plaques

Atherosclerotic plaques from *Apoe*$^{-/-}$ and DKO animals were stained using Picrosirius red stain for collagen (A). Plaques from 6 month old *Apoe*$^{-/-}$ mice show more intense and abundant staining for collagen than plaques from DKO mice at either 3 or 6 months of age. Representative images from *Apoe*$^{-/-}$ and DKO mice, captured at x10 magnification. Scale bar = 250 µm. The area of collagen staining was quantified using Photoshop CS3 Extended software and expressed as a % of total plaque area (B). Collagen content was reduced in brachiocephalic plaques from 3 and 6 month DKO mice compared to those from *Apoe*$^{-/-}$ mice at 6 months of age. Data are mean ± sem, n= 5-6. Analysed by two-way ANOVA: * $p<0.01$.

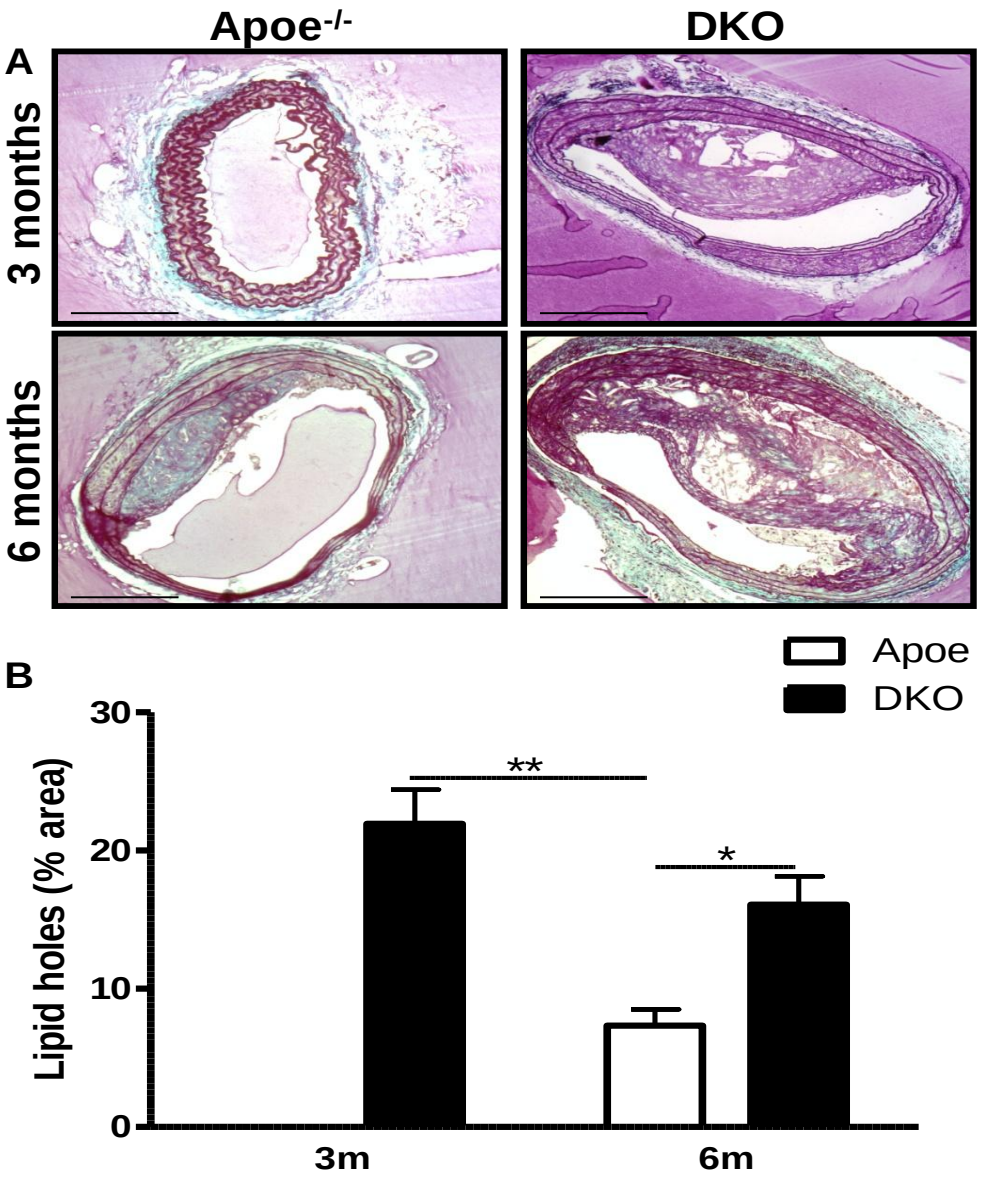

Figure 4.5 Lipid content is increased in DKO plaques

Atherosclerotic plaques from *Apoe*$^{-/-}$ and DKO animals stained with UST to reveal lipid holes left behind by histological processing (A). DKO mice at 3 and 6 months of age show larger areas of lipid holes in their plaques than *Apoe*$^{-/-}$ mice at 6 months of age. Representative images from *Apoe*$^{-/-}$ and DKO mice, captured at x10 magnification. Scale bar = 250 µm. The area of lipid was quantified using Photoshop CS3 Extended software and expressed as a % of total plaque area (B). Lipid content was increased in brachiocephalic plaques from 3 and 6 month DKO mice compared to those from *Apoe*$^{-/-}$ mice at 6 months of age. Data are mean ± sem, n= 6-8. Analysed by two-way ANOVA: * $p<0.01$; ** $p<0.001$.

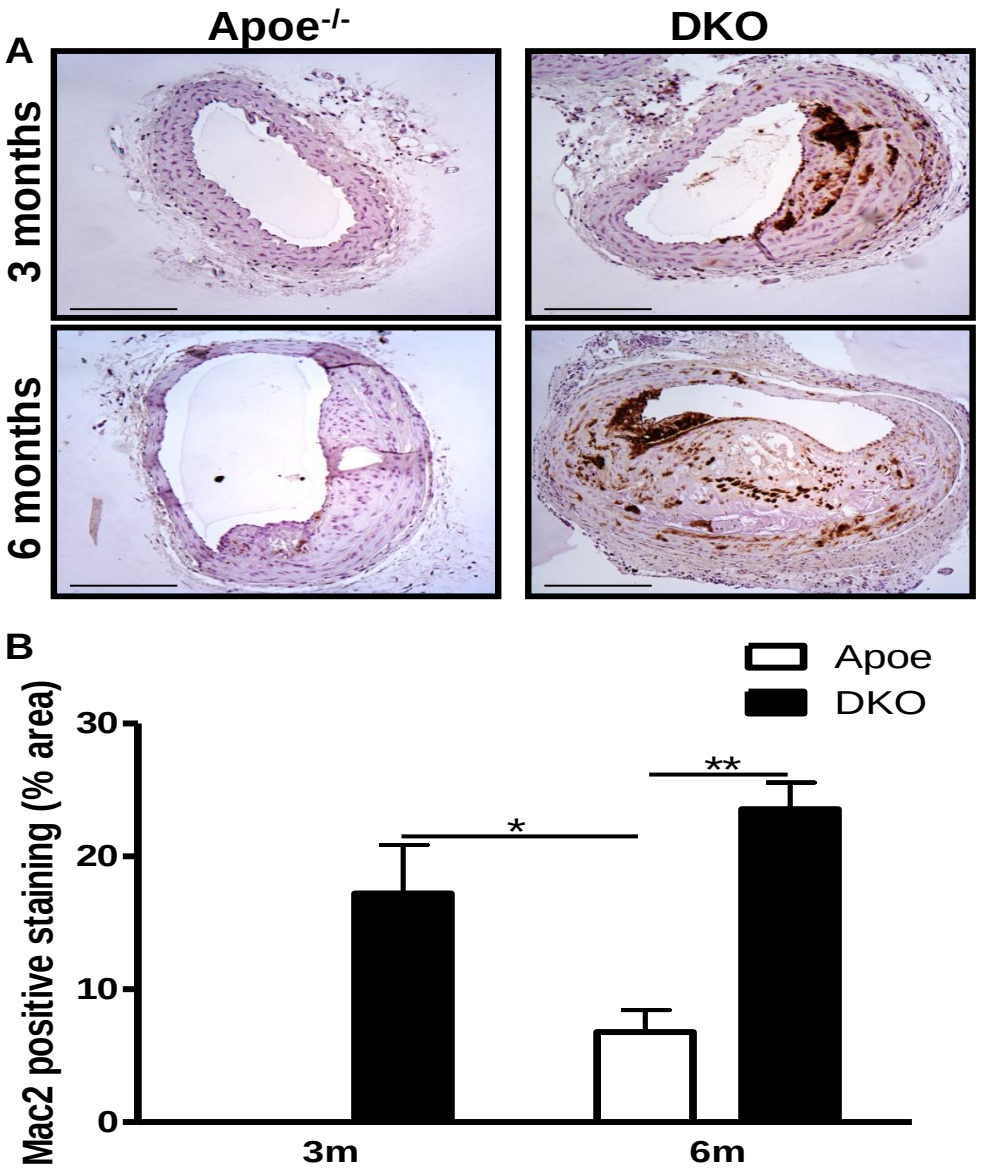

Figure 4.6 Macrophage content is increased in DKO plaques

Sections of brachiocephalic arteries from DKO and *Apoe*$^{-/-}$ mice were stained with antibody against Mac-2 (A). Plaque macrophage abundance appeared greater in 3 and 6 month old DKO mice compared to that in 6 month old *Apoe*$^{-/-}$ mice. Representative images from *Apoe*$^{-/-}$ and DKO mice, captured at x10 magnification. Scale bar = 250 µm. The area of macrophage staining was quantified using Photoshop CS3 Extended software and expressed as a % of total plaque area (B). Macrophage content was increased in brachiocephalic plaques from 3 and 6 month DKO mice compared to those from *Apoe*$^{-/-}$ mice at 6 months of age. Data are mean ± sem, n= 6-8. Analysed by two-way ANOVA: * $p<0.01$; ** $p<0.001$.

4.3.4 Influence of 11β-HSD2 inactivation on overall plaque stability in *Apoe*$^{-/-}$ mice

In the previous chapter it was shown that MR blockade stabilised DKO plaques by increasing the ratio of stabilising (SMC + collagen) to degrading (lipids + macrophages) forces. To determine whether or not loss of 11β-HSD2 in DKO mice promotes plaque vulnerability, a stacked bar graph was created (

Figure 4.7) to enable a direct comparison of plaque composition between *Apoe*$^{-/-}$ and DKO mice. The graph suggests that lack of 11β-HSD2 alters the composition of plaques, favouring a more vulnerable phenotype. At 6 months of age, *Apoe*$^{-/-}$ mice show stable plaques consisting of 62% stabilising components, largely collagen, and only 14% destabilising components, almost equal parts lipids and macrophages. Despite having similar plaque sizes to the 6 month *Apoe*$^{-/-}$ mice, 3 month old DKO mice show more vulnerable plaques with only 22% stabilising components, mainly collagen, and 39% destabilising components, almost equal lipids and macrophages. By 6 months of age, plaques in DKO mice have gained stability with equal stabilising (39%) and destabilising (39%) components, but are still more vulnerable than those in age-matched *Apoe*$^{-/-}$ counterparts. The stabilising component of 6 month DKO plaques is mostly collagen whilst the destabilising component is mostly macrophages.

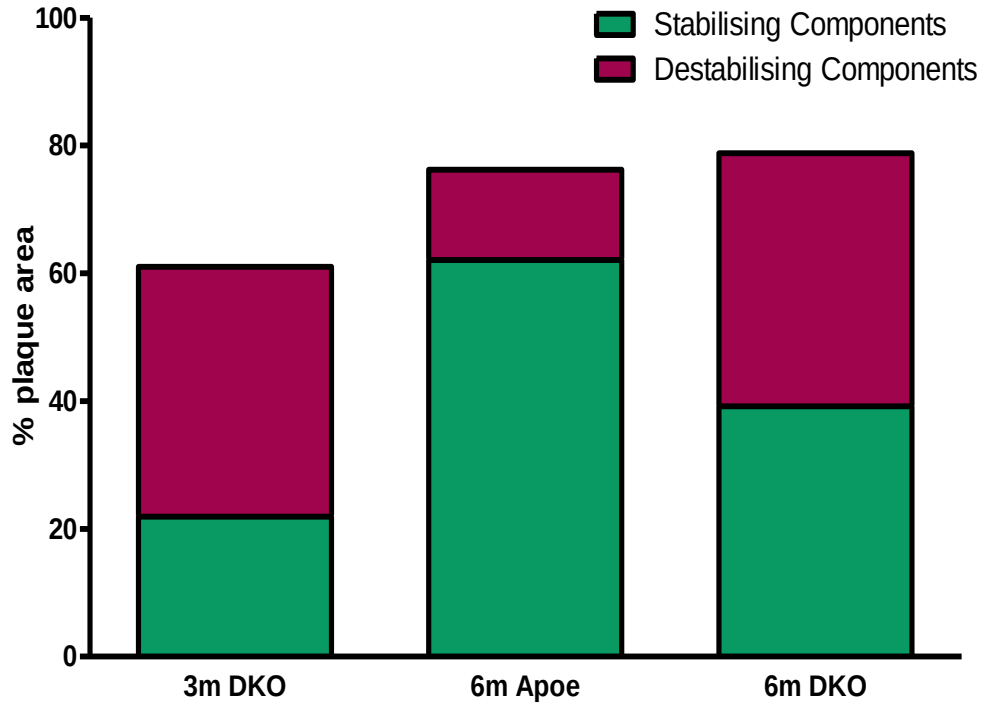

Figure 4.7 Effect of 11β-HSD2 inactivation on the stability of plaques

The contribution that stabilising and destabilising components make to the overall plaque gives an indication of plaque stability. 11β-HSD2 inactivation promotes plaque instability by altering plaque composition such that the ratio of stabilising (SMC and collagen) to degrading (lipid and macrophages) forces is reduced in DKO mice compared to *Apoe*$^{-/-}$ mice.

4.4 Discussion

The studies detailed in this chapter have demonstrated that loss of 11β-HSD2 activity on the *Apoe*$^{-/-}$ background accelerates the progression of atherosclerosis and vascular remodelling in DKO mice. Plaque composition was altered in DKO mice, revealing an important function for 11β-HSD2 in protection against the formation of vulnerable plaques. Lack of 11β-HSD2 activity promotes vascular inflammation in DKO mice as shown by enhanced macrophage infiltration into brachiocephalic plaques during the early stages of atherogenesis.

Effects of 11β-HSD2 inactivation on atherogenesis and vascular remodelling

The results of the present study confirm those of the preliminary studies showing significantly increased atherosclerotic plaques in 3 and 6 month old DKO mice compared to age-matched *Apoe*$^{-/-}$ mice (Deuchar *et al.,* 2009). On a normal chow diet, *Apoe*$^{-/-}$ mice did not develop plaques until after 3 months of age and this is consistent with a study demonstrating the time course of lesion development in the aortic sinus of chow fed *Apoe*$^{-/-}$ mice which reported that composite plaques were not evident until 5 – 7 months of age (Reddick *et al.*, 1994). In addition, brachiocephalic plaques were only observed in chow fed *Apoe*$^{-/-}$ mice at around 6 months of age in another study (von Holt *et al.*, 2009). By contrast, chow fed DKO mice presented with full atherosclerotic plaques at 3 months, suggesting very *early* pro-atherogenic consequences of 11β-HSD2 inactivation. At 6 months of age plaques from DKO mice were significantly larger than plaques from age-matched *Apoe*$^{-/-}$ mice and whilst all DKO animals studied had plaques at this age; the same was not true of the *Apoe*$^{-/-}$ animals. It is note-worthy that 3 month old DKO mice had brachiocephalic plaques of comparable size to those in 6 month old *Apoe*$^{-/-}$ mice. This not only highlights the accelerated nature of atherogenesis in DKO mice, but it also allows for comparisons of atherosclerosis between DKO and *Apoe*$^{-/-}$ plaques that are size-matched, and thus are at similar stages of development.

In the drug study (chapter 3), eplerenone treatment of DKO mice normalised plaque size to the dimensions observed in 6 month *Apoe*$^{-/-}$ mice, implying that MR activation is causal in the accelerated atherosclerotic phenotype. However, it should be noted that the plaques in vehicle treated mice in the drug study were smaller than those in 6 month old DKO mice, possibly because the vehicle mice were studied at 5 months of age. This suggests that caution should be employed when comparing the results of the present chapter with those of chapter 3. Nonetheless, it is clear that inappropriate activation of MR due to loss of protection by 11β-HSD2 plays a major role in accelerating the atherogenic process in DKO mice. The benefits of MR antagonists in atherosclerosis are well established (Strawn, 2005) and it has been reported that inhibition of 11β-HSD1-mediated local glucocorticoid regeneration reduces atherogenesis in *Apoe*$^{-/-}$ mice (Hermanowski-Vosatka *et al.*, 2005). These studies provide an indirect link between inappropriate activation of MR by glucocorticoids and the pathogenesis of atherosclerosis. However, there are no published data as yet describing a specific role for 11β-HSD2-mediated protection of MR in atherosclerosis. Therefore, the present investigations provide novel evidence that compromised 11β-HSD2 activity, in the setting of hypercholesterolemia, promotes atherogenesis via MR-mediated mechanisms.

The atherosclerosis in DKO mice was associated with compensatory outwards remodelling of the vascular wall such that luminal patency was preserved in the face of increased lesion size. Brachiocephalic arteries from DKO mice at 3 months of age were comparable to those from *Apoe*$^{-/-}$ mice at 6 months of age in all parameters except the medial area. A significant increase in medial area was observed in DKO arteries at 3 and 6 months of age compared to both age- and plaque size-matched *Apoe*$^{-/-}$ arteries, suggesting that 11β-HSD2 inactivation, and not purely atherogenesis, promotes proliferation and/or hypertrophy of medial cells. The results from chapter 3 show that eplerenone treatment of DKO mice had no effect on the medial area. Taken together, these results suggest that loss of 11β-HSD2 activity leads to medial proliferation via MR-independent mechanisms. However, the dose of eplerenone used did not alter blood pressure in DKO mice (Deuchar *et al.*, 2009) and so the increased medial area observed upon 11β-HSD2 deficiency may be secondary to

hypertension (Deuchar *et al.*, 2009) as a result of renal MR activation. Alternatively, the eplerenone treatment may not have commenced early enough or continued long enough to inhibit or reverse some of the consequences of inappropriate vascular MR activation in DKO mice. This idea is supported by the fact that aldosterone caused hypertrophy of rat aortic smooth muscle cells (Fan *et al.*, 2008) and proliferation of human vascular smooth muscle cells (Nakamura *et al.*, 2006), effects that were reversed by eplerenone. This implies a role for activation of SMC MR in the DKO phenotype. However, the differential effects of renal and extra-renal MR activation on DKO vascular pathology cannot be fully dissected by the present studies.

DKO mice have total plasma cholesterol levels that are comparable to those found in *Apoe*$^{-/-}$ mice and so the accelerated atherogenesis in DKO mice is not simply a result of high plasma cholesterol levels. Yet, differences in lipid profiles between *Apoe*$^{-/-}$ and DKO mice cannot be ruled out and may impact upon atherogenesis. Indeed, it is well known that certain lipid profiles (e.g. high LDL cholesterol, high triglycerides, and low HDL cholesterol) are associated with coronary heart disease in humans (Kreisberg, 2002). In addition to this, there is evidence to suggest that glucocorticoids affect lipid profiles with one study showing that glucocorticoid treatment of patients with congenital adrenal hyperplasia was associated with increased triglyceride levels (Botero *et al.*, 2000). Also, the atherogenic lipid profile found in patients with rheumatoid arthritis is thought to be partially due to the exogenous glucocorticoid therapy employed to treat the disease (White *et al.*, 2006). Thus, increased intracellular glucocorticoid levels in DKO mice may act to detrimentally alter lipid profiles. This is most likely to occur through activation of glucocorticoid receptors (GR) and is in agreement with a study in 11β-HSD1 knockout mice which have improved lipid profiles (Morton *et al.*, 2001). However, since there is no conversion of corticosterone into 11-dehydrocorticosterone in DKO mice, there is no substrate available for 11β-HSD1 in DKO animals, rendering them essentially 11β-HSD1 knockouts. In this case it might be suggested that lipid profiles would be improved in DKO animals. Without actually comparing full lipid profiles in DKO and *Apoe*$^{-/-}$ mice, however, we can only speculate as to how this particular phenotype may manifest and so no solid conclusions can be drawn.

Effects of 11β-HSD2 inactivation on plaque composition and inflammation

As might be expected from the results of the eplerenone study (chapter 3), the increase in plaque size in DKO mice was accompanied by an alteration in the cellular composition of plaques. Plaque smooth muscle cell (SMC) content was not different between *Apoe*$^{-/-}$ mice at 6 months and either plaque size- (3 months) or age- (6 months) matched DKO mice. This was surprising given that MR blockade significantly increased the SMC content of plaques in DKO mice in the drug study. Since loss of 11β-HSD2 activity was not sufficient to affect SMC content but blockade of MR increased it, it could be that blockade of MR in cells that do not express 11β-HSD2 is responsible for the beneficial result. In this case, it is predicted that treatment of *Apoe*$^{-/-}$ mice with eplerenone will produce the same effects on plaque SMC content. Alternatively, illicit activation of MR in DKO mice may have no effect on SMC content, but blockade of MR in the DKO may result in increased activation of GR by glucocorticoids, via which glucocorticoids could enhance proliferation and/or migration of SMCs. In support of this, it was reported that treatment of rat aortic smooth muscle cells with short bursts of glucocorticoid increased proliferation (Kawai *et al.*, 1998). Plaques from DKO mice demonstrated decreased collagen content at both 3 and 6 months compared to plaques from 6 month old *Apoe*$^{-/-}$ mice. Since blockade of MR with eplerenone significantly increased collagen content in DKO mice, it is likely that the reduction in collagen content in DKO mice when compared to *Apoe*$^{-/-}$ mice occurs as a result of loss of 11β-HSD2-mediated protection of MR from glucocorticoids. It has previously been shown that glucocorticoid treatment of rat chondrocytes inhibited collagen mRNA expression (Miyazaki *et al.*, 2000) and collagen synthesis was reduced in chick embryos by glucocorticoid treatment (Oikarinen *et al.*, 1988). However, both of these studies employed dexamethasone and so the effects were most likely GR-mediated (Ramsahoye *et al.*, 1995). Activation of MR is associated with *increased* collagen synthesis in the heart (Chai *et al.*, 2006; Young *et al.*, 1994), clearly contrasting with the observations of the present study in which MR activation is

associated with decreased plaque collagen content. Perhaps activation of MR promotes collagen synthesis whilst activation of GR, which is also protected by 11β-HSD2, results in reduced synthesis or increased degradation. Also, it is likely that activation of MR produces different effects in different cells and tissues, which could be dependent upon other local factors such as inflammatory status or redox state. Although the mechanism of decreased plaque collagen content in DKO mice cannot be determined from the present study, or predicted from other studies, it is evident that 11β-HSD2 activity is key in protecting against the formation of a vulnerable collagen-poor plaque.

Plaque SMC content was unaltered and collagen content was decreased in DKO mice, so what is responsible for the increased plaque size? It was found that macrophage staining was increased in plaques from DKO mice at 3 and 6 months of age compared to plaques from 6 month old *Apoe*$^{-/-}$ mice. This suggests that despite comparable plaque sizes between 3 month DKO and 6 month *Apoe*$^{-/-}$ mice, there is an enhanced inflammatory environment in the vasculature of DKO mice. Eplerenone treatment of DKO mice significantly reduced macrophage infiltration into plaques (chapter 3) suggesting an MR-mediated mechanism. That inactivation of 11β-HSD2 is pro-inflammatory is supported by a study in rats which demonstrated that pharmacological inhibition of 11β-HSD2 mimicked the effects of DOC on coronary artery inflammation, reversible in both cases by eplerenone (Young *et al.*, 2003a). This study in combination with the present studies indicates that loss of 11β-HSD2 activity allows endogenous glucocorticoids to activate MR, consequently promoting a pro-inflammatory vascular environment. However, this proposal is complicated by the fact that glucocorticoids are anti-inflammatory (Newton, 2000) and that glucocorticoid treatment decreased macrophage accumulation in a rabbit model of atherogenesis (Asai *et al.*, 1993). Again, the glucocorticoid employed in this study was dexamethasone and so will activate GR, thus, the result of this study is not surprising given that the anti-inflammatory properties of glucocorticoids are attributed to activation of GR. Based on the results of the present study, it might then be suggested that the conflict between the anti-inflammatory and pro-atherogenic properties of glucocorticoids may simply reflect differential receptor

activation, i.e. GR versus MR. This in turn will depend on 11β-HSD2 status. However, this explanation may be a bit simplistic, especially since glucocorticoid activation of GR is associated with insulin resistance (Andrews *et al.*, 1999; Wang, 2005), which is thought to be a major linking factor between the metabolic syndrome and CVD. Thus, increased activation of GR may exacerbate atherosclerosis in DKO mice through promotion of insulin resistance.

Compared to plaques in 6 month old *Apoe*$^{-/-}$ mice, plaques in both 3 and 6 month old DKO mice showed significantly increased lipid levels, as assessed by measuring the area of lipid holes left behind by histological processing. Lipid content was not altered by MR blockade in the eplerenone study (chapter 3) and so it appears that lipid accumulation in plaques from DKO mice is not a result of inappropriate MR activation. Having said this, as mentioned earlier it might be that the length of eplerenone treatment was insufficient to fully reverse some of the consequences of MR activation. On the other hand, the accumulation of lipids may be associated with the hypertension in DKO mice (Deuchar *et al.*, 2009) which was not normalised by eplerenone. Whilst there are few data linking hypertension and plaque lipid content, it is well established that hypertension precipitates endothelial dysfunction (De Meyer *et al.*, 1997), which in turn allows the entry of lipids into the vascular wall (Rafflenbeul, 1994). Thus, hypertension may indeed increase plaque lipid content through promotion of endothelial cell dysfunction. The main sources of plaque lipids are blood lipids and lipids released by necrotic macrophage foam cells (Falk *et al.*, 1995), but the relative contribution of each to total plaque lipid is a controversial issue. Given that total plasma cholesterol levels were unaltered but plaque macrophage content was increased in DKO mice, it is tempting to speculate that the increased lipid content is due to deposition by macrophages.

Alternative theories

It is clear from the results of both chapter 3 and the present chapter that illicit activation of MR plays a major role in the atherosclerotic phenotype of the DKO mouse. However, there may be other consequences of 11β-HSD2 inactivation that contribute towards atherogenesis. Loss of 11β-HSD2 may not only lead to over-

activation of MR but also GR, leading to increased negative feedback control of the hypothalamic-pituitary-adrenal (HPA) axis (De Kloet, 1991). This has the effect of inhibiting the release of cortisol/corticosterone from the adrenal glands thereby reducing the levels of circulating glucocorticoids. Whilst the findings of the present thesis might indicate that decreased *local* glucocorticoid levels are beneficial during atherogenesis, it is well known that high circulating glucocorticoid levels are important during inflammation and that glucocorticoid deficiency is associated with pathological overshoot of inflammatory responses (Sapolsky *et al.*, 2000). Thus, suppression of circulating glucocorticoid levels may enhance inflammation which could drive the atherogenic process. Renal MR plays an important role in maintaining normal electrolyte balance through actions on the epithelial sodium channel (ENaC) in the distal tubules (White, 1994). Over-activation of renal MR results in increased sodium re-absorption and potassium excretion (Scheinman *et al.*, 1999). Indeed, young 11β-HSD2 knockout mice have low urinary sodium levels and are hypokalemic, a phenotype that results from illicit activation of MR by endogenous glucocorticoids (Kotelevtsev *et al.*, 1999). It has been reported that sodium can promote endothelial cell dysfunction (Oberleithner *et al.*, 2007) and so the situation could be envisaged where sodium retention in the vasculature of the DKO mouse initiates endothelial dysfunction sufficient to be pro-atherogenic. Sudden death occurs in DKO (Deuchar *et al.*, 2009) and 11β-HSD2 single knockout (Kotelevtsev *et al.*, 1999) mice and this is likely a consequence of sudden cardiac death due to the hypokalaemia. However, hypokalaemia also causes haemodynamic changes (Galvez *et al.*, 1977) and it is possible that consequent alterations in shear stress could predispose certain vascular beds to atherogenesis.

In the normal physiological state MR is occupied by glucocorticoids, even in mineralocorticoid target tissues, but is not activated (Funder *et al.*, 1996). When 11β-HSD2 is inhibited, glucocorticoids can then activate MR and it has been suggested that this change in activation state may be due to alterations in cellular redox state (Funder, 2005b). When 11β-HSD2 is active, for each molecule of corticosterone that is converted into 11-dehydrocorticosterone one molecule of NAD is converted into NADH (Funder, 2005b). Thus, when 11β-HSD2 is inactive there

will be a rise in the NAD/NADH ratio which could have an effect on the intracellular redox environment. Not only will this change in redox state allow glucocorticoids to activate MR, but it may also contribute to dysfunction of cells of the vasculature, particularly endothelial cells (Cai *et al.*, 2000), thereby accelerating the initiation of atherogenesis. In addition to this, tissue damage, during inflammation for example, leads to the production of ROS and a subsequent change in intracellular redox state (Funder, 2005b). This in combination with the proposal that intracellular redox changes allow for glucocorticoid activation of MR provides a possible mechanism by which MR may be illicitly activated by glucocorticoids during pathological conditions even when 11β-HSD2 is functional.

Effects of 11β-HSD2 inactivation on plaque stability

The overall effect of loss of 11β-HSD2 activity on atherogenesis was a destabilisation of the plaque. *Apoe*$^{-/-}$ mice at 6 months of age exhibited a stable plaque phenotype with a larger SMC + collagen content compared to lipid + macrophage content. Despite having similar plaque sizes to the 6 month *Apoe*$^{-/-}$ mice, 3 month old DKO mice had more vulnerable plaques with a low SMC + collagen component and a high lipid + macrophage content. By 6 months of age, plaques in DKO mice had gained stability with equal contents of SMC + collagen and lipid + macrophages, but were still more vulnerable than those in age-matched *Apoe*$^{-/-}$ counterparts. Eplerenone increased the ratio of stabilising/destabilising components in plaques from DKO mice in the drug study (chapter 3), suggesting that illicit activation of MR is key in the formation of a vulnerable plaque during compromised 11β-HSD2 activity. The decrease in collagen content in DKO plaques could be due to increased MMP activity which, in turn, may be a result of enhanced macrophage infiltration into plaques. Evidence to support the idea that macrophages are destabilising components comes from a study in humans that reported significantly more macrophages in lesions that underwent rupture than in those that were responsible for stable angina pectoris, and did not rupture (Moreno *et al.*, 1994). DKO mice also demonstrated an increase in plaque lipid content compared to *Apoe*$^{-/-}$ mice and that this correlates with plaque instability is substantiated by post-mortem studies in human atherosclerotic arteries which found much larger lipid cores

in arterial segments with plaque disruption than in the segments with an intact surface (Gertz *et al.*, 1990). The observation that plaques in DKO mice stabilised between 3 and 6 months of age was quite surprising given that the atherogenesis and inflammation were clearly still ongoing in these later stages. However, this result does reinforce the concept that *early* pro-inflammatory events accelerate the atherogenic process in DKO mice. It would be of interest to investigate the atherosclerosis in older DKO mice to determine whether plaques continue to stabilise or whether they go through cycles of vulnerability. In line with this, more DKO mice at 6 months of age had buried fibrous caps within their plaques than DKO mice at 3 months of age, showing that this rupture/healing growth cycle continues. Also, a greater percentage of DKO mice at 3 months of age had buried fibrous caps than did *Apoe*$^{-/-}$ mice at 6 months of age, despite comparable plaque sizes between these two groups. Again, this highlights the increased vulnerability of plaques upon 11β-HSD2 inactivation and shows that this occurs during early stages of plaque development.

Conclusions

Loss of 11β-HSD2 activity accelerates atherogenesis in hyperlipidemic mice and promotes a vulnerable plaque phenotype through alteration of plaque composition and enhanced vascular inflammation. The DKO mouse provides a useful test-bed for the development of new anti-atherosclerotic drugs and the assessment of already existing drugs such as statins. Indeed the so called 'pleiotropic' effects of statins on atherosclerosis could be studied in the DKO mouse to determine whether or not these benefits are associated with plaque stabilisation. The results of this chapter combined with those of the previous chapter suggest that illicit activation of *extra-renal* MR is largely causative in the DKO atherosclerotic phenotype. This idea is further explored in the next chapter which aims to dissect possible vascular mechanisms of the enhanced inflammatory cell content of DKO plaques.

Chapter 5
Mechanisms of enhanced vascular inflammation in the DKO mouse

5.1 Introduction

This thesis has so far demonstrated that 11β-HSD2 inactivation enhances macrophage infiltration into brachiocephalic plaques on the *Apoe*$^{-/-}$ background, and that this is at least partially an MR mediated mechanism was shown by reversal with eplerenone. This phenotype could result from activation of MR in a number of cells and so to begin to isolate roles for specific cell types, the potential of the endothelium in mediating increased macrophage infiltration was investigated.

The endothelium plays a vital role in the infiltration of monocytes into the intimal space during the early stages of atherogenesis, partially through the expression of cellular adhesion molecules. Vascular Cell Adhesion Molecule 1 (VCAM-1) and intercellular cellular adhesion molecule 1 (ICAM-1) largely bind monocytes and T-lymphocytes (Libby *et al.*, 2002) and the finding that lesion development is disrupted in both ICAM-1 (Collins *et al.*, 2000) and VCAM-1 deficient mice (Cybulsky *et al.*, 2001) highlights the important role of these pro-inflammatory molecules in atherogenesis. Given that endothelial cells express both MR and 11β-HSD2 (Caprio *et al.*, 2008; Christy *et al.*, 2003), and that MR over-activation causes enhanced macrophage infiltration in the DKO mouse, it is reasonable to postulate that adhesion molecule expression may be regulated by MR-mediated mechanisms. In support of this, a study in human vascular endothelial cells found that aldosterone mediated activation of MR lead to up-regulation of ICAM-1 mRNA and protein (Caprio *et al.*, 2008). Also, MR antagonism in mice with heart failure resulted in reduced expression of ICAM-1 (Kuster *et al.*, 2005). However, a direct role for 11β-HSD2 in protection against MR-mediated up-regulation of adhesion molecules remains to be defined.

The endothelium not only expresses adhesion molecules during atherogenesis, but it also releases pro-inflammatory cytokines such as monocyte chemoattractant protein 1 (MCP-1). A role for MR in stimulating MCP-1 expression has been shown in the

rat heart, where treatment with aldosterone and salt resulted in increased MCP-1 mRNA, an effect that was reversed by MR blockade with spironolactone (Sun *et al.*, 2002). However, there is little data on the effect of MR activation on MCP-1 expression in cells of the murine vasculature, particularly during atherogenesis. In addition to cytokines, the endothelium can also shed adhesion molecules (Pigott *et al.*, 1992), producing soluble forms (sCAM) that circulate in the plasma (Rothlein *et al.*, 1991). It is thought that plasma concentrations of soluble adhesion molecules could be useful markers for predicting the presence and severity of cardiovascular pathologies. Indeed, sICAM-1, sVCAM-1 and sE-selectin are elevated during inflammatory conditions (Gearing *et al.*, 1993) and in individuals with cardiovascular disease (Caulin-Glaser *et al.*, 1998; Haught *et al.*, 1996). Also, the fact that a positive correlation has been reported between the extent of atherosclerosis and the plasma concentrations of sICAM-1 (Rohde *et al.*, 1998) and sVCAM-1 (Peter *et al.*, 1997) indicates that these markers may be enhanced in DKO mice.

To begin to explore the possible cellular mechanisms by which 11β-HSD2 inactivation leads to enhanced macrophage infiltration into DKO plaques, it was hypothesised that the endothelial cell expression of adhesion molecules, and cytokine release, would be enhanced in DKO mice compared to *Apoe*$^{-/-}$ mice. With this in mind, the specific aims of this chapter were:

(i) To compare VCAM-1 and ICAM-1 expression in brachiocephalic arteries and MCP-1 and sVCAM-1 levels in plasma between DKO and *Apoe*$^{-/-}$ mice.

(ii) To determine whether there is a role for 11β-HSD2 in protection against endothelial up-regulation of pro-inflammatory molecules during atherogenesis.

5.2 Methods

5.2.1 Adhesion molecule expression

Histological and immunohistochemical techniques were performed according to the methods detailed in section 2.3.2.

5.2.2 Subjective scoring

In order to allow quantification of vascular endothelial cell staining for adhesion molecules, a subjective scoring system was employed. A representative section, chosen from roughly the same portion of each vessel, was quantified per mouse for ICAM-1 or VCAM-1 staining. The system was based on the proportion of the circumference of the endothelium that was stained for each adhesion molecule and the scores were applied as follows: 0 = staining absent; 1 = < 25% circumference stained; 2 = 25-50% circumference stained; 3 = 50-75% circumference stained; and 4 = > 75% circumference stained.

5.2.3 Cytokine expression

ELISA kits for mouse MCP-1 (Invitrogen) and soluble VCAM-1 (sVCAM-1) (R&D Systems) were used according to the manufacturer's instructions in the measurement of plasma levels of these pro-inflammatory molecules (see section 2.4.4.2).

5.2.4 Statistical analysis

Data are mean ± sem and were analysed by 2-way Anova for sVCAM-1 data and the non-parametric Kruskal-Wallis test was employed for the analysis of endothelial cell staining.

5.3 Results

5.3.1 Effect of 11β-HSD2 inactivation on the endothelial expression of ICAM-1 in *Apoe*$^{-/-}$ mice

Immunohistochemistry with specific antibodies against ICAM-1 was used to investigate the importance of this molecule in the enhanced macrophage content of plaques from DKO mice. It was immediately clear from observing the stained sections (Figure 5.1a) that ICAM-1 was constitutively expressed throughout the endothelium of both DKO and *Apoe*$^{-/-}$ mice at 3 and 6 months of age. Quantitative analysis, using the semi-quantitative scoring system detailed in section 5.2.4, confirmed that ICAM-1 expression was not different in DKO mice at either 3 or 6 months of age compared to either age- or plaque size- matched *Apoe*$^{-/-}$ mice (figure 5.1b).

5.3.2 Effect of 11β-HSD2 inactivation on the endothelial expression of VCAM-1 in *Apoe*$^{-/-}$ mice

Immunohistochemistry was performed with specific antibodies against VCAM-1 and it was evident from observing the stained sections (Figure 5.2a) that VCAM-1 was more abundant on the endothelium of DKO mice at 3 and 6 months of age when compared to age-matched *Apoe*$^{-/-}$ mice. Quantitative analysis, using the semi-quantitative scoring system detailed in section 5.2.4, confirmed that VCAM-1 expression was significantly increased in DKO mice compared to *Apoe*$^{-/-}$ mice at both 3 and 6 months of age (figure 5.2b). This analysis also demonstrated that VCAM-1 expression was significantly increased in DKO mice at 3 months of age compared to *Apoe*$^{-/-}$ mice at 6 months of age, despite similar plaque sizes between these two groups (see chapter 4).

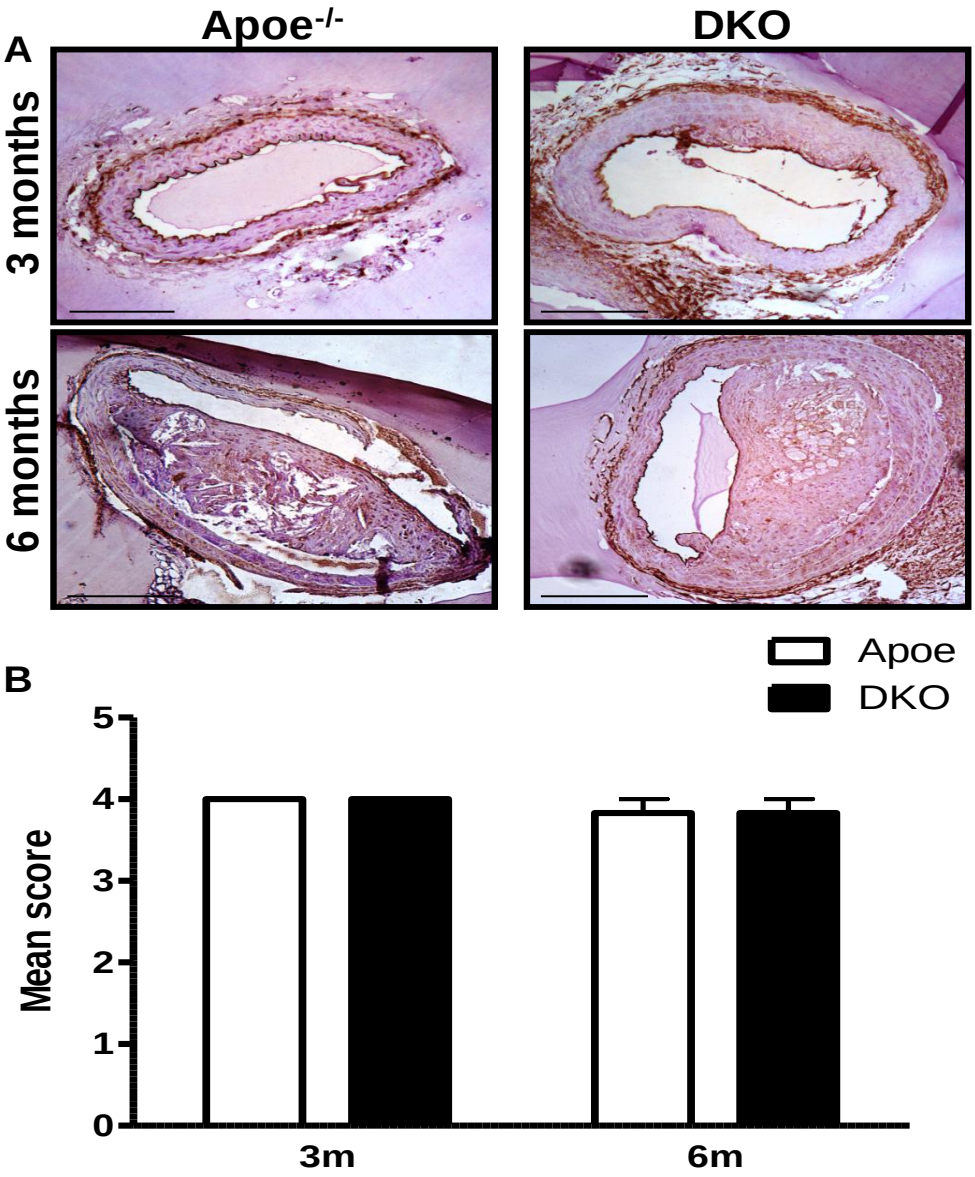

Figure 5.1 Loss of 11β-HSD2 activity has no effect on endothelial expression of ICAM-1

Sections of brachiocephalic arteries from *Apoe*$^{-/-}$ and DKO animals were stained with antibody against ICAM-1 (A). DKO and *Apoe*$^{-/-}$ mice constitutively express ICAM-1 at 3 and 6 months of age. Representative images from *Apoe*$^{-/-}$ and DKO animals, captured at x10 magnification. Scale bar = 250 µm. Circumferential staining was quantified using a semi-quantitative scoring system (B). ICAM-1 expression was comparable between DKO and *Apoe*$^{-/-}$ mice at both 3 and 6 months of age. Data are mean ± sem, n= 4-6 per group. Analysed by Kruksal-Wallis test: p=ns.

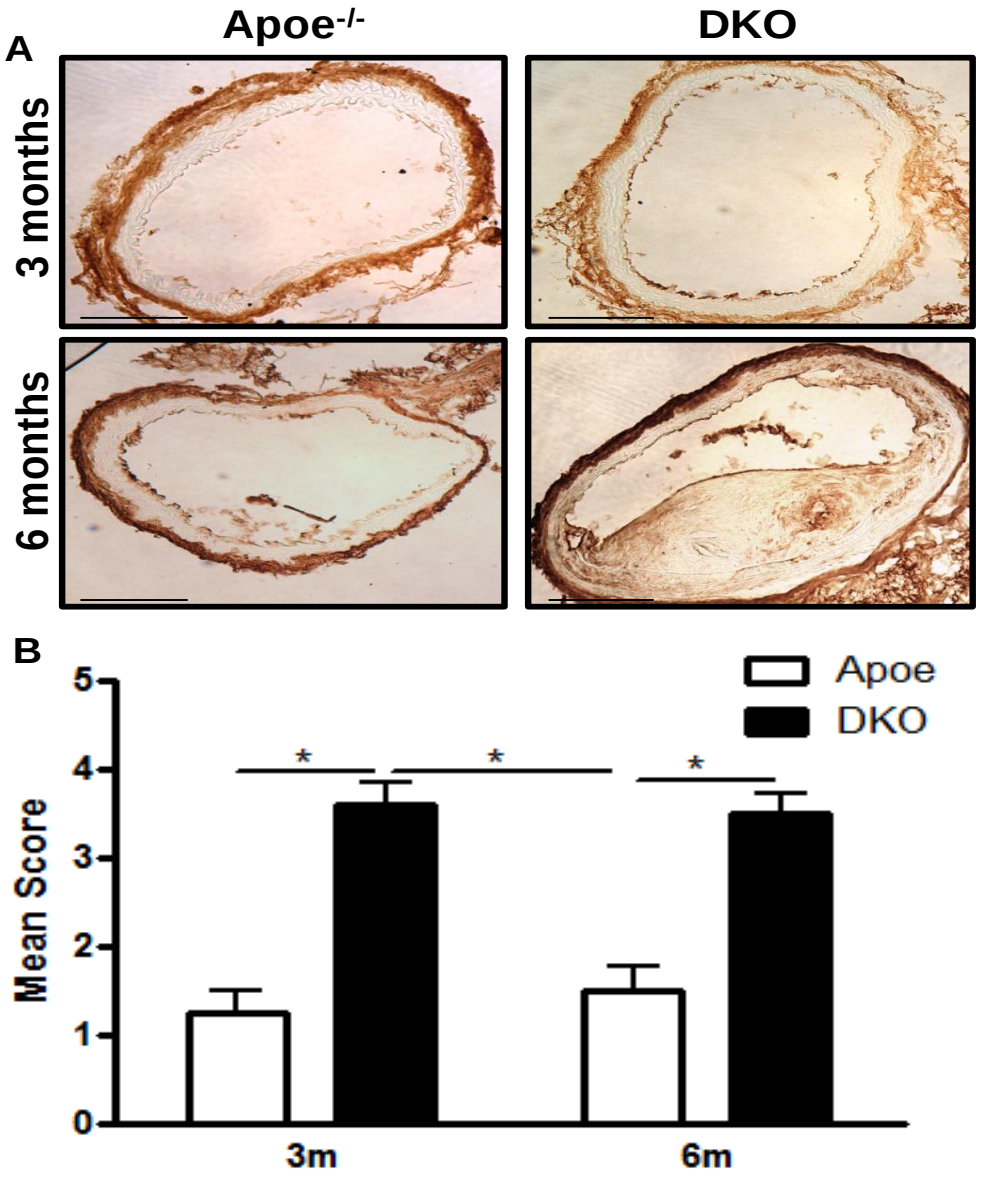

Figure 5.2 Loss of 11β-HSD2 activity increases endothelial expression of VCAM-1

Sections of brachiocephalic arteries from *Apoe*$^{-/-}$ and DKO animals were stained with antibody against VCAM-1 (A). DKO mice appear to have more abundant VCAM-1 staining at 3 and 6 months compared to age-matched *Apoe*$^{-/-}$ mice. Representative images from *Apoe*$^{-/-}$ and DKO animals, captured at x10 magnification. Scale bar = 250 µm. Circumferential staining was quantified using a semi-quantitative scoring system (B). At 3 months of age, DKO mice had increased VCAM-1 expression compared to both age- (3 months) and plaque size- (6 months) matched *Apoe*$^{-/-}$ mice. At 6 months, VCAM-1 expression remained increased in DKO compared to *Apoe*$^{-/-}$ mice. Data are mean ± sem, n= 4-6 per group. Analysed by Kruskal-Wallis test: *p<0.01.

5.3.3 Influence of 11β-HSD2 inactivation on levels of sVCAM-1

Plasma levels of sVCAM-1 are thought to correlate with inflammation (Gearing *et al.*, 1993) and atherosclerosis (Peter *et al.*, 1997). Thus, ELISA for sVCAM-1 was performed in plasma samples from *Apoe*$^{-/-}$ and DKO mice at 3 and 6 months of age. There was no difference in the levels of sVCAM-1 present in plasma from *Apoe*$^{-/-}$ and DKO mice at either 3 or 6 months of age (Figure 5.3).

5.3.4 Influence of 11β-HSD2 inactivation on MCP-1 levels

MCP-1 is important in attracting macrophages to sites of atherosclerosis (see chapter 1) and so to determine whether or not increased levels of MCP-1 may be involved in the increased recruitment of macrophages to DKO plaques, plasma MCP-1 levels were measured by ELISA. Unfortunately, MCP-1 levels were below the limit of detection for the assay in both *Apoe*$^{-/-}$ and DKO mice at 3 and 6 months of age (data not shown).

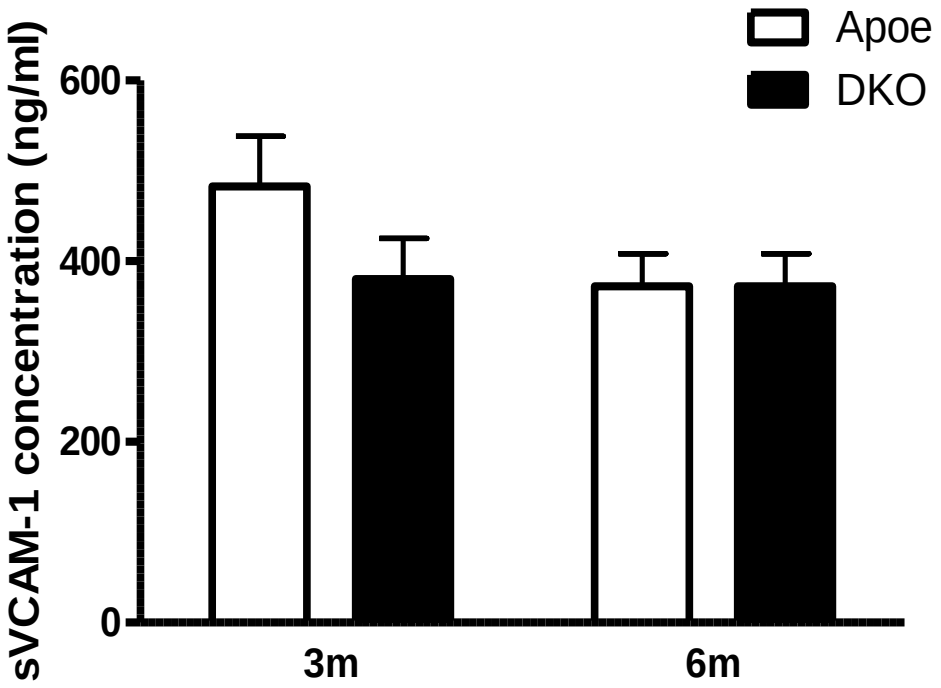

Figure 5.3 11β-HSD2 inactivation has no effect on sVCAM-1 levels in plasma

Plasma sVCAM-1 levels were measured in *Apoe*$^{-/-}$ and DKO mice at 3 and 6 months of age using a commercial kit. sVCAM-1 levels were comparable between DKO and *Apoe*$^{-/-}$ mice at both ages. Data are mean ± sem, n= 4 per group. Analysed by two-way ANOVA: p=ns.

5.4 Discussion

Loss of 11β-HSD2 activity results in increased endothelial cell expression of VCAM-1, but not ICAM-1, in brachiocephalic arteries during the early stages of atherogenesis in *Apoe*$^{-/-}$ mice. This enhanced vascular inflammation may be responsible for, or contribute to, the increased recruitment of macrophages to plaques from DKO mice and it exposes an important role for 11β-HSD2 in modulating inflammatory responses in the vasculature.

Influence of 11β-HSD2 inactivation on vascular expression of adhesion molecules

The present studies found that ICAM-1 was constitutively expressed on the endothelium of *Apoe*$^{-/-}$ and DKO mice at 3 and 6 months of age. This contrasts with other studies showing up-regulation of ICAM-1 in response to MR activation in the rat coronary vasculature (Rocha *et al.*, 2002b), the rat heart (Sun *et al.*, 2002), rat aortic tissue (Hirono *et al.*, 2007), and the murine myocardium (Kuster *et al.*, 2005). In addition to this, it was recently shown that MR activation *in vitro* in human vascular endothelial cells resulted in increased ICAM-1 expression (Caprio *et al.*, 2008), providing a direct link between MR activation and ICAM-1 expression without the confounding variables that come with *in vivo* studies. The reason for the discrepancy between the previously reported results and the observations made in the present work is unclear although it may be due to a species variance in ICAM-1 expression. The majority of studies on the role of MR activation in the cardiovascular expression of adhesion molecules have been carried out in rats or in human cells in culture; there are very few data on the effect of MR activation on ICAM-1 expression in murine vasculature cells. Thus, ICAM-1 may be constitutively expressed in murine blood vessels and not subject to the same regulatory mechanisms present in other species. In support of this, it was reported that ICAM-1 was expressed in the aortas of both wild type and *Apoe*$^{-/-}$ mice and was independent of cholesterol levels (Nakashima *et al.*, 1998). However, RT-PCR methodology has been used to show that ICAM-1 mRNA can be up-regulated by TNF-α in murine cerebral blood vessels (Rudin *et al.*, 1997). Perhaps the methods used to investigate ICAM-1 expression in the current studies were not sensitive enough to detect alterations from the high baseline levels of expression.

Alternatively, whilst mRNA levels may be altered, protein levels may be unchanged. Another possible source of variance is the vascular bed used; most of the studies that show regulation of ICAM-1 expression by MR-mediated mechanisms are performed in either the coronary vasculature, the aorta, or human umbilical vein endothelial cells (HUVECs) in culture. There are no reports on the effects of MR activation on ICAM-1 expression in the brachiocephalic artery. It is well established that large and small vessels differ in their ability to express adhesion molecules (Carlos *et al.*, 1994) and so it might be that the endothelial cells of the murine brachiocephalic artery constitutively express ICAM-1 and do not up-regulate this particular molecule in response to pro-inflammatory stimuli.

Another possibility is that ICAM-1 expression was investigated too late in DKO mice. Comparing expression at an earlier age (1 or 2 months) may have revealed differences between DKO and *Apoe*$^{-/-}$ mice. Alternatively, the difference between the results of the present study and those reported in the literature may reflect differential ligand effects on MR-mediated regulation of ICAM-1. The studies by Rocha *et al.*, Sun *et al.*, Hirono *et al.*, and Caprio *et al.* detailed above all employed aldosterone as the MR ligand whereas it is more likely that the ligand for MR in the present study will be corticosterone. Perhaps unlike aldosterone, *glucocorticoid* activation of MR has no effect on the transcriptional activity of the ICAM-1 gene. The increased local glucocorticoids in the DKO mouse will not only activate MR, but they may also activate GR. Given that activation of GR has been shown to *suppress* cytokine-induced ICAM-1 expression in HUVECs (Cronstein *et al.*, 1992) and in a human monocytic cell line (van de Stolpe *et al.*, 1994), it might be proposed that activation of GR in DKO mice counters any stimulatory effects of MR activation on ICAM-1 expression. Brachiocephalic sections from the DKO mice that received eplerenone treatment (chapter 3) were stained for ICAM-1 (data not shown) and, in line with the results of the present chapter ICAM-1 remained constitutive throughout the endothelium. Taken together, these results suggest that ICAM-1 expression is not an MR-mediated mechanism in the murine brachiocephalic artery.

It has been suggested that VCAM-1 is more important in the pathogenesis of atherosclerosis than ICAM-1 (Cybulsky *et al.*, 2001), particularly in the initiation of atherosclerosis. The present study found significant up-regulation of VCAM-1 on the endothelium of brachiocephalic arteries from DKO mice at 3 and 6 months of age compared to *Apoe*$^{-/-}$ mice. The increased VCAM-1 expression at 3 months of age may be partially responsible for the accelerated development of atherosclerosis in DKO mice and is consistent with the hypothesis that DKO mice have enhanced vascular inflammation during the *early* stages of disease. Importantly, despite similar plaque sizes, 3 month old DKO mice had significantly increased VCAM-1 expression and macrophage infiltration (chapter 4) compared to 6 month old *Apoe*$^{-/-}$ mice. This provides an indirect link between endothelial VCAM-1 expression and macrophage infiltration into plaques. Indeed, the vital role that VCAM-1 plays in monocyte emigration *in vivo* was demonstrated in a study that showed blockade of emigration into the peritoneum of rabbits upon treatment with neutralising antibody against VCAM-1 (Winn *et al.*, 1993). In addition to this, it has been reported that not only is VCAM-1 required for the firm attachment of rolling monocytes to sites of atherosclerosis (Ramos *et al.*, 1999), but that VCAM-1 expression *precedes* sub-endothelial monocyte accumulation in a model of vein graft atherosclerosis (Hanyu *et al.*, 2001). Furthermore, there is evidence to suggest that intimal macrophage recruitment in humans is dependent upon the expression level of adhesion molecules, particularly VCAM-1 (Duplàa *et al.*, 1996). However, whilst it is likely that the increased macrophage content in DKO mice is due to the increased endothelial expression of VCAM-1, the present study does not prove that this is the case. In order to determine a direct relationship between VCAM-1 expression and macrophage infiltration in DKO mice, the effects of VCAM-1 ablation, via gene disruption or neutralising antibodies, on macrophage content of plaques would need to be investigated.

The main stimulus for investigating VCAM-1 expression in DKO mice was to determine whether it might underlie the enhanced macrophage infiltration into plaques, particularly during the early stages of atherogenesis. However, increased macrophage recruitment may not be the only consequence of VCAM-1 up-

regulation. It has been reported that VCAM-1 signalling in endothelial cells is important not only in leukocyte migration (Matheny *et al.*, 2000) but also in the production of MMPs via ROS generation (Deem *et al.*, 2004). It is thought that this endothelial production of MMPs aids in leukocyte migration across endothelial cells (Deem *et al.*, 2004). In the setting of atherosclerosis, increased MMP production may also be implicated in promoting a vulnerable plaque phenotype through collagen degradation. Thus, in the case of the DKO mouse, it is possible that MR-mediated up-regulation of VCAM-1 leads to increased macrophage infiltration and production of MMPs in endothelial cells which, in turn, promotes the breakdown of plaque integrity and the consequent formation of the macrophage-rich/collagen-poor vulnerable plaques observed in DKO mice.

That VCAM-1 expression was increased in DKO mice compared to *Apoe*$^{-/-}$ mice implicates 11β-HSD2 in protection against endothelial expression of pro-inflammatory molecules. It also suggests that illicit MR activation in endothelial cells plays a key role in promoting vascular inflammation and the initiation of atherogenesis in hyperlipidaemic mice. In line with the present results, it was recently reported that aldosterone significantly increased VCAM-1 mRNA in HUVECs (Hashikabe *et al.*, 2006) and that MR blockade in aldosterone-treated rats reduced aortic expression of VCAM-1 mRNA (Hirono *et al.*, 2007). Taken all together, the evidence suggests that illicit activation of MR in vascular endothelial cells promotes up-regulation of VCAM-1. Also, the fact that 11β-HSD2 is protective against this implies that endogenous glucocorticoids are the MR ligands responsible. However, there are no data concerning glucocorticoid-mediated MR activation and VCAM-1 expression in the literature.

The question now arises as to how activation of MR can lead to increased expression of VCAM-1 in the brachiocephalic artery. There are no known mineralocorticoid response elements (MRE) in the VCAM-1 gene promoter (Caprio *et al.*, 2008; Neish *et al.*, 1992) so the mechanism, which has not been investigated, must involve intermediate steps. It is well established that cytokines are the major regulators of adhesion molecule expression (Carlos *et al.*, 1994) and so it is possible that

activation of MR leads to increased secretion of cytokines from endothelial cells. Both interleukin 4 (IL-4) (Masinovsky *et al.*, 1990) and tumor necrosis factor α (TNF-α) (Osborn *et al.*, 1989) induce endothelial VCAM-1 expression and it has previously been reported that activation of MR increases expression of TNF-α in human mononuclear cells (Miura *et al.*, 2006) and in plasma of rats with experimentally induced heart failure (Kang *et al.*, 2006). Thus, perhaps the MR-mediated up-regulation of VCAM-1 in DKO mice is via increased production of TNF-α and/or other cytokines. It would be beneficial to subject plasma samples from young DKO and *Apoe*$^{-/-}$ mice to a cytokine array assay to discover whether or not any particular cytokines are differentially regulated between the two genotypes. In addition to cytokines, it is known that endothelial nitric oxide (NO) has an inhibitory role in VCAM-1 gene expression (De Caterina *et al.*, 1995). Therefore, it might be that activation of MR inhibits endothelial NO production which, in turn, results in increased VCAM-1 expression. In support of this, it was shown that both aldosterone and glucocorticoid activation of MR in rats led to decreased endothelial nitric oxide synthase (eNOS) mRNA expression in the vascular wall (Wilson *et al.*, 2009). It was also previously demonstrated that NO production was decreased by aldosterone in rat vascular smooth muscle cells *in vitro* (Ikeda *et al.*, 1995). A further possibility is that MR activation leads to up-regulation of VCAM-1 expression via its effects on oxidative stress, which have been repeatedly demonstrated both *in vivo (*Keidar *et al.*, 2003*;* Keidar *et al.*, 2004*;* Nishiyama *et al.*, 2004) and *in vitro* (Calo *et al.*, 2004; Mazak *et al.*, 2004). Indeed, it was reported that IL-4-induced VCAM-1 expression in HUVECs (Lee *et al.*, 2001) and AngII-induced VCAM-1 expression in rat aortic endothelial cells (Pueyo *et al.*, 2000) was mediated by increased oxidative stress. These studies, in combination with the present data, provide the link between MR activation, oxidative stress, and VCAM-1 expression in endothelial cells. A final factor to consider in the MR-mediated expression of VCAM-1 is the involvement of transcription factors, which are also intimately involved with the other intracellular mechanisms described above. This particular area is studied and discussed in the next chapter.

Influence of 11β-HSD2 inactivation on vascular production of MCP-1 and sVCAM-1

The endothelium, along with macrophages and SMCs, releases pro-inflammatory cytokines that attract macrophages to the developing atherosclerosis, the best characterised of which is monocyte chemoattractant protein 1 (MCP-1) (Libby *et al.*, 1995). MR activation in humans was associated with increased levels of MCP-1 in the urine of diabetic patients (Takebayashi *et al.*, 2006) and in rats, with increased MCP-1 mRNA in the heart (Sun *et al.*, 2002). Aldosterone has also been shown to increase MCP-1 mRNA expression in the kidneys of wild type mice (Ma *et al.*, 2006). However, there are few data on the effect of MR activation on MCP-1 expression in cells of the murine vasculature. In the present study, MCP-1 levels in plasma of DKO and *Apoe*$^{-/-}$ mice were measured by ELISA but unfortunately were below the limit of detection for the assay. It is believed that MCP-1 plays a vital role in the recruitment of macrophages to sites of atherogenesis (Gu *et al.*, 1998; Harrington, 2000) and MCP-1 is detectable in *Apoe*$^{-/-}$ mice (Dol *et al.*, 2001), so the failure to detect MCP-1 in the present study was surprising. Perhaps the assay used was unsuitably optimised for detecting MCP-1 in plasma samples or perhaps MCP-1 protein degrades rapidly once the blood sample has been taken. It could be that MCP-1 levels in the plasma peak early on, prior to the onset of atherosclerosis and so maybe this assay should be performed at a younger age. On the other hand, MCP-1 just may not be an important mediator of macrophage recruitment in the current model. Activation of GR has been shown to inhibit MCP-1 production in vascular smooth muscle cells (Dhawan *et al.*, 2007), in endothelial cells (Shyy *et al.*, 1995) and *in vivo* in rats (Lopez *et al.*, 2008). Therefore, it could be that activation of GR is sufficient to counteract any stimulatory effects of MR activation on MCP-1 production in the DKO mouse. However, if this were the case then MCP-1 would still have been detectable in *Apoe*$^{-/-}$ mice. No conclusion could be drawn from the present results about the role of MCP-1 in the increased recruitment of macrophages to plaques from DKO mice.

The lack of difference in levels of sVCAM-1 in plasma from *Apoe*$^{-/-}$ and DKO mice at either 3 or 6 months of age was quite surprising given that endothelial cell surface expression of VCAM-1 was up-regulated in DKO mice and plasma levels of

sVCAM-1 are thought to correlate with cell surface expression (Garton *et al.*, 2003), inflammation (Gearing *et al.*, 1993) and atherosclerosis (Peter *et al.*, 1997). There are several possible explanations for this result. First of all, and in line with several other studies (Blann *et al.*, 1994; Frijns *et al.*, 1997; Morisaki *et al.*, 1997), sVCAM-1 levels may not correlate all that well with the presence of cardiovascular disease. There are conflicting data in the literature about which particular soluble adhesion molecules are increased in various pathologies. These discrepancies could be a result of different methods of detection or natural variances between different groups of patients. It could be that, as suggested for MCP-1, the time-points chosen were not optimal for detecting differences in sVCAM-1 levels. Alternatively, the loss of 11β-HSD2 activity may be insufficient to raise plasma levels of soluble adhesion molecules above that already afforded by the *Apoe*$^{-/-}$ state. However, since sVCAM-1 levels are a reflection of cell surface VCAM-1 levels (Garton *et al.*, 2003), it seems more likely that the increased VCAM-1 in DKO mice is not being shed properly. At 3 months of age, sVCAM-1 levels were comparable between *Apoe*$^{-/-}$ and DKO mice whilst cell surface VCAM-1 was virtually absent from *Apoe*$^{-/-}$ mice. This suggests that *Apoe*$^{-/-}$ mice are able to shed VCAM-1, perhaps as a regulatory mechanism to prevent macrophage accumulation. Indeed, it has been reported that sVCAM-1 at pathophysiological levels significantly inhibited monocyte adhesion to endothelial cells in culture (Abe *et al.*, 1998) , implicating elevated sVCAM-1 levels in protection against monocyte adherence. In contrast, a dysregulation in the mechanisms responsible for sVCAM-1 shedding may partially explain the increased cell surface VCAM-1 levels and enhanced macrophage accumulation in DKO mice. Perhaps constant MR activation in DKO mice results in continual VCAM-1 expression such that shedding cannot occur fast enough to have a significant impact. Nonetheless, sVCAM-1 levels are not a good marker of disease severity in the DKO model.

Clinical relevance of findings

Based on the present findings it might be proposed that illicit activation of MR, perhaps due to inflammatory down-regulation of 11β-HSD2 (Suzuki *et al.*, 2005), promotes endothelial up-regulation of VCAM-1 and subsequent monocyte

infiltration into the vascular wall with the consequence of accelerating atherogenesis. Thus, the benefits of MR blockade may arise from inhibition of the initial pro-inflammatory consequences of MR activation, i.e. VCAM-1 expression. Clearly, it would be useful to repeat the eplerenone study in DKO mice in order to obtain frozen vessels to perform VCAM-1 staining. This would help elucidate the role that VCAM-1 plays in the MR-mediated phenotype of the DKO mouse.

Patients with chronic inflammatory diseases, such as rheumatoid arthritis (RA), suffer from accelerated forms of atherosclerosis. It is thought that this may be due to the exogenous glucocorticoid therapy employed to treat the disorder (Nashel, 1986), which certainly corresponds well with the present thesis, but given the inflammatory nature of both of these conditions it is tempting to speculate that there may be other linking factors. It is known that patients with RA are insulin resistant, irrespective of therapy (Gonzalez-Gay *et al.*, 2005) and insulin resistance is associated with inflammation (Svenson *et al.*, 1988). In line with this, the presence of foam cells in the blood vessels of the connective tissue was reported in patients with RA (Winyard *et al.*, 1993), implying that cellular adhesion molecules may be up-regulated. Indeed, endothelial expression of E-selectin, VCAM-1, and ICAM-1 is known to be increased in RA (Bevilacqua *et al.*, 1994; Koch *et al.*, 1991). This, in combination with the present studies, suggests the hypothesis that in rheumatoid arthritis, compromised 11β-HSD2 activity by the pro-inflammatory environment in combination with exogenous glucocorticoid therapy may overwhelm the MR leading to up-regulation of adhesion molecules and accelerated atherogenesis. This predicts that eplerenone treatment would be beneficial in patients with RA and it has in fact been recently reported that spironolactone treatment improved endothelial dysfunction and inflammatory disease activity in RA patients (Syngle *et al.*, 2009). This supports a role for inappropriate MR activation in RA and suggests that 11β-HSD2 could be a major link between rheumatoid arthritis and atherosclerosis.

Conclusions

Inactivation of 11β-HSD2 selectively up-regulates endothelial cell expression of VCAM-1, providing a mechanism by which enhanced macrophage recruitment may

occur in DKO mice. This implicates MR activation in *endothelial cells* as a major contributing factor to the early pro-inflammatory changes that accelerate atherogenesis in DKO mice. Endothelial cell specific knockout of 11β-HSD2 on the *Apoe*$^{-/-}$ background would aid in defining a more specific role for endothelial MR activation in the DKO atherosclerotic phenotype. Whilst this is not within the scope of the present thesis, the experiments detailed in the next chapter were designed to determine whether or not MR activation specifically in endothelial cells accounts for the findings of the current chapter.

Chapter 6
The role of the endothelial cell in MR-mediated pro-inflammatory pathways

6.1 Introduction

It was shown in the previous chapter that 11β-HSD2 inactivation results in up-regulation of VCAM-1 on the endothelial cell surface of DKO brachiocephalic arteries. However, these studies did not determine whether or not this was due to illicit MR activation, or another effect of loss of 11β-HSD2 activity. It was also not established whether this increase in VCAM-1 was a direct result of MR activation in endothelial cells or an indirect result of MR activation in other cells types. Given that blood pressure is increased in DKO mice (Deuchar *et al.,* 2009) the possibility that VCAM-1 expression was affected by hypertension cannot be ruled out. The literature is deficient in studies investigating the role of MR activation, and 11β-HSD2-mediated protection of MR, in VCAM-1 expression specifically in endothelial cells. Given the early endothelial expression of VCAM-1 in DKO mice and the importance of endothelial cell dysfunction in the initial stages of atherogenesis, investigations into endothelial MR-mediated effects on VCAM-1 are clearly warranted.

In order to overcome some of the difficulties associated with *in vivo* experiments, an *in vitro* cell culture model was employed. This allows the assessment of the role of endothelial cell MR activation without the confounding variables present in the mouse; such as the presence of other cell types, haemodynamic and humoral factors, and the influence of disease progression. Mouse Aortic Endothelial Cells (MAECs) were obtained from the lab of Dr Saito at Tsurumi University in Japan (Nishiyama *et al.*, 2007). These immortalised cells were isolated from the aortas of p53-deficient mice and the group initially cultured the MAECs for over 100 passages to ensure they retained endothelial cell (EC) properties, such as cobblestone morphology, active uptake of acetylated low-density lipoprotein, and expression of EC markers (Nishiyama *et al.*, 2007). As well as this, tumour necrosis factor α (TNF-α) treatment promoted lymphocyte adhesion to MAECs (Nishiyama *et al.,* 2007), lending these cells to the study of inflammatory responses and atherosclerosis.

A further advantage of cell culture is that the study of intracellular mechanisms is straightforward and less time-consuming than it is *in vivo*. As mentioned in the

previous chapter, there are no known mineralocorticoid response elements (MRE) in the promoter of the VCAM-1 gene and so other intracellular pathways must be involved. The transcription factor NF-κB is involved in a whole host of inflammatory responses (Ghosh *et al.*, 2002; Hayden *et al.*, 2008; Vallabhapurapu *et al.*, 2009) and is activated in atherosclerosis (Brand *et al.*, 1996; de Winther *et al.*, 2005; Gareus *et al.*, 2008). It is also known that *endothelial cell* NF-κB plays a major role in many pro-atherogenic processes (Collins *et al.*, 2001; Gareus *et al.*, 2008). In addition to this, NF-κB, is a known regulator of VCAM-1 (Binion *et al.*, 2009; Neish *et al.*, 1992), and rats over-expressing human renin and angiotensin II have increased NF-kB activity which is inhibited by MR antagonism (Fiebeler *et al.*, 2001). NF-κB activity in rats with heart failure was also shown to be inhibited by MR antagonism (Kobayashi *et al.*, 2006). Taken together, these studies provide a link between MR activation, NF-κB, and VCAM-1 expression and it is likely, but to date unconfirmed, that this pathway is operational in endothelial cells.

It was hypothesised that VCAM-1, but not ICAM-1 or MCP-1, would be up-regulated in MAECs in response to activation of MR by both mineralocorticoid and glucocorticoid and that 11β-HSD2 plays a protective role. This pathway likely involves activation of NF-κB. Thus, the aims of this chapter were:

(i) To determine the effects of MR activation in endothelial cells on the expression of VCAM-1, ICAM-1, and MCP-1.

(ii) To elucidate the intracellular pathways involved in MR-mediated up-regulation of VCAM-1.

6.2 Methods

6.2.1 Treatment of MAECs

The following hormones and drugs were employed at the indicated concentrations: TNF-α (10ng/mL), Aldosterone (1nM), Corticosterone (1nM), Spironolactone (1μM), and glycyrrhetinic acid (1μM). In all studies, MAECs were first pre-treated with the inhibitor drugs (spironolactone or glycyrrhetinic acid) for 2 hours prior to the addition of the hormone treatments to ensure maximal inhibition at the time of treatment. For justification of the use of these treatments, see section 2.4.2.

6.2.2 Adhesion molecule expression

For details of immunocytochemistry staining protocols and image analysis, see section 2.4.3.

6.2.3 Cytokine expression

A mouse MCP-1 sandwich ELISA kit (Invitrogen) was used according to the manufacturer's instructions. For full methodological description, see section 2.4.4.

6.2.4 Electromobility shift assay (EMSA)

6.2.4.1 Nuclear protein extractions

Nuclear proteins were extracted using a modified version of the protocol described by Dignam et al (Dignam JD, 1983). See chapter 2.4.5 for full description.

6.2.4.2 NF-κB band shift assay

The activity of NF-κB in nuclear protein extracts was determined by EMSA using NF-κB IRDye 700-labelled DNA oligonucleotides. Binding reactions containing crude nuclear extract (10μg), binding buffer and labelled oligonucleotide were separated by electrophoresis at 20mA in pre-run 6% polyacrylamide gels for around 2 hours. Specific NF-κB binding was shown using an antibody to supershift the band. The Odyssey infrared imaging system was use to analyse the gel. For full methodological details, see section 2.4.5.

6.2.5 Statistical analysis

Data are mean ± sem, analysed by one-way Anova with Bonferroni post-test.

6.3 Results

6.3.1 The role of endothelial MR activation on VCAM-1 expression

VCAM-1 was shown to be increased on the brachiocephalic endothelium of DKO mice compared to *Apoe*$^{-/-}$ mice in the previous chapter. In an attempt to determine a direct role for endothelial cell MR activation in this phenotype, immunocytochemistry was performed on treated MAECs with specific antibody against VCAM-1 (Figure 6.1a). The number of VCAM-1-positive cells per field at x40 magnification was counted in four randomly selected fields per treatment and the mean of five separate experiments was used to construct the graph (Figure 6.1b). Images of stained MAECs show that, compared to untreated cells, aldosterone treatment dramatically increased VCAM-1 expression in MAECs (Figure 6.1a) with the number of cells positively stained for VCAM-1 increased >7-fold (Figure 6.1b), comparable to the 13-fold increase observed with TNF-α (Figure 6.1b), included as a positive control (Wajant *et al.*, 2003). Spironolactone pre-treatment blocked the effect of aldosterone (Figure 6.1a & b), suggesting an MR-mediated mechanism. Corticosterone alone had no effect on VCAM-1 expression (Figure 6.1a & b). However, inhibition of 11β-HSD2 by pre-treatment with glycyrrhetinic acid, an 11β-HSD2 inhibitor (Bujalska *et al.*, 1997) which had no effect on VCAM-1 expression on its own (Figure 6.1b), allowed corticosterone to induce a >9-fold increase in the number of VCAM-1-stained MAECs (Figure 6.1b), demonstrating functional expression of 11β-HSD2 in MAECs. Consistent with MR involvement, VCAM-1 up-regulation by corticosterone in the presence of glycyrrhetinic acid was reversed by blockade of MR with spironolactone (Figure 6.1b).

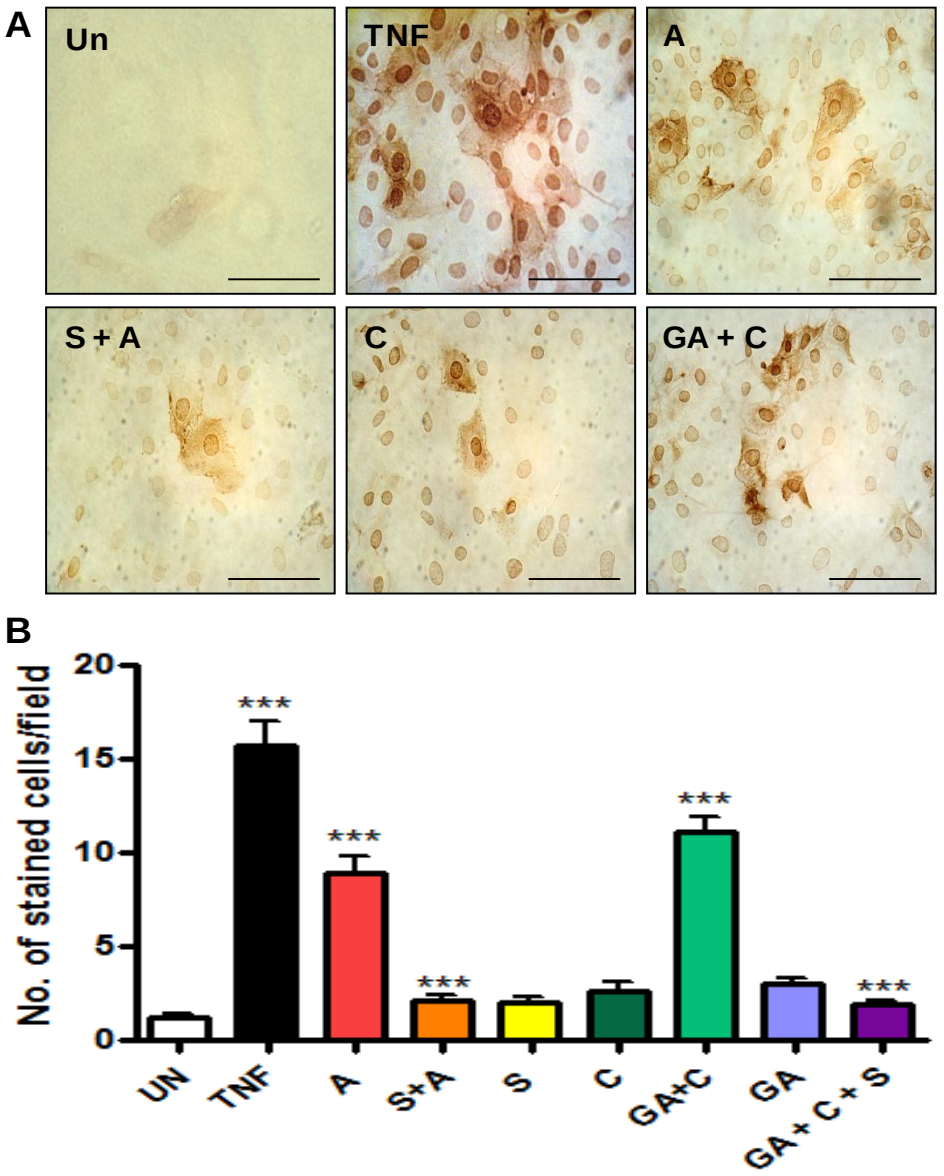

Figure 6.1 VCAM-1 is induced following MR activation in MAECs

MAECs were treated for 24h with 10ng/mL TNF-α, 1nM aldosterone, or 1nM corticosterone, with or without pre-treatment with 1μM spironolactone or 1μM glycyrrhetinic acid for 2h, as indicated. (A) brown staining shows VCAM-1 immunoreactivity. Images captured at x40 magnification. Scale bar = 62.5 μm. VCAM-1 immunopositive cells were counted in 4 randomly selected fields (x40 magnification) per treatment in 5 separate experiments. Aldosterone increased VCAM-1 expression, an effect that was reversible by MR blockade with spironolactone. When 11β-HSD2 was inhibited with glycyrrhetinic acid, corticosterone was able to increase VCAM-1 expression, an effect that was reversible by spironolactone pre-treatment. Data are means +/- sem of 5 experiments. Data were analysed by one-way ANOVA and *** $p<0.0001$. Un = untreated, A = aldosterone, S = spironolactone, C = corticosterone, GA = glycyrrhetinic acid.

6.3.2 The role of endothelial MR activation on ICAM-1 expression

The results of the previous chapter suggest that ICAM-1 expression is not an MR-mediated mechanism as it was constitutively expressed throughout the endothelium in *Apoe*$^{-/-}$ and DKO mice. However, much of the literature contrasts with this finding and so it was decided to determine whether or not MR activation in endothelial cells had an effect on the *level* of ICAM-1 expression. Thus, immunocytochemistry was performed on treated MAECs with a specific antibody to ICAM-1 (Figure 6.2a) and the intensity of staining was measured by replacing the DAB in the last step of the staining protocol with the soluble substrate OPD. This allowed colorimetric measurement of staining intensity and the absorbance at 490nm was used to construct the graph (Figure 6.2b). It was evident from observation of images of ICAM-1 stained MAECs (obtained using the same procedure as was used for VCAM-1 staining) that these cells constitutively expressed ICAM-1, even in the untreated state (Figure 6.2a). It appeared as though some of the treatments might have increased the staining intensity (Figure 6.2a), however, quantification in the plate reader demonstrated no significant effect of any of the treatments on ICAM-1 expression level, including TNF-α (Figure 6.2b).

6.3.3 The influence of MR activation on MCP-1 secretion in MAECs

In the previous chapter, plasma MCP-1 levels were below the limit of detection for the ELISA kit used and so no conclusion could be drawn about the role of MR activation in MCP-1 production. MAECs were used to determine whether MCP-1 is truly not up-regulated by MR activation, which is in contrast to the literature, or whether the kit used was just not suitable for detection of MCP-1 in plasma samples. MAECs were treated for 16h and any MCP-1 protein that was secreted into the cell culture medium was analysed by ELISA. It was found that the only treatment to significantly increase MCP-1 secretion from MAECs was the positive control, TNF-α (Figure 6.3). None of the treatments that activate MR pathways had an effect on MCP-1 production compared to baseline levels in untreated cells (Figure 6.3).

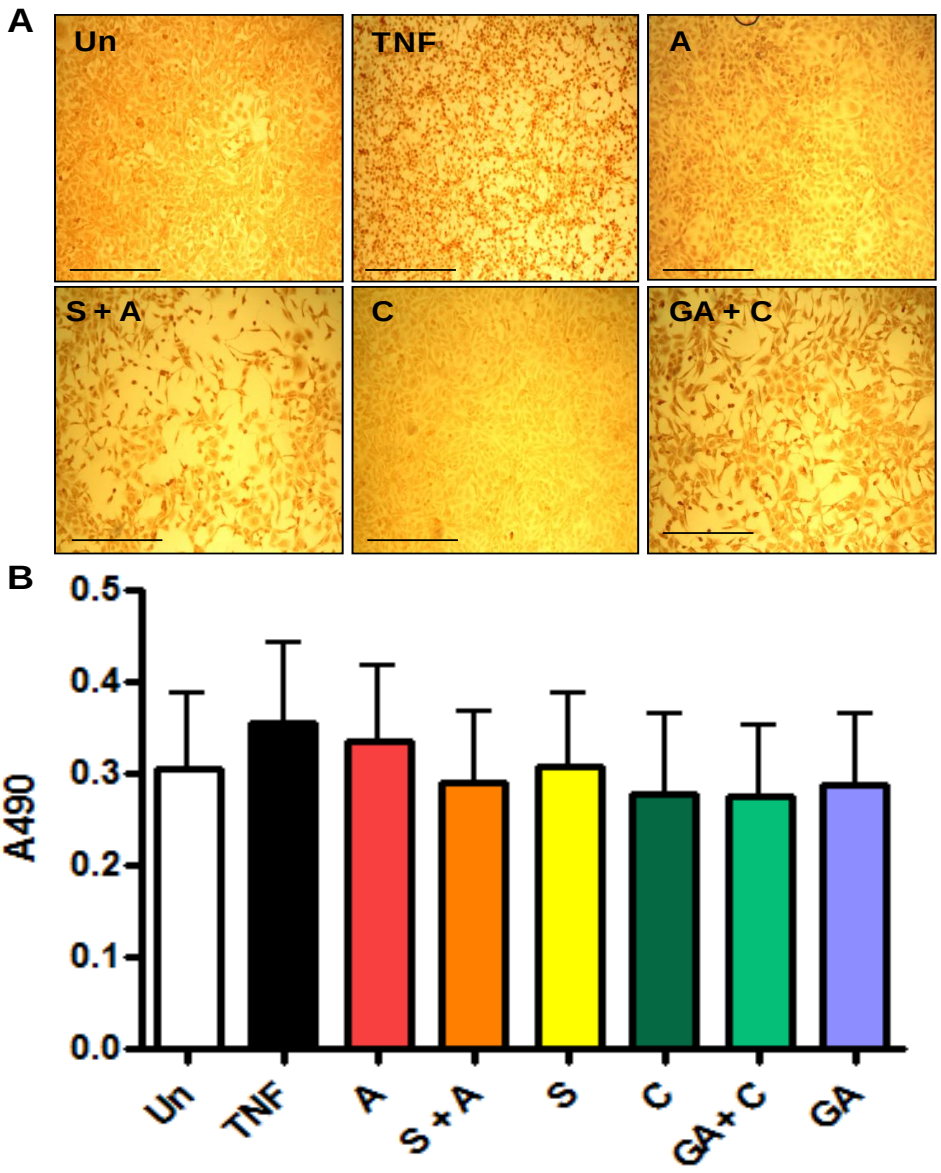

Figure 6.2 ICAM-1 is not regulated by MR-mediated mechanisms in MAECs

MAECs were treated for 24h with 10ng/mL TNF-α, 1nM aldosterone, or 1nM corticosterone, with or without pre-treatment with 1µM spironolactone or 1µM glycyrrhetinic acid for 2h, as indicated. (A) brown staining shows ICAM-1 immunoreactivity. Images captured at x10 magnification. Scale bar = 250 µm. ICAM-1 expression intensity was measured colorimetrically (B). ICAM-1 expression levels were unaffected by any of the treatments employed, including the positive control, TNF-α. Data are means +/- sem. Data were analysed by one-way ANOVA and p=ns. Un = untreated, A = aldosterone, S = spironolactone, C = corticosterone, GA = glycyrrhetinic acid.

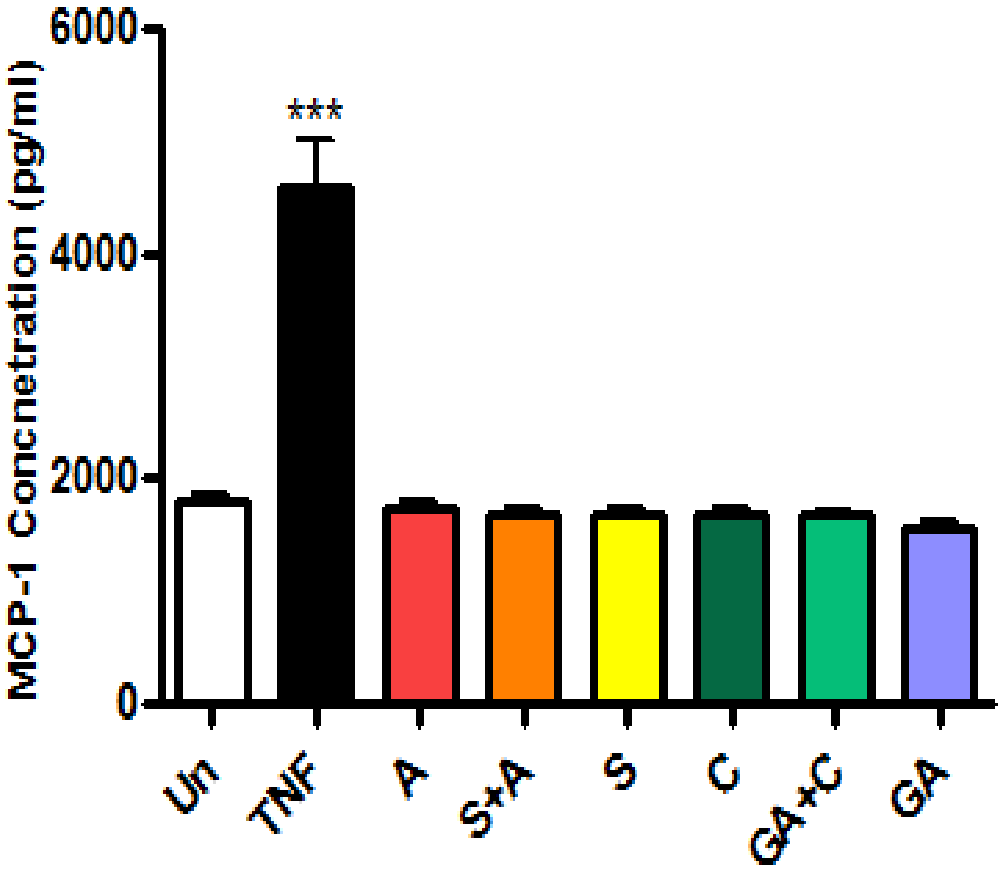

Figure 6.3 MCP-1 secretion is not affected by MR activation in MAECs

MAECs were treated for 16h as indicated prior to measurement of MCP-1 levels in cell supernatants. TNF-α, included as a positive control, increased MCP-1 secretion from MAECs whilst activation of MR had no effect on MCP-1 secretion from MAECs. ELISA was performed in quadruplicate for each treatment. Data are means +/- sem. Data were analysed by one-way ANOVA: *** = $p<0.0001$. Un = untreated, A = aldosterone, S = spironolactone, C = corticosterone, GA = glycyrrhetinic acid.

6.3.4 Involvement of NF-κB in MR-mediated mechanisms

To determine whether the pro-inflammatory effect of MR activation in MAECs involved NF-κB pathways, activation of NF-κB was investigated by electromobility shift assay (EMSA). MAECs were treated with the MR-activating hormones shown to be effective in increasing VCAM-1 expression for 2h before extraction of nuclear proteins and subsequent gel shift assay analysis of NF-κB activation. If NF-κB has been activated by any of the treatments the protein will be present in the nuclear extracts and it will bind to the IR-labelled NF-κB oligo, causing a shift on the gel due to increased size compared to the oligo alone. To ensure that the oligo is specifically binding to NF-κB, an antibody against NF-κB is added to some of the samples which will disrupt the protein-oligo complex thereby causing a supershift on the gel. It can be seen from the gel (Figure 6.4) that NF-κB was activated in the positive control sample (TNF-α) as shown by the presence of a darker band compared to the untreated sample. The specificity of binding was shown by disruption of the band in the second TNF-α lane, marked with a + to indicate the presence of antibody. Thus, the assay is optimised to detect specific activation of NF-κB in MAECs. The next two control lanes, representing spironolactone and glycyrrhetinic acid, showed bands of comparable intensity to those in the untreated samples. NF-κB was activated by aldosterone and the band was disrupted in the presence of antibody. Co-administration of the MR blocker spironolactone reversed this affect of aldosterone on NF-κB activation. Corticosterone alone had no effect on NF-κB activity, however pre-treatment with the 11β-HSD2 inhibitor glycyrrhetinic acid allowed corticosterone to minimally activate NF-κB in MAECs. This band was not disrupted by the presence of the specific antibody.

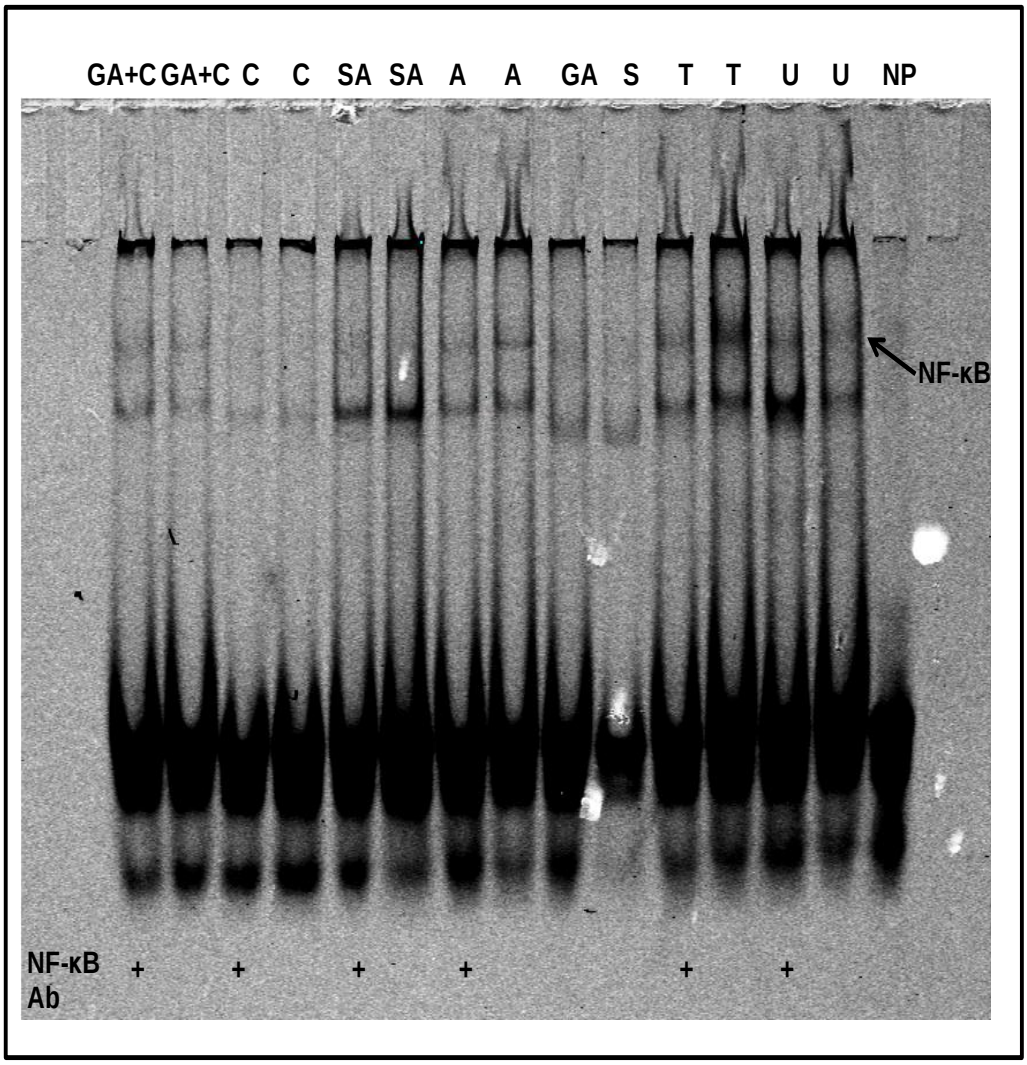

Figure 6.4 Activation of MR in MAECs activates the NF-κB pathway

NF-κB activity was investigated in MAEC nuclear extracts by EMSA. Compared to untreated samples (U), TNF-α (T) and aldosterone (A) activated NF-κB, the specificity of protein-DNA binding in these samples was shown by disruption of the bands in the presence of an NF-κB antibody (Ab) (+ lanes). This affect of aldosterone was reversed by co-administration of spironolactone (SA), demonstrating an MR-mediated mechanism. Spironolactone alone had no effect on NF-κB (S). Corticosterone (C) was unable to activate NF-κB whilst pre-treatment with glycyrrhetinic acid (GA+C), which had no effect on its own (GA), enabled corticosterone to minimally activate NF-κB. There was no binding in the no protein (NP) control sample.

6.4 Discussion

Activation of MR specifically increased VCAM-1, and not ICAM-1 or MCP-1, expression in MAECs, suggesting that the increased expression of VCAM-1 in DKO mice could be due to illicit activation of MR directly in endothelial cells. The protective role of endothelial 11β-HSD2 was demonstrated by the finding that glucocorticoids mimicked the pro-inflammatory actions of mineralocorticoids when 11β-HSD2 activity was compromised.

Pathways of VCAM-1 up-regulation in endothelial cells

In order to determine the possible cellular and molecular mechanisms responsible for the increased endothelial VCAM-1 observed in DKO mice in the previous chapter, activation of MR-mediated pathways was investigated *in vitro* in MAECs. The findings of the present chapter revealed that activation of MR in endothelial cells does indeed lead to increased expression of VCAM-1. Significantly, 11β-HSD2 prevents glucocorticoids from illicitly activating pro-inflammatory pathways in MAECs. It was shown that under conditions of compromised 11β-HSD2 activity, glucocorticoids became MR agonists and were able to promote the same intracellular events as mineralocorticoids. In line with this, it has been reported that glucocorticoids can activate MREs in human coronary and aortic endothelial cells when 11β-HSD2 enzyme is inhibited (Caprio *et al.*, 2008). Also, the beneficial effects of MR blockade in salt-sensitive rats with heart failure were attributed to inhibition of *glucocorticoid-mediated* activation of MR in light of the low aldosterone levels found in these animals (Nagata *et al.*, 2006). However, the present study provides novel direct evidence that activation of MR by glucocorticoids in endothelial cells is pro-inflammatory and, therefore, likely pro-atherogenic. It also supports the concept that extra-renal MR activation is important in the DKO phenotype, as implied by the results of the eplerenone study (chapter 3), and that VCAM-1 up-regulation is not simply a result of hypertension in DKO mice.

Glucocorticoids have been reported to antagonise the actions of mineralocorticoids at the MR in rats (Kenyon *et al.*, 1984) and in the toad bladder (Brem *et al.*, 1991) and it was more recently reported that low concentrations of cortisol blocked aldosterone-

induced MR activation in the presence, but not in the absence, of 11βHSD2 in HEK293 cells (Odermatt *et al.*, 2001). Thus, in MAECs, the lack of effect of glucocorticoids administered alone on VCAM-1 may have been a result of antagonism of the MR. Then, when 11β-HSD2 is inhibited, glucocorticoids might become agonists and mimic the effects of aldosterone at the MR. It would be useful to pre-treat MAECs with glucocorticoid before co-administering aldosterone to establish whether or not glucocorticoids do antagonise the actions of aldosterone at the MR with respect to VCAM-1 expression. Perhaps this idea may explain the finding that physiological levels of aldosterone were able to up-regulate VCAM-1 on MAECs. Given that vascular endothelial cells might normally be exposed to these levels of aldosterone *in vivo* it might not be expected that aldosterone would be pro-inflammatory under normal physiological conditions. However, unlike in the cell culture experiments, vascular endothelial cells *in vivo* will also be exposed to glucocorticoids, which may normally prevent aldosterone activation of MR. This suggests that whilst *excess* glucocorticoids, and/or 11β-HSD2 inactivation, are detrimental to the vasculature, normal physiological levels may be required to protect against the pathological actions of aldosterone. How and why glucocorticoids can switch from antagonism to agonism of MR remains to be investigated. On the other hand, 1nM is considered to be in the 'high' physiological range of aldosterone, as it has been shown to circulate at around 0.2nM in mice (Spyroglou, 2008). Therefore, it could be that small fluctuations of aldosterone within the physiological range are sufficient to compete with glucocorticoids *in vivo* and over-activate the MR, producing pathophysiological effects. This could be a relevant mechanism in the cardiovascular pathologies associated with conditions of mineralocorticoid excess, such as Conn's syndrome (Conn, 1955).

The ultimate result of VCAM-1 up-regulation on endothelial cells is increased adherence and infiltration of monocytes into the intimal space. It would therefore be interesting to perform monocyte adhesion and transmigration experiments on treated MAECs to determine whether or not MR activation, with the associated increase in VCAM-1, can enhance monocyte attachment to the endothelium and subsequent migration. The fact that macrophage content of DKO plaques was significantly

increased compared to *Apoe*$^{-/-}$ plaques suggests that this is in fact the case. Indeed, it was recently demonstrated that MR activation by aldosterone in human coronary and aortic endothelial cells led to increased adherence of monocytes (Caprio *et al.*, 2008). However, this was shown to be through up-regulation of ICAM-1, not VCAM-1, and the ability of glucocorticoids to affect adherence was not studied. Nonetheless, this study does verify that activation of MR in endothelial cells promotes monocyte adhesion through up-regulation of adhesion molecules.

VCAM-1 up-regulation in response to both mineralocorticoid- and glucocorticoid-mediated activation of MR in endothelial cells likely involves a common intracellular pathway. As previously mentioned, there are no known mineralocorticoid response elements (MRE) in the VCAM-1 gene promoter (Caprio *et al.*, 2008; Neish *et al.*, 1992) and so it could be that MR activation promotes activity of other transcription factors which, in turn, regulate VCAM-1 gene transcription. NF-κB, a known regulator of VCAM-1 (de Martin *et al.*, 2000; Neish *et al.*, 1992), was a prime candidate for this role since it has been reported that MR activity is associated with activation of this transcription factor (Fiebeler *et al.*, 2001; Kobayashi *et al.*, 2006). To determine whether or not NF-κB might be the link between MR activation and VCAM-1 expression in endothelial cells, activation of NF-κB was assessed in treated MAECs by EMSA. It was found that MR activation by aldosterone caused activation of NF-κB. In line with this, it was previously reported that mice treated with aldosterone had increased NF-κB activity in the heart (Johar *et al.*, 2006). Also, aldosterone treatment of diabetic rats led to an increase in renal NF-κB activation which was reversed by spironolactone, demonstrating the involvement of MR (Cha *et al.*, 2005). In addition to this, it was recently reported that MR activation by aldosterone in mouse VSMCs resulted in activation of NF-κB (Lemarie *et al.*, 2009). This suggests that this pathway is active in the vasculature and, therefore, could contribute to the pathogenesis of atherosclerosis in DKO mice. Indeed, it is tempting to speculate that MR-mediated up-regulation of VCAM-1 in MAECs involves NF-κB pathways. However, a previous study reported that aldosterone treatment of HUVECs caused up-regulation of mRNA for VCAM-1 without activation of NF-κB (Hashikabe *et al.*, 2006). Perhaps this reflects differences in methodologies or in species, or it could be that other signalling pathways are important in MR-mediated

VCAM-1 expression in endothelial cells. For example, it has been demonstrated that aldosterone induces not only NF-κB, but also active protein 1 (AP-1) activity in hepatic cells in culture (Li *et al.*, 2007). In the present study, corticosterone alone had no effect on NF-κB activation in MAECs, which mirrors the VCAM-1 data. Pre-treatment with the 11β-HSD2 inhibitor glycyrrhetinic acid allowed corticosterone to minimally activate NF-κB, suggesting an MR-dependent mechanism. However, the band for corticosterone-induced NF-κB on the gel (see figure 6.4) was very pale and the presence of NF-κB antibody did not disrupt the band. Thus, it might be concluded that corticosterone in the presence of glycyrrhetinic acid did not specifically activate NF-κB. However, given that the intensity of the band was not convincingly increased compared to untreated control samples, no solid conclusions can be drawn. Perhaps glucocorticoid-mediated up-regulation of VCAM-1 in MAECs was due to activation of alternative pathways. Indeed, it has been shown that the VCAM-1 promoter in HUVECs contains a potential AP-1 binding site (Iademarco *et al.*, 1992). This, in combination with the afore mentioned study demonstrating aldosterone-mediated activation of AP-1 in hepatic cells (Li *et al.*, 2007) suggests a potential role for this pathway in MR-mediated VCAM-1 expression in MAECs. The most reliable way to investigate the importance of NF-κB activation in MR-mediated VCAM-1 expression would be to repeat the VCAM-1 staining experiments in MAECs (see section 6.3.1) in the presence of an NF-κB inhibitor.

ICAM-1 and MCP-1 expression in endothelial cells

Whilst MR-mediated activation of NF-κB was likely involved in VCAM-1 up-regulation on MAECs, this pathway does not appear to affect ICAM-1 or MCP-1 expression. This was surprising given that both ICAM-1 (Roy *et al.*, 2001) and MCP-1 (Landry *et al.*, 1997; Pindolia *et al.*, 1996) are also known to be regulated by NF-κB. Perhaps the particular set of co-activator and co-repressor proteins recruited upon MR activation in MAECs preferentially directs NF-κB activity towards the VCAM-1 promoter. It was reported that inhibition of NF-κB by pyrrolidine dithiocarbamate (PDTC) in HUVECs repressed TNF-α-induced VCAM-1, but not ICAM-1, mRNA expression (Marui *et al.*, 1993). As mentioned above, other

transcription factors may be involved in VCAM-1 expression and so it could be that MR activation in MAECs leads to an interaction between the specific transcription factors that are required to promote VCAM-1 expression, but not ICAM-1 or MCP-1. Alternatively, the methods of detection employed may not have been sensitive enough to expose an effect of MR activation on expression in MAECs.

The fact that the positive control, TNF-α, significantly enhanced MCP-1 secretion from MAECs suggests that the protocol was suitably optimised for detecting changes in MCP-1 production. Time points ranging from 2-24h of treatment were initially studied and activation of MR pathways had no effect on MCP-1 levels at any time point studied. Also, the results are in agreement with those obtained from plasma samples (chapter 5) where MCP-1 levels were equally undetectable in DKO and *Apoe*$^{-/-}$ mice. This contrasts with previous studies where MR activation in humans was associated with increased levels of MCP-1 in the urine of diabetic patients (Takebayashi *et al.*, 2006) and in rats with increased MCP-1 mRNA in the heart (Sun *et al.*, 2002). Aldosterone has also been shown to increase MCP-1 mRNA expression in the kidneys of wild type mice (Ma *et al.*, 2006). However, there is little data on the effect of MR activation on MCP-1 expression in cells of the murine vasculature. Our data demonstrate that MR activation in mouse endothelial cells has no effect on MCP-1 secretion and MCP-1, therefore, is unlikely to play a significant role in the initial recruitment of macrophages to DKO plaques.

The lack of effect of MR activation on ICAM-1 expression in MAECs mirrors the constitutive endothelial expression observed in *Apoe*$^{-/-}$ and DKO mice in the previous chapter. However, TNF-α, a known mediator of ICAM-1 expression (Rothlein *et al.*, 1988), failed to up-regulate ICAM-1 in MAECs, suggesting that the methods used were not sensitive enough to detect changes in ICAM-1. The basal expression levels were high on untreated MAECs and so perhaps they could not be increased further by stimuli. If ICAM-1 was maximally expressed on MAECs under normal conditions then it might be suggested that some factor present in the cell culture medium was responsible for this. Culture medium, particularly that supplemented with serum, contains growth factors and other components that can affect cell

physiology. Importantly, it has recently been reported that one of the components of the endothelial basal medium used in the present study, epidermal growth factor, increases ICAM-1 expression in bronchial epithelial cells (Liu *et al.*, 2008). Thus, it could be that in order to detect changes in ICAM-1 expression on MAECs, the culture medium needs to be altered. Indeed, the study in which MR activation was shown to increase ICAM-1 levels in human endothelial cells (Caprio *et al.*, 2008) employed medium that had been charcoal-stripped to remove factors that may interfere with expression levels. Given the high constitutive expression of ICAM-1 observed both *in vitro* and *in vivo*, it is difficult to draw any definite conclusions about the role of MR activation in ICAM-1 expression.

Conclusions

Inactivation of 11β-HSD2 in endothelial cells allows glucocorticoids to illicitly activate the MR, promoting up-regulation of VCAM-1 possibly through NF-κB activation. This confirms that the pro-atherosclerotic effects of 11β-HSD2 inactivation are not purely due to inappropriate activation of renal MR with associated hypertension but that extra-renal, and specifically endothelial, MR activation likely plays a significant role. Given the protective effect of MR blockade on aldosterone- and glucocorticoid- mediated up-regulation of VCAM-1 in MAECs, the benefits of eplerenone treatment both in DKO mice and in humans may be partially due to inhibition of pro-inflammatory molecule expression in the vasculature.

Chapter 7
Discussion

The work described in this thesis used a transgenic mouse model to assess the role of inappropriate MR activation, and the protective role of 11β-HSD2, in atherogenesis. The potential of MR antagonist administration for the inhibition of atherosclerosis has been demonstrated in several animal models and the cardio-protective effects of MR blockade in humans were greater than expected for the moderate decrease in blood pressure observed. However, the roles of MR signalling during atherosclerosis are largely unknown. Furthermore, whilst glucocorticoids and mineralocorticoids can influence certain aspects of vascular structure and function, the role of endogenous steroid hormones and 11β-HSD2 in modulating atherogenic processes has not been investigated. Therefore, the overall objective of the present studies was to advance understanding of how MR activation influences atherogenesis and to determine a protective role for 11β-HSD2 in vascular pathology.

7.1 The DKO mouse as a model of atherosclerosis

This is the first thesis describing the *Apoe*$^{-/-}$/11β-HSD2$^{-/-}$ DKO mouse and therefore it is very important to discuss the suitability of this model in the study of atherosclerosis. The *Apoe*$^{-/-}$ mouse has been extensively used to investigate numerous aspects of atherosclerotic disease (Meir *et al.*, 2004) and has proved to be a very convenient and reliable model for these purposes. This model has also been used as a test bed for studying the effects of a variety of endogenous and exogenous agents on atherosclerosis. For example, the effects of dietary components (Guo *et al.*, 2002; Kaplan *et al.*, 2001; Stocker *et al.*, 2004) , anti-oxidant therapy (Nakata *et al.*, 2002; Pratico *et al.*, 1998), steroid hormones (Bourassa *et al.*, 1996; Elhage *et al.*, 1997), lipid-lowering drugs (Chiwata *et al.*, 2001; Kusunoki *et al.*, 2001), and immunomodulatory agents (Daugherty *et al.*, 1997; Inoue *et al.*, 2002; Paul *et al.*, 2004) on atherogenesis have been investigated in the *Apoe*$^{-/-}$ mouse. In recent years, other genes that may affect atherosclerosis have been studied through the generation of DKO mice or *Apoe*$^{-/-}$ mice over-expressing a transgene. Each of these methods has advantages and disadvantages. Over-expressing a transgene can be particularly useful in studying the function of proteins that are not normally expressed in the mouse, however this technique is limited by the fact that integration into the mouse genome occurs randomly and the copy number of the transgene cannot be controlled.

This results in different expression levels between mice and the accidental insertion of the transgene into an endogenous mouse gene sequence can produce a non-specific phenotype (Marschang *et al.*, 2003). The use of gene targeting to knockout genes of interest overcomes some of the problems of transgene over-expression and crossing these mice with *Apoe*$^{-/-}$ mice enables the effects of the gene of interest on atherosclerosis to be investigated. Indeed, a variety of mice in which genes involved in lipid metabolism (Suzuki *et al.*, 1997; Willner *et al.*, 2003), inflammation (Caligiuri *et al.*, 2003; Dong *et al.*, 2000), and haemostasis (Xiao *et al.*, 1997; Xiao *et al.*, 1998) have been knocked out and crossed with *Apoe*$^{-/-}$ mice to generate DKO models have been successfully used to study atherosclerosis. However, the current *Apoe*$^{-/-}$/11β-HSD2$^{-/-}$ DKO mouse offers several advantages over other DKO models of atherosclerosis. In the current model, both mutations are on a pure C57Bl/6 background, which is in contrast to other models in which mice from mixed backgrounds were used (Willner *et al.*, 2003; Xiao *et al.*, 1997; Xiao *et al.*, 1998). It is known that mutations may manifest differentially on different genetic backgrounds and so by maintaining genetic uniformity through in-breeding, inter-individual variances in phenotype are minimized. Importantly, the current model also has the advantage that advanced lesions develop rapidly on a normal chow diet, removing the need to expose the mice to abnormally high levels of cholesterol, which may itself affect lesion properties (Jawien *et al.*, 2004). The observation that DKO mice have buried fibrous caps in their plaques is indicative of previous plaque ruptures and instability. Whilst there is evidence to suggest that plaque rupture may occur in *Apoe*$^{-/-}$ mice fed a high-fat high-cholesterol diet (Johnson *et al.*, 2005; Johnson *et al.*, 2001), there is no widely accepted model of murine plaque rupture to date. Thus, the DKO mouse may prove to be a more clinically significant model of human atherosclerosis. This is supported by the finding that DKO mice also suffer from an as yet undetermined form of cardiac sudden death, which whilst thought not to be due to plaque rupture, might be a result of cardiac ischaemia induced by coronary atherosclerosis (Deuchar *et al.*, 2009a).

With relevance to the themes of the present thesis, investigations into roles of the renin-angiotensin-aldosterone system (RAAS) in atherosclerosis and the cardio-

protective mechanisms of MR antagonists using *Apoe*$^{-/-}$ mice have revealed important insights into the pathological consequences of dysregulation of this system. However, many of these studies employ supra-physiological concentrations of aldosterone and so do not reflect the consequences of endogenous steroid hormone action. Also, the majority of the investigations into MR activation in CVD focus on aldosterone and neglect to mention glucocorticoids. Furthermore, a role for 11β-HSD2 in protection against MR-mediated pro-atherogenic events remains to be determined. The DKO mouse counters these problems by allowing the effects of endogenous steroid hormones inappropriately activating the MR in the absence of 11β-HSD2 to be studied. Thus, the DKO mouse is an ideal model for investigating the roles of illicit MR activation during atherogenesis.

7.2 The role of MR activation in atherosclerosis

Treatment of DKO mice with eplerenone allowed an assessment of the contribution of illicit MR activation to the accelerated atherogenesis observed in these mice. It was shown that MR activation was responsible, at least partially, for the accelerated nature of atherogenesis, the promotion of an unstable plaque phenotype, and an enhanced vascular inflammatory environment. A comparison between DKO and *Apoe*$^{-/-}$ mice supported the results of the eplerenone study, demonstrating that loss of 11β-HSD2 activity accelerates the formation of unstable plaques and promotes a pro-inflammatory vascular environment. Taken together, these results suggest that 11β-HSD2 plays a vital role in protecting against MR-mediated pro-atherogenic changes in the vasculature. However, these studies did not determine whether it was aldosterone or glucocorticoids that were activating the MR in DKO mice. The much greater circulating concentrations of glucocorticoids compared to aldosterone makes it tempting to assign this action to glucocorticoids. Indeed, 11β-HSD2$^{-/-}$ mice have decreased circulating levels of aldosterone (Kotelevtsev *et al.*, 1999) and so, presuming that loss of *ApoE* has no effect on mineralocorticoid levels, DKO mice are expected to also have low aldosterone levels. Thus, the demonstration that MR blockade was anti-atherosclerotic in DKO mice, with low aldosterone levels, lends support to the notion that *glucocorticoid* activation of MR precipitates vascular

disease in this model. One method of resolving this would be to adrenalectomise the DKO mice and exogenously replace either aldosterone or glucocorticoids.

In recent years it has become increasingly apparent that activation of MR in non-epithelial, non-classical aldosterone target tissues is very important in various cardiovascular pathologies. The work in the present thesis supports this idea and extends the knowledge in this area by providing mechanistic information about MR activation in the vasculature. Whilst renal MR activation with associated hypertension is likely to play a role in the atherosclerotic phenotype of the DKO mouse, it is clear that activation of MR directly in cells of the vasculature is also key to the pathology. It is well established that hypertension is a major risk factor for atherosclerosis and may well contribute towards endothelial dysfunction during the initial stages of atherogenesis in DKO mice. That this is possible is supported by the fact that patients with Cushing's disease (Setola *et al.*, 2007) and 11β-HSD2$^{-/-}$ mice (Christy *et al.*, 2003) both have hypertension and endothelial dysfunction. Further, it was concluded that glucocorticoids did not promote the endothelial dysfunction in 11β-HSD2$^{-/-}$ mice through direct actions on the vascular wall (Christy *et al.*, 2003), but rather through indirect effects, likely hypertension. Thus, hypertension cannot be ruled out as an important mediator of atherosclerosis in DKO mice. However, the finding that blockade of MR without a reduction in blood pressure in DKO mice had a significant inhibitory effect on atherogenesis suggests that hypertension is not the only, and probably not the main, factor involved. It has been noted throughout this thesis that the vast majority of studies showing cardio-protective benefits of MR blockade find that this is independent of blood pressure lowering. Endothelial cells are not only intimately involved in the pathogenesis of atherosclerosis but they also express the necessary receptors and enzymes to be glucocorticoid/mineralocorticoid responsive. The finding that VCAM-1 was significantly up-regulated on brachiocephalic endothelial cells in DKO mice compared to *Apoe*$^{-/-}$ mice further supported a role for endothelial cell MR activation in atherosclerosis. The need for frozen instead of paraffin embedded sections in the VCAM-1 staining procedure prevented the expression of VCAM-1 being studied in mice treated with eplerenone. However, whilst this could have shown whether or not the increase in VCAM-1 was MR-mediated, it would not have proven that this phenotype was a direct result of

MR activation in the endothelial cells themselves. This issue was addressed in cell culture using a mouse aortic endothelial cell (MAEC) immortalised secondary cell line. The results of these experiments were very important in that they demonstrated a causative role for endothelial MR activation in up-regulation of VCAM-1. A novel role for endothelial 11β-HSD2 in protection against glucocorticoid-mediated expression of VCAM-1 through the MR was also revealed. This in combination with the *in vivo* data for VCAM-1 provides one of the non-renal mechanisms by which illicit MR activation may promote atherogenesis.

In an attempt to further distinguish between the consequences of renal and extra-renal MR activation, the kidney-rescue DKO mouse was generated (KRDKO). A wild-type mouse expressing human 11β-HSD2 under the control of the aquaporin 2 (AQP2) promoter was crossed with a DKO mouse in order to obtain DKO mice that have been 'rescued' for 11β-HSD2 in the AQP-2 expressing collecting duct cells of the kidney. It was expected that these mice should have normalised blood pressure and electrolyte balance and therefore any atheroma still present over and above that afforded by the *Apoe*$^{-/-}$ state would be due to activation of extra-renal MR. These mice were not ready in sufficient numbers until very recently and so could not be included in the present thesis. However, some preliminary experiments have been recently been performed and suggest that blood pressure is significantly reduced compared to DKO mice but is still significantly greater than that in *Apoe*$^{-/-}$ mice. Thus the rescue is likely not complete and requires further characterisation.

7.3 Mechanisms of accelerated atherogenesis in DKO mice

Based on the results of the present studies along with those reported in the literature, a schematic diagram illustrating the possible mechanisms involved in MR-mediated atherogenesis in DKO mice has been composed (Figure 7.1). The early increased expression of VCAM-1 in DKO brachiocephalic arteries (chapter 5), and the finding that glucocorticoids illicitly activate endothelial cell MR in the absence of 11β-HSD2 activity to cause up-regulation of VCAM-1 (chapter 6); led to the hypothesis that VCAM-1 may be the initiating event in atherogenesis in DKO mice. In order to more fully investigate this possibility, it would be constructive to study VCAM-1 expression at a younger age in DKO mice (1-2 months). This would show whether

or not VCAM-1 up-regulation precedes the development of atherosclerotic lesions. In support of this, it was previously shown that VCAM-1 expression preceded sub-endothelial monocyte accumulation in a model of vein graft atherosclerosis (Hanyu *et al.*, 2001). As well as direct effects on VCAM-1 expression, MR activation may also indirectly increase VCAM-1 through inhibition of NO synthesis in the endothelium (Wilson *et al.*, 2009).

In the current proposal, this initial increase in endothelial VCAM-1 would then lead to enhanced capture of macrophages, thereby contributing to the increased infiltration of macrophages observed in plaques from DKO mice (chapter 4). That this was an MR-mediated mechanism was demonstrated by reversal with eplerenone treatment (chapter 3). In addition to this, it has been reported that VCAM-1 expression is also associated with the production of MMPs via ROS generation (Deem *et al.*, 2004). It is thought that this endothelial production of MMPs aids in leukocyte migration across endothelial cells (Deem *et al.*, 2004), providing a further mechanism by which VCAM-1 may increase macrophage recruitment to plaques. In turn, these MMPs in union with MMPs that are likely to be secreted by the increased numbers of macrophages, could promote the breakdown of collagen within the plaque. In order to determine if this might be an important mechanism in the significantly decreased collagen content found in plaques from DKO mice (chapter 4), it would be beneficial to perform zymography experiments on plaque homogenates from *Apoe*$^{-/-}$ and DKO mice to assess MMP activity.

The current hypothesis then proposes that the MR-mediated reduction in plaque collagen content in DKO mice (chapter 3) could alter SMC content, shown to be increased by MR blockade (chapter 3), through a concomitant decrease in migration of SMCs into the intimal space (Rocnik *et al.*, 1998). SMC content may also be directly affected by macrophages through release of pro-apoptotic factors which have been shown to deplete plaque-derived SMCs in culture (Boyle *et al.*, 2001b). Finally, the macrophage may also be partially responsible for the increased plaque lipid content observed in DKO mice (chapter 4). The main sources of plaque lipids are blood lipids and lipids released by necrotic macrophage foam cells (Falk *et al.*, 1995), but the relative contribution of each to total plaque lipid is a controversial

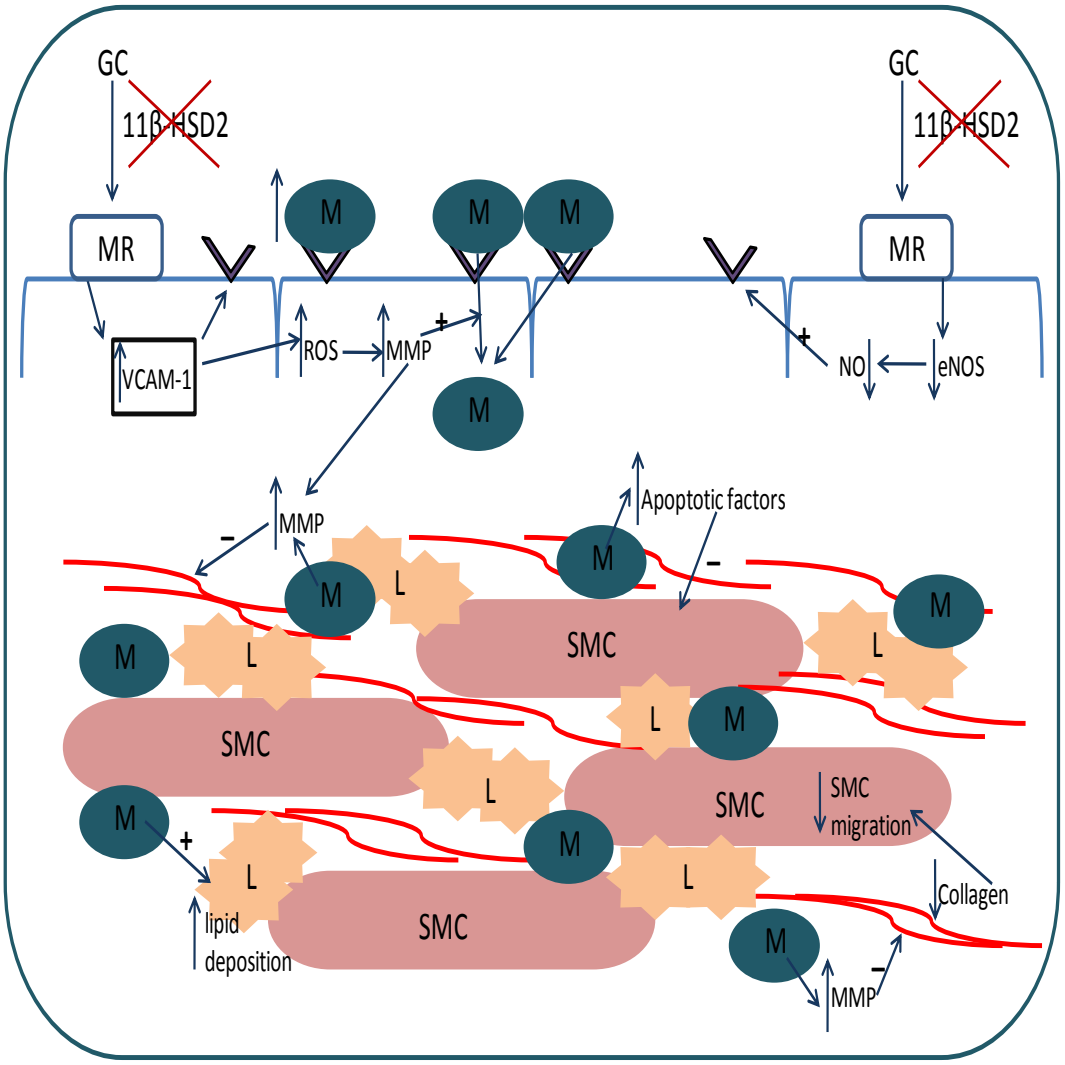

Figure 7.1 Mechanisms of atherogenesis in DKO mice

Schematic representation of atherogenesis in DKO mice. MR-mediated up-regulation of VCAM-1 in endothelial cells, either directly or indirectly through reduced NO synthesis, may precipitate a host of pro-inflammatory and pro-atherogenic events responsible for the accelerated atherosclerotic phenotype. VCAM-1 may aid enhanced capture of macrophages resulting in the increased plaque macrophage content observed in DKO mice. Macrophages may then lead to increased collagen breakdown through release of MMPs, enhanced SMC apoptosis through release of pro-apoptotic factors, and increased lipid deposition via the formation and necrosis of lipid-laden foam-cells. The proposed mechanism involves a complex interplay of cellular and molecular events with the macrophage being central to pathology. M = macrophages, SMC = smooth muscle cells, L = lipids, and collagen is represented by the red fibres.

issue. Given that total plasma cholesterol levels were unaltered (chapter 4) but plaque macrophage content was increased in DKO mice, it is tempting to speculate that the increased lipid content is due to deposition by macrophages.

In summary, the results of this thesis have enabled the development of a reasonable theory of the mechanisms by which illicit MR activation, specifically in endothelial cells, may accelerate the atherosclerotic process in *Apoe*$^{-/-}$ mice. This combined with the evidence in the literature suggests a variety of inter-dependent mechanisms through which atherogenesis may occur in DKO mice. Whilst it is more than likely that a complex interplay of mechanisms are involved, it is tempting to speculate that a very early increase in endothelial VCAM-1 expression may be the initiating MR-mediated factor.

7.4 Potential clinical significance of results

Studies assessing the actions of illicit MR activation on atherosclerosis have implications for the clinical use of both steroids and MR antagonists in humans for the treatment of various diseases. The present findings further the knowledge on how eplerenone produces cardioprotective benefits in patients with heart failure by providing possible mechanisms of action in the vasculature. It could be suggested that illicit activation of MR, perhaps due to inflammatory down-regulation of 11β-HSD2 (Suzuki *et al.*, 2005) during chronic disease, promotes endothelial up-regulation of VCAM-1 and subsequent monocyte infiltration into the vascular wall with the consequence of *accelerating* atherogenesis. Continuing MR activation may then result in the formation of macrophage and lipid rich plaques that lack structural integrity due to diminished collagen content, thereby increasing the likelihood of plaque rupture and the associated clinical sequalae. Thus, MR blockade in patients might be expected to halt the progression of atherosclerosis and favour the formation of more stable plaques. This, in turn, would decrease the frequency and/or severity of clinical endpoints. The results of this thesis also support previous evidence for the positive relationship between exogenous glucocorticoid therapy and cardiovascular risk in humans. Whilst in the present studies endogenous glucocorticoids had unrestricted access to the MR, which is not the case in patients treated with exogenous glucocorticoids, it has previously been reported that high concentrations

of glucocorticoids can overwhelm 11β-HSD2 and subsequently illicitly activate the MR (Odermatt *et al.*, 2001). Whether these increased levels of glucocorticoids in humans undergoing therapy promote CVD through saturation of 11β-HSD2, and activation of MR, in renal or extra-renal tissues remains to be determined. Perhaps there is a case for employing local treatment with glucocorticoids in the future rather than subjecting the whole systemic circulation to abnormally high levels of these steroids.

The observed detrimental actions of glucocorticoids on the vasculature in the present study point towards the use of 11β-HSD1 inhibitors in atherosclerosis. In line with this, 11β-HSD1 inhibition has been shown to delay the progression of atherosclerosis in mice (Hermanowski-Vosatka *et al.* 2005). Recent evidence suggests that increased tissue 11β-HSD1 activity is associated with symptoms of the metabolic syndrome (Walker, 2006a). Thus, intracellular glucocorticoids may contribute to this condition, and inhibitors of 11β-HSD1 have become an important novel therapeutic target for the treatment of its underlying cardiovascular risk factors (hypertension, insulin resistance, dyslipidemia and atherosclerosis). However, whilst this appears to be an attractive target, other aspects relating to the systemic inhibition of tissue 11β-HSD1 activity need to be considered. A reduction in inflammatory cell glucocorticoid levels may have pro-inflammatory effects and delay the resolution of inflammatory responses (Gilmour *et al.* 2006). This has important implications in the development of chronic inflammatory conditions, including atherosclerosis. Also, enhancement of angiogenesis via 11β-HSD1 inhibition (Small *et al.*, 2005) would be detrimental in some pathological conditions, such as cancer or diabetic retinopathy. Therefore a balance between the 'positive' and 'potentially adverse' affects of 11β-HSD1 inhibition needs to be established if these agents are to be successfully used in the clinic.

Blockade of MR with currently available antagonists has clear benefits in cardiovascular pathologies, however, the use of these drugs is limited in patients due to inactivation of renal MR and associated hyperkalemia (Pitt *et al.*, 1999). Systematic investigations into the effects of MR activation in specific cells of the cardiovascular system are required to aid in the development of tissue and/or cell

specific antagonists. Knowing the exact detrimental mechanisms caused by MR activation in individual cells will be important in determining which cells to target for treating various aspects of disease. For example, the results of the present thesis implicate *endothelial cell* MR activation in the pathogenesis of the DKO phenotype and therefore suggest that an endothelial cell specific MR antagonist may be efficacious in the treatment of atherosclerosis. A recent study showing a protective effect of macrophage-specific MR knockout against hypertension in the DOC/salt mouse model (Rickard *et al.*, 2009a) is suggestive that targeting macrophage MR with a cell-specific antagonist would be beneficial in hypertensive disorders. This promising evidence should lead to the development of cell-specific MR antagonists in the future.

7.5 Future directions

As well as highlighting important aspects regarding the effects of adrenal steroids and MR activation on the pathogenesis of atherosclerosis, the work described in this thesis has also provided a basis for further experiments. The introduction of the DKO mouse as a model of MR activation in atherosclerosis will allow the study of many other potential factors and pathways in atherogenesis. In addition, there are several prospective studies that could extend the work described here.

7.5.1 The DKO mouse as a 'test-bed'

The DKO mouse has clear potential as a test-bed for anti-atherosclerotic agents, and not only those associated with MR/11β-HSD pathways but also agents that act on other pathways. Given the hypertensive phenotype of the DKO mouse it could be a good model for testing new and existing anti-hypertensive drugs. As well as testing their ability to lower blood pressure, the impact of these drugs upon atherosclerosis could also be investigated. It was recently reported that in addition to their cholesterol lowering abilities, statins also reduced systolic blood pressure in hypertensive hypercholesterolaemic patients (Chopra *et al.*, 2007). The DKO mouse would be ideal for investigating the mechanisms involved in both the anti-atherosclerotic and anti-hypertensive actions of statins. One of the main advantages of the DKO mouse over the *Apoe*$^{-/-}$ mouse is that they develop complex lesions early

in life without the need for high-fat feeding. The present studies have shown that plaque stability can easily be measured in DKO mice through comparisons of plaque composition, lending the DKO mouse to investigations of the plaque-stabilising effects of statins (Libby *et al.*, 2003) and other drugs. The DKO mouse may also prove useful for testing anti-inflammatory agents targeted towards atherosclerosis due to the enhanced inflammatory nature of the atherosclerosis in this model.

Recent advances in non-invasive imaging techniques have allowed atherosclerosis to be assessed in live mice (Fayad *et al.*, 1998). These techniques are becoming increasingly sensitive and it is now possible to differentiate between different plaque components (Itskovich *et al.*, 2003). Given that DKO mice develop large complex plaques on a chow diet, they would be particularly useful in the development of techniques that allow a detailed examination of plaque composition through non-invasive imaging. The fact that the composition of plaques in DKO mice can be quite dramatically altered with drug treatment further supports the idea that this model would be particularly useful in developing this type of technology.

7.5.2 MR vs. GR

The pro-atherogenic actions of mineralocorticoids/glucocorticoids in the DKO mouse have been attributed to MR activation which, given the loss of 11β-HSD2-mediated protection of MR, is a sound hypothesis. In addition to this, the results of the drug study and the cell culture work provide direct evidence that MR activation is causative in the DKO phenotype. However, 11β-HSD2 also limits glucocorticoid access to the GR (Paterson *et al.*, 2005) and so effects of GR activation of atherogenesis cannot be completely ruled out. It is thought that 11β-HSD2 mediated protection of GR is particularly important during pre-natal development where 11β-HSD2 in the placenta may protect against the effects of abundant maternal glucocorticoids (Seckl, 2001). Foetal exposure to glucocorticoids is associated with increased cardiovascular risk factors (hypertension, hyperglycaemia, and hyperinsulinaemia) and disease in adult life (Seckl, 2001). Thus, it might be suggested that increased glucocorticoid access to GR during pre-natal development would play an important role in the DKO atherosclerotic phenotype later in life. In order to try and minimise the *in utero* effects of glucocorticoids in DKO mice,

females that were heterozygous, and not complete knockout, for 11β-HSD2 were used for breeding. However, it was recently demonstrated that 11β-HSD2$^{-/-}$ mice born to either 11β-HSD2 homozygous or heterozygous null mothers exhibited features of excess foetal glucocorticoid exposure (Holmes *et al.*, 2006). Therefore, DKO mice born to 11β-HSD2 heterozygous mothers will likely still suffer from the effects of enhanced GR activation in pre-natal life.

Whilst GR activation may be important in 'programming' DKO mice *in utero* to increase their susceptibility to cardiovascular disease, MR activation is most likely responsible for the accelerated atherosclerotic disease. Indeed, previous studies suggest that activation of GR would be anti-atherosclerotic (Asai *et al.*, 1993; Tauchi *et al.*, 2001). To investigate this further, a pharmacological approach to confirm the role of GR in atherosclerosis in the DKO mouse could be employed. The GR antagonist RU38486 could be administered to pregnant females such that the effects of pre-natal glucocorticoid exposure on atherosclerosis in the offspring could be investigated. RU38486 could also be administered to DKO mice in the same way that eplerenone was in this thesis to study the effects of GR activation on atherogenesis later in life.

7.5.3 Mechanisms of unstable plaque formation

If cell-specific drugs are to be developed for the treatment of atherosclerosis, it will be important to determine the cellular and molecular mechanisms by which MR activation accelerates the formation of vulnerable plaques in this model. Since it is very likely that MR antagonists act by inhibiting the early inflammation in DKO mice, experiments to investigate this hypothesis are an important next step. Treating DKO mice with a neutralising antibody against VCAM-1 would aid in determining the contribution that increased endothelial VCAM-1 expression makes to the formation of macrophage-rich plaques. As well as this, the macrophages themselves may be phenotypically different in DKO mice. It is known that macrophages can be polarized by the microenvironment to mount specific functions and they can be broadly classified into two main groups; classically activated and alternatively activated (Martinez *et al.*, 2008). It was recently shown that knockout of MR in macrophages reduced the inflammatory response in hearts of DOCA/salt-treated

mice (Rickard *et al.*, 2009a), suggesting a specific role for macrophage MR activation in the inflammatory response to injury. Obtaining primary cultures of macrophages from DKO mice may be informative in determining their specific phenotype. If it were found that macrophages in DKO mice were polarised towards the classically activated 'inflammatory' phenotype (Mosser *et al.*, 2008) it might be worth considering the development of a macrophage-specific MR blocker. Only a small proportion of the possible inflammatory mechanisms involved in atherogenesis were studied in this thesis and so it would be worth more fully characterising the inflammatory response elicited by MR activation in DKO mice. This could be investigated using a cytokine array to determine which molecules are differentially regulated between DKO and *Apoe*$^{-/-}$ mice.

As previously mentioned, the role of MMPs in degrading collagen in DKO plaques should be investigated to dissect the mechanisms by which MR activation reduces plaque collagen content and thus integrity. It would also be important to determine the cellular source of MMPs in plaques, this could be done using confocal microscopy to co-localise MMP-specific immunostaining with cell-specific markers (e.g. Mac-2, SMA, and CD31). Whilst it would be challenging to determine the contributions of plasma and macrophage lipids to the increased plaque lipid content observed in DKO mice, it would be possible to investigate each separately. Cultured macrophages from DKO and *Apoe*$^{-/-}$ mice could be compared in their abilities to differentiate into lipid-laden foam-cells. Also, primary cultures of endothelial cells from *Apoe*$^{-/-}$ and DKO mice could be tested for their potential to oxidise and take-up LDL particles.

7.5.4 Renal vs. extra-renal MR activation

Whilst blood pressure was not fully normalised in the KRDKO mouse, it would still be worth investigating the atherosclerosis in these animals. First of all, the extent of the renal 11β-HSD2 rescue would need to be established by performing radioactive enzyme activity assays on kidneys from KRDKO, DKO and *Apoe*$^{-/-}$ mice. It would also be useful to perform immunohistochemistry on kidneys from KRDKO mice to investigate the expression pattern of the human transgene. It has previously been reported that a physical association between the MR and 11β-HSD2 is required for

normal function of the receptor (Odermatt *et al.*, 2001). Therefore, co-localisation studies using antibodies against murine MR and human 11β-HSD2 could be performed to determine whether or not this interaction occurs in KRDKO mice. In line with the blood pressure results, plasma potassium levels were also not normalised in KRDKO mice, further supporting the idea that the rescue is not complete. However, if it were found that the atherosclerotic burden, plaque composition, and VCAM-1 expression was not altered in KRDKO mice compared to DKO mice then it could reasonably be postulated that renal hypertension is not the determining factor in the DKO phenotype. It might be more informative to generate vascular cell-specific 11β-HSD2 KO mice on the *Apoe*$^{-/-}$ background to distinguish between renal and non-renal MR-mediated effects. Given the results of this thesis, the obvious target for a cell-specific 11β-HSD2 KO would be the endothelial cell.

7.6 Conclusions

In conclusion, these studies have provided valuable insight into the effects of MR activation on atherosclerosis. The role of endogenous glucocorticoids and their metabolism by 11β-HSD2 during atherogenesis was investigated for the first time. The importance of continued research into the mechanisms of eplerenone action is highlighted by the results of this thesis. One of the most important observations of these studies is the detrimental consequences of compromised 11β-HSD2 activity on atherosclerotic disease. Investigations of the regulation of 11β-HSD2 activity, particularly by inflammatory factors, during different pathological conditions might aid in determining the potential efficacy of MR blockade in certain diseases. Until very recently, the detrimental actions of MR activation were attributed to mineralocorticoid activity, this thesis demonstrates a potential role for glucocorticoid-mediated activation of MR in pathophysiological conditions. Perhaps in the future, attention should be focused on the receptor and not the hormone.

Reference List

Abe, Y, El-Masri, B, Kimball, KT, Pownall, H, Reilly, CF, Osmundsen, K, Smith, CW, Ballantyne, CM (1998) Soluble cell adhesion molecules in hypertriglyceridemia and potential significance on monocyte adhesion. *Arterioscler Thromb Vasc Biol* **18**(5)**:** 723-731.

Agarwal, AK, Monder, C, Eckstein, B, White, PC (1989) Cloning and expression of rat cDNA encoding corticosteroid 11 beta-dehydrogenase. *J Biol Chem* **264**(32)**:** 18939-18943.

Aguilera, G, Parker, DS, Catt, KJ (1982) Characterization of somatostatin receptors in the rat adrenal glomerulosa zone. *Endocrinology* **111**(4)**:** 1376-1384.

Albano, JD, Brown, BL, Ekins, RP, Tait, SA, Tait, JF (1974) The effects of potassium, 5-hydrocytryptamine, adrenocorticotrophin and angiotensin II on the concentration of adenosine 3':5'-cyclic monophosphate in suspensions of dispersed rat adrenal zona glomerulosa and zona fasciculata cells. *Biochem J* **142**(2)**:** 391-400.

Amelung, D, Hubener, HJ, Roka, L, Meyerheim, G (1953) Conversion of cortisone to compound F. *J Clin Endocrinol Metab* **13**(9)**:** 1125-1126.

Amento, EP, Ehsani, N, Palmer, H, Libby, P (1991) Cytokines and growth factors positively and negatively regulate interstitial collagen gene expression in human vascular smooth muscle cells. *Arterioscler Thromb* **11**(5)**:** 1223-1230.

Andrews, RC, Walker, BR (1999) Glucocorticoids and insulin resistance: old hormones, new targets. *Clin Sci (Lond)* **96**(5)**:** 513-523.

Arriza, JL, Weinberger, C, Cerelli, G, Glaser, TM, Handelin, BL, Housman, DE, Evans, RM (1987) Cloning of human mineralocorticoid receptor complementary DNA: structural and functional kinship with the glucocorticoid receptor. *Science* **237**(4812)**:** 268-275.

Asai, K, Funaki, C, Hayashi, T, Yamada, K, Naito, M, Kuzuya, M, Yoshida, F, Yoshimine, N, Kuzuya, F (1993) Dexamethasone-induced suppression of aortic atherosclerosis in cholesterol-fed rabbits. Possible mechanisms. *Arterioscler Thromb* **13**(6)**:** 892-899.

Badimon, JJ, Fuster, V, Chesebro, JH, Badimon, L (1993) Coronary atherosclerosis. A multifactorial disease. *Circulation* **87**(3 Suppl)**:** II3-16.

Ball, RY, Stowers, EC, Burton, JH, Cary, NR, Skepper, JN, Mitchinson, MJ (1995) Evidence that the death of macrophage foam cells contributes to the lipid core of atheroma. *Atherosclerosis* **114**(1)**:** 45-54.

Balla, T, Enyedi, P, Spat, A, Antoni, FA (1985) Pressor-type vasopressin receptors in the adrenal cortex: properties of binding, effects on phosphoinositide metabolism and aldosterone secretion. *Endocrinology* **117**(1)**:** 421-423.

Barath, P, Fishbein, MC, Cao, J, Berenson, J, Helfant, RH, Forrester, JS (1990) Detection and localization of tumor necrosis factor in human atheroma. *Am J Cardiol* **65**(5)**:** 297-302.

Barish, GD, Downes, M, Alaynick, WA, Yu, RT, Ocampo, CB, Bookout, AL, Mangelsdorf, DJ, Evans, RM (2005) A Nuclear Receptor Atlas: Macrophage Activation. *Mol Endocrinol* **19**(10)**:** 2466-2477.

Barnes, PJ, Adcock, I (1993) Anti-inflammatory actions of steroids: molecular mechanisms. *Trends Pharmacol Sci* **14**(12)**:** 436-441.

Benetos, A, Lacolley, P, Safar, ME (1997) Prevention of aortic fibrosis by spironolactone in spontaneously hypertensive rats. *Arterioscler Thromb Vasc Biol* **17**(6)**:** 1152-1156.

Bevilacqua, MP, Nelson, RM., Mannori, G, Cecconi, O (1994) Endothelial-leukocyte adhesion molecules in human disease. *Annual Review of Medicine* **45**(1)**:** 361-378.

Binion, DG, Heidemann, J, Li, MS, Nelson, VM, Otterson, MF, Rafiee, P (2009) Vascular cell adhesion molecule-1 expression in human intestinal microvascular endothelial cells is regulated by PI 3-kinase/Akt/MAPK/NF-kappaB: inhibitory role of curcumin. *Am J Physiol Gastrointest Liver Physiol* **297**(2)**:** G259-268.

Blann, AD, McCollum, CN (1994) Circulating endothelial cell/leukocyte adhesion molecules in atherosclerosis. *Thromb Haemost* **72**(1)**:** 151-154.

Borkowski, A, Delcroix, C, Levin, S (1972) Metabolism of adrenal cholesterol in man. II. In vitro studies including a comparison of adrenal cholesterol synthesis with the synthesis of the clucocorticosteroid hormones. *J Clin Invest* **51**(7)**:** 1679-1687.

Botero, D, Arango, A, Danon, M, Lifshitz, F (2000) Lipid profile in congenital adrenal hyperplasia. *Metabolism* **49**(6)**:** 790-793.

Bourassa, PA, Milos, PM, Gaynor, BJ, Breslow, JL, Aiello, RJ (1996) Estrogen reduces atherosclerotic lesion development in apolipoprotein E-deficient mice. *Proc Natl Acad Sci U S A* **93**(19)**:** 10022-10027.

Bourdillon, MC, Poston, RN, Covacho, C, Chignier, E, Bricca, G, McGregor, JL (2000) ICAM-1 deficiency reduces atherosclerotic lesions in double-knockout mice (ApoE(-/-)/ICAM-1(-/-)) fed a fat or a chow diet. *Arterioscler Thromb Vasc Biol* **20**(12)**:** 2630-2635.

Bousette, N, D'Orleans-Juste, P, Kiss, RS, You, Z, Genest, J, Al-Ramli, W, Qureshi, ST, Gramolini, A, Behm, D, Ohlstein, EH, Harrison, SM, Douglas, SA, Giaid, A (2009) Urotensin II receptor knockout mice on an ApoE knockout background fed a high-fat diet exhibit an enhanced hyperlipidemic and atherosclerotic phenotype. *Circ Res* **105**(7)**:** 686-695, 619 p following 695.

Boyd, JE, Palmore, WP, Mulrow, PJ (1971) Role of potassium in the control of aldosterone secretion in the rat. *Endocrinology* **88**(3)**:** 556-565.

Boyle, JJ, Bowyer, DE, Weissberg, PL, Bennett, MR (2001a) Human Blood-Derived Macrophages Induce Apoptosis in Human Plaque-Derived Vascular Smooth Muscle Cells by Fas-Ligand/Fas Interactions. *Arterioscler Thromb Vasc Biol* **21**(9)**:** 1402-1407.

Boyle, JJ, Bowyer, DE, Weissberg, PL, Bennett, MR (2001b) Human blood-derived macrophages induce apoptosis in human plaque-derived vascular smooth muscle cells by Fas-ligand/Fas interactions. *Arterioscler Thromb Vasc Biol* **21**(9)**:** 1402-1407.

Bradford, M (1976) A rapid and sensitive method for quantitation of microgram quantities of protein utilizing the principle of protein-dye-binding.
. *Anal Biochem* **72:** 248-254.

Brand, K, Page, S, Rogler, G, Bartsch, A, Brandl, R, Knuechel, R, Page, M, Kaltschmidt, C, Baeuerle, PA, Neumeier, D (1996) Activated transcription factor nuclear factor-kappa B is present in the atherosclerotic lesion. *J Clin Invest* **97**(7)**:** 1715-1722.

Brem, AS (2001) Insights Into Glucocorticoid-Associated Hypertension. *Am J Kidney Dis* **37**(1)**:** 1-10.

Brem, AS, Bina, RB, King, T, Morris, DJ (1995) Bidirectional activity of 11 beta-hydroxysteroid dehydrogenase in vascular smooth muscle cells. *Steroids* **60**(5)**:** 406-410.

Brem, AS, Bina, RB, King, TC, Morris, DJ (1998) Localization of 2 11beta-OH steroid dehydrogenase isoforms in aortic endothelial cells. *Hypertension* **31**(1 Pt 2)**:** 459-462.

Brem, AS, Matheson, KL, Barnes, JL, Morris, DJ (1991) 11-Dehydrocorticosterone, a glucocorticoid metabolite, inhibits aldosterone action in toad bladder. *Am J Physiol* **261**(5 Pt 2)**:** F873-879.

Brem, AS, Matheson, KL, Latif, S, Morris, DJ (1993) Activity of 11 beta-hydroxysteroid dehydrogenase in toad bladder: effects of 11-dehydrocorticosterone. *Am J Physiol* **264**(5 Pt 2)**:** F854-858.

Breslow, JL (1993) Transgenic mouse models of lipoprotein metabolism and atherosclerosis. *Proc Natl Acad Sci U S A* **90**(18)**:** 8314-8318.

Breuner, CW, Orchinik, M (2002) Plasma binding proteins as mediators of corticosteroid action in vertebrates. *J Endocrinol* **175**(1)**:** 99-112.

Brilla, CG, Weber, KT (1992) Reactive and reparative myocardial fibrosis in arterial hypertension in the rat. *Cardiovasc Res* **26**(7)**:** 671-677.

Brown, MS, Goldstein, JL (1983) Lipoprotein metabolism in the macrophage: implications for cholesterol deposition in atherosclerosis. *Annu Rev Biochem* **52:** 223-261.

Brown, NJ (2008) Aldosterone and Vascular Inflammation. *Hypertension* **51**(2)**:** 161-167.

Bujalska, I, Shimojo, M, Howie, A, Stewart, PM (1997) Human 11[beta]-hydroxysteroid dehydrogenase: Studies on the stably transfected isoforms and localization of the type 2 isozyme within renal tissue. *Steroids* **62**(1)**:** 77-82.

Bujalska, IJ, Draper, N, Michailidou, Z, Tomlinson, JW, White, PC, Chapman, KE, Walker, EA, Stewart, PM (2005) Hexose-6-phosphate dehydrogenase confers oxo-reductase activity upon 11 beta-hydroxysteroid dehydrogenase type 1. *J Mol Endocrinol* **34**(3)**:** 675-684.

Cai, H, Harrison, DG (2000) Endothelial Dysfunction in Cardiovascular Diseases: The Role of Oxidant Stress. *Circ Res* **87**(10)**:** 840-844.

Cai, TQ, Wong, B, Mundt, SS, Thieringer, R, Wright, SD, Hermanowski-Vosatka, A (2001) Induction of 11beta-hydroxysteroid dehydrogenase type 1 but not -2 in human aortic smooth muscle cells by inflammatory stimuli. *J Steroid Biochem Mol Biol* **77**(2-3)**:** 117-122.

Calara, F, Silvestre, M, Casanada, F, Yuan, N, Napoli, C, Palinski, W (2001) Spontaneous plaque rupture and secondary thrombosis in apolipoprotein E- deficient and LDL receptor-deficient mice. *J Pathol* **195**(2)**:** 257-263.

Caligiuri, G, Rudling, M, Ollivier, V, Jacob, MP, Michel, JB, Hansson, GK, Nicoletti, A (2003) Interleukin-10 deficiency increases atherosclerosis, thrombosis, and low-density lipoproteins in apolipoprotein E knockout mice. *Mol Med* **9**(1-2)**:** 10-17.

Callera, GE, Touyz, RM, Tostes, RC, Yogi, A, He, Y, Malkinson, S, Schiffrin, EL (2005) Aldosterone activates vascular p38MAP kinase and NADPH oxidase via c-Src. *Hypertension* **45**(4)**:** 773-779.

Calo, LA, Zaghetto, F, Pagnin, E, Davis, PA, de Mozzi, P, Sartorato, P, Martire, G, Fiore, C, Armanini, D (2004) Effect of Aldosterone and Glycyrrhetinic Acid on the

Protein Expression of PAI-1 and p22phox in Human Mononuclear Leukocytes. *J Clin Endocrinol Metab* **89**(4)**:** 1973-1976.

Capponi, AM, Lew, PD, Jornot, L, Vallotton, MB (1984) Correlation between cytosolic free Ca2+ and aldosterone production in bovine adrenal glomerulosa cells. Evidence for a difference in the mode of action of angiotensin II and potassium. *Journal of Biological Chemistry* **259**(14)**:** 8863-8869.

Caprio, M, Newfell, BG, la Sala, A, Baur, W, Fabbri, A, Rosano, G, Mendelsohn, ME, Jaffe, IZ (2008) Functional Mineralocorticoid Receptors in Human Vascular Endothelial Cells Regulate Intercellular Adhesion Molecule-1 Expression and Promote Leukocyte Adhesion. *Circ Res* **102**(11)**:** 1359-1367.

Carlos, T, Harlan, J (1994) Leukocyte-endothelial adhesion molecules. *Blood* **84**(7)**:** 2068-2101.

Caulin-Glaser, T, Farrell, WJ, Pfau, SE, Zaret, B, Bunger, K, Setaro, JF, Brennan, JJ, Bender, JR, Cleman, MW, Cabin, HS, Remetz, MS (1998) Modulation of circulating cellular adhesion molecules in postmenopausal women with coronary artery disease. *J Am Coll Cardiol* **31**(7)**:** 1555-1560.

Cha, DR, Kang, YS, Han, SY, Jee, YH, Han, KH, Kim, HK, Han, JY, Kim, YS (2005) Role of aldosterone in diabetic nephropathy. *Nephrology* **10**(s2)**:** S37-S39.

Chai, W, Danser, AH (2006) Why are mineralocorticoid receptor antagonists cardioprotective? *Naunyn Schmiedebergs Arch Pharmacol* **374**(3)**:** 153-162.

Chamley-Campbell, JH, Campbell, GR (1981) What controls smooth muscle phenotype? *Atherosclerosis* **40**(3-4)**:** 347-357.

Chiwata, T, Aragane, K, Fujinami, K, Kojima, K, Ishibashi, S, Yamada, N, Kusunoki, J (2001) Direct effect of an acyl-CoA:cholesterol acyltransferase inhibitor, F-1394, on atherosclerosis in apolipoprotein E and low density lipoprotein receptor double knockout mice. *Br J Pharmacol* **133**(7)**:** 1005-1012.

Chopra, V, Choksi, PU, Cavusoglu, E (2007) Beyond lipid lowering: the anti-hypertensive role of statins. *Cardiovasc Drugs Ther* **21**(3)**:** 161-169.

Christy, C, Hadoke, PW, Paterson, JM, Mullins, JJ, Seckl, JR, Walker, BR (2003) 11beta-hydroxysteroid dehydrogenase type 2 in mouse aorta: localization and influence on response to glucocorticoids. *Hypertension* **42**(4)**:** 580-587.

Collins, RG, Velji, R, Guevara, NV, Hicks, MJ, Chan, L, Beaudet, AL (2000) P-Selectin or Intercellular Adhesion Molecule (ICAM)-1 Deficiency Substantially Protects against Atherosclerosis in Apolipoprotein E-deficient Mice. *J. Exp. Med.* **191**(1)**:** 189-194.

Collins, T, Cybulsky, MI (2001) NF-ÎºB: pivotal mediator or innocent bystander in atherogenesis? *The Journal of Clinical Investigation* **107**(3)**:** 255-264.

Conn, JW (1955) Presidential address. I. Painting background. II. Primary aldosteronism, a new clinical syndrome. *J Lab Clin Med* **45**(1)**:** 3-17.

Cronstein, BN, Kimmel, SC, Levin, RI, Martiniuk, F, Weissmann, G (1992) A mechanism for the antiinflammatory effects of corticosteroids: the glucocorticoid receptor regulates leukocyte adhesion to endothelial cells and expression of endothelial-leukocyte adhesion molecule 1 and intercellular adhesion molecule 1. *Proceedings of the National Academy of Sciences of the United States of America* **89**(21)**:** 9991-9995.

Cugini, P, Manconi, R, Mancini, A, Serdoz, R, Meucci, T, Scavo, D (1980) Beta-adrenergic regulation of circadian rhythmicity of the renin-angiotensin-aldosterone system in five subtypes of essential hypertension. *G Ital Cardiol* **10**(2)**:** 184-190.

Cybulsky, MI, Iiyama, K, Li, H, Zhu, S, Chen, M, Iiyama, M, Davis, V, Gutierrez-Ramos, J-C, Connelly, PW, Milstone, DS (2001) A major role for VCAM-1, but not ICAM-1, in early atherosclerosis. *The Journal of Clinical Investigation* **107**(10)**:** 1255-1262.

Dallman, MF, Strack, AM, Akana, SF, Bradbury, MJ, Hanson, ES, Scribner, KA, Smith, M (1993) Feast and famine: critical role of glucocorticoids with insulin in daily energy flow. *Front Neuroendocrinol* **14**(4)**:** 303-347.

Daugherty, A, Pure, E, Delfel-Butteiger, D, Chen, S, Leferovich, J, Roselaar, SE, Rader, DJ (1997) The effects of total lymphocyte deficiency on the extent of atherosclerosis in apolipoprotein E-/- mice. *J Clin Invest* **100**(6)**:** 1575-1580.

Davies, M, Thomas, A (1984) Thrombosis and acute coronary-artery lesions in sudden cardiac ischemic death. *N Engl J Med* **310**(18)**:** 1137-1140.

Davies, MJ (1996) Stability and Instability: Two Faces of Coronary Atherosclerosis: The Paul Dudley White Lecture 1995. *Circulation* **94**(8)**:** 2013-2020.

Davies, MJ, Richardson, PD, Woolf, N, Katz, DR, Mann, J (1993) Risk of thrombosis in human atherosclerotic plaques: role of extracellular lipid, macrophage, and smooth muscle cell content. *Br. Heart J.* **69**(5)**:** 377-381.

Davis, JM, 3rd, Maradit-Kremers, H, Gabriel, SE (2005) Use of low-dose glucocorticoids and the risk of cardiovascular morbidity and mortality in rheumatoid arthritis: what is the true direction of effect? *J Rheumatol* **32**(10)**:** 1856-1862.

De Caterina, R, Libby, P, Peng, HB, Thannickal, VJ, Rajavashisth, TB, Gimbrone, MA, Jr., Shin, WS, Liao, JK (1995) Nitric oxide decreases cytokine-induced endothelial activation. Nitric oxide selectively reduces endothelial expression of adhesion molecules and proinflammatory cytokines. *J Clin Invest* **96**(1)**:** 60-68.

De Kloet, E (1991) Brain corticosteroid receptor balance and homeostatic control *Frontiers in Neuroendocrinology* **12:** 95-164.

de Martin, R, Martina, H, Hofer-Warbinek, Schmid, R, A., J (2000) The Transcription Factor NF-{kappa}B and the Regulation of Vascular Cell Function. *Arterioscler Thromb Vasc Biol* **20**(11)**:** e83-88.

De Meyer, GRY, Herman, AG (1997) Vascular endothelial dysfunction. *Progress in Cardiovascular Diseases* **39**(4)**:** 325-342.

de Winther, MPJ, Kanters, E, Kraal, G, Hofker, MH (2005) Nuclear Factor {kappa}B Signaling in Atherogenesis. *Arterioscler Thromb Vasc Biol* **25**(5)**:** 904-914.

Deem, TL, Cook-Mills, JM (2004) Vascular cell adhesion molecule 1 (VCAM-1) activation of endothelial cell matrix metalloproteinases: role of reactive oxygen species. *Blood* **104**(8)**:** 2385-2393.

Delyani, JA (2000) Mineralocorticoid receptor antagonists: The evolution of utility and pharmacology. *Kidney Int* **57**(4)**:** 1408-1411.

Deuchar, G, Hadoke, P, Armour, D, Brownstein, D, Webb, D, Mullins, J, Seckl, J, Kotelevtsev, Y (2009) Glucocorticoid-mediated activation of extra-renal mineralocorticoid receptors exacerbates atherosclerosis in mice. *Submitted to Circ. Res.*

Dhanya, SP, Hema, CG (2008) Small animal models of atherosclerosis. *Calicut Medical Journal* **6**(4)**:** e4.

Dhawan, L, Liu, B, Blaxall, BC, Taubman, MB (2007) A Novel Role for the Glucocorticoid Receptor in the Regulation of Monocyte Chemoattractant Protein-1 mRNA Stability. *J. Biol. Chem.* **282**(14)**:** 10146-10152.

Dignam JD, LR, Roeder RG (1983) Accurate transcription initiation by RNA polymerase II in a soluble extract from isolated mammalian nuclei. *Neucleic Acids Res.* **11:** 1475-1489.

Dol, F, Martin, G, Staels, B, Mares, AM, Cazaubon, C, Nisato, D, Bidouard, JP, Janiak, P, Schaeffer, P, Herbert, JM (2001) Angiotensin AT1 receptor antagonist irbesartan decreases lesion size, chemokine expression, and macrophage accumulation in apolipoprotein E-deficient mice. *J Cardiovasc Pharmacol* **38**(3)**:** 395-405.

Dong, ZM, Brown, AA, Wagner, DD (2000) Prominent role of P-selectin in the development of advanced atherosclerosis in ApoE-deficient mice. *Circulation* **101**(19)**:** 2290-2295.

Doyle, AE (1990) Does hypertension predispose to coronary artery disease? In Hypertension: pathophysiology, diagnosis and management. *J.H. Laragh and B.M. Brenner, editors. Raven Press Ltd. New York, NY.***:** 119–125.

Duplàa, C, Couffinhal, T, Labat, L, Moreau, C, Petit-Jean, M-E, Doutre, M-S, Lamazière, J-MD, Bonnet, J (1996) Monocyte/macrophage recruitment and expression of endothelial adhesion proteins in human atherosclerotic lesions. *Atherosclerosis* **121**(2)**:** 253-266.

Duprez, D, De Buyzere, M, Rietzschel, ER, Clement, DL (2000) Aldosterone and vascular damage. *Curr Hypertens Rep* **2**(3)**:** 327-334.

Elhage, R, Arnal, JF, Pieraggi, MT, Duverger, N, Fievet, C, Faye, JC, Bayard, F (1997) 17 beta-estradiol prevents fatty streak formation in apolipoprotein E-deficient mice. *Arterioscler Thromb Vasc Biol* **17**(11)**:** 2679-2684.

Eto, H, Miyata, M, Shirasawa, T, Akasaki, Y, Hamada, N, Nagaki, A, Orihara, K, Biro, S, Tei, C (2008) The long-term effect of angiotensin II type 1a receptor deficiency on hypercholesterolemia-induced atherosclerosis. *Hypertens Res* **31**(8)**:** 1631-1642.

Faggiano, A, Pivonello, R, Spiezia, S, De Martino, MC, Filippella, M, Di Somma, C, Lombardi, G, Colao, A (2003) Cardiovascular Risk Factors and Common Carotid Artery Caliber and Stiffness in Patients with Cushing's Disease during Active Disease and 1 Year after Disease Remission. *J Clin Endocrinol Metab* **88**(6)**:** 2527-2533.

Falk, E (1983) Plaque rupture with severe pre-existing stenosis precipitating coronary thrombosis. Characteristics of coronary atherosclerotic plaques underlying fatal occlusive thrombi. *British Heart Journal* **50**(2)**:** 127-134.

Falk, E, Shah, PK, Fuster, V (1995) Coronary Plaque Disruption. *Circulation* **92**(3)**:** 657-671.

Fan, C, Kawai, Y, Inaba, S, Arakawa, K, Katsuyama, M, Kajinami, K, Yasuda, T, Yabe-Nishimura, C, Konoshita, T, Miyamori, I (2008) Synergy of aldosterone and high salt induces vascular smooth muscle hypertrophy through up-regulation of NOX1. *The Journal of Steroid Biochemistry and Molecular Biology* **111**(1-2)**:** 29-36.

Fayad, ZA, Fallon, JT, Shinnar, M, Wehrli, S, Dansky, HM, Poon, M, Badimon, JJ, Charlton, SA, Fisher, EA, Breslow, JL, Fuster, V (1998) Noninvasive In Vivo High-Resolution Magnetic Resonance Imaging of Atherosclerotic Lesions in Genetically Engineered Mice. *Circulation* **98**(15)**:** 1541-1547.

Fiebeler, A, Schmidt, F, Muller, DN, Park, JK, Dechend, R, Bieringer, M, Shagdarsuren, E, Breu, V, Haller, H, Luft, FC (2001) Mineralocorticoid receptor affects AP-1 and nuclear factor-kappab activation in angiotensin II-induced cardiac injury. *Hypertension* **37**(2 Part 2)**:** 787-793.

Finking, G, Hanke, H (1997) Nikolaj Nikolajewitsch Anitschkow (1885-1964) established the cholesterol-fed rabbit as a model for atherosclerosis research. *Atherosclerosis* **135**(1)**:** 1-7.

Franchimont, D, Kino, T, Galon, J, Meduri, GU, Chrousos, G (2002) Glucocorticoids and inflammation revisited: the state of the art. NIH clinical staff conference. *Neuroimmunomodulation* **10**(5)**:** 247-260.

Frijns, CJ, Kappelle, LJ, van Gijn, J, Nieuwenhuis, HK, Sixma, JJ, Fijnheer, R (1997) Soluble adhesion molecules reflect endothelial cell activation in ischemic stroke and in carotid atherosclerosis. *Stroke* **28**(11)**:** 2214-2218.

Fujita, K, Aguilera, G, Catt, KJ (1979) The role of cyclic AMP in aldosterone production by isolated zona glomerulosa cells. *J Biol Chem* **254**(17)**:** 8567-8574.

Funder, J, Myles, K (1996) Exclusion of corticosterone from epithelial mineralocorticoid receptors is insufficient for selectivity of aldosterone action: in vivo binding studies. *Endocrinology* **137**(12)**:** 5264-5268.

Funder, JW (1997) Glucocorticoid and mineralocorticoid receptors: biology and clinical relevance. *Annu Rev Med* **48:** 231-240.

Funder, JW (2006) Mineralocorticoid Receptors and Cardiovascular Damage: It's Not Just Aldosterone. *Hypertension* **47**(4)**:** 634-635.

Funder, JW (2005a) Mineralocorticoid Receptors: Distribution and Activation. *Heart Failure Reviews* **10**(1)**:** 15-22.

Funder, JW (2005b) RALES, EPHESUS and redox. *J Steroid Biochem Mol Biol* **93**(2-5)**:** 121-125.

Furchgott, RF, Zawadzki, JV (1980) The obligatory role of endothelial cells in the relaxation of arterial smooth muscle by acetylcholine. *Nature* **288**(5789)**:** 373-376.

Galis, ZS, Sukhova, GK, Libby, P (1995) Microscopic localization of active proteases by in situ zymography: detection of matrix metalloproteinase activity in vascular tissue. *FASEB J.* **9**(10)**:** 974-980.

Galvez, OG, Bay, WH, Roberts, BW, Ferris, TF (1977) The hemodynamic effects of potassium deficiency in the dog. *Circ Res* **40**(5 Suppl 1)**:** I11-16.

Gareus, R, Kotsaki, E, Xanthoulea, S, van der Made, I, Gijbels, MJJ, Kardakaris, R, Polykratis, A, Kollias, G, de Winther, MPJ, Pasparakis, M (2008) Endothelial Cell-Specific NF-[kappa]B Inhibition Protects Mice from Atherosclerosis. *Cell Metabolism* **8**(5)**:** 372-383.

Garner, MM, Revzin, A (1981) A gel electrophoresis method for quantifying the binding of proteins to specific DNA regions: application to components of the Escherichia coli lactose operon regulatory system. *Nucl. Acids Res.* **9**(13)**:** 3047-3060.

Garton, KJ, Gough, PJ, Philalay, J, Wille, PT, Blobel, CP, Whitehead, RH, Dempsey, PJ, Raines, EW (2003) Stimulated shedding of vascular cell adhesion molecule 1 (VCAM-1) is mediated by tumor necrosis factor-alpha-converting enzyme (ADAM 17). *J Biol Chem* **278**(39)**:** 37459-37464.

Gearing, AJ, Newman, W (1993) Circulating adhesion molecules in disease. *Immunol Today* **14**(10)**:** 506-512.

Gertz, SD, Roberts, WC (1990) Hemodynamic shear force in rupture of coronary arterial atherosclerotic plaques. *Am J Cardiol* **66**(19)**:** 1368-1372.

Ghosh, S, Karin, M (2002) Missing Pieces in the NF-[kappa]B Puzzle. *Cell* **109**(2, Supplement 1)**:** S81-S96.

Gilmour, JS, Coutinho, AE, Cailhier, J-F, Man, TY, Clay, M, Thomas, G, Harris, HJ, Mullins, JJ, Seckl, JR, Savill, JS, Chapman, KE (2006) Local Amplification of Glucocorticoids by 11beta-Hydroxysteroid Dehydrogenase Type 1 Promotes Macrophage Phagocytosis of Apoptotic Leukocytes. *J Immunol* **176**(12)**:** 7605-7611.

Glagov, S, Weisenberg, E, Zarins, CK, Stankunavicius, R, Kolettis, GJ (1987) Compensatory enlargement of human atherosclerotic coronary arteries. *N Engl J Med* **316**(22)**:** 1371-1375.

Glass, CK, Witztum, JL (2001) Atherosclerosis. the road ahead. *Cell* **104**(4)**:** 503-516.

Golestaneh, N, Klein, C, Valamanesh, F, Suarez, G, Agarwal, MK, Mirshahi, M (2001) Mineralocorticoid Receptor-Mediated Signaling Regulates the Ion Gated Sodium Channel in Vascular Endothelial Cells and Requires an Intact Cytoskeleton. *Biochemical and Biophysical Research Communications* **280**(5)**:** 1300-1306.

Gonzalez-Gay, MA, Gonzalez-Juanatey, C, Martin, J (2005) Rheumatoid Arthritis: A Disease Associated with Accelerated Atherogenesis. *Seminars in Arthritis and Rheumatism* **35**(1)**:** 8-17.

Gu, L, Okada, Y, Clinton, SK, Gerard, C, Sukhova, GK, Libby, P, Rollins, BJ (1998) Absence of Monocyte Chemoattractant Protein-1 Reduces Atherosclerosis in Low Density Lipoprotein Receptor-Deficient Mice. *Molecular Cell* **2**(2)**:** 275-281.

Guo, Z, Mitchell-Raymundo, F, Yang, H, Ikeno, Y, Nelson, J, Diaz, V, Richardson, A, Reddick, R (2002) Dietary restriction reduces atherosclerosis and oxidative stress in the aorta of apolipoprotein E-deficient mice. *Mech Ageing Dev* **123**(8)**:** 1121-1131.

Guyton, JR, Klemp, KF (1993) Transitional features in human atherosclerosis. Intimal thickening, cholesterol clefts, and cell loss in human aortic fatty streaks. *Am J Pathol* **143**(5)**:** 1444-1457.

Hadoke, P, Wainwright, CL, Wadsworth, RM, Butler, K, Giddings, MJ (1995) Characterization of the morphological and functional alterations in rabbit subclavian artery subjected to balloon angioplasty. *Coron Artery Dis* **6**(5)**:** 403-415.

Hadoke, PW, Christy, C, Kotelevtsev, YV, Williams, BC, Kenyon, CJ, Seckl, JR, Mullins, JJ, Walker, BR (2001) Endothelial cell dysfunction in mice after transgenic knockout of type 2, but not type 1, 11beta-hydroxysteroid dehydrogenase. *Circulation* **104**(23)**:** 2832-2837.

Hadoke, PW, Macdonald, L, Logie, JJ, Small, GR, Dover, AR, Walker, BR (2006) Intra-vascular glucocorticoid metabolism as a modulator of vascular structure and function. *Cell Mol Life Sci* **63**(5)**:** 565-578.

Hadoke, PWF, Iqbal, J, Walker, BR (2009) Therapeutic manipulation of glucocorticoid metabolism in cardiovascular disease. *British Journal of Pharmacology* **156**(5)**:** 689-712.

Hanyu, M, Kume, N, Ikeda, T, Minami, M, Kita, T, Komeda, M (2001) VCAM-1 expression precedes macrophage infiltration into subendothelium of vein grafts interposed into carotid arteries in hypercholesterolemic rabbits -- a potential role in vein graft atherosclerosis. *Atherosclerosis* **158**(2)**:** 313-319.

Harrington, JR (2000) The Role of MCP-1 in Atherosclerosis. *Stem Cells* **18**(1)**:** 65-66.

Hashikabe, Y, Suzuki, K, Jojima, T, Uchida, K, Hattori, Y (2006) Aldosterone Impairs Vascular Endothelial Cell Function. *Journal of Cardiovascular Pharmacology* **47**(4)**:** 609-613

Hatakeyama, H, Inaba, S, Miyamori, I (1999) 11beta-hydroxysteroid dehydrogenase in cultured human vascular cells. Possible role in the development of hypertension. *Hypertension* **33**(5)**:** 1179-1184.

Hatakeyama, H, Miyamori, I, Fujita, T, Takeda, Y, Takeda, R, Yamamoto, H (1994) Vascular aldosterone. Biosynthesis and a link to angiotensin II-induced hypertrophy of vascular smooth muscle cells. *J Biol Chem* **269**(39)**:** 24316-24320.

Haught, WH, Mansour, M, Rothlein, R, Kishimoto, TK, Mainolfi, EA, Hendricks, JB, Hendricks, C, Mehta, JL (1996) Alterations in circulating intercellular adhesion molecule-1 and L-selectin: further evidence for chronic inflammation in ischemic heart disease. *Am Heart J* **132**(1 Pt 1)**:** 1-8.

Hayden, MS, Ghosh, S (2008) Shared Principles in NF-[kappa]B Signaling. *Cell* **132**(3)**:** 344-362.

Heistad, DD (2003) Unstable Coronary-Artery Plaques. *N Engl J Med* **349**(24)**:** 2285-2287.

Hermanowski-Vosatka, A, Balkovec, JM, Cheng, K, Chen, HY, Hernandez, M, Koo, GC, Le Grand, CB, Li, Z, Metzger, JM, Mundt, SS, Noonan, H, Nunes, CN, Olson, SH, Pikounis, B, Ren, N, Robertson, N, Schaeffer, JM, Shah, K, Springer, MS, Strack, AM, Strowski, M, Wu, K, Wu, T, Xiao, J, Zhang, BB, Wright, SD, Thieringer, R (2005) 11beta-HSD1 inhibition ameliorates metabolic syndrome and prevents progression of atherosclerosis in mice. *J Exp Med* **202**(4)**:** 517-527.

Hewitt, KN, Walker, EA, Stewart, PM (2005) Minireview: hexose-6-phosphate dehydrogenase and redox control of 11{beta}-hydroxysteroid dehydrogenase type 1 activity. *Endocrinology* **146**(6)**:** 2539-2543.

Hirono, Y, Yoshimoto, T, Suzuki, N, Sugiyama, T, Sakurada, M, Takai, S, Kobayashi, N, Shichiri, M, Hirata, Y (2007) Angiotensin II Receptor Type 1-Mediated Vascular Oxidative Stress and Proinflammatory Gene Expression in Aldosterone-Induced Hypertension: The Possible Role of Local Renin-Angiotensin System. *Endocrinology* **148**(4)**:** 1688-1696.

Ho, MK, Springer, TA (1982) Mac-2, a novel 32,000 Mr mouse macrophage subpopulation-specific antigen defined by monoclonal antibodies. *J Immunol* **128**(3)**:** 1221-1228.

Holmes, MC, Abrahamsen, CT, French, KL, Paterson, JM, Mullins, JJ, Seckl, JR (2006) The Mother or the Fetus? 11beta-Hydroxysteroid Dehydrogenase Type 2 Null Mice Provide Evidence for Direct Fetal Programming of Behavior by Endogenous Glucocorticoids. *J. Neurosci.* **26**(14)**:** 3840-3844.

Horie, T, Sekiguchi, M, Hirosawa, K (1978) Coronary thrombosis in pathogenesis of acute myocardial infarction. Histopathological study of coronary arteries in 108 necropsied cases using serial section. *British Heart Journal* **40**(2)**:** 153-161.

Horrocks, PM, Jones, AF, Ratcliffe, WA, Holder, G, White, A, Holder, R, Ratcliffe, JG, London, DR (1990) Patterns of ACTH and cortisol pulsatility over twenty-four hours in normal males and females. *Clin Endocrinol (oxf)* **32**(1)**:** 127-134.

Iademarco, MF, McQuillan, JJ, Rosen, GD, Dean, DC (1992) Characterization of the promoter for vascular cell adhesion molecule-1 (VCAM-1). *J Biol Chem* **267**(23)**:** 16323-16329.

Ignarro, LJ, Buga, GM, Wood, KS, Byrns, RE, Chaudhuri, G (1987) Endothelium-derived relaxing factor produced and released from artery and vein is nitric oxide. *Proc Natl Acad Sci U S A* **84**(24)**:** 9265-9269.

Ignatova, ID, Kostadinova, RM, Goldring, CE, Nawrocki, AR, Frey, FJ, Frey, BM (2009) Tumor necrosis factor-{alpha} upregulates 11{beta}-hydroxysteroid dehydrogenase type 1 expression by CCAAT/enhancer binding protein-{beta} in HepG2 cells. *Am J Physiol Endocrinol Metab* **296**(2)**:** E367-377.

Ikeda, U, Kanbe, T, Nakayama, I, Kawahara, Y, Yokoyama, M, Shimada, K (1995) Aldosterone inhibits nitric oxide synthesis in rat vascular smooth muscle cells induced by interleukin-1 beta. *Eur J Pharmacol* **290**(2)**:** 69-73.

Inagaki, Y, Yamagishi, S, Amano, S, Okamoto, T, Koga, K, Makita, Z (2002) Interferon-gamma-induced apoptosis and activation of THP-1 macrophages. *Life Sci* **71**(21)**:** 2499-2508.

Inoue, H, Umesono, K, Nishimori, T, Hirata, Y, Tanabe, T (1999) Glucocorticoid-mediated suppression of the promoter activity of the cyclooxygenase-2 gene is modulated by expression of its receptor in vascular endothelial cells. *Biochem Biophys Res Commun* **254**(2)**:** 292-298.

Inoue, S, Egashira, K, Ni, W, Kitamoto, S, Usui, M, Otani, K, Ishibashi, M, Hiasa, K, Nishida, K, Takeshita, A (2002) Anti-monocyte chemoattractant protein-1 gene therapy limits progression and destabilization of established atherosclerosis in apolipoprotein E-knockout mice. *Circulation* **106**(21)**:** 2700-2706.

Ishikawa, T, Kondoh, H, Nakagawa, S, Koiwaya, Y, Tanaka, K (1984) Steroid therapy in cardiac sarcoidosis. Increased left ventricular contractility concomitant with electrocardiographic improvement after prednisolone. *Chest* **85**(3)**:** 445-447.

Itskovich, VV, Choudhury, RP, Aguinaldo, JGS, Fallon, JT, Omerhodzic, S, Fisher, EA, Fayad, ZA (2003) Characterization of aortic root atherosclerosis in ApoE knockout mice: High-resolution in vivo and ex vivo MRM with histological correlation. *Magnetic Resonance in Medicine* **49**(2)**:** 381-385.

Iuchi, T, Akaike, M, Mitsui, T, Ohshima, Y, Shintani, Y, Azuma, H, Matsumoto, T (2003) Glucocorticoid Excess Induces Superoxide Production in Vascular Endothelial Cells and Elicits Vascular Endothelial Dysfunction. *Circ Res* **92**(1)**:** 81-87.

Jaffe, IZ, Mendelsohn, ME (2005) Angiotensin II and aldosterone regulate gene transcription via functional mineralocortocoid receptors in human coronary artery smooth muscle cells. *Circ Res* **96**(6)**:** 643-650.

Jamieson, PM, Chapman, KE, Edwards, CR, Seckl, JR (1995) 11 beta-hydroxysteroid dehydrogenase is an exclusive 11 beta- reductase in primary cultures of rat hepatocytes: effect of physicochemical and hormonal manipulations. *Endocrinology* **136**(11)**:** 4754-4761.

Jawien, J, Nastalek, P, Korbut, R (2004) Mouse models of experimental atherosclerosis. *J Physiol Pharmacol* **55**(3)**:** 503-517.

Johar, S, Cave, AC, Narayanapanicker, A, Grieve, DJ, Shah, AM (2006) Aldosterone mediates angiotensin II-induced interstitial cardiac fibrosis via a Nox2-containing NADPH oxidase. *FASEB J.* **20**(9)**:** 1546-1548.

Johnson, J, Carson, K, Williams, H, Karanam, S, Newby, A, Angelini, G, George, S, Jackson, C (2005) Plaque rupture after short periods of fat feeding in the apolipoprotein E-knockout mouse: model characterization and effects of pravastatin treatment. *Circulation* **111**(11)**:** 1422-1430.

Johnson, JL, Jackson, CL (2001) Atherosclerotic plaque rupture in the apolipoprotein E knockout mouse. *Atherosclerosis* **154**(2)**:** 399-406.

Kang, Y-M, Zhang, Z-H, Johnson, RF, Yu, Y, Beltz, T, Johnson, AK, Weiss, RM, Felder, RB (2006) Novel Effect of Mineralocorticoid Receptor Antagonism to Reduce Proinflammatory Cytokines and Hypothalamic Activation in Rats With Ischemia-Induced Heart Failure. *Circ Res* **99**(7)**:** 758-766.

Kaplan, M, Hayek, T, Raz, A, Coleman, R, Dornfeld, L, Vaya, J, Aviram, M (2001) Pomegranate juice supplementation to atherosclerotic mice reduces macrophage lipid peroxidation, cellular cholesterol accumulation and development of atherosclerosis. *J Nutr* **131**(8)**:** 2082-2089.

Karlberg, BE (1983) Adrenergic regulation of renin release and effects on angiotensin and aldosterone. *Acta Med Scand Suppl* **672:** 33-40.

Kawai, Y, Hayashi, T, Eguchi, K, Asazuma, K-y, Masamura, K, Iwamuro, A, Takano, Y, Tada, H, Matsukawa, S, Miyamori, I (1998) Effects of Brief Glucocorticoid Exposure on Growth of Vascular Smooth Muscle Cells in Culture. *Biochemical and Biophysical Research Communications* **245**(2)**:** 493-496.

Keidar, S, Hayek, T, Kaplan, M, Pavlotzky, E, Hamoud, S, Coleman, R, Aviram, M (2003) Effect of eplerenone, a selective aldosterone blocker, on blood pressure, serum and macrophage oxidative stress, and atherosclerosis in apolipoprotein E-deficient mice. *J Cardiovasc Pharmacol* **41**(6)**:** 955-963.

Keidar, S, Kaplan, M, Pavlotzky, E, Coleman, R, Hayek, T, Hamoud, S, Aviram, M (2004) Aldosterone administration to mice stimulates macrophage NADPH oxidase and increases atherosclerosis development: a possible role for angiotensin-converting enzyme and the receptors for angiotensin II and aldosterone. *Circulation* **109**(18)**:** 2213-2220.

Kenyon, CJ, Saccoccio, NA, Morris, DJ (1984) Glucocorticoid inhibition of mineralocorticoid action in the rat. *Clin Sci (Lond)* **67**(3)**:** 329-335.

Knowles, JW, Reddick, RL, Jennette, JC, Shesely, EG, Smithies, O, Maeda, N (2000) Enhanced atherosclerosis and kidney dysfunction in eNOS(-/-)Apoe(-/-) mice are ameliorated by enalapril treatment. *J Clin Invest* **105**(4)**:** 451-458.

Kobayashi, N, Yoshida, K, Nakano, S, Ohno, T, Honda, T, Tsubokou, Y, Matsuoka, H (2006) Cardioprotective mechanisms of eplerenone on cardiac performance and remodeling in failing rat hearts. *Hypertension* **47**(4)**:** 671-679.

Koch, AE, Burrows, JC, Haines, GK, Carlos, TM, Harlan, JM, Leibovich, SJ (1991) Immunolocalization of endothelial and leukocyte adhesion molecules in human rheumatoid and osteoarthritic synovial tissues. *Lab Invest* **64**(3)**:** 313-320.

Kojima, I, Kojima, K, Rasmussen, H (1985a) Intracellular calcium and adenosine 3',5'-cyclic monophosphate as mediators of potassium-induced aldosterone secretion. *Biochem J* **228**(1)**:** 69-76.

Kojima, I, Kojima, K, Rasmussen, H (1985b) Role of calcium and cAMP in the action of adrenocorticotropin on aldosterone secretion. *J Biol Chem* **260**(7)**:** 4248-4256.

Kojima, Y, Kundu, R, Leeper, NJ, Quertermous, T (2008) Abstract 3756: Atherosclerosis Development is Increased in Apelin/Apoe Double Knockout Mice. *Circulation* **118**(18_MeetingAbstracts)**:** S_481-.

Kornel, L (1993) The role of vascular steroid receptors in the control of vascular contractility and peripheral vascular resistance. *The Journal of Steroid Biochemistry and Molecular Biology* **45**(1-3)**:** 195-203.

Kornel, L, Kanamarlapudi, N, Travers, T, Taff, DJ, Patel, N, Chen, C, Baum, RM, Raynor, WJ (1982) Studies on high affinity binding of mineralo- and glucocorticoids in rabbit aorta cytosol. *J Steroid Biochem* **16**(2)**:** 245-264.

Kornel, L, Nelson, WA, Manisundaram, B, Chigurupati, R, Hayashi, T (1993) Mechanism of the effects of glucocorticoids and mineralocorticoids on vascular smooth muscle contractility. *Steroids* **58**(12)**:** 580-587.

Kostadinova, RM, Nawrocki, AR, Frey, FJ, Frey, BM (2005) Tumor necrosis factor alpha and phorbol 12-myristate-13-acetate down-regulate human 11β-hydroxysteroid dehydrogenase type 2 through p50/p50 NF-κB homodimers and Egr-1. *FASEB J.***:** 04-2820fje.

Kotelevtsev, Y, Brown, RW, Fleming, S, Kenyon, C, Edwards, CR, Seckl, JR, Mullins, JJ (1999) Hypertension in mice lacking 11beta-hydroxysteroid dehydrogenase type 2. *J Clin Invest* **103**(5)**:** 683-689.

Kotelevtsev, Y, Holmes, MC, Burchell, A, Houston, PM, Schmoll, D, Jamieson, P, Best, R, Brown, R, Edwards, CRW, Seckl, JR, Mullins, JJ (1997) 11Î²-Hydroxysteroid dehydrogenase type 1 knockout mice show attenuated glucocorticoid-inducible responses and resist hyperglycemia on obesity orâ€‰stress. *Proceedings of the National Academy of Sciences of the United States of America* **94**(26)**:** 14924-14929.

Krosch, H, Schabitz, J (1977) [High-dosage glucocorticoid therapy in acute heart infarct and in cardiogenic shock]. *Z Gesamte Inn Med* **32**(22)**:** 631-633.

Kuster, GM, Kotlyar, E, Rude, MK, Siwik, DA, Liao, R, Colucci, WS, Sam, F (2005) Mineralocorticoid Receptor Inhibition Ameliorates the Transition to Myocardial Failure and Decreases Oxidative Stress and Inflammation in Mice With Chronic Pressure Overload. *Circulation* **111**(4)**:** 420-427.

Kusunoki, J, Hansoty, DK, Aragane, K, Fallon, JT, Badimon, JJ, Fisher, EA (2001) Acyl-CoA:cholesterol acyltransferase inhibition reduces atherosclerosis in apolipoprotein E-deficient mice. *Circulation* **103**(21)**:** 2604-2609.

Lakshmi, V, Monder, C (1988) Purification and characterization of the corticosteroid 11 beta-dehydrogenase component of the rat liver 11 beta-hydroxysteroid dehydrogenase complex. *Endocrinology* **123**(5)**:** 2390-2398.

Landry, DB, Couper, LL, Bryant, SR, Lindner, V (1997) Activation of the NF-kappa B and I kappa B system in smooth muscle cells after rat arterial injury. Induction of vascular cell adhesion molecule-1 and monocyte chemoattractant protein-1. *Am J Pathol* **151**(4)**:** 1085-1095.

Langford, HG, Snavely, JR (1959) Effect of DCA on development of renoprival hypertension. *Am J Physiol* **196**(2)**:** 449-450.

Lee, RT, Libby, P (1997) The Unstable Atheroma. *Arterioscler Thromb Vasc Biol* **17**(10)**:** 1859-1867.

Lee, YW, Kühn, H, Hennig, B, Neish, AS, Toborek, M (2001) IL-4-induced Oxidative Stress Upregulates VCAM-1 Gene Expression in Human Endothelial Cells. *Journal of Molecular and Cellular Cardiology* **33**(1)**:** 83-94.

Lemarie, CA, Simeone, SM, Nikonova, A, Ebrahimian, T, Deschenes, ME, Coffman, TM, Paradis, P, Schiffrin, EL (2009) Aldosterone-induced activation of signaling pathways requires activity of angiotensin type 1a receptors. *Circ Res* **105**(9)**:** 852-859.

Lendon, CL, Davies, MJ, Born, GV, Richardson, PD (1991) Atherosclerotic plaque caps are locally weakened when macrophages density is increased. *Atherosclerosis* **87**(1)**:** 87-90.

Letizia, C, De Toma, G, Cerci, S, Scuro, L, De Ciocchis, A, D'Ambrosio, C, Massa, R, Cavallaro, A, Scavo, D (1996) Plasma endothelin-1 levels in patients with aldosterone-producing adenoma and pheochromocytoma. *Clin Exp Hypertens* **18**(7)**:** 921-931.

Levick, WR (2003) Blood vessels casting a shadow. *Science* **299**(5615)**:** 1983-1985; author reply 1983-1985.

Li, X, Meng, Y, Wu, P, Zhang, Z, Yang, X (2007) Angiotensin II and Aldosterone stimulating NF-kappaB and AP-1 activation in hepatic fibrosis of rat. *Regul Pept* **138**(1)**:** 15-25.

Libby, P (2008a) The molecular mechanisms of the thrombotic complications of atherosclerosis. *J Intern Med* **263**(5)**:** 517-527.

Libby, P (2008b) Role of inflammation in atherosclerosis associated with rheumatoid arthritis. *Am J Med* **121**(10 Suppl 1)**:** S21-31.

Libby, P, Aikawa, M (2003) Mechanisms of plaque stabilization with statins. *The American Journal of Cardiology* **91**(4, Supplement 1)**:** 4-8.

Libby, P, Ridker, PM, Maseri, A (2002) Inflammation and Atherosclerosis. *Circulation* **105**(9)**:** 1135-1143.

Libby, P, Sukhova, G, Lee, RT, Galis, ZS (1995) Cytokines regulate vascular functions related to stability of the atherosclerotic plaque. *J Cardiovasc Pharmacol* **25**(Suppl 2)**:** S9-12.

Libby, P, Theroux, P (2005) Pathophysiology of coronary artery disease. *Circulation* **111**(25)**:** 3481-3488.

Liu, K, Gualano, RC, Hibbs, ML, Anderson, GP, Bozinovski, S (2008) Epidermal growth factor receptor signaling to Erk1/2 and STATs control the intensity of the epithelial inflammatory responses to rhinovirus infection. *J Biol Chem* **283**(15)**:** 9977-9985.

Lommer, D, Distler, A, Nast, HP, Sinterhauf, K, Walter, U, Wolff, HP, Sieler, K (1976) [Diurnal profiles of plasma aldosterone, cortisol, renin, angiotensinogen and angiotensinases in normal subjects (author's transl)]. *Klin Wochenschr* **54**(3)**:** 123-130.

Lopez, FJ, Ardecky, RJ, Bebo, B, Benbatoul, K, De Grandpre, L, Liu, S, Leibowitz, MD, Marschke, K, Rosen, J, Rungta, D, Viveros, HO, Yen, W-C, Zhi, L, Negro-Vilar, A, Miner, JN (2008) LGD-5552, an Antiinflammatory Glucocorticoid Receptor Ligand with Reduced Side Effects, in Vivo. *Endocrinology* **149**(5)**:** 2080-2089.

Lucas, AD, Greaves, DR (2001) Atherosclerosis: role of chemokines and macrophages. *Expert Rev Mol Med* **3**(25)**:** 1-18.

Ma, J, Weisberg, A, Griffin, JP, Vaughan, DE, Fogo, AB, Brown, NJ (2006) Plasminogen activator inhibitor-1 deficiency protects against aldosterone-induced glomerular injury. *Kidney Int* **69**(6)**:** 1064-1072.

Marschang, P, Herz, J (2003) Mouse models as tools for dissecting disorders of lipoprotein metabolism. *Seminars in Cell & Developmental Biology* **14**(1)**:** 25-35.

Martinez, FO, Sica, A, Mantovani, A, Locati, M (2008) Macrophage activation and polarization. *Front Biosci* **13:** 453-461.

Marui, N, Offermann, MK, Swerlick, R, Kunsch, C, Rosen, CA, Ahmad, M, Alexander, RW, Medford, RM (1993) Vascular cell adhesion molecule-1 (VCAM-1) gene transcription and expression are regulated through an antioxidant-sensitive mechanism in human vascular endothelial cells. *J Clin Invest* **92**(4)**:** 1866-1874.

Masaki, T (1989) The discovery, the present state, and the future prospects of endothelin. *J Cardiovasc Pharmacol* **13 Suppl 5:** S1-4; discussion S18.

Masinovsky, B, Urdal, D, Gallatin, WM (1990) IL-4 acts synergistically with IL-1 beta to promote lymphocyte adhesion to microvascular endothelium by induction of vascular cell adhesion molecule-1. *J Immunol* **145**(9)**:** 2886-2895.

Masuzaki, H, Paterson, J, Shinyama, H, Morton, NM, Mullins, JJ, Seckl, JR, Flier, JS (2001) A transgenic model of visceral obesity and the metabolic syndrome. *Science* **294**(5549)**:** 2166-2170.

Matheny, HE, Deem, TL, Cook-Mills, JM (2000) Lymphocyte Migration Through Monolayers of Endothelial Cell Lines Involves VCAM-1 Signaling Via Endothelial Cell NADPH Oxidase. *J Immunol* **164**(12)**:** 6550-6559.

Mazak, I, Fiebeler, A, Muller, DN, Park, J-K, Shagdarsuren, E, Lindschau, C, Dechend, R, Viedt, C, Pilz, B, Haller, H, Luft, FC (2004) Aldosterone Potentiates Angiotensin II-Induced Signaling in Vascular Smooth Muscle Cells. *Circulation* **109**(22)**:** 2792-2800.

McClelland, S, Gawaz, M, Kennerknecht, E, Konrad, CS, Sauer, S, Schuerzinger, K, Massberg, S, Fitzgerald, DJ, Belton, O (2009) Contribution of cyclooxygenase-1 to thromboxane formation, platelet-vessel wall interactions and atherosclerosis in the ApoE null mouse. *Atherosclerosis* **202**(1)**:** 84-91.

Mehta, D, Angelini, GD, Bryan, AJ (1996) Experimental models of accelerated atherosclerosis syndromes. *Int J Cardiol* **56**(3)**:** 235-257.

Meir, KS, Leitersdorf, E (2004) Atherosclerosis in the Apolipoprotein E-Deficient Mouse: A Decade of Progress. *Arterioscler Thromb Vasc Biol* **24**(6)**:** 1006-1014.

Mendelsohn, FA, Lloyd, CJ, Kachel, C, Funder, JW (1982) Induction by glucocorticoids of angiotensin converting enzyme production from bovine endothelial cells in culture and rat lung in vivo. *J Clin Invest* **70**(3)**:** 684-692.

Mercer, WR, Krozowski, ZS (1992) Localization of an 11 beta hydroxysteroid dehydrogenase activity to the distal nephron. Evidence for the existence of two species of dehydrogenase in the rat kidney. *Endocrinology* **130**(1)**:** 540-543.

Miura, R, Nakamura, K, Miura, D, Miura, A, Hisamatsu, K, Kajiya, M, Hashimoto, K, Nagase, S, Morita, H, Fukushima Kusano, K, Emori, T, Ishihara, K, Ohe, T (2006) Aldosterone synthesis and cytokine production in human peripheral blood mononuclear cells. *J Pharmacol Sci* **102**(3)**:** 288-295.

Miyazaki, Y, Tsukazaki, T, Hirota, Y, Yonekura, A, Osaki, M, Shindo, H, Yamashita, S (2000) Dexamethasone inhibition of TGF[beta]-induced cell growth and type II collagen mRNA expression through ERK-integrated AP-1 activity in cultured rat articular chondrocytes. *Osteoarthritis and Cartilage* **8**(5)**:** 378-385.

Molnar, GA, Lindschau, C, Dubrovska, G, Mertens, PR, Kirsch, T, Quinkler, M, Gollasch, M, Wresche, S, Luft, FC, Muller, DN, Fiebeler, A (2008) Glucocorticoid-Related Signaling Effects in Vascular Smooth Muscle Cells. *Hypertension* **51**(5)**:** 1372-1378.

Monder, C, Lakshmi, V (1989) Evidence for kinetically distinct forms of corticosteroid 11 beta-dehydrogenase in rat liver microsomes. *J Steroid Biochem* **32**(1A)**:** 77-83.

Monder, C, Shackleton, CH, Bradlow, HL, New, MI, Stoner, E, Iohan, F, Lakshmi, V (1986) The syndrome of apparent mineralocorticoid excess: its association with 11 beta-dehydrogenase and 5 beta-reductase deficiency and some consequences for corticosteroid metabolism. *J Clin Endocrinol Metab* **63**(3)**:** 550-557.

Montrella-Waybill, M, Clore, JN, Schoolwerth, AC, Watlington, CO (1991) Evidence that high dose cortisol-induced Na+ retention in man is not mediated by the mineralocorticoid receptor. *J Clin Endocrinol Metab* **72**(5)**:** 1060-1066.

Moore, S, Ihnatowycz, TO (1978) Vessel injury and atherosclerosis. *Adv Exp Med Biol* **102:** 145-161.

Morand, EF, Leech, M, Bernhagen, J (2006) MIF: a new cytokine link between rheumatoid arthritis and atherosclerosis. *Nat Rev Drug Discov* **5**(5)**:** 399-410.

Moreno, P, Falk, E, Palacios, I, Newell, J, Fuster, V, Fallon, J (1994) Macrophage infiltration in acute coronary syndromes. Implications for plaque rupture. *Circulation* **90**(2)**:** 775-778.

Morin, C, Asselin, C, Boudreau, F, Provencher, PH (1998) Transcriptional regulation of pre-pro-endothelin-1 gene by glucocorticoids in vascular smooth muscle cells. *Biochem Biophys Res Commun* **244**(2)**:** 583-587.

Morisaki, N, Saito, I, Tamura, K, Tashiro, J, Masuda, M, Kanzaki, T, Watanabe, S, Masuda, Y, Saito, Y (1997) New indices of ischemic heart disease and aging: studies

on the serum levels of soluble intercellular adhesion molecule-1 (ICAM-1) and soluble vascular cell adhesion molecule-1 (VCAM-1) in patients with hypercholesterolemia and ischemic heart disease. *Atherosclerosis* **131**(1)**:** 43-48.

Morris, DJ, Latif, SA, Brem, AS (2009) Interactions of mineralocorticoids and glucocorticoids in epithelial target tissues revisited. *Steroids* **74**(1)**:** 1-6.

Morton, NM, Holmes, MC, Fievet, C, Staels, B, Tailleux, A, Mullins, JJ, Seckl, JR (2001) Improved Lipid and Lipoprotein Profile, Hepatic Insulin Sensitivity, and Glucose Tolerance in 11beta -Hydroxysteroid Dehydrogenase Type 1 Null Mice. *J. Biol. Chem.* **276**(44)**:** 41293-41300.

Mosser, DM, Edwards, JP (2008) Exploring the full spectrum of macrophage activation. *Nat Rev Immunol* **8**(12)**:** 958-969.

Muller, B, Kleschyov, AL, Gyorgy, K, Stoclet, JC (2000) Inducible NO synthase activity in blood vessels and heart: new insight into cell origin and consequences. *Physiol Res* **49**(1)**:** 19-26.

Munck, A, Guyre, PM, Holbrook, NJ (1984) Physiological functions of glucocorticoids in stress and their relation to pharmacological actions. *Endocr Rev* **5**(1)**:** 25-44.

Nagata, K, Obata, K, Xu, J, Ichihara, S, Noda, A, Kimata, H, Kato, T, Izawa, H, Murohara, T, Yokota, M (2006) Mineralocorticoid Receptor Antagonism Attenuates Cardiac Hypertrophy and Failure in Low-Aldosterone Hypertensive Rats. *Hypertension* **47**(4)**:** 656-664.

Nakamura, Y, Suzuki, S, Suzuki, T, Ono, K, Miura, I, Satoh, F, Moriya, T, Saito, H, Yamada, S, Ito, S, Sasano, H (2006) MDM2: A Novel Mineralocorticoid-Responsive Gene Involved in Aldosterone-Induced Human Vascular Structural Remodeling. *Am J Pathol* **169**(2)**:** 362-371.

Nakashima, Y, Plump, AS, Raines, EW, Breslow, JL, Ross, R (1994) ApoE-deficient mice develop lesions of all phases of atherosclerosis throughout the arterial tree. *Arterioscler Thromb* **14**(1)**:** 133-140.

Nakashima, Y, Raines, EW, Plump, AS, Breslow, JL, Ross, R (1998) Upregulation of VCAM-1 and ICAM-1 at Atherosclerosis-Prone Sites on the Endothelium in the ApoE-Deficient Mouse. *Arterioscler Thromb Vasc Biol* **18**(5)**:** 842-851.

Nakata, Y, Maeda, N (2002) Vulnerable atherosclerotic plaque morphology in apolipoprotein E-deficient mice unable to make ascorbic Acid. *Circulation* **105**(12)**:** 1485-1490.

Naray-Fejes-Toth, A, Watlington, CO, Fejes-Toth, G (1991) 11 beta-Hydroxysteroid dehydrogenase activity in the renal target cells of aldosterone. *Endocrinology* **129**(1)**:** 17-21.

Narayanaswamy, M, Wright, KC, Kandarpa, K (2000) Animal models for atherosclerosis, restenosis, and endovascular graft research. *J Vasc Interv Radiol* **11**(1)**:** 5-17.

Nashel, DJ (1986) Is atherosclerosis a complication of long-term corticosteroid treatment? *The American Journal of Medicine* **80**(5)**:** 925-929.

Neish, AS, Williams, AJ, Palmer, HJ, Whitley, MZ, Collins, T (1992) Functional analysis of the human vascular cell adhesion molecule 1 promoter. *J. Exp. Med.* **176**(6)**:** 1583-1593.

Newton, R (2000) Molecular mechanisms of glucocorticoid action: what is important? *Thorax* **55**(7)**:** 603-613.

Nishimura, H, Ito, Y, Mizuno, M, Tanaka, A, Morita, Y, Maruyama, S, Yuzawa, Y, Matsuo, S (2008) Mineralocorticoid receptor blockade ameliorates peritoneal fibrosis in new rat peritonitis model. *Am J Physiol Renal Physiol* **294**(5)**:** F1084-1093.

Nishiyama, A, Yao, L, Nagai, Y, Miyata, K, Yoshizumi, M, Kagami, S, Kondo, S, Kiyomoto, H, Shokoji, T, Kimura, S, Kohno, M, Abe, Y (2004) Possible Contributions of Reactive Oxygen Species and Mitogen-Activated Protein Kinase to Renal Injury in Aldosterone/Salt-Induced Hypertensive Rats. *Hypertension* **43**(4)**:** 841-848.

Nishiyama, T, Mishima, K, Ide, F, Yamada, K, Obara, K, Sato, A, Hitosugi, N, Inoue, H, Tsubota, K, Saito, I (2007) Functional analysis of an established mouse vascular endothelial cell line. *J Vasc Res.* **44**(2)**:** 138-148.

Oberleithner, H, Ludwig, T, Riethmuller, C, Hillebrand, U, Albermann, L, Schafer, C, Shahin, V, Schillers, H (2004) Human endothelium: target for aldosterone. *Hypertension* **43**(5)**:** 952-956.

Oberleithner, H, RiethmÃ¼ller, C, Schillers, H, MacGregor, GA, de Wardener, HE, Hausberg, M (2007) Plasma sodium stiffens vascular endothelium and reduces nitric oxide release. *Proceedings of the National Academy of Sciences* **104**(41)**:** 16281-16286.

Oberleithner, H, Riethmuller, C, Ludwig, T, Hausberg, M, Schillers, H (2006) Aldosterone remodels human endothelium. *Acta Physiol (Oxf)* **187**(1-2)**:** 305-312.

Oberleithner, H, Schneider, SW, Albermann, L, Hillebrand, U, Ludwig, T, Riethmüller, C, Shahin, V, Schäfer, C, Schillers, H (2003) Endothelial Cell Swelling by Aldosterone. *Journal of Membrane Biology* **196**(3)**:** 163-172.

Odermatt, A, Arnold, P, Frey, FJ (2001) The Intracellular Localization of the Mineralocorticoid Receptor Is Regulated by 11beta -Hydroxysteroid Dehydrogenase Type 2. *J. Biol. Chem.* **276**(30)**:** 28484-28492.

Oikarinen, AI, Vuorio, EI, Zaragoza, EJ, Palotie, A, Chu, ML, Uitto, J (1988) Modulation of collagen metabolism by glucocorticoids. Receptor-mediated effects of dexamethasone on collagen biosynthesis in chick embryo fibroblasts and chondrocytes. *Biochem Pharmacol* **37**(8)**:** 1451-1462.

Osborn, L, Hession, C, Tizard, R, Vassallo, C, Luhowskyj, S, Chi-Rosso, G, Lobb, R (1989) Direct expression cloning of vascular cell adhesion molecule 1, a cytokine-induced endothelial protein that binds to lymphocytes. *Cell* **59**(6)**:** 1203-1211.

Ouali, R, LeBrethon, M, Saez, J (1993) Identification and characterization of angiotensin-II receptor subtypes in cultured bovine and human adrenal fasciculata cells and PC12W cells. *Endocrinology* **133**(6)**:** 2766-2772.

Paigen, B, Plump, AS, Rubin, EM (1994) The mouse as a model for human cardiovascular disease and hyperlipidemia. *Curr Opin Lipidol* **5**(4)**:** 258-264.

Parker, MG (1993) Steroid and related receptors. *Curr Opin Cell Biol* **5**(3)**:** 499-504.

Paterson, JM, Morton, NM, Fievet, C, Kenyon, CJ, Holmes, MC, Staels, B, Seckl, JR, Mullins, JJ (2004) Metabolic syndrome without obesity: Hepatic overexpression of 11beta-hydroxysteroid dehydrogenase type 1 in transgenic mice. *Proc Natl Acad Sci U S A* **101**(18)**:** 7088-7093.

Paterson, JM, Seckl, JR, Mullins, JJ (2005) Genetic manipulation of 11{beta}-hydroxysteroid dehydrogenases in mice. *Am J Physiol Regul Integr Comp Physiol* **289**(3)**:** R642-652.

Paul, A, Ko, KW, Li, L, Yechoor, V, McCrory, MA, Szalai, AJ, Chan, L (2004) C-reactive protein accelerates the progression of atherosclerosis in apolipoprotein E-deficient mice. *Circulation* **109**(5)**:** 647-655.

Paul, M, Poyan Mehr, A, Kreutz, R (2006) Physiology of Local Renin-Angiotensin Systems. *Physiol. Rev.* **86**(3)**:** 747-803.

Pellman, J, Lyon, RC, Sheikh, F (2009) Extracellular matrix remodeling in atrial fibrosis: Mechanisms and implications in atrial fibrillation. *Journal of Molecular and Cellular Cardiology* **In Press, Corrected Proof**.

Peter, K, Nawroth, P, Conradt, C, Nordt, T, Weiss, T, Boehme, M, Wunsch, A, Allenberg, J, Kubler, W, Bode, C (1997) Circulating vascular cell adhesion molecule-1 correlates with the extent of human atherosclerosis in contrast to circulating intercellular adhesion molecule-1, E-selectin, P-selectin, and thrombomodulin. *Arterioscler Thromb Vasc Biol* **17**(3)**:** 505-512.

Pigott, R, Dillon, LP, Hemingway, IH, Gearing, AJ (1992) Soluble forms of E-selectin, ICAM-1 and VCAM-1 are present in the supernatants of cytokine activated cultured endothelial cells. *Biochem Biophys Res Commun* **187**(2)**:** 584-589.

Pindolia, KR, Noth, CJ, Xu, YX, Janakiraman, N, Chapman, RA, Gautam, SC (1996) IL-4 upregulates IL-1-induced chemokine gene expression in bone marrow stromal cells by enhancing NF-kB activation. *Hematopathol Mol Hematol* **10**(4)**:** 171-185.

Pitt, B, Williams, G, Remme, W, Martinez, F, Lopez-Sendon, J, Zannad, F, Neaton, J, Roniker, B, Hurley, S, Burns, D, Bittman, R, Kleiman, J (2001) The EPHESUS trial: eplerenone in patients with heart failure due to systolic dysfunction complicating acute myocardial infarction. Eplerenone Post-AMI Heart Failure Efficacy and Survival Study. *Cardiovasc Drugs Ther* **15**(1)**:** 79-87.

Pitt, B, Zannad, F, Remme, WJ, Cody, R, Castaigne, A, Perez, A, Palensky, J, Wittes, J (1999) The effect of spironolactone on morbidity and mortality in patients with severe heart failure. Randomized Aldactone Evaluation Study Investigators. *N Engl J Med* **341**(10)**:** 709-717.

Plump, AS, Smith, JD, Hayek, T, Aalto-Setala, K, Walsh, A, Verstuyft, JG, Rubin, EM, Breslow, JL (1992) Severe hypercholesterolemia and atherosclerosis in apolipoprotein E- deficient mice created by homologous recombination in ES cells. *Cell* **71**(2)**:** 343-353.

Pluta, RM (2006) Dysfunction of nitric oxide synthases as a cause and therapeutic target in delayed cerebral vasospasm after SAH. *Neurol Res* **28**(7)**:** 730-737.

Ponnuswamy, P, Ostermeier, E, Schrottle, A, Chen, J, Huang, PL, Ertl, G, Nieswandt, B, Kuhlencordt, PJ (2009) Oxidative stress and compartment of gene expression determine proatherosclerotic effects of inducible nitric oxide synthase. *Am J Pathol* **174**(6)**:** 2400-2410.

Pratico, D, Tangirala, RK, Rader, DJ, Rokach, J, FitzGerald, GA (1998) Vitamin E suppresses isoprostane generation in vivo and reduces atherosclerosis in ApoE-deficient mice. *Nat Med* **4**(10)**:** 1189-1192.

Pratt, JH (1982) Role of angiotensin II in potassium-mediated stimulation of aldosterone secretion in the dog. *J Clin Invest* **70**(3)**:** 667-672.

Prior, JT, Kurtz, DM, Ziegler, DD (1961) The hypercholesteremic rabbit. An aid to understanding arteriosclerosis in man? *Arch Pathol* **71:** 672-684.

Puchtler, H, Waldrop, F, Valentine, L (1973) Polarization microscopic studies of connective tissue stained with picro-sirius red FBA. *Beitr Pathol* **150**(2)**:** 174-187.

Pueyo, ME, Gonzalez, W, Nicoletti, A, Savoie, F, Arnal, J-F, Michel, J-B (2000) Angiotensin II Stimulates Endothelial Vascular Cell Adhesion Molecule-1 via Nuclear Factor-{kappa}B Activation Induced by Intracellular Oxidative Stress. *Arterioscler Thromb Vasc Biol* **20**(3)**:** 645-651.

Quinn, SJ, Cornwall, MC, Williams, GH (1987) Electrical properties of isolated rat adrenal glomerulosa and fasciculata cells. *Endocrinology* **120**(3)**:** 903-914.

Quinn, SJ, Williams, GH (1988) Regulation of aldosterone secretion. *Annu Rev Physiol* **50:** 409-426.

Rafflenbeul, W (1994) Hypertension treatment and prevention of new atherosclerotic plaque formation. *Drugs* **48 Suppl 1:** 11-15.

Rajagopalan, S, Duquaine, D, King, S, Pitt, B, Patel, P (2002) Mineralocorticoid receptor antagonism in experimental atherosclerosis. *Circulation* **105**(18)**:** 2212-2216.

Rajagopalan, S, Meng, XP, Ramasamy, S, Harrison, DG, Galis, ZS (1996) Reactive oxygen species produced by macrophage-derived foam cells regulate the activity of vascular matrix metalloproteinases in vitro. Implications for atherosclerotic plaque stability. *J Clin Invest* **98**(11)**:** 2572-2579.

Rajagopalan, S, Pitt, B (2001) Aldosterone antagonists in the treatment of hypertension and target organ damage. *Curr Hypertens Rep* **3**(3)**:** 240-248.

Rajan, V, Edwards, CR, Seckl, JR (1996) 11 beta-Hydroxysteroid dehydrogenase in cultured hippocampal cells reactivates inert 11-dehydrocorticosterone, potentiating neurotoxicity. *J Neurosci* **16**(1)**:** 65-70.

Ramos, CL, Huo, Y, Jung, U, Ghosh, S, Manka, DR, Sarembock, IJ, Ley, K (1999) Direct Demonstration of P-Selectin– and VCAM-1–Dependent Mononuclear Cell Rolling in Early Atherosclerotic Lesions of Apolipoprotein E–Deficient Mice. *Circ Res* **84**(11)**:** 1237-1244.

Ramsahoye, BH, Davies, SV, el-Gaylani, N, Sandeman, D, Scanlon, MF (1995) The mineralocorticoid effects of high dose hydrocortisone. *BMJ* **310**(6980)**:** 656-657.

Rask, E, Olsson, T, Soderberg, S, Andrew, R, Livingstone, DE, Johnson, O, Walker, BR (2001) Tissue-specific dysregulation of cortisol metabolism in human obesity. *J Clin Endocrinol Metab* **86**(3)**:** 1418-1421.

Reddick, RL, Zhang, SH, Maeda, N (1994) Atherosclerosis in mice lacking apo E. Evaluation of lesional development and progression. *Arterioscler Thromb* **14**(1)**:** 141-147.

Rekhter, MD (1999) Collagen synthesis in atherosclerosis: too much and not enough. *Cardiovasc Res* **41**(2)**:** 376-384.

Rensen, SS, Doevendans, PA, van Eys, GJ (2007) Regulation and characteristics of vascular smooth muscle cell phenotypic diversity. *Neth Heart J* **15**(3)**:** 100-108.

Reul, JM, de Kloet, ER (1985) Two receptor systems for corticosterone in rat brain: microdistribution and differential occupation. *Endocrinology* **117**(6)**:** 2505-2511.

Reul, JM, Pearce, PT, Funder, JW, Krozowski, ZS (1989) Type I and type II corticosteroid receptor gene expression in the rat: effect of adrenalectomy and dexamethasone administration. *Mol Endocrinol* **3**(10)**:** 1674-1680.

Rickard AJ, Morgan, J, Tesch, G, Funder, JW, Fuller, PJ, Young, MJ (2009) Deletion of mineralocorticoid receptors from macrophages protects against deoxycorticosterone/salt-induced cardiac fibrosis and increased blood pressure. *Hypertension* **54**(3)**:** 537-543.

Rocha, R, Chander, PN, Khanna, K, Zuckerman, A, Stier, CT, Jr. (1998) Mineralocorticoid blockade reduces vascular injury in stroke-prone hypertensive rats. *Hypertension* **31**(1 Pt 2)**:** 451-458.

Rocha, R, Funder, J (2002a) The Pathophysiology of Aldosterone in the Cardiovascular System. *Annals of the New York Academy of Sciences* **970**(ENDOCRINE HYPERTENSION)**:** 89-100.

Rocha, R, Rudolph, AE, Frierdich, GE, Nachowiak, DA, Kekec, BK, Blomme, EA, McMahon, EG, Delyani, JA (2002b) Aldosterone induces a vascular inflammatory phenotype in the rat heart. *Am J Physiol Heart Circ Physiol* **283**(5)**:** H1802-1810.

Rocnik, EF, Chan, BM, Pickering, JG (1998) Evidence for a role of collagen synthesis in arterial smooth muscle cell migration. *J Clin Invest* **101**(9)**:** 1889-1898.

Rohde, LE, Lee, RT, Rivero, J, Jamacochian, M, Arroyo, LH, Briggs, W, Rifai, N, Libby, P, Creager, MA, Ridker, PM (1998) Circulating cell adhesion molecules are correlated with ultrasound-based assessment of carotid atherosclerosis. *Arterioscler Thromb Vasc Biol* **18**(11)**:** 1765-1770.

Roman, M, Saba, P, Pini, R, Spitzer, M, Pickering, T, Rosen, S, Alderman, M, Devereux, R (1992) Parallel cardiac and vascular adaptation in hypertension. *Circulation* **86**(6)**:** 1909-1918.

Rosenbaum, RM, Cheli, CD, Gerritsen, ME (1986) Dexamethasone inhibits prostaglandin release from rabbit coronary microvessel endothelium. *Am J Physiol* **250**(6 Pt 1)**:** C970-977.

Rosenfeld, ME, Polinsky, P, Virmani, R, Kauser, K, Rubanyi, G, Schwartz, SM (2000) Advanced atherosclerotic lesions in the innominate artery of the ApoE knockout mouse. *Arterioscler Thromb Vasc Biol* **20**(12)**:** 2587-2592.

Ross, EJ, Linch, DC (1982) Cushing's syndrome--killing disease: discriminatory value of signs and symptoms aiding early diagnosis. *Lancet* **2**(8299)**:** 646-649.

Ross, R (1999) Atherosclerosis is an inflammatory disease. *Am Heart J* **138**(5 Pt 2)**:** S419-420.

Ross, R (1986) The pathogenesis of atherosclerosis--an update. *N Engl J Med* **314**(8)**:** 488-500.

Ross, R (1993) Rous-Whipple Award Lecture. Atherosclerosis: a defense mechanism gone awry. *Am J Pathol* **143**(4)**:** 987-1002.

Ross, R, Glomset, JA (1976a) The pathogenesis of atherosclerosis (first of two parts). *N Engl J Med* **295**(7)**:** 369-377.

Ross, R, Glomset, JA (1976b) The pathogenesis of atherosclerosis (second of two parts). *N Engl J Med* **295**(8)**:** 420-425.

Rossi, GP, Cavallin, M, Nussdorfer, GG, Pessina, AC (2001) The endothelin-aldosterone axis and cardiovascular diseases. *J Cardiovasc Pharmacol* **38 Suppl 2:** S49-52.

Rossier, BC (1997) 1996 Homer Smith Award Lecture. Cum grano salis: the epithelial sodium channel and the control of blood pressure. *J Am Soc Nephrol* **8**(6)**:** 980-992.

Rothlein, R, Czajkowski, M, O'Neill, MM, Marlin, SD, Mainolfi, E, Merluzzi, VJ (1988) Induction of intercellular adhesion molecule 1 on primary and continuous cell lines by pro-inflammatory cytokines. Regulation by pharmacologic agents and neutralizing antibodies. *J Immunol* **141**(5)**:** 1665-1669.

Rothlein, R, Mainolfi, EA, Czajkowski, M, Marlin, SD (1991) A form of circulating ICAM-1 in human serum. *J Immunol* **147**(11)**:** 3788-3793.

Roy, J, Audette, M, Tremblay, MJ (2001) Intercellular adhesion molecule-1 (ICAM-1) gene expression in human T cells is regulated by phosphotyrosyl phosphatase activity. Involvement of NF-kappaB, Ets, and palindromic interferon-gamma-responsive element-binding sites. *J Biol Chem* **276**(18)**:** 14553-14561.

Rudin, W, Eugster, HP, Bordmann, G, Bonato, J, Muller, M, Yamage, M, Ryffel, B (1997) Resistance to cerebral malaria in tumor necrosis factor-alpha/beta-deficient mice is associated with a reduction of intercellular adhesion molecule-1 up-regulation and T helper type 1 response. *Am J Pathol* **150**(1)**:** 257-266.

Safar, ME, London, GM, Asmar, R, Frohlich, ED (1998) Recent Advances on Large Arteries in Hypertension. *Hypertension* **32**(1)**:** 156-161.

Sapolsky, RM, Romero, LM, Munck, AU (2000) How Do Glucocorticoids Influence Stress Responses? Integrating Permissive, Suppressive, Stimulatory, and Preparative Actions. *Endocr Rev* **21**(1)**:** 55-89.

Scheinman, SJ, Guay-Woodford, LM, Thakker, RV, Warnock, DG (1999) Genetic Disorders of Renal Electrolyte Transport. *N Engl J Med* **340**(15)**:** 1177-1187.

Schiffrin, EL (2006a) Effects of Aldosterone on the Vasculature. *Hypertension* **47**(3)**:** 312-318.

Schiffrin, EL (2006b) Effects of aldosterone on the vasculature. *Hypertension* **47**(3)**:** 312-318.

Schiffrin, EL, Touyz, RM (2004) From bedside to bench to bedside: role of renin-angiotensin-aldosterone system in remodeling of resistance arteries in hypertension. *Am J Physiol Heart Circ Physiol* **287**(2)**:** H435-446.

Schneider, EG, Radke, KJ, Ulderich, DA, Taylor, RE, Jr. (1985) Effect of osmolality on aldosterone secretion. *Endocrinology* **116**(4)**:** 1621-1626.

Scott, BA, Lawrence, B, Nguyen, HH, Meyer, WJ, 3rd (1987) Aldosterone and dexamethasone binding in human arterial smooth muscle cells. *J Hypertens* **5**(6)**:** 739-744.

Seckl, JR (2001) Glucocorticoid programming of the fetus; adult phenotypes and molecular mechanisms. *Molecular and Cellular Endocrinology* **185**(1-2)**:** 61-71.

Seckl, JR, Morton, NM, Chapman, KE, Walker, BR (2004) Glucocorticoids and 11beta-Hydroxysteroid Dehydrogenase in Adipose Tissue. *Recent Prog Horm Res* **59**(1)**:** 359-393.

Seckl, JR, Walker, BR (2001) Minireview: 11beta-hydroxysteroid dehydrogenase type 1- a tissue-specific amplifier of glucocorticoid action. *Endocrinology* **142**(4)**:** 1371-1376.

Setola, E, Losa, M, Lanzi, R, Lucotti, P, Monti, LD, Castrignano, T, Galluccio, E, Giovanelli, M, Piatti, P (2007) Increased insulin-stimulated endothelin-1 release is a distinct vascular phenotype distinguishing Cushing's disease from metabolic syndrome. *Clin Endocrinol (oxf)* **66**(4)**:** 586-592.

Shackleton CH, RJ, Arteaga E, Lopez JM, Winter JS (1985) Cogenital 11beta-Hydroxysteroid Dehydrogenase deficiency associated with juvenile hypertension: corticosteroid metabolite profiles of four patients and their families. *Clin Endocrinol (oxf)* **22:** 701-712.

Shah, PK, Falk, E, Badimon, JJ, Fernandez-Ortiz, A, Mailhac, A, Villareal-Levy, G, Fallon, JT, Regnstrom, J, Fuster, V (1995) Human monocyte-derived macrophages induce collagen breakdown in fibrous caps of atherosclerotic plaques. Potential role of matrix-degrading metalloproteinases and implications for plaque rupture. *Circulation* **92**(6)**:** 1565-1569.

Sheppard, K, Funder, JW (1987) Mineralocorticoid specificity of renal type I receptors: in vivo binding studies. *Am J Physiol* **252**(2 Pt 1)**:** E224-229.

Shiomi, M, Yamada, S, Amano, Y, Nishimoto, T, Ito, T (2008) Lapaquistat acetate, a squalene synthase inhibitor, changes macrophage/lipid-rich coronary plaques of hypercholesterolaemic rabbits into fibrous lesions. *Br J Pharmacol* **154**(5)**:** 949-957.

Shyy, JYJ, Li, Y-S, Lin, M-C, Chen, W, Yuan, S, Usami, S, Chien, S (1995) Multiple cis-elements mediate shear stress-induced gene expression. *Journal of Biomechanics* **28**(12)**:** 1451-1457.

Small, GR, Hadoke, PW, Sharif, I, Dover, AR, Armour, D, Kenyon, CJ, Gray, GA, Walker, BR (2005) Preventing local regeneration of glucocorticoids by 11beta-hydroxysteroid dehydrogenase type 1 enhances angiogenesis. *Proc Natl Acad Sci U S A* **102**(34)**:** 12165-12170.

Smith, JD, Breslow, JL (1997) The emergence of mouse models of atherosclerosis and their relevance to clinical research. *J Intern Med* **242**(2)**:** 99-109.

Smith, JD, Trogan, E, Ginsberg, M, Grigaux, C, Tian, J, Miyata, M (1995) Decreased atherosclerosis in mice deficient in both macrophage colony-stimulating factor (op) and apolipoprotein E. *Proc Natl Acad Sci U S A* **92**(18)**:** 8264-8268.

Soro-Paavonen, A, Watson, AM, Li, J, Paavonen, K, Koitka, A, Calkin, AC, Barit, D, Coughlan, MT, Drew, BG, Lancaster, GI, Thomas, M, Forbes, JM, Nawroth, PP, Bierhaus, A, Cooper, ME, Jandeleit-Dahm, KA (2008) Receptor for advanced glycation end products (RAGE) deficiency attenuates the development of atherosclerosis in diabetes. *Diabetes* **57**(9)**:** 2461-2469.

Souverein, PC, Berard, A, Van Staa, TP, Cooper, C, Egberts, AC, Leufkens, HG, Walker, BR (2004) Use of oral glucocorticoids and risk of cardiovascular and cerebrovascular disease in a population based case-control study. *Heart* **90**(8)**:** 859-865.

Spyroglou, SW, Jenny Manolopoulou, Constanze Hantel, Martin Reincke, Martin Bidlingmaier, Martin Hrabé de Angelis & Felix Beuschlein (2008) Establishment of a mutagenesis screen to identify mice with high aldosterone levels
Endocrine Abstracts **16:** 28.

Stary, HC (1989) Evolution and progression of atherosclerotic lesions in coronary arteries of children and young adults. *Arteriosclerosis* **9**(1 Suppl)**:** I19-32.

Stas, S, Whaley-Connell, A, Habibi, J, Appesh, L, Hayden, MR, Karuparthi, PR, Qazi, M, Morris, EM, Cooper, SA, Link, CD, Stump, C, Hay, M, Ferrario, C, Sowers, JR (2007) Mineralocorticoid Receptor Blockade Attenuates Chronic Overexpression of the Renin-Angiotensin-Aldosterone System Stimulation of Reduced Nicotinamide Adenine Dinucleotide Phosphate Oxidase and Cardiac Remodeling. *Endocrinology* **148**(8)**:** 3773-3780.

Stevens, HY, Melchior, B, Bell, KS, Yun, S, Yeh, JC, Frangos, JA (2008) PECAM-1 is a critical mediator of atherosclerosis. *Dis Model Mech* **1**(2-3)**:** 175-181; discussion 179.

Stewart, PM, Krozowski, ZS (1999) 11 beta-Hydroxysteroid dehydrogenase. *Vitam Horm* **57:** 249-324.

Stewart, PM, Murry, BA, Mason, JI (1994a) Human kidney 11 beta-hydroxysteroid dehydrogenase is a high affinity nicotinamide adenine dinucleotide-dependent enzyme and differs from the cloned type I isoform. *J Clin Endocrinol Metab* **79**(2)**:** 480-484.

Stewart, PM, Whorwood, CB (1994b) 11 beta-Hydroxysteroid dehydrogenase activity and corticosteroid hormone action. *Steroids* **59**(2)**:** 90-95.

Stocker, R, O'Halloran, RA (2004) Dealcoholized red wine decreases atherosclerosis in apolipoprotein E gene-deficient mice independently of inhibition of lipid peroxidation in the artery wall. *Am J Clin Nutr* **79**(1)**:** 123-130.

Strawn, WB (2005) Eplerenone Antagonizes Atherosclerosis, But What Is the Agonist? *Hypertension* **46**(5)**:** 1093-1094.

Sugiyama, T, Yoshimoto, T, Tsuchiya, K, Gochou, N, Hirono, Y, Tateno, T, Fukai, N, Shichiri, M, Hirata, Y (2005) Aldosterone induces angiotensin converting enzyme gene expression via a JAK2-dependent pathway in rat endothelial cells. *Endocrinology* **146**(9)**:** 3900-3906.

Sun, Y, Zhang, J, Lu, L, Chen, SS, Quinn, MT, Weber, KT (2002) Aldosterone-Induced Inflammation in the Rat Heart : Role of Oxidative Stress. *Am J Pathol* **161**(5)**:** 1773-1781.

Suzuki, G, Morita, H, Mishima, T, Sharov, VG, Todor, A, Tanhehco, EJ, Rudolph, AE, McMahon, EG, Goldstein, S, Sabbah, HN (2002) Effects of Long-Term Monotherapy With Eplerenone, a Novel Aldosterone Blocker, on Progression of Left Ventricular Dysfunction and Remodeling in Dogs With Heart Failure. *Circulation* **106**(23)**:** 2967-2972.

Suzuki, H, Kurihara, Y, Takeya, M, Kamada, N, Kataoka, M, Jishage, K, Ueda, O, Sakaguchi, H, Higashi, T, Suzuki, T, Takashima, Y, Kawabe, Y, Cynshi, O, Wada, Y, Honda, M, Kurihara, H, Aburatani, H, Doi, T, Matsumoto, A, Azuma, S, Noda, T, Toyoda, Y, Itakura, H, Yazaki, Y, Kodama, T, et al. (1997) A role for macrophage scavenger receptors in atherosclerosis and susceptibility to infection. *Nature* **386**(6622)**:** 292-296.

Suzuki, J, Iwai, M, Mogi, M, Oshita, A, Yoshii, T, Higaki, J, Horiuchi, M (2006) Eplerenone with valsartan effectively reduces atherosclerotic lesion by attenuation of oxidative stress and inflammation. *Arterioscler Thromb Vasc Biol* **26**(4)**:** 917-921.

Suzuki, S, Tsubochi, H, Ishibashi, H, Matsuda, Y, Suzuki, T, Krozowski, ZS, Sasano, H, Kondo, T (2005) Inflammatory mediators down-regulate 11beta-hydroxysteroid dehydrogenase type 2 in a human lung epithelial cell line BEAS-2B and the rat lung. *Tohoku J Exp Med* **207**(4)**:** 293-301.

Svenson, KL, Pollare, T, Lithell, H, Hallgren, R (1988) Impaired glucose handling in active rheumatoid arthritis: relationship to peripheral insulin resistance. *Metabolism* **37**(2)**:** 125-130.

Syngle, A, Vohra, K, Kaur, L, Sharma, S (2009) Effect of spironolactone on endothelial dysfunction in rheumatoid arthritis. *Scand J Rheumatol* **38**(1)**:** 15-22.

Takai, S, Jin, D, Muramatsu, M, Kirimura, K, Sakonjo, H, Miyazaki, M (2005) Eplerenone inhibits atherosclerosis in nonhuman primates. *Hypertension* **46**(5)**:** 1135-1139.

Takebayashi, K, Matsumoto, S, Aso, Y, Inukai, T (2006) Aldosterone Blockade Attenuates Urinary Monocyte Chemoattractant Protein-1 and Oxidative Stress in Patients with Type 2 Diabetes Complicated by Diabetic Nephropathy. *J Clin Endocrinol Metab* **91**(6)**:** 2214-2217.

Takeda, R (1993) Production of mineralocorticoid and enzyme expression for steroidogenesis in blood vessels as components of the vascular auto-/paracrine system. *Nippon Naibunpi Gakkai Zasshi* **69**(11)**:** 1101-1122.

Tauchi, Y, Zushida, L, Chono, S, Sato, J, Ito, K, Morimoto, K (2001) Effect of dexamethasone palmitate-low density lipoprotein complex on cholesterol ester accumulation in aorta of atherogenic model mice. *Biol Pharm Bull* **24**(8)**:** 925-929.

Tomlinson, JW, Walker, EA, Bujalska, IJ, Draper, N, Lavery, GG, Cooper, MS, Hewison, M, Stewart, PM (2004) 11beta-hydroxysteroid dehydrogenase type 1: a tissue-specific regulator of glucocorticoid response. *Endocr Rev* **25**(5)**:** 831-866.

Ulick, S, Levine, LS, Gunczler, P, Zanconato, G, Ramirez, LC, Rauh, W, Rosler, A, Bradlow, HL, New, MI (1979) A syndrome of apparent mineralocorticoid excess associated with defects in the peripheral metabolism of cortisol. *J Clin Endocrinol Metab* **49**(5)**:** 757-764.

Ullian, ME (1999) The role of corticosteriods in the regulation of vascular tone. *Cardiovasc Res* **41**(1)**:** 55-64.

Vale, W, Spiess, J, Rivier, C, Rivier, J (1981) Characterization of a 41-residue ovine hypothalamic peptide that stimulates secretion of corticotropin and beta-endorphin. *Science* **213**(4514)**:** 1394-1397.

Vallabhapurapu, S, Karin, M (2009) Regulation and Function of NF-ÎºB Transcription Factors in the Immune System. *Annual Review of Immunology* **27**(1)**:** 693-733.

van de Stolpe, A, Caldenhoven, E, Stade, B, Koenderman, L, Raaijmakers, J, Johnson, J, van der Saag, P (1994) 12-O-tetradecanoylphorbol-13-acetate- and tumor necrosis factor alpha- mediated induction of intercellular adhesion molecule-1 is inhibited by dexamethasone. Functional analysis of the human intercellular adhesion molecular-1 promoter. *J. Biol. Chem.* **269**(8)**:** 6185-6192.

van der Wal, AC, Becker, AE, Das, PK (1994) The expression of adhesion molecules on endothelial cells in atherosclerosis has a topographic relationship with the underlying inflammatory process. *Histopathology* **24**(2)**:** 200-201.

VanderLaan, PA, Reardon, CA, Getz, GS (2004) Site specificity of atherosclerosis: site-selective responses to atherosclerotic modulators. *Arterioscler Thromb Vasc Biol* **24**(1)**:** 12-22.

Vassalli, JD, Belin, D (1987) Amiloride selectively inhibits the urokinase-type plasminogen activator. *FEBS Lett* **214**(1)**:** 187-191.

Velican, C, Velican, D (1976) Coronary arteries in children up to the age of ten years II. Intimal thickening and its role in atherosclerotic involvement. *Med Interne* **14**(1)**:** 17-24.

von Holt, K, Lebrun, S, Stinn, W, Conroy, L, Wallerath, T, Schleef, R (2009) Progression of atherosclerosis in the Apo E-/- model: 12-Month exposure to cigarette mainstream smoke combined with high-cholesterol/fat diet. *Atherosclerosis* **205**(1)**:** 135-143.

Wagner, CA, Devuyst, O, Bourgeois, S, Mohebbi, N (2009) Regulated acid-base transport in the collecting duct. *Pflugers Arch* **458**(1)**:** 137-156.

Wajant, H, Pfizenmaier, K, Scheurich, P (2003) Tumor necrosis factor signaling. *Cell Death Differ* **10**(1)**:** 45-65.

Walker, BR (2006a) Cortisol--cause and cure for metabolic syndrome? *Diabetic Medicine* **23**(12)**:** 1281-1288.

Walker, BR (2006b) Cortisol--cause and cure for metabolic syndrome? *Diabet Med* **23**(12)**:** 1281-1288.

Walker, BR, Phillips, DI, Noon, JP, Panarelli, M, Andrew, R, Edwards, HV, Holton, DW, Seckl, JR, Webb, DJ, Watt, GC (1998) Increased glucocorticoid activity in men with cardiovascular risk factors. *Hypertension* **31**(4)**:** 891-895.

Wang, D, Liu, YH, Yang, XP, Rhaleb, NE, Xu, J, Peterson, E, Rudolph, AE, Carretero, OA (2004) Role of a selective aldosterone blocker in mice with chronic heart failure. *J Card Fail* **10**(1)**:** 67-73.

Wang, M (2005) The role of glucocorticoid action in the pathophysiology of the Metabolic Syndrome. *Nutr Metab (Lond)* **2**(1)**:** 3.

Watanabe, Y (1980) Serial inbreeding of rabbits with hereditary hyperlipidemia (WHHL-rabbit). *Atherosclerosis* **36**(2)**:** 261-268.

Welgus, HG, Campbell, EJ, Cury, JD, Eisen, AZ, Senior, RM, Wilhelm, SM, Goldberg, GI (1990) Neutral metalloproteinases produced by human mononuclear phagocytes. Enzyme profile, regulation, and expression during cellular development. *J Clin Invest* **86**(5)**:** 1496-1502.

Westphal, U (1971) Steroid-protein interactions. *Monogr Endocrinol* **4:** 1-567.

Wexler, BC, Greenberg, BP (1978) Metyrapone-induced cardiovascular degenerative changes in non- arteriosclerotic and arteriosclerotic rats. *Br J Exp Pathol* **59**(1)**:** 52-63.

White, D, Fayez, S, Doube, A (2006) Atherogenic lipid profiles in rheumatoid arthritis. *N Z Med J* **119**(1240)**:** U2125.

White, PC (1994) Disorders of Aldosterone Biosynthesis and Action. *N Engl J Med* **331**(4)**:** 250-258.

Whitworth, JA (1992) Adrenocorticotrophin and steroid-induced hypertension in humans. *Kidney Int Suppl* **37:** S34-37.

Whitworth, JA, Schyvens, CG, Zhang, Y, Andrews, MC, Mangos, GJ, Kelly, JJ (2002) The nitric oxide system in glucocorticoid-induced hypertension. *J Hypertens* **20**(6)**:** 1035-1043.

Whorwood, C, Sheppard, M, Stewart, P (1993) Licorice inhibits 11 beta-hydroxysteroid dehydrogenase messenger ribonucleic acid levels and potentiates glucocorticoid hormone action. *Endocrinology* **132**(6)**:** 2287-2292.

Williams, H, Johnson, JL, Carson, KG, Jackson, CL (2002) Characteristics of intact and ruptured atherosclerotic plaques in brachiocephalic arteries of apolipoprotein E knockout mice. *Arterioscler Thromb Vasc Biol* **22**(5)**:** 788-792.

Williams, JS, Williams, GH (2003) 50th Anniversary of Aldosterone. *J Clin Endocrinol Metab* **88**(6)**:** 2364-2372.

Willner, EL, Tow, B, Buhman, KK, Wilson, M, Sanan, DA, Rudel, LL, Farese, RV, Jr. (2003) Deficiency of acyl CoA:cholesterol acyltransferase 2 prevents

atherosclerosis in apolipoprotein E-deficient mice. *Proc Natl Acad Sci U S A* **100**(3)**:** 1262-1267.

Wilson, P, Morgan, J, Funder, JW, Fuller, PJ, Young, MJ (2009) Mediators of mineralocorticoid receptor-induced profibrotic inflammatory responses in the heart. *Clinical Science* **116**(9)**:** 731-739.

Winn, RK, Harlan, JM (1993) CD18-independent neutrophil and mononuclear leukocyte emigration into the peritoneum of rabbits. *J Clin Invest* **92**(3)**:** 1168-1173.

Winyard, PG, Tatzber, F, Esterbauer, H, Kus, ML, Blake, DR, Morris, CJ (1993) Presence of foam cells containing oxidised low density lipoprotein in the synovial membrane from patients with rheumatoid arthritis. *Ann Rheum Dis* **52**(9)**:** 677-680.

Wissler, RW (1992) Theories and new horizons in the pathogenesis of atherosclerosis and the mechanisms of clinical effects. *Arch Pathol Lab Med* **116**(12)**:** 1281-1291.

Wissler, RW, Vesselinovitch, D (1968) Experimental models of human atherosclerosis. *Ann N Y Acad Sci* **149**(2)**:** 907-922.

Xiao, Q, Danton, MJ, Witte, DP, Kowala, MC, Valentine, MT, Bugge, TH, Degen, JL (1997) Plasminogen deficiency accelerates vessel wall disease in mice predisposed to atherosclerosis. *Proc Natl Acad Sci U S A* **94**(19)**:** 10335-10340.

Xiao, Q, Danton, MJ, Witte, DP, Kowala, MC, Valentine, MT, Degen, JL (1998) Fibrinogen deficiency is compatible with the development of atherosclerosis in mice. *J Clin Invest* **101**(5)**:** 1184-1194.

Yamada, Y, Doi, T, Hamakubo, T, Kodama, T (1998) Scavenger receptor family proteins: roles for atherosclerosis, host defence and disorders of the central nervous system. *Cell Mol Life Sci* **54**(7)**:** 628-640.

Young, M, Fullerton, M, Dilley, R, Funder, J (1994) Mineralocorticoids, hypertension, and cardiac fibrosis. *J Clin Invest* **93**(6)**:** 2578-2583.

Young, MJ, Moussa, L, Dilley, R, Funder, JW (2003a) Early inflammatory responses in experimental cardiac hypertrophy and fibrosis: effects of 11 beta-hydroxysteroid dehydrogenase inactivation. *Endocrinology* **144**(3)**:** 1121-1125.

Young, MJ, Moussa, L, Dilley, R, Funder, JW (2003b) Early Inflammatory Responses in Experimental Cardiac Hypertrophy and Fibrosis: Effects of 11{beta}-Hydroxysteroid Dehydrogenase Inactivation. *Endocrinology* **144**(3)**:** 1121-1125.

Zhang, SH, Reddick, RL, Piedrahita, JA, Maeda, N (1992) Spontaneous hypercholesterolemia and arterial lesions in mice lacking apolipoprotein E. *Science* **258**(5081)**:** 468-471.

Publications from thesis

Papers

Graeme A Deuchar, Patrick W.F. Hadoke, **Danielle Armour**, David G Brownstein, David J Webb, John J Mullins, Jonathan R Seckl, Yuri V Kotelevtsev. 'Glucocorticoid-mediated activation of extra-renal mineralocorticoid receptors exacerbates atherosclerosis in mice'. Manuscript in preparation for submission to Circulation Research, 2009.

Danielle Armour, Graeme A Deuchar, Karen E Chapman, Jonathon R Seckl and Yuri V Kotelevtsev. 'Accelerated atherosclerosis in the ApoE null mouse with 11β-HSD2 inactivation is associated with early pro-inflammatory changes in the vasculature'. Manuscript in preparation for submission to Arteriosclerosis Thrombosis and Vascular Biology.

Abstracts

Danielle Armour, Graeme Deuchar, Karen Chapman, and Yuri Kotelevtsev. Accelerated Atherosclerosis with 11β-HSD2-Deficiencey is Associated with Increased Inflammation in Early Stages of Plaque Development. *Abstract oral presentation (1st prize young investigators award),* XV International Symposium on Atherosclerosis, Boston USA 2009.

Danielle Armour, Graeme Deuchar, Karen Chapman, and Yuri Kotelevtsev. Can pro-inflammatory changes in the endothelium promote atherogenesis in the ApoE/11β-HSD2 double knockout mouse? *Oral presentation,* Centre for Cardiovascular Sciences annual symposium day, Edinburgh UK 2009.

Danielle Armour, Karen Chapman, and Yuri Kotelevtsev. The role of 11β-HSD2 in Protection against Inflammation during Atherogenesis'. *Abstract,* the Scottish Cardiovascular Forum, Inverness 2009.

Graeme Deuchar, **Danielle Armour**, Patrick Hadoke, David Brownstein, David Webb, Jonathon Seckl, and Yuri Kotelevtsev. Compromised Inactivation of Glucocorticoids in ApoE/HSD11B2 Deficient Mice Promotes Fulminant and Diet Independent Atherosclerosis Accompanied by Pro-Inflammatory Changes in Endothelium'. Abstract, Presented as second author at The European Atherosclerosis Society 77th Congress, Istanbul Turkey, 2008.